



universität
wien

DISSERTATION

Titel der Dissertation

„Synthesis of novel aminophosphonate scaffolds from
UGI-multicomponent reaction and their application as
selectors for liquid chromatography“

Verfasser

Msc. Andrea Gargano

angestrebter akademischer Grad

Doktor der Naturwissenschaften (Dr. rer.nat)

Wien, April 2013

Studienkennzahl lt. Studienblatt:

A 091 419

Dissertationsgebiet lt. Studienblatt:

Chemie

Betreuerin / Betreuer:

Univ.Prof.Dr. Michael Lämmerhofer

Abstract

Synthesis of novel aminophosphonate scaffolds from Ugi-multicomponent reaction and their application as selectors for liquid chromatography.

The present doctoral thesis describes a novel Ugi Multicomponent Reaction for the production of potential phosphopeptidomimetic functional molecules and its application to the development of novel zwitterionic chromatographic selectors. These novel amido aminophosphonate structures were synthesized as racemic mixtures starting from aminophosphonic acids reacted together with aldehydes and isonitriles educts. The design and the optimization of such one pot microwave based Ugi five-center four-component reaction (U-5C-4CR) synthetic pathway constitute the first part of the present work. Reaction conditions such as temperature, solvent and reaction time were extensively investigated in order to obtain optimal parameters. Based on the established reaction conditions we explored the synthetic scope using a variety of educts, generating the corresponding amido-aminophosphonates in moderate to high yields.

Since in the development of bioactive structures the chirality is a fundamental parameter to be investigated, part of my research interest has been invested in the development of liquid chromatography methods to enantiomerically resolve both the aminophosphonic acid educts and the Ugi products. Aminophosphonic acids synthons were separated by means of HPLC on cinchona-based chiral zwitterionic ion-exchangers under polar organic chromatographic elution conditions. The application of this method for chiral educts in preparative scale offers the possibility of using enantiomerically pure synthons, conditions that reduce the stereochemical complexity of the generated product (e.g. yielding two diastereomers instead of four stereoisomers). The separation of the Ugi-MCR phosphonate molecules was investigated as well adopting cinchona carbamate based stationary phases under chiral anion exchange conditions. This method offered the important advantage of obtaining by a single step both chemically and (when this was possible) enantiomerically pure compounds. Moreover from both of these studies the heterogeneity in terms of structural elements of the analytes allowed us to evaluate the influence of various structural motifs on enantioselectivity. Such elements of structure-enantioselectivity relationship are useful for the application of these methods to other structurally related analytes.

The developed Ugi combinatorial chemistry concept was exploited to devise new chromatographic ligands. Molecules selected for their interesting structural motifs were immobilized by thiol-ene click chemistry on silica beads. The chromatographic characteristics of these stationary phases were evaluated comparatively to corresponding commercially available columns. Interestingly multimodal separation capabilities were found for the novel selectors i.e. columns can be operated both in interaction liquid chromatography (HILIC) and in reversed-phase (RP) mode with good selectivity and efficiency. Moreover, the adopted synthetic approach offer the capability to generate chemical diversity simply by the variation of the starting aldehyde, aminophosphonic acid and/or isonitrile components. This unique characteristic offers great flexibility for the design of novel selectors for mixed mode chromatography, HILIC, affinity and chiral chromatography.

Synthese von neuartigen Aminophosphonat Gerüste aus UGI-Mehrkomponenten-Reaktion und ihre Anwendungen als Selektoren für die Flüssigchromatographie.

Die vorliegende Dissertation beschreibt eine neue Ugi Mehrkomponentenreaktion zur Herstellung von potentiellen phosphopeptidomimetic funktionalen Molekülen und ihre Anwendung bei der Entwicklung von neuartigen, zwitterionischen, chromatographischen Selektoren.

*“Nel mezzo del
cammin di nostra
vita..*

Table Of Contents

<u>A.</u>	<u>INTRODUCTION.....</u>	<u>3</u>
1.1	Liquid Chromatography.....	3
1.1.1.	Normal Phase Chromatography (NPC)	7
1.1.2.	Hydrophilic Interaction Chromatography (HILIC).....	8
1.1.3.	Reversed Phase Liquid Chromatography	10
1.1.4.	Ion exchange chromatography	11
1.1.4.a.	<i>Retention mechanism in IEC</i>	11
1.1.5.	Mixed-Mode Separations.....	14
1.1.6.	Enantioselective Liquid Chromatography	15
1.1.6.a.	<i>Basis of the chiral recognition</i>	15
1.1.6.b.	<i>Chiral Stationary phases</i>	18
1.1.6.c.	<i>Low molecular weight ion-exchange CSPs</i>	19
1.2	Multicomponent reactions.....	21
1.2.1	Isocyanide multicomponent reactions.....	22
1.2.1.a	<i>The Passerini and Ugi reaction</i>	22
<u>A.</u>	<u>REFERENCES.....</u>	<u>25</u>
<u>B.</u>	<u>AIM OF THE THESIS</u>	<u>27</u>
<u>C.</u>	<u>RESULTS AND DISCUSSION</u>	<u>29</u>
1.	Development of an Ugi multicomponent reaction for the synthesis of novel amido-aminophosphonate scaffolds	29
2.	Chromatographic enantioseparation of aminophosphonic acid synthons and amido-aminophosphonates structures by the means of carbamoylated cinchonan based ion exchangers.....	30
3.	Amido-aminophosphonate scaffolds from Ugi multicomponent reaction as multimodal chromatographic selectors	31
<u>D.</u>	<u>PUBLICATIONS AND MANUSCRIPTS</u>	<u>32</u>
	Manuscript 1	33
	Manuscript 2	94
	Manuscript 3	123

Manuscript 4	155
<u>E. THESIS STATISTICS:</u>	<u>216</u>
<u>F. ACKNOWLEDGEMENTS</u>	<u>218</u>
<u>G. CURRICULUM VITAE</u>	<u>220</u>
<u>CONFERENCE CONTRIBUTIONS</u>	<u>222</u>

I endeavoured to ascertain the copyright holders of all illustrations and secure their consent to the utilisation of their illustrations in the present paper. If, in spite of my efforts, a copyright infringement should have occurred, I kindly request the relevant parties to contact me.”

11/03/2013 Andrea Gargano

A. Introduction

The presented doctoral thesis describes the development of a Ugi Multicomponent Reaction for the synthesis of novel amido aminophosphonate structures (*Manuscript 1*) and the application of the synthetic protocol to the generation of novel chromatographic selectors (*Manuscript 4*). To achieve such aim in the course of the study we developed chromatographic methods for the purification of both the aminophosphonic educts (*Publication 1*) and the phosphonate products (*Manuscript 2*) adopted during the synthesis.

In the first chapter of the introduction (1.1) is reported a brief description over the chromatographic principles adopted either for the purification or used to evaluate the newly produced stationary phases. The second chapter (1.2) on the other hand, offers a brief background introduction about Multicomponent Reactions (MCR) and focuses particularly on the isocyanide based UGI MCR.

1.1 *Liquid Chromatography*

Chromatography is a technique that has a long tradition in the field of analytical chemistry. Its origins date back to the beginning of the last century ^[1]. To its development and understanding contributed important achievements from chemistry, physics but also engineering, electronics and computer science. This resulted in High Pressure Liquid Chromatography (HPLC), considered nowadays as THE analytical method for the separation, analysis and purification of small and large molecules. A decade ago, further advancements brought us UHPLC with further benefits in efficiency and speed of analysis. Applications of these techniques are established both in the production and analysis processes of the pharmaceutical, bio- pharmaceutical and synthetic industry as well as in applied research.

The separation principle in chromatography originates from the difference in migration velocities between solutes dispersed in a mobile fluidic medium and a stationary phase. Solute having weak affinity for the stationary phase will migrate with a velocity close to the one of the mobile phase. Thus they will elute before solutes, which are strongly distributed into the stationary phase, as a matter of fact, will possess lower migration velocity (*Figure 1*).

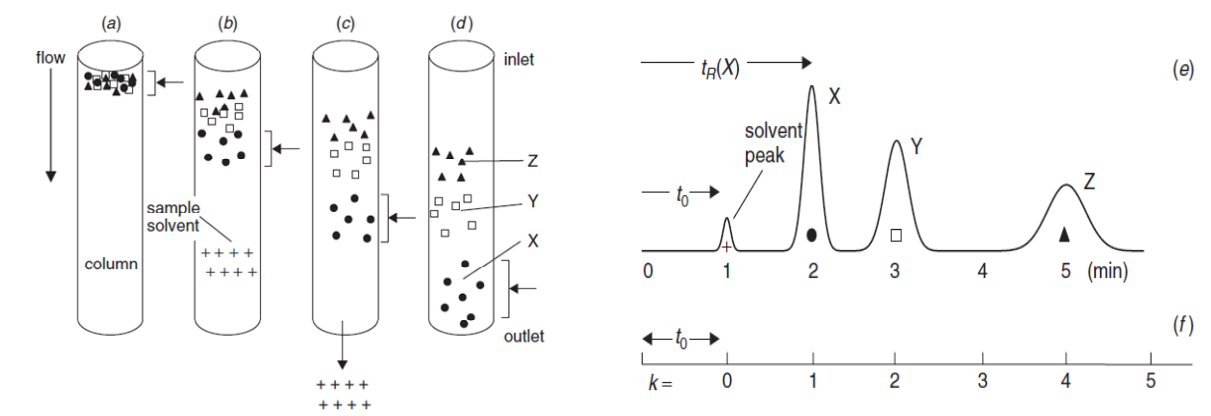


Figure 1: Illustration of the separation process in HPLC. (a–d) Sequential separation process of the analytes on the basis of different migration velocities; (e) the final chromatogram; (f) analysis of the elution profiles as function of time. Solute molecules X, Y, and Z are represented by •, □ and ▲ respectively; sample solvent molecules are shown by +. Reprinted from John Wiley & Sons inc. [2]

The most commonly adopted chromatographic set-up is composed by a liquid mobile phase that percolates a solid phase and takes the name of Liquid Solid Chromatography. In this set-up two phenomena determine the migration velocity of the analyte: the competitive adsorption between the analytes / solvent components on the stationary phase and the solvation of the analytes in the mobile phase. As obvious consequence, in the development of a separation method in order to generate different migration velocities between analytes the characteristics of both the mobile and stationary phases can or have to be tuned. The extensive research in liquid chromatography resulted in a categorization of the combinations of mobile and stationary phases expressing similar separation principles, namely chromatographic modes.

In the separation process a primary source of selectivity (parameter identifying the capability of the system of generating differential elution velocity) is represented by the chemistry of the accessible surfaces of the stationary phase. The chemistry of the surface determines both type(s) and strength of the molecular interaction(s) towards solutes. Therefore in the development of chromatography a key rule was, and still is, played by begetting novel separation materials that can overcome the limits of the one existing. In this context can be seen the final goal of my PhD, which deals with the modification of the chemical surface of silica (material commonly employed as support material for stationary phases) adopting compounds generated through combinatorial chemistry. This synthetic strategy offers the advantage of generating wide chemical heterogeneity adopting simple synthetic protocols. In particular my research has been focused on developing a multicomponent reaction for the chemical modification of aminophosphonic acids and the immobilization of novel structural motifs generated by this approach. Interesting novel multimodal separation capabilities were observed for the newly produced stationary phases (*Manuscript 4*).

Typically, chromatographic separation processes can be classified on the basis of the type of interaction of the solutes with the stationary phase. Adsorption chromatography is a term adopted to define a system in which the separation is based on the different affinity of solutes for the stationary phase and their binding to the solid surface (*Figure 2a*). When instead an analyte is undergoing a partition phenomenon between the two phases the method is classified as partition chromatography (*Figure 2b*).

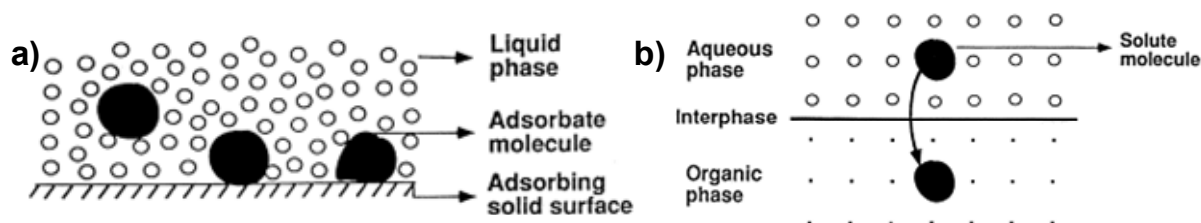


Figure 2: a) Schematic illustration of adsorption from aqueous solution onto an adsorptive solid surface, b) schematic illustration of partitioning between an aqueous and an organic phase. Reprinted with permission from Elsevier^[3]

Other means of separating molecules are based on charge or size (or shape) differences, approaches referred to as ion-exchange and size exclusion chromatography.

Last but not least, yet another chromatographic interaction principle is affinity chromatography in which specific retention is present towards a particular molecule or a class of molecules due to the concomitant presence of several interactions.

The suitability of a certain method for a specific separation is determined by analyte characteristics in terms of polarity and dimension (a schematic representation of this principle is reported in *Figure 3*).

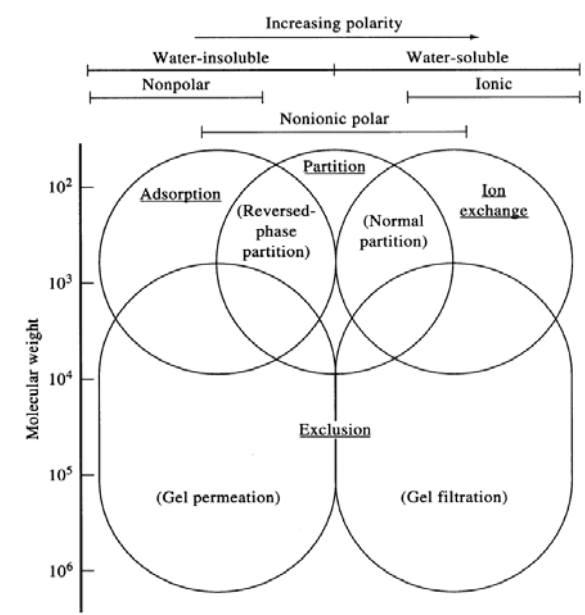


Figure 3: Schematic representation of the area of applicability of chromatographic methodologies with respect to analytes' characteristics and molecular weight. Reprinted from John Wiley & Sons inc^[2].

Besides its selectivity another important factor characterizing the separation process is its efficiency. This parameter is a miscellaneous indicator of the properties of the chromatographic set-up and is determined as the number of interactions between a solute/stationary phase (mass transefer properties) as well as by the axial dispersion of the solute molecules. The contributions characterizing this parameter arise from the structural properties of the separation material. Porous silica particles are the most widely adopted separation material thanks to their high surface areas, good mechanical properties, established chemical modification techniques and a well characterized operational range. Beside this material, interesting results have been obtained by the use of diverse stationary phase formats (e.g. silica monolith ^[4], fused core ^[5], non-porous phases ^[5]) and materials (e.g. polymeric ^[6], zirconia ^[7] based materials). Such different supports offer solutions to overcome some of the limitations of porous silica particles such as operational back pressure/efficiency (e.g. monolith), pH resistance (e.g. polymeric, zirconia materials), thermal stability (e.g. zirconia) and mass transfer properties for biomolecules (monolith, resins). However, these materials are currently adopted mainly in special chromatographic applications, leaving silica as the general support for HPLC.

1.1.1. Normal Phase Chromatography (NPC)

In its origins chromatography was performed on stationary phases having polar properties (packed inorganic particles like calcium carbonate or alumina), using mobile phases constituted of apolar or moderately polar solvents (addressed as “less polar”, in comparison to the stationary phase). This mobile/stationary phase set up was the main type of chromatography adopted till the 1960/70 and named as Normal Phase Chromatography. Bare inorganic materials with different purity grades are still the main stationary phases used in this technique, although other materials such as alumina, magnesia, Celite or chemically bounded stationary phases are also found. Amongst the chemically modified stationary phases, in particular cyano, diol, and amino ligands offer different elution properties and can be adopted for particular separations ^[8].

NPC is described as a separation process in which the retention of the solutes occurs due to a displacement of the solvent molecules on the silica surface (*Figure 4*). The displacement is therefore influenced by the polarity of the analyte and by the polarity of the solvent (solvent strength). For a more detailed discussion of the theory a comprehensive description can be found in ^[8].

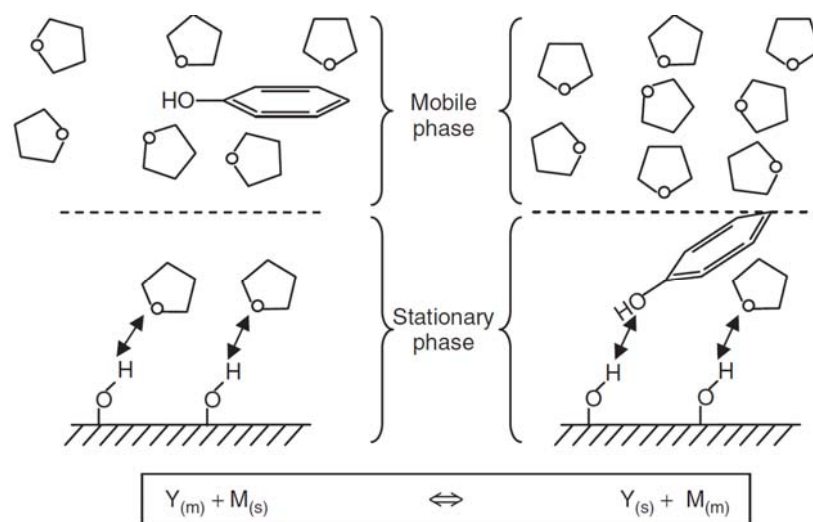


Figure 4: Hypothetical examples of solute retention on silica for phenol binding to bare silica in NPC with tetrahydrofuran as solvent. Reprinted with permission from John Wiley and Sons of ^[8]

With the introduction of reversed phase liquid chromatography (RPC) the popularity of NPC decreased, nowadays this technique is mainly adopted for column chromatography (for lab scale preparative purifications), thin layer chromatography and often with (polysaccharide based) chiral separation materials. Important advantages that contributed to the shift towards RPC are: the possibility of analyzing samples with water based media (biological samples) and the use of less toxic solvents.

1.1.2. Hydrophilic Interaction Chromatography (HILIC)

Hydrophilic interaction chromatography is an HPLC separation technique traditionally classified as part of the NPC because of the similarity in the use of polar stationary phases and relatively apolar bulk solvent. The mobile phases in this chromatographic set up are aqueous-organic with high concentration of organic solvent (usually ACN) and a water phase containing buffers (usually in the range between 2-50mM). Thanks to its capability of generating retention towards charged and uncharged polar compounds, its complementarity to RPC and its high MS compatibility (*Figure 5a*) the interest in this technique is rapidly rising in proteomic, glycomic and metabolomic research as well as drug and natural products analysis.

The retention mechanism regulating this separation technique is currently under debate. Albert et. al in the first publication that addresses this chromatographic technique as HILIC, describes the process as a partition between the stagnant water rich layer adsorbed onto the polar stationary phase and the water poor organic bulk medium, supported in some cases by adsorption phenomena ^[9] (*Figure 5b*).

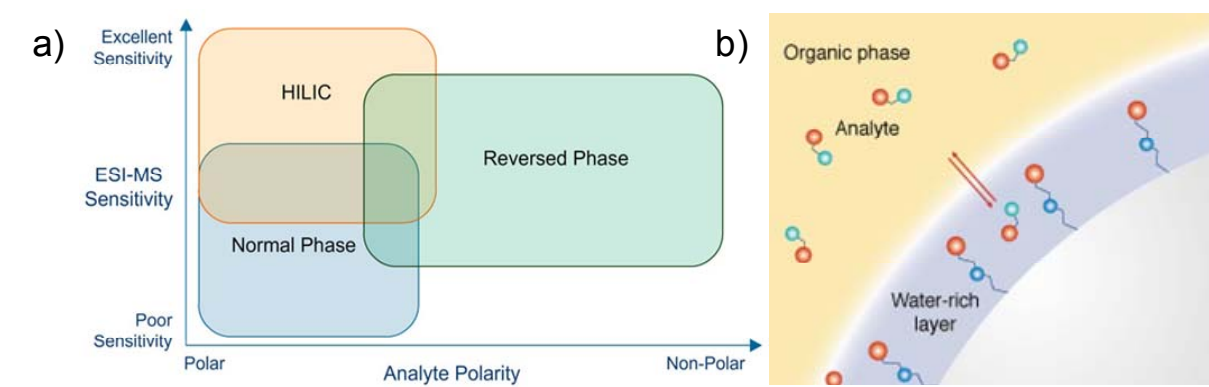


Figure 5: a) Schematic representation of the partition mechanism in HILIC chromatography. b) Range of applicability of HILIC, NPC and RPC chromatography with respect to the analyte polarity and MS compatibility. Reprinted with permissions of Caword Scientific (a) and Macherey-Nagel (b).

Several research groups investigated the mechanism of HILIC in order to prove or disprove the initial hypothesis of the existence of a water layer but till now no absolute conclusion was achieved. Interestingly what emerged from these studies is that in addition to the hydrophilic partition also hydrogen bonding and repulsive or attractive electrostatic forces may occur (the latter with charged stationary phases) ^[10]. Thus, HILIC chromatography can be described as a mixed type of chromatography in which a mixture of partition and adsorption mechanisms (including ionic interactions) takes place (*Figure 6*).

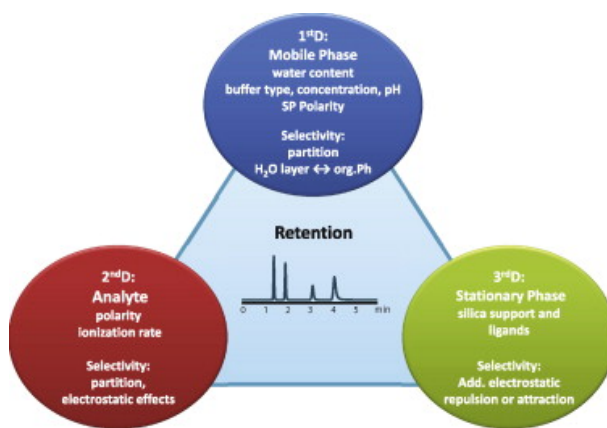


Figure 6: Retention contribution in HILIC chromatography, Reprinted with permission of Elsevier from [11].

Bare silica offers excellent properties in HILIC separation, but its use is limited due to the irreversible bonding of certain compounds on the support. Due to the novelty of the technique several bonded phases have been developed and are commercially available: polar neutral (e.g., cyanopropyl), diol-bonded, amide-bonded, polypeptide-bonded, positively charged amine-bonded (anion-exchange), negatively charged (cation-exchange), and zwitterionic phases. It is evident that the introduction of additional interaction sites affects the retention properties in HILIC but due to the presence of several parameters regulating this mixed mode interaction no general prediction¹ system was yet achieved.

¹ Correlation between structural analyte elements, stationary phase and mobile phase composition with respect to the retention observed

1.1.3. Reversed Phase Liquid Chromatography

Reversed-phase chromatography (RPC) is the most widely used branch of high-performance liquid chromatography (HPLC) finding applications for the analysis and purification of a wide variety of substances ^[12]. The technique is addressed as reversed since in comparison to normal phase it reverses the polarity of the original adsorbent and of the mobile phase.

The very high selectivity capability that such separation approach offers makes this method first choice for the separation of non-polar, polar, or ionic molecules. Exceptions from this generalization have to be made for big molecules (for which IEC or HIC chromatography are generally preferred), highly hydrophilic compounds (NPC, HILIC) and of achiral isomers (often better resolved in NPC).

The mechanism of solute retention in RPC is governed by hydrophobic interactions between the elute molecules and the stationary phase (*Figure 7*); although, depending on the characteristics of the column, polar, ionic, and other types of interactions can also be present in the separation process.

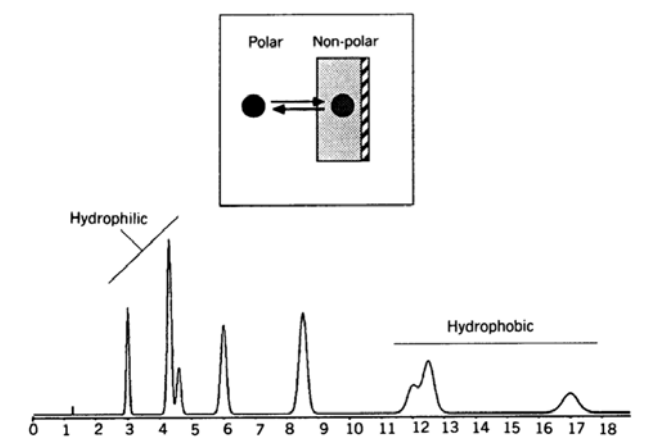


Figure 7: Schematic representation of the retention mechanism for reversed phase chromatography. a) Representation of the partition mechanism taking place within mobile phase and stationary phase. b) Example of a reverse phase separation of compounds differing in hydrophobicity properties. Reprinted with permission from John Wiley and Sons of ^[13].

The reason for the success of this chromatographic methodology relies on its robustness, versatility, efficiency and easiness in the development of chromatographic methods. Due to its broad utility most of the achievements in column technology were directly transferred to this technique, resulting in wide range of commercially available choices including column dimensions, particle size and stationary-phase type (C₁ –C₃₀, phenyl, cyano, etc.).

1.1.4. Ion exchange chromatography

Ion-exchange chromatography (IEC) is a chromatographic mode used to separate ions or ionizable species (from small ions to large biomacromolecules) on the base of their charge properties. The materials adopted as stationary phases are characterized by the presence of charged groups: anion-exchange columns carry positive charges (usually quaternary or tertiary ammonium groups) and are used for the separation of anionic or acidic samples while the cation-exchange columns carry negative charges (sulfonate or carboxylate groups) and are used to separate cationic or basic samples. Retention arises because of electrostatic attraction between the opposite charges of the analytes and stationary phase and elution is achieved by displacement of the analytes from the ion-exchange sites of the stationary phase by competing ions present in the mobile phase. In this context it is worth to mention that the mobile phase composition will also affect the charged status of the analyte.

With respect to the charged groups exposed, ion-exchange columns can be classified into strong and weak ion-exchangers. Strong ion-exchangers (anion: SAX and cation: SCX) carry ionic groups whose ionization does not change over the usual pH range ($2 < \text{pH} < 12$, e.g. SO_3^- group for SCX and NR_4^+ for SAX). Weak IEX lose their charge at certain pH ranges (e.g. COO^- for WCX show a progressive loss in charge for $\text{pH} < 5$) and changes in the pH conditions can be used as means of changing selectivity or for reducing retention.

Generally, the specific parameters that can be adopted to influence the strength of the chromatographic interaction are the pH, the concentration of the counter-ions as well as the percentage of organic modifier in the mobile phase.

This chromatographic technique has been extensively adopted in the course of the present study. Hence, a more detailed description of the separation mechanism will be discussed.

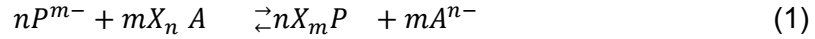
1.1.4.a. Retention mechanism in IEC

Retention in IEC results from the competition between the analyte (in its ionic form) and the counterions present in the mobile phase for the charged groups of the stationary phase driven by Coulombic attractions.

Describing a model regulating the electrostatic interaction between charged species in a medium requires a deep understanding of the physical chemistry phenomena and is not part of the aim of this introduction. The interested reader is referred to a review ^[14] for an extensive discussion of the topic.

To explain the ion-exchange phenomena a less rigorous but more descriptive system namely the stoichiometric displacement mode is adopted ^[15] (derived in this particular case from applied IEC of proteins).

Equation 1 depicts a generic ion exchange mechanism where P^{m-} represent the analyte, X^+ the stationary phase (in case of an anion exchanger) A^{n-} are the counterions present in the mobile phase and n and m express the charge status of the analytes and counterions.



The mass action law for this equilibrium can be written as:

$$K = \frac{[A^{n-}]^Z \{X_m P\}}{\{X_m A\}^Z [P^{m-}]} \quad (2)$$

where $[]$ are molar conc., $\{ \}$ are the amount of ion fixed/unit sorbent and $Z = \frac{m(\text{analyte})}{n(\text{counterion})}$

Expressing with q the the amount of analyte adsorbed per unit of surface area (in mol m^{-2}), q_x the total amount of accessible IEX site in the stationary phase and with C the concentration of the analyte the mass action law can be expressed as follows.

$$C = \frac{q [A^{n-}]^Z}{K (q_x - q)^Z} \quad (3)$$

This equation represents the adsorption isotherm relating the amount of analyte adsorbed to the concentration of counterion in solution.

In chromatography the migration of analytes is expressed in terms of retention factor. This parameter defines the time that a solute resides in the stationary phase and is derived from the slope of the adsorption isotherm (3) at the origin (alias when the concentration of the analyte in the MP, $C = 0$) where V_o is the mobile phase volume and S the surface area accessible:

$$k = \frac{S}{V_o} \left(\frac{dq}{dC} \right)_{C=0} = \frac{K S}{V_o} \frac{(q_x)^Z}{[A^{n-}]^Z} \quad (4)$$

Equation 4 mathematically represent the dependency of the retention factor in ion-exchange chromatography as function of the charge of the surface area exposed by the stationary phase, the counterion concentration and the ion exchange equilibrium constant (in L mol^{-1} , (*Equation 2*)).

By plotting in a double logarithmic manner the retention factors versus the displacement ion (counterion) concentrations a linear relationship is obtained and the equation derived by this relationship is referred to as stoichiometric displacement model (refer to *Equation 5* and *Figure 8*).

$$\log k = \log K_z + Z \log \frac{1}{[A^{n-}]} \quad (5)$$

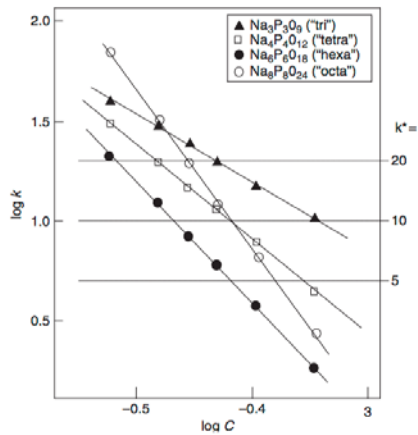


Figure 8: Illustration of the dependence of log k on counter-ion concentration (log C) ($[A^{n-}]$ in eq. 5) in isocratic IEC. Sample: four polyphosphates as defined in the figure legend; conditions: 500 × 4.0 mm TSKgel SAX anion exchange column; aqueous KCl salt solutions (buffered at pH 10.2 with EDTA) as mobile phase; 30°C. Reprinted with permission from John Wiley and Sons of ^[15]

The constant K_z can be calculated from the intercept of the slope:

$$K_z = \frac{K S (q_x)^Z}{V_o} \quad (6)$$

$\text{Log}K_z$ represents a system specific constant expressing the log k value at a 1M concentration of counter-ion.

In the case of weak ion exchanger the variation of the proton activity of the medium strongly influences the retention phenomena. The parameter q_x of *Equation 4* has therefore to be adjusted for the ionization state of the solute and the stationary phase. Resulting in *Equation 7* as illustrated by Sellergreen and co-workers ^[16]

$$k = \Phi \frac{1}{[A^{n-}]} K \alpha_P \alpha_X (q_x)^Z \quad (7)$$

Where Φ represent a system constant $\left(\frac{S}{V_o}\right)$ and α the ionization status of the analyte (P) and the stationary phase (X).

1.1.5. Mixed-Mode Separations

The analysis of biomatrices by means of RPC-MS can be problematic because of the weak retention properties offered by this technique towards highly polar molecules. Therefore, for analytes of biological interest such as metabolites or physiological intermediates alternatives to bare RPC have been introduced such as the addition of an ion pair in the mobile phase (IPC) or the use of HILIC chromatography. However, both the methods suffer from limitations such as ion suppression in MS detection for IPC or lack of retentivity of HILIC for lipophilic compounds.

In this context the use of mixed-mode columns, offering combined orthogonal separation principles (e.g. RP-WAX) results in novel selectivity profiles that allow the differentiation of the analytes on the basis of various different characteristics rather than just hydrophobicity. Although the application of this chemistry is known in solid-phase extraction materials ^[17] and capillary electrochromatography ^[18], this approach has rarely been exploited in LC ^[19] and has only become more popular recently ^[20]

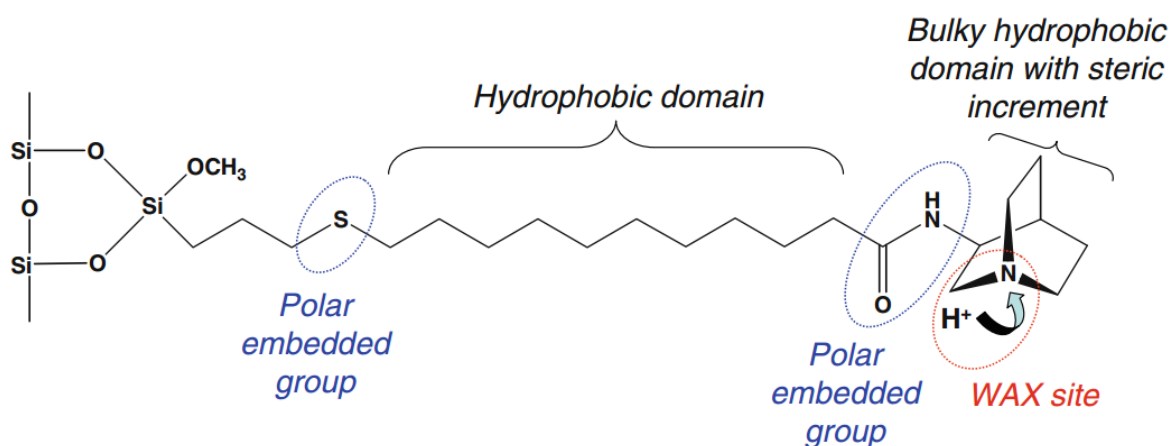


Figure 9: Structure of mixed-mode reversed-phase/weak anion-exchange (RP/WAX) stationary phase utilized in this study. Reprinted with permission from Springer of ^[20c, 20d].

Adopting these stationary phases the binding at the individual interaction sites can be adjusted by varying a broad range of parameters, such as the nature and amount of organic modifier in the eluent as well as the buffer type and concentration, pH, and temperature. Various modes of gradient elution (positive and negative organic modifier gradients, mixed modifier/buffer gradients, pH gradients) add further flexibility during method development. Depending on the elution conditions and the characteristics of the solutes used, these materials can be operated in a variety of chromatographic modes, such as classical RP mode (e.g. for neutral molecules), WAX mode (for negatively charged solutes), ion exclusion chromatography mode (cationic solutes), HILIC mode (polar neutral, basic, amphoteric, and acidic compounds), and HIC mode (for e.g. larger peptides) ^[20c].

1.1.6. Enantioselective Liquid Chromatography

Enantioselective chromatography is a branch of chromatography which is utilized for the separation of molecules that have identical atom-to-atom connections but distinct orientation of atoms or groups in three-dimensional space. Such entities are defined as stereoisomers and in particular as enantiomers when an element of chirality² is present within the molecule. The application of this technique is particularly relevant in the field of drug discovery, agrochemicals, fragrance and toxicology research. Enantiomers of potentially bioactive molecules often express different bioactivities and therefore have to be distinctly characterized. Within the possible strategies applicable to obtain single enantiomers, asymmetric synthesis is the methodology that guarantees the production of a single enantiomer of the investigated compound. However, such approaches (when applicable) are requiring long development time and beside that have to be characterized for their enantioselectivity. In this context, liquid chromatographic enantiomer separation methods are important tools for both the analytical characterization (determination of enantiomeric excess) and as preparative technique to give rapid access to individual enantiomers for biological testing.

1.1.6.a. Basis of the chiral recognition

Typically, enantiomer separations are performed employing a chiral selector (SO) immobilized or adsorbed onto a chromatographic support material (mostly spherical silica gel) yielding a chiral stationary phase (CSP). The interaction between the analyte (selectand (SA)) and the SO results in the generation of a diastereomeric associate (R-CS...X or S-CS...X of *Figure 10*). In case of a successful chiral separation the difference in binding energies between these two associates determines the generation of different migration velocities and thus elution properties.

Amongst the models proposed to rationalize the requirements for molecular recognition of different enantiomers, the “three-point interaction model” is the one frequently adopted to practically visualize a chiral discrimination process ^[22]. This model defines as minimum requirement for the creation of a chiral recognition process the presence of a minimum of three simultaneous interactions within SO-SA, out of which at least one must be spatially oriented. A fourth essential requirement consists in the accessibility of the SO only from one direction.

² Chirality refers to the geometrical property of an object of being nonsuperimposable on its mirror image (for a more detailed description the reader can refer to [21] M. Lämmerhofer, *Journal of Chromatography A* **2010**, 1217, 814-856.)

The validity and definition of this model has been debated over the years, but its use is nowadays commonly accepted (for a more detailed description the reader can refer to ^[21, 23]).

In *Figure 10* is depicted the “three-point interaction model”. Under the ideal assumption that the SA interact solely with the SO (and not with other elements of the stationary phase) the relative retentions of the enantiomers are determined by the strength of the interactions with the selector. Due to the presence of at least one stereochemically oriented interaction point the formation of the SA-SO associates will be influenced by the three-dimensional orientation and spatial arrangement of complementary sites in the binding partners. In case of chiral recognition one of the two enantiomers will show a better complementarity with respect to the SO and thus will have a higher equilibrium constant leading to a stronger complex.

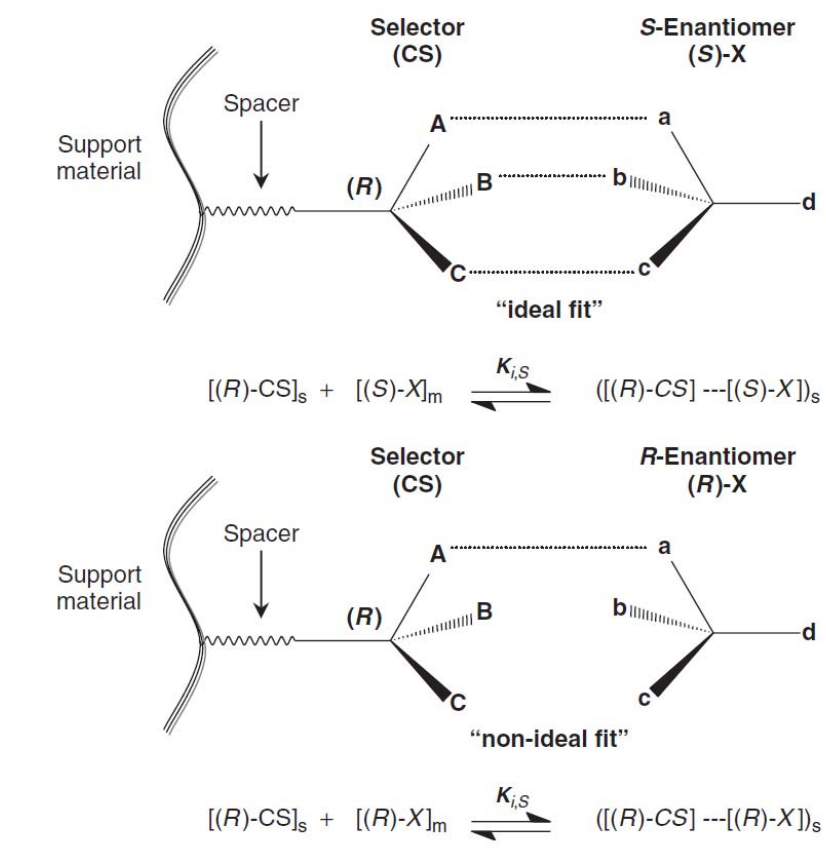


Figure 10: Three-point interaction model and associated interactions between R- or S-enantiomers and the CSP. Reprinted with permission from John Wiley and Sons of ^[23].

The elements of chiral recognition can be classified on the basis of the nature of their interaction as *sterical* or *functional* fit. In the first case there is a size and shape complementarity between the selector and one of the enantiomers (meaning that one analyte sterically fits the SA). A functional fit is instead observed when analytes and the selector have complementary interaction sites arranged in a favorable geometric and spatial orientation.

The non-covalent interaction forces that can take part in the association between analyte and selector (functional fit) are several and comprise:

- ionic interactions (electrostatic interactions between positively and negatively charged groups)
- hydrogen bonding (between H-donor and H-acceptor groups)
- ion–dipole, dipole–dipole (orientation forces), dipole–induced dipole (induction forces), and induced dipole–instantaneous dipole (dispersion forces) interactions
- π – π -interactions (face-to-face or face-to-edge arrangement of electron-rich and electron-poor aromatic groups)
- others such as quadrupolar, π –cation, π –anion interactions

In this context, the use of different solvents can interfere or promote specific SA-SO interactions and thus affect enantiorecognition. Solvents of high polarity attenuate the strength of electrostatic interactions, whereas hydrophobic interactions are present only in aqueous or hydro-organic mobile phases. The mobile phase pH or apparent pH is also another important parameter because of its influence on the charge status of the analyte and of the stationary phase (in the case that ionic interactions are involved in the recognition process).

1.1.6.b. Chiral Stationary phases

Chiral separation among the branches of chromatography remains one of the more challenging. In the course of the development of this technique several hundreds of chiral stationary phases (CSPs) proved their capability in resolving enantiomers, employing different mechanism of recognition. However, no general chromatographic set up could be established. Therefore, for every analyte the most suitable combination of CSP/mobile has to be identified.

Databases such as ChirBase^[24] were developed in order to collect information of successful separations of chiral structures under specified CSP/mobile phase combinations, but this information is often useless in the case of new structures. Moreover, the possibility of publishing separation protocols on new chemical entities is often not in the interest of chemical industries, a factor that considerably reduced the information input in this ChirBase project.

In the process of drug discovery pharmaceutical companies developed automated fast screening procedures employing the combination of the statistically more successful chiral separation phases and mobile phases. This is possible because between the hundreds of CSPs available on the market with a column set of about 20/30 of them virtually all the enantiomers can be separated.

A commonly accepted classification of CSPs is based on the nature of the chiral selector^[21]:

- *macromolecular selectors of semisynthetic origin* (polysaccharides)
- *macromolecular selectors of synthetic origin* (poly(meth)acrylamides, poly- tartramides)
- *macromolecular selectors of natural origin* (proteins)
- *macrocylic oligomeric or intermediate-sized selectors* (cyclodextrins, macrocylic antibiotics, chiral crown ethers)
- *synthetic, neutral entities of low molecular weight* (Pirkle-type phases, brush-type CSPs)
- *synthetic, ionic entities of low molecular weight that provide for ion-exchange*
- *chelating selectors for chiral ligand-exchange chromatography*

In the course of this PhD thesis work on low molecular weight ion-exchange selectors were adopted and therefore elements of the principles of their enantioseparation will be discussed in the following chapter. For a detailed discussion of the listed stationary phase the reader can refer to^[21, 23].

1.1.6.c. Low molecular weight ion-exchange CSPs

Chiral ion-exchangers are a class of CSPs developed for the enantioseparation of ionized species in which the main contribution to the retention is given by long range ionic interactions. The possibility of exploiting this type of interaction for chiral separation was deeply investigated by the group of professor Lindner in the last 20 years ^[25].

Several examples of chiral ion-exchangers are reported in literature: cinchona alkaloids and ergot alkaloids derivatives as anion-exchangers for chiral acids ^[26], chiral amino sulfonic acids as cation exchangers for the separation of chiral bases ^[27] and zwitterionic ion-exchangers for the separation of both acids, bases, and zwitterionic solutes such as amino acids and peptides ^[28] (some of the structures of the selectors are reported in *Figure 11*).

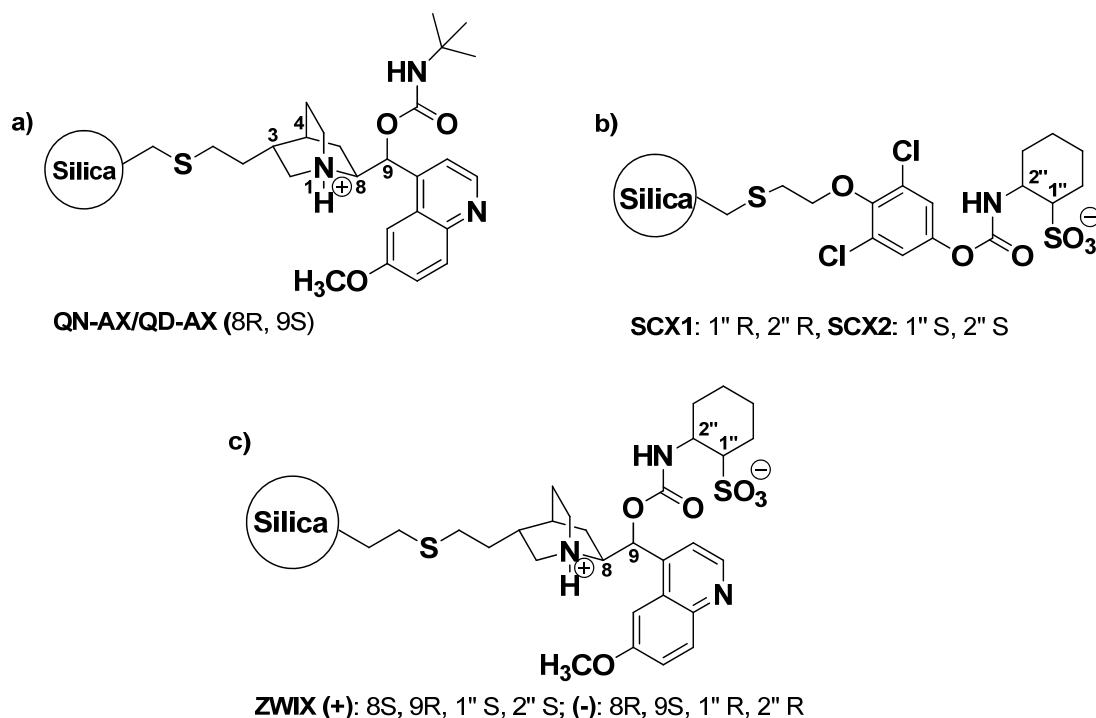


Figure 11: Chiral ion-exchangers. (a) Cinchona alkaloid-derived weak chiral anion-exchangers (WAX) ^[26a]: quinine-derived, Chiralpak QN-AX (8S,9R); quinidine-derived, Chiralpak QD-AX (8R,9S); configurations in position N1, C3, C4 are always (1S,3R,4S). (b) Strong chiral cation exchanger (SCX) derived from cis/trans-2-aminohexanesulfonic acid ^[27]. (c) Zwitterionic ion-exchangers (ZWIX) obtained by merging structural elements of above anion and cation exchangers ^[28].

The original study on the enantiorecognition properties of a stationary phase based on the chiral catalyst quinine and quinidine was performed by the group of Salvadori et al ^[29]. From this starting point the research work of Lämmerhofer and Lindner significantly improved the enantiodiscrimination capability of these phases by the introduction of different carbamoylated substituents in the OH-group in C9 position ^[26a, 30]. Moreover, the operation mode was shifted from NPC conditions to weakly acidic hydro-organic or polar organic mode (thus the selector was not operated as Pirkle type but as ion-exchanger).

The enantiorecognition power of these selectors is a result of a binding pocket constituted of five stereogenic centers: N₁, C₃, C₄ that possess the same configuration between quinine (QN) and quinidine (QD) and C₈, C₉ that possess instead opposite configurations (QN:8S, 9R; QD: 8R, 9S). The chiral recognition behavior of these phases is often driven by the interactions arising from the stereogenic center C₉ resulting in a pseudo-enantiomeric behavior which causes an inversion of the enantiomer elution order between QN and QD selectors.

Under weakly acidic hydro-organic or polar organic mobile phases the quinuclidine amine is protonated enabling the establishment of non-oriented long range electrostatic interaction that dominate the retention process while H-bond mediated ionic interactions can orient the selectand (SA) at the chiral selector (SO) resulting in a chiral recognition process. This recognition process can be additionally supported by other interacting groups capable of giving π - π interaction (quinoline ring) or steric hindrance (by the bulky quinuclidine and tert-butyl residues).

Lämmerhofer and Lindner's group continued the research in the field of chiral ion exchangers investigating the possibility of creating a novel chiral cation exchanger. The results were strong cation exchangers derived from cis and trans-2-aminohexanesulfonic acid, reporting excellent enantiorecognition properties for the separation of selected chiral secondary and tertiary amine ^[27]. Extension to this achievement was the combination of the anion (cinchona alkaloids) and cation (sulfonic acid) exchanger in a zwitterionic selector (ZWIX CSP) offering the possibility of resolving chiral acids, bases and amphoteric compounds ^[28]. Zwitterionic stationary phases overcame the limitation presented by WAX and SCX of only addressing analytes that carry charges of opposite sign and with respect to their uni-ionic exchangers this chromatographic selector reported significantly reduced retention times. This phenomenon was termed as "intra-molecular counterion (IMCI) effect" ^[27-28].

In the course of this study both the cinchona carbamate based chiral zwitterionic ion-exchanger were successfully applied for the enantioseparation of underivatized aminophosphonic acids and cinchona carbamate anion exchangers for the purification and enantioseparation of amido aminophosphonate Ugi products.

1.2 Multicomponent reactions

A multicomponent condensation reaction (MCR) or simply multicomponent reaction is a process in which three or more reactants are combined together in a single chemical step to generate products that incorporate substantial portions of all the educts. Typically these reactions undergo sequences of reversible equilibrium combined with a last irreversible step that pull the reaction towards the formation of the product(s). With respect to traditional multistep approaches multicomponent reactions have the advantage of enabling to produce great molecular diversity per step by use of distinct educts with a minimum of synthetic time and effort (reactions performed in a single vessel, only one purification step; *Figure 12*).

In the last decades the significant progress in the field of molecular biology and the development of high-throughput biological screening methodology has led to an ever-increasing demand for prospective drug compounds. In this context, multicomponent reactions (MCRs), thanks to their efficiency, ease of automation together with their chemical diversity-generating power, have attracted the attention of both, the academic and the industrial scientific community. Within the class of MCRs, those based on the peculiar reactivity of isocyanides, and in particular the Passerini and Ugi reactions, have been among the most widely used ^[31].

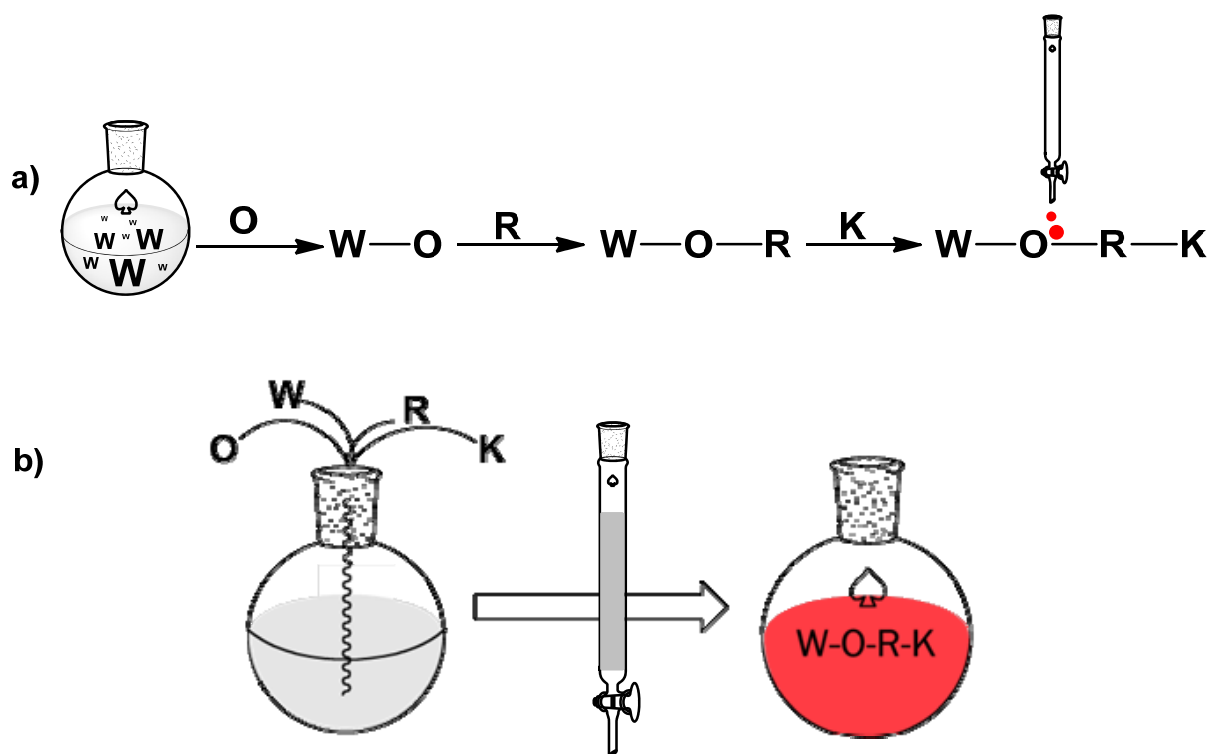


Figure 12: Schematic representation of the traditional multi-step synthetic approach (a) with respect to the multicomponent reaction (b).

1.2.1 Isocyanide multicomponent reactions

Isocyanide (also named isonitriles) are a class of organic compounds having a formally divalent carbon responsible for the characteristic properties of α -acidity, α -addition and easy formation of radicals. One of the reasons that make them very popular in a laboratory environment is their penetrating and intense odor. Almost all commercially available isocyanides are volatile and carry an interesting repulsive odor which is described by Gautier in 1869 as: “reminiscent of artichokes and phosphorus at the same time”^[32]. Dömling in his review on multicomponent reaction states that prolonged inhalation of isocyanides is “believed to increase the intensity of dreams at night”^[31i]. The author of this thesis did not experience such phenomena by these compounds *per se*.

Historically, the synthesis of isocyanides is dated back to 1859 by Lieke, who first believed them to be nitriles^[33]. In 1867 Gautier discovered the isomeric nature of the relationship between isocyanides and nitriles^[34]. Nowadays, the most commonly adopted method for the preparation of isocyanides is the reaction of the N-formamides with phosgene or phosgene surrogates or other inorganic dehydratants and matching bases^[35].

1.2.1.a The Passerini and Ugi reaction

A large and important class of MCRs are the isocyanide multicomponent reactions that origin from the pioneering studies performed by Mario Passerini in 1921 that developed the reaction that now bears his name almost a century ago^[36]. What was observed was that the reaction of an aldehyde or ketone with an isocyanide and a carboxylic acid lead to the formation of an α -acyloxyamide (*Figure 13*) with a new stereocenter. The reaction demonstrated excellent atom economy as every portion of the three components is incorporated into the product. However, limitations related to the availability of isonitriles as well as the limited knowledge on the reaction mechanism available at that time limited the use of this synthetic approach.

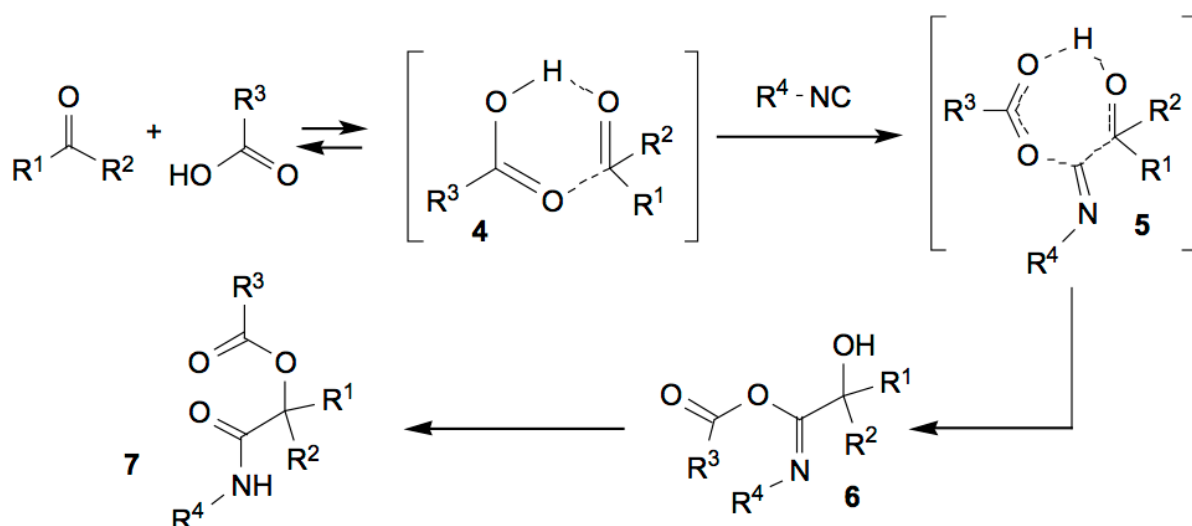


Figure 13: Schematic representation of the Passerini reaction. Reprinted with permission from John Wiley and Sons of ^[37]

Ivar Ugi entered the field many decades later and discovered that an amine could also be included, giving us a four-component reaction of a carbonyl component, a carboxylic acid, an amine and the isocyanide (*Figure 14*).

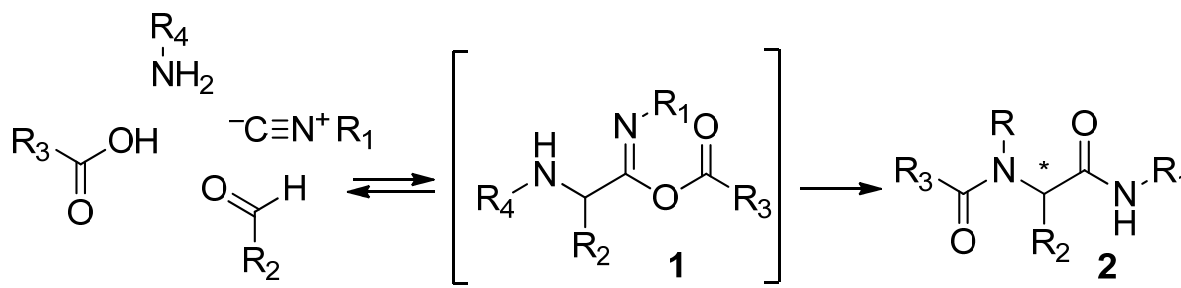


Figure 14: Schematic representation of the Ugi multicomponent reaction.

The reaction represents only a small variation on the Passerini reaction and the output is similar. However, the Ugi reaction is much more widely used. In this reaction the components combine reversibly to form the acylimidate (1). This intermediate undergoes irreversible Mumm rearrangement to form the product N-acylamino acid amide (2) with a new stereocenter(*). The elucidation of the reaction mechanism is still under investigation and is not objective of this introduction. The author refers to reference ^[38] for recent results on this topic.

Variations of the U-4-CR are the Ugi five-center four-component reaction (U-5C-4CR) and the Ugi-4-center-3-component reaction (U-4C-3CR). In these intramolecular versions of the Ugi reaction α - and β -AAs are used as bifunctional educts, the former to generate methyl esters of 1,1-iminodicarboxylic acids ^[39] (*Figure 15*) and the latter providing alicyclic β -lactams (*Figure 16*) ^[40].

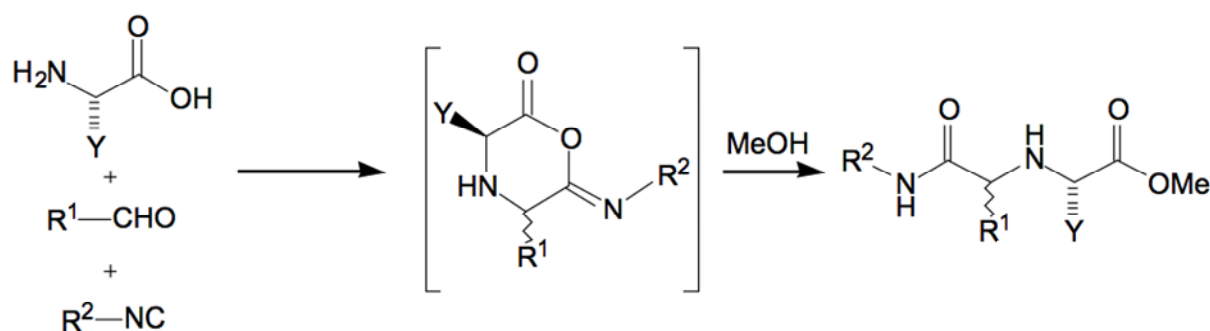


Figure 15: Schematic representation of the Ugi 5 component 4 center reaction (U-5C-4CR). Methanol is the fourth component. Reprinted with permission from John Wiley and Sons of ^[37].

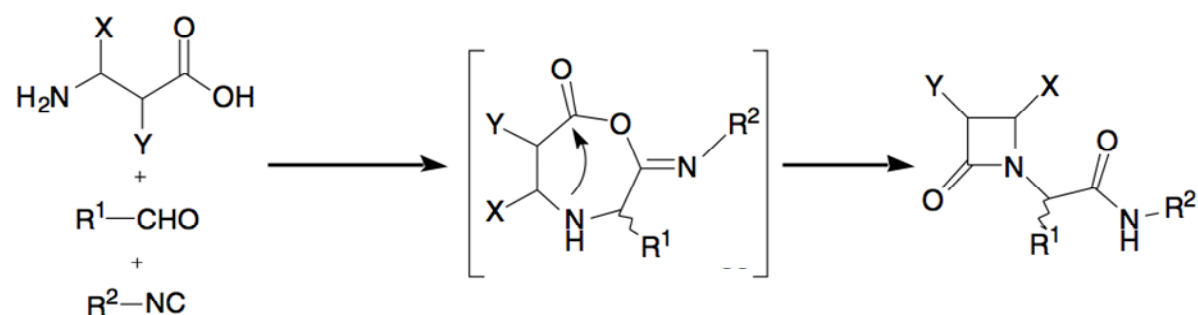


Figure 16: Schematic representation of a Ugi 3 component 3 center reaction (U-3C-3CR). Reprinted with permission from John Wiley and Sons of ^[37].

From my work experience with this synthesis I can conclude that Ugi MCRs are an excellent tool for synthesis of libraries of compounds. However, a consistent limitation is represented by the challenging task of purifying the chemically complex mixtures generated by the one pot synthesis. The possibility of applying this synthesis adopting one of the compounds immobilized on a solid support (namely solid phase synthesis) would be beneficial ^[41]. Unfortunately, due to time limitations this approach was not evaluated in this work and can just be suggested as an opportunity for further work on this topic.

A. References

- [1] M. S. Tswett, *Proceedings of the Warsaw Society of Naturalists, Biology Section* **1905**, 14, 20-39.
- [2] L. R. Snyder, J. J. Kirkland, J. W. Dolan, in *Introduction to Modern Liquid Chromatography*, John Wiley & Sons, Inc., **2010**, pp. 2-13.
- [3] A. Vailaya, C. Horváth, *Journal of Chromatography A* **1998**, 829, 1-27.
- [4] F. Švec, Z. Děyl, T. B. Tennikova, in *Journal of Chromatography Library, Vol. Volume 67* (Eds.: T. B. T. František Švec, D. Zdeněk), Elsevier, **2003**, pp. V-VI.
- [5] D. Guillarme, J. Ruta, S. Rudaz, J.-L. Veuthey, *Anal Bioanal Chem* **2010**, 397, 1069-1082.
- [6] F. Svec, J. M. J. Frechet, *Analytical Chemistry* **1992**, 64, 820-822.
- [7] J. Nawrocki, M. Rigney, A. McCormick, P. W. Carr, *Journal of Chromatography A* **1993**, 657, 229-282.
- [8] L. R. Snyder, J. J. Kirkland, J. W. Dolan, in *Introduction to Modern Liquid Chromatography*, John Wiley & Sons, Inc., **2010**, pp. 361-402.
- [9] A. J. Alpert, *J Chromatogr* **1990**, 499, 177-196.
- [10] aA. J. Alpert, *Analytical Chemistry* **2007**, 80, 62-76; bA. E. Karatapanis, Y. C. Fiamegos, C. D. Stalikas, *Journal of Chromatography A* **2011**, 1218, 2871-2879.
- [11] G. Schuster, W. Lindner, *Journal of Chromatography A* **2013**, 1273, 73-94.
- [12] C. Horvath, W. Melander, *Journal of Chromatographic Science* **1977**, 15, 393-404.
- [13] L. Lloyd, J. Kennedy, *Bioseparation* **1999**, 8, 330-331.
- [14] J. Ståhlberg, *Journal of Chromatography A* **1999**, 855, 3-55.
- [15] M. C. Millot, T. Debranché, A. Pantazaki, I. Gherghi, B. Sébille, C. Vidal-Madjar, *Chromatographia* **2003**, 58, 365-373.
- [16] B. Sellergren, K. J. Shea, *Journal of Chromatography A* **1993**, 654, 17-28.
- [17] N. Fontanals, R. M. Marcé, F. Borrull, *Journal of Chromatography A* **2007**, 1152, 14-31.
- [18] F. Progent, M. Taverna, A. Banco, A. Tchaplá, C. Smadja, *Journal of Chromatography A* **2006**, 1136, 221-225.
- [19] L. W. McLaughlin, *Chemical Reviews* **1989**, 89, 309-319.
- [20] aW. Bicker, M. Lämmerhofer, T. Keller, R. Schuhmacher, R. Krska, W. Lindner, *Analytical Chemistry* **2006**, 78, 5884-5892; bH. Hinterwirth, M. Lämmerhofer, B. Preinerstorfer, A. Gargano, R. Reischl, W. Bicker, O. Trapp, L. Brecker, W. Lindner, *Journal of Separation Science* **2010**, 33, 3273-3282; cM. Lämmerhofer, R. Nogueira, W. Lindner, *Anal Bioanal Chem* **2011**, 400, 2517-2530; dR. Nogueira, M. Lämmerhofer, W. Lindner, *Journal of Chromatography A* **2005**, 1089, 158-169.
- [21] M. Lämmerhofer, *Journal of Chromatography A* **2010**, 1217, 814-856.
- [22] aS. Topiol, M. Sabio, *Journal of the American Chemical Society* **1989**, 111, 4109-4110; bT. D. Booth, D. Wahnnon, I. W. Wainer, *Chirality* **1997**, 9, 96-98.
- [23] L. R. Snyder, J. J. Kirkland, J. W. Dolan, in *Introduction to Modern Liquid Chromatography*, John Wiley & Sons, Inc., **2010**, pp. 665-724.
- [24] S. L. Cui, X. F. Lin, Y. G. Wang, *J. Org. Chem.* **2005**, 70, 2866-2869.
- [25] M. Laemmerhofer, W. Lindner, *Liquid chromatographic enantiomer separation and chiral recognition by cinchona alkaloid-derived enantioselective separation materials*, Vol. 46, **2008**.
- [26] aM. Lämmerhofer, W. Lindner, *Journal of Chromatography A* **1996**, 741, 33-48; bJ. Olšovská, M. Flieger, F. Bachechi, A. Messina, M. Sinibaldi, *Chirality* **1999**, 11, 291-300.
- [27] C. V. Hoffmann, M. Laemmerhofer, W. Lindner, *Journal of Chromatography A* **2007**, 1161, 242-251.
- [28] C. V. Hoffmann, R. Pell, M. Lämmerhofer, W. Lindner, *Analytical Chemistry* **2008**, 80, 8780-8789.

- [29] C. Rosini, C. Bertucci, D. Pini, P. Altemura, P. Salvadori, *Chromatographia* **1987**, *24*, 671-676.
- [30] A. Mandl, L. Nicoletti, M. Lämmerhofer, W. Lindner, *Journal of Chromatography A* **1999**, *858*, 1-11.
- [31] aC. Hulme, *Multicomponent Reactions* **2005**, 311-341; bC. C. Musonda, D. Taylor, J. Lehman, J. Gut, P. J. Rosenthal, K. Chibale, *Bioorg. Med. Chem. Lett.* **2004**, *14*, 3901-3905; cC. Musonda Chitalu, D. Taylor, J. Lehman, J. Gut, J. Rosenthal Philip, K. Chibale, *Bioorg Med Chem Lett* **2004**, *14*, 3901-3905; dW. Wang, A. Domling, *Journal of Combinatorial Chemistry* **2009**, *11*, 403-409; eC. Hulme, V. Gore, *Current Medicinal Chemistry* **2003**, *10*, 51-80; fG. Miao, R. Lan, C. Le, Y. Kan, S. Kandasamy, V. Joshi, L. Yu, *Abstracts of Papers, 231st ACS National Meeting, Atlanta, GA, United States, March 26-30, 2006* **2006**, ORGN-310; gG. Miao, Y. Kan, C. Le, V. Joshi, R. Qiu, L. Yu, C. Baldino, *Abstracts of Papers, 229th ACS National Meeting, San Diego, CA, United States, March 13-17, 2005* **2005**, ORGN-061; hP. A. Tempest, *Current Opinion in Drug Discovery & Development* **2005**, *8*, 776-788; iA. Dömling, I. Ugi, *Angewandte Chemie International Edition* **2000**, *39*, 3168-3210.
- [32] A. Gautier, *Ann.Chim. (Paris)* **1869**, *17*, 218.
- [33] W. Lieke, *Justus Liebigs Ann. Chem.* **1859**, 316.
- [34] A. Arizpe, F. J. Sayago, A. I. Jiménez, M. Ordóñez, C. Cativiela, *European Journal of Organic Chemistry* **2011**, *2011*, 3074-3081.
- [35] aG. Skorna, I. Ugi, *Angewandte Chemie International Edition in English* **1977**, *16*, 259-260; bH. Eckert, B. Forster, *Angewandte Chemie International Edition in English* **1987**, *26*, 894-895.
- [36] aM. Passerini, *Gazzetta Chimica Italiana* **1921**, *51*, 121; bM. Passerini, *Gazzetta Chimica Italiana* **1921**, *51*, 181.
- [37] L. Banfi, A. Basso, G. Guanti, R. Riva, in *Multicomponent Reactions*, Wiley-VCH Verlag GmbH & Co. KGaA, **2005**, pp. 1-32.
- [38] N. Cheron, R. Ramozzi, L. El Kaim, L. Grimaud, P. Fleurat-Lessard, *The Journal of Organic Chemistry* **2012**.
- [39] al. Ugi, A. Demharter, W. Hörl, T. Schmid, *Tetrahedron* **1996**, *52*, 11657-11664; bA. Demharter, W. Hörl, E. Herdtweck, I. Ugi, *Angewandte Chemie International Edition in English* **1996**, *35*, 173-175.
- [40] al. Ugi, C. Steinbrückner, *Chemische Berichte* **1961**, *94*, 734-742; bH. P. Isenring, W. Hofheinz, *Synthesis* **1981**, *1981*, 385-387.
- [41] J. J. Chen, A. Golebiowski, S. R. Klopfenstein, L. West, *Tetrahedron Letters* **2002**, *43*, 4083-4085.

B. Aim of the thesis

The aim of the present thesis work has been to extend the Ugi multicomponent reaction to aminophosphonic acids educts and through this synthetic approach design chromatographic materials characterized by novel chemoselective properties (Figure 18).

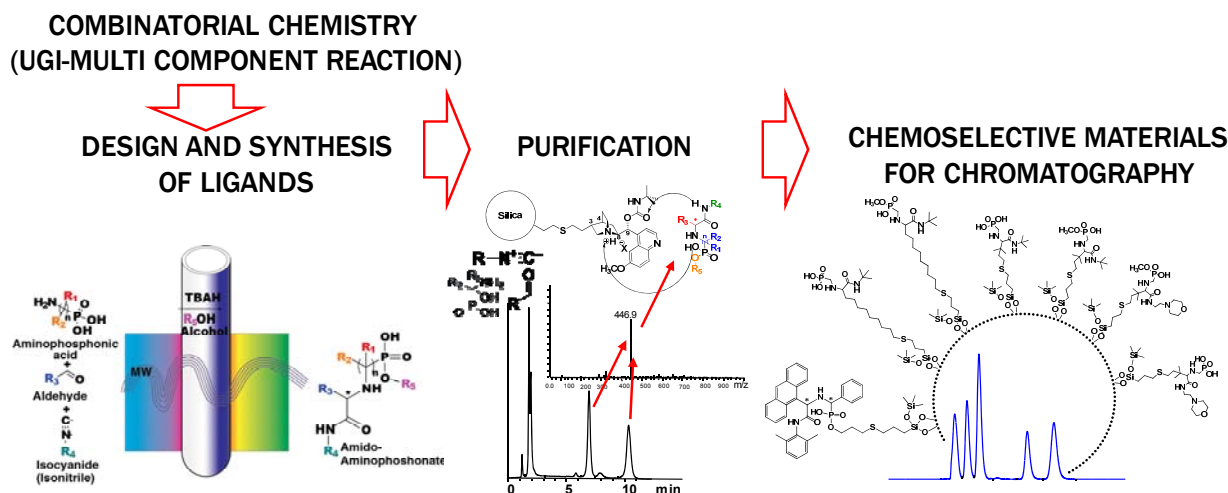


Figure 18: Schematic representation of the objective of this PhD investigation

Primary objective of this work, on the one hand, has been the investigation of synthesis parameters and reaction conditions that could lead to an efficient production of a novel class of chemical entities, namely amido aminophosphonate compounds. In order to prove the generation of such chemical entities and illustrate the applicability to generate chemical diversity we extended the synthetic scope to diverse educts and adopted several analytical and spectroscopic techniques for the analysis of the product such as X-Ray, NMR, High Resolution Mass Spectrometry, IR and liquid chromatography to obtain the necessary structural information of the generated species.

Due to the racemic nature of the products generated from aldehydes of the general formula $R_1HC=O$ and high level of chemical complexity of the reaction products (consisting of educts, product(s) and side product(s) that possess similar properties) that characterizes this synthetic procedure, a second aim of this study has been the development of chromatographic methods which can be used to give access to enantiomerically pure products and can be used for analytical quality control. Such objective has been successfully achieved applying chromatographic methods on cinchona carbamate based ion exchangers. Chemical and enantiomeric (when possible) purification of the Ugi-MCR reaction mixtures was achieved by means of cinchona carbamate anion exchangers under polar organic conditions. Moreover, cinchona-based chiral zwitterionic ion-exchangers were found to be capable of offering good separation properties towards chiral aminophosphonic acid educts,

offering the possibility of using enantiomerically pure synthons and therefore reducing the stereochemical complexity of the generated products.

Finally, in order to accomplish the initial scope of our investigation, we adopted the developed synthetic method to design selectors, bearing chemically diverse functional groups, for various modes of chromatography, such as polar reversed-phase (RP) chromatography, hydrophilic interaction liquid chromatography (HILIC), chiral separation, ligand-exchange, chemoaffinity separations and immobilized metal affinity chromatography (IMAC), amongst others. Structural variability via the various residues of the selectors allows tailoring of their retention increments and thus flexible adjustment of the selectivity of the stationary phases for given applications. Herein, the principle was documented for mixed-mode chromatography. Thus, the chromatographic ligands were immobilized onto silica gels, generating materials with interesting multimodal separation capabilities i.e. columns which can be operated both in HILIC and in RP mode with good selectivity and efficiency.

C. Results and Discussion

In the present chapter is reported a brief overview over the most important results achieved during my PhD thesis. A more detailed description of the approach, methods, results and discussions is given in the manuscripts in the appendix of this thesis. The results are organized into three different sections according to their general topic.

1. Development of an Ugi multicomponent reaction for the synthesis of novel amido-aminophosphonate scaffolds

In the first manuscript reported (Manuscript 1) is described the development of a multicomponent reaction strategy (Ugi 5 components 4 centers reaction) to produce a novel class of molecules, namely zwitterionic amido-aminophosphonates. In the course of the study we investigated the effects of structural variation of educts, temperature, reaction time, heating strategy and solvent on the yield of the product. Optimized reaction conditions were worked out by thoroughly studying each of these influential variables.

The newly developed method makes use of microwave heating, in order to enhance reaction rates, generating the corresponding amido-aminophosphonate products from α -, β - and γ -aminophosphonic acids, aldehydes, isocyanides and alcohols in moderate to high yields. A full characterization of the compound structures employing X-ray, Nuclear Magnetic Resonance, High Resolution Mass Spectrometry, Vibrational Circular Dichroism and chromatographic techniques is described. As an extension of the work are described conditions for quantitative hydrolysis of this novel class of mono-alkyl phosphonate ester compounds to generate the corresponding phosphonic acids.

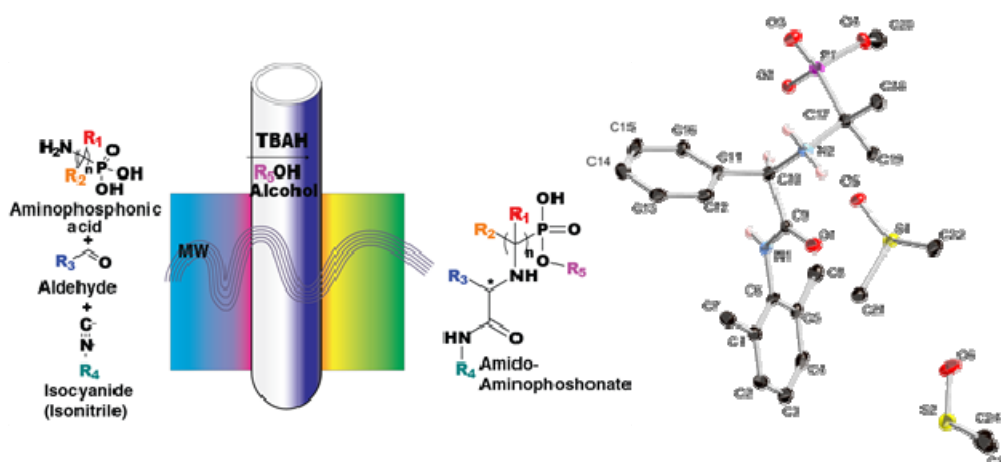


Figure 19: Graphical abstract of manuscript 1

2. *Chromatographic enantioseparation of aminophosphonic acid synthons and amido-aminophosphonates structures by the means of carbamoylated cinchonan based ion exchangers*

In manuscript 2 and 3 are reported chromatographic methods to enantioseparate aminophosphonic acids (2) and amido-aminophosphonates structures (3). These separation procedures were successfully applied to reduce the high level of chemical complexity that characterize this synthetic procedure previously described.

Cinchona-based chiral zwitterionic ion-exchangers demonstrated good separation properties towards chiral aminophosphonic acid educts, offering the possibility of using enantiomerically pure synthons and therefore reducing the stereochemical complexity of the generated products (Manuscript 2). Cinchona carbamate anion exchangers were instead adopted for the chemical and enantiomeric (when possible) purification of the Ugi-MCR reaction mixtures (Manuscript 3).

Beside their usefulness in the purification procedures of the reported work, such procedures can be widely applied for the enantiopurification and/or for the determination of the enantiomeric purity of these novel classes of molecules with which studies on bioactivity are conducted, substituting the indirect ^{31}P -NMR methods currently adopted.

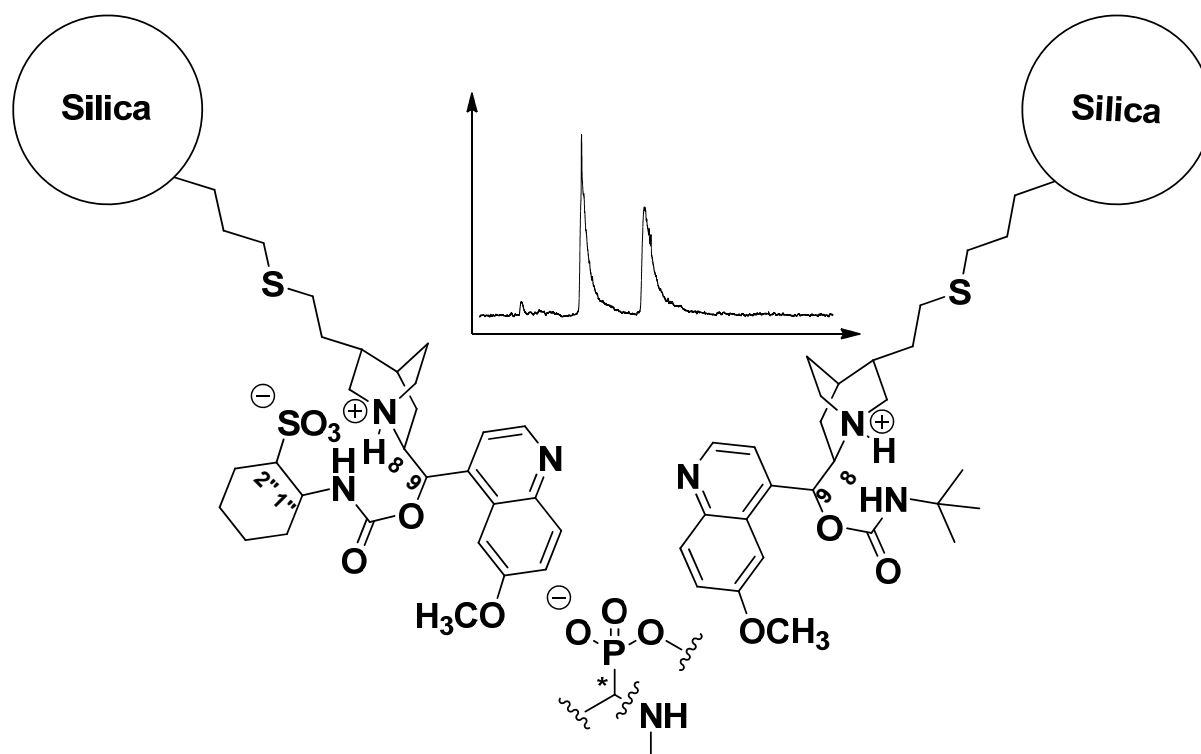


Figure 20: Graphical abstract of manuscript 2 and 3

3. *Amido-aminophosphonate scaffolds from Ugi multicomponent reaction as multimodal chromatographic selectors*

In manuscript 4 is described the design and immobilization of amido-aminophosphonate derivatives obtained by Ugi reaction onto thiopropyl silica and the investigation of their chromatographic properties. Such phases combining alkyl groups with ion exchange moieties and polar embedded groups exhibited typical multimodal retention capabilities and due to their chemical nature where classified as reversed-phase/zwitterionic ion-exchangers (RP/ZWIX).

The contribution describes the observed retention properties in dependence of the mobile phase composition with respect to a set of analytes with diverse lipophilicity and charge properties. As conclusive study the novel stationary phases were chromatographically evaluated under HILIC elution modes (i.e., ACN-rich hydroorganic eluents) as well as RP conditions (i.e., employing aqueous-rich hydroorganic eluents). The results obtained were analyzed on the basis of the different structural elements inserted in the molecular scaffold. Complementary retention profiles distinct to common HILIC and RPLC phases were found. The RP/ZWIX phases generated hold therefore considerable promise to be useful as complementary stationary phases in impurity profiling and 2D-HPLC.

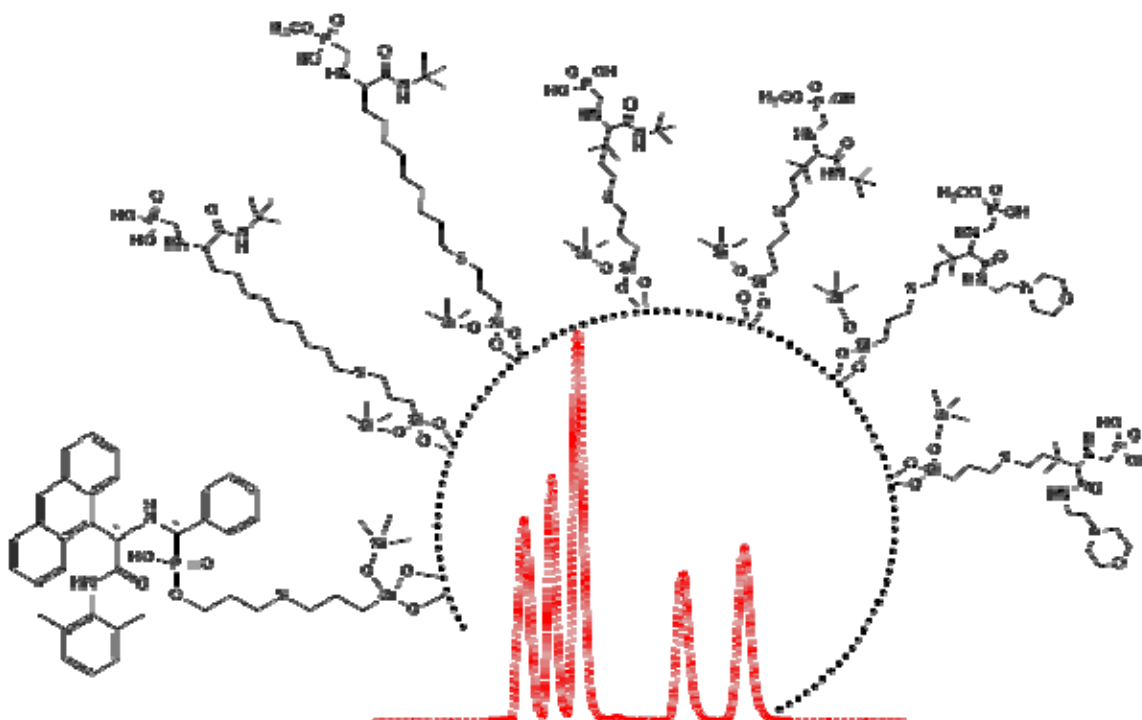
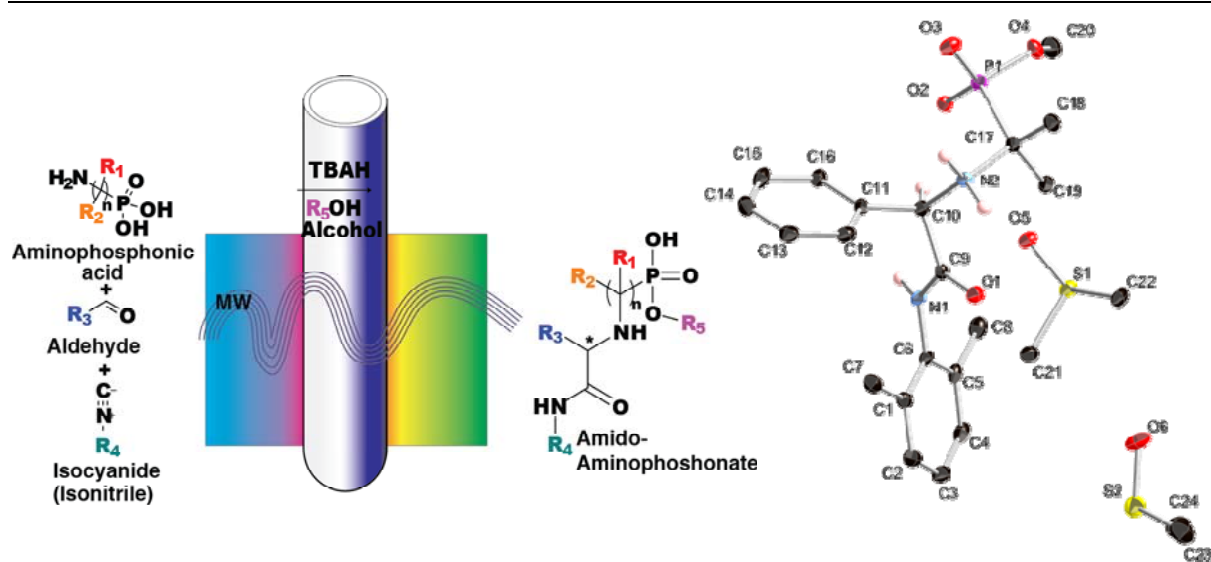


Figure 21: Graphical abstract manuscript 4

D. Publications and Manuscripts

Manuscript 1



Graphical abstract:

Novel UGI microwave assisted multicomponent reaction for the synthesis of **phosphopeptidomimetic compounds**. Aminophosphonic acids (α , β , γ), aldehydes, and isocyanides as educts, react together to create amido-aminophosphonate compounds.

Facile route to phosphopeptidomimetics by single step Ugi Multicomponent Reaction

Andrea Gargano¹, Stefanie Buchinger¹, Michal Kohout¹, Wolfgang Lindner¹, Michael Lämmerhofer^{1,2*}

¹ Department of Analytical Chemistry, University of Vienna, Waehringer Strasse 38, 1090 Vienna, Austria

²Institute of Pharmaceutical Sciences, University of Tübingen, Auf der Morgenstelle 8, 72076 Tübingen, Germany

Correspondence:

Michael Lämmerhofer

Institute of Pharmaceutical Sciences

University of Tübingen

Auf der Morgenstelle 8

72076 Tübingen, Germany

T +49 7071 29 78793

F +49 7071 29 4565

<mailto:michael.laemmerhofer@uni-tuebingen.de>

Keywords:

Combinatorial chemistry, Multicomponent reaction, Microwave sythesis, Ugi five center four component reaction, Amino phosphonic acid, Phosphopeptidomimetic compounds, Isocyanides

Abstract

This article describes the design and optimization of an effective microwave-assisted multicomponent reaction to produce a novel class of phosphopeptidomimetic compounds. When using aminophosphonic acids (α , β , γ), aldehydes and isocyanides as educts with alcohols as solvents these building blocks are merged to functionalized amido-aminophosphonate structures in a novel Ugi-type one-pot transformation.

A high level of structural diversity can be achieved through this synthetic approach, providing a platform for the production of functionalized building blocks for novel bioactive molecules. The general scope of this multicomponent synthetic protocol is explored by variation of reaction parameters together with an evaluation of a diverse set of reaction educts

1. Introduction

Amino acids (AAs) play a key role in biochemistry, constituting the structural units of peptides, proteins and enzymes. As phosphorus analogues of AAs, aminophosphonic acids can very efficiently act as biomimetics undergoing competing interactions at the active site of enzymes^[42] and cell receptors^[42a, 43]. In addition, phosphonates have demonstrated to be effective chelating agents, capable of controlling the uptake or the removal of metal ions in living systems. These unique characteristics render aminophosphonic acids and phosphonates of considerable biological and pharmacological interest, with applications as antitumor^[44], neuroactive^[44c, 45], antihypertensive^[44c, 46], antimicrobial^[44c, 47], herbicidal^[42a, 44c] and imaging agents^[48].

In the last decades a significant progress in the field of molecular biology and the development of high-throughput biological screening methodology in drug discovery has led to an ever-increasing demand for prospective drug compounds. In this context, multicomponent reactions (MCRs), thanks to their efficiency, ease of automation together with their chemical diversity-generating power, have attracted the attention of both, the academic and the industrial scientific community^[49]. Within the class of MCRs, those based on the peculiar reactivity of isocyanides, and in particular the Ugi reactions, have been among the most widely used^[31].

Ugi four component reactions (U-4-CR) provide access to peptide-like derivatives by condensing an aldehyde, an amine, a carboxylic acid and an isocyanide efficiently in one pot. Effective variations of the U-4-CR are the Ugi five-center four-component reaction (U-5C-4CR) and the Ugi-4-centre-3-component reaction (U-4C-3CR). In these intramolecular

versions of the Ugi reaction α - and β -AAs are used as bifunctional educts, the former to generate 1,1-iminodicarboxylic acids^[39] and the latter providing alicyclic β -lactams^[40]. It has been postulated that in both cases the reaction evolves through a cyclic intermediate (6 and 7-membered ring, respectively; *vide infra*)^[50]. In the case of β -amino carboxylic acids, a lactam structure is generated via ring contraction of a 7-membered intermediate (U-4C-3CR). With α -AAs the intermediate cannot undergo such reaction and methanol (used as solvent) acts as nucleophile generating iminodiacetic adducts. These synthetic procedures are restricted to amino carboxylic acids and typically are carried out at low temperature (-30 °C, 0 °C or r.t.) and require extended reaction times (often in the range of days)^[31i, 39b]

The aim of the present study was to extend the preparative simplicity of the Ugi reaction to aminophosphonic acid educts to access a novel class of amido-aminophosphonate molecules. The newly developed method makes use of microwave heating in order to enhance reaction rates^[51], generating the corresponding amido-aminophosphonate products from α -, β - and γ - aminophosphonic acid, aldehyde, isocyanide and alcohol via U-5C-4CR (Scheme 1). As an extension of our work we also describe conditions for quantitative hydrolysis of this novel class of phosphonate compounds to generate the corresponding phosphonic acids.

2. Result and discussion

2.1. Reaction mechanism:

A reaction mechanism similar to that suggested by Ugi *et al* ^[39a] for amino carboxylic acids can be postulated (*Scheme 2*). In the first step of the cascade reaction, the amino group of the aminophosphonic acid (**a**) condenses with the aldehyde (**b**) to form the imine intermediate (**I**). The Schiff's base is then protonated by the phosphonic acid group followed by addition of the isocyanide (**c**) to create a nitrilium intermediate (**II**) ^[38]. Subsequently, the nucleophilic attack of the phosphonate anion generates an O-phosphorylimine intermediate (**III**), which is then subject to nucleophilic attack by the solvent (**d**; alcohol, fifth reacting center), followed by a Mumm rearrangement to the corresponding 1-amido-1-aminomonophosphonate acid derivative (**e**). The compound characterization of the obtained product was accomplished by the means of X-Ray (*Figure 1 and 2*), NMR and VCD and chromatographic methods (supporting information).

2.2. Synthesis optimization:

As mentioned above Ugi-5C-4CRs are typically carried out at low temperature (-30 °C and then gradually warmed up to ambient temperature^[39a]), requiring extended reaction times in the range of 24-48 h. However, with APAs as educts we did not observe formation of the desired products under such conditions. Thus, reaction conditions were optimized using a single set of educts, namely (1-amino-1-methylethyl)phosphonic acid with benzaldehyde and 2,6-dimethylphenyl isocyanide as well as methanol as solvent (*Table 1*). In the course of the optimization studies, the impact of temperature, mode of heating, solvent and ion-pairing reagents were systematically evaluated by reversed phase liquid chromatography coupled to mass spectrometry (RPLC-MS) for reaction monitoring (for conditions see Supplementary Information).

Increasing the temperature up to 50 °C provided the desired product in 35% yield after two days (*Table 1*). Given this rather low reaction rate we decided to employ microwave (MW) heating ^[52] in order to increase the heat-exchange efficacy, and thus shorten the reaction time. The acceleration of the reaction using MW heating instead of conventional heating proved to be significant. Employing identical conditions reaction time could be reduced from 2 days to 90 min at comparable yields (compare entries 5 and 9 in *Table 1*). Increasing the reaction temperature to 100 °C with slightly prolonged reaction time provided the best results. Maximal yield of 45% was achieved with a temperature of 100 °C under microwave heating for 150 min (maximum power set to 100 W).

In the following experiments we evaluated the influence of the reaction medium. We employed apolar and dipolar aprotic solvents under MW heating at 100 °C. As can be seen from the results summarized in *Table 1*, formation of the target compound was observed only in methanol and thus this was selected as optimum solvent.

Reaction yields could have been impaired by poor solubility of the zwitterionic aminophosphonic acids. Thus, we decided to introduce an ion-pair reagent to enhance solubility of the amino phosphonic acid. We tested both acidic (methanolic HCl, acetic acid, trifluoroacetic acid) and basic (NaOH, Hünig base, tetra-*n*-butylammonium hydroxide) additives. The results, summarized in *Table 2*, indicate that protonation of the amino group in an acidic environment hinders the initial nucleophilic attack of the amino group at the carbonyl group of the aldehyde. This behavior diminishes the benefit of higher solubility of the substrate given by acidic media. Thus, basic media are favorable for the synthesis. The best results were achieved using tetra-*n*-butylammonium hydroxide (TBAH) in a molar ratio of 1:2 with respect to the aminophosphonic acid (*table 2*). This finding suggests that strong organic bases capable of forming free ion-pairs with the phosphonic functional group do not represent an impediment to intramolecular cyclization. The purification of this new type of phosphonate compounds can be easily accomplished employing normal-phase chromatography on silica (entry 6 of *Table 3*). Alternatively, chiral anion exchange chromatography employing CHIRALPAK QD-AX or QN-AX™ chiral stationary phases can be chosen as a general purification process to obtain the target compounds in their enantiomerically pure forms with high chemical and stereochemical purity as well as good recovery.

2.3. Effect of educts on the reaction:

Based on the established optimized reaction conditions (summarized in *Scheme 1*), we explored the synthetic scope using a variety of aldehydes, isocyanides and aminophosphonic acids (*table 3*). We did not observe significant differences in the reactivity of aliphatic and aromatic aldehydes or isonitriles. Surprisingly, the use of APAs of a different spacer length between the amino and the phosphonic group (α -, β - and γ -APAs, *Table 4*) affected just the product formation in terms of yield but not the general reaction mechanism. In contrast, it has been reported that β - or γ -amino carboxylic acids in Ugi reactions led to the formation of lactam structures (U-4C-3CR)^[40]. On the other hand, no cyclic product was generated under the conditions reported here. The lack of cyclization in the final product could be attributed to higher thermodynamic stability of the 1-amido-1-aminophosphonate structure (**II**, *Scheme 2*) with respect to its phosphoramidate lactam equivalent (**IV**). Additionally, using high temperature, pressure and pH the reactivity of methanol in the methanolysis reaction of the cyclic intermediate (**III**) is much higher than under reported conditions^[40]. The reduced

thermal stability of the cyclic intermediate and lower solubility of APAs with longer aliphatic spacers between reaction centers (β - and γ -APAs) could possibly be the reasons of the decrease of yield in comparison to α -APAs.

In the course of this study we also investigated the efficiency of the established MCR reaction scheme upon replacing the APA component by different types of amino acids (carboxylic, sulfonic, and phosphonic acid moiety; *Table 4*). The reaction protocol was successful for amino carboxylic acids, although with lower yields^[39b]. However, the protocol failed to produce detectable amounts of products when aminosulfonic acids were employed.

In order to assess the possibility of generating further molecular diversity via the phosphoester residue (R^5), we also tested allyl alcohol as the reaction solvent. The incorporation of this solvent into the product was indeed confirmed (compound **7**, *Table 4*). Also other educts were tested in this solvent and LC-MS confirmed incorporation of the alcoholic component in the product. However, yields were generally lower with this solvent, indicating that probably a specific optimization of the reaction conditions has to be performed to improve the reaction rate and yield when this or another solvent is used.

2.4. Hydrolysis of Phosphonic Acid Ester:

In order to quantitatively obtain phosphonic acid derivatives of the amido-amino phosphonate compounds without the risk of hydrolysis of the amide bond we tested various conditions^[46, 53], monitoring the product formation with LC-MS. The use of trimethylsilyl bromide in DCM proved to be the most convenient and efficient method. Under these conditions, generally quantitative yields were obtained and the integrity of the stereogenic center(s) within the substrates remained unaffected (entry 1, 12, 13 *table 3*, detailed results in Supporting Information).

3. Conclusions

In summary, we devised a generally applicable multicomponent reaction protocol which enables synthesis of 1-amido-1-aminophosphonate structures in a fast and efficient manner from α -, β -, γ - aminophosphonic acids, aldehydes, isocyanides and methanol. We investigated the influence of structural variation of educts, temperature, reaction time, and solvent on the yield of the product. The established protocol can be used with a large variety of substrates providing corresponding 1-amido-1-aminophosphonates in moderate to high yields. This novel type of Ugi five center four component reaction opens up the possibility to obtain libraries of phosphopeptidomimetic compounds as new lead structures with potential bioactivity.

4. Experimental Section

4.1. General Methods

Microwave-assisted reactions were performed in sealed glass vials using a temperature and pressure controlled microwave (90801 CEM discovery system) operated through Chem Driver Software 3.6.0. Temperature was set to 100 °C under stirring in “discovery mode”, the maximum power to 100 W, and maximum pressure to 20 bar. The ramp time was set to 2 min and the given conditions were maintained for 150 min. Purity grade of reagents and solvents are listed in the material and method section of the supporting information.

^1H , ^{13}C , ^{31}P NMR spectra were acquired at 25 °C on a Bruker DRX 400 MHz spectrometer in CD_3OD if not specified differently. Chemical shifts (δ) are given in parts per million (*ppm*) and the coupling constants (*J*) in Hertz (*Hz*). COSY, HSQC and HMBC experiments were performed in order to clarify the assignment of ^1H and ^{13}C resonances.

Analytical HPLC experiments were performed using an 1100 series LC system from Agilent Technologies (Waldbronn, Germany) equipped with a binary gradient pump, autosampler, thermostat, vacuum degasser, temperature-controlled column compartment and a diode-array detector. The data were processed with the Agilent ChemStation software (Rev. A. 10.01).

Mass spectrometric detection was carried out using an electrospray interface (ESI) on an ion trap MS G244D LC/MSD trap SL (Agilent Technologies). Data processing interpretation was carried out in LC/MSD trap software 4.2. High-resolution mass spectra were recorded by direct injection (2 μL of a 2 μM solution in water/acetonitrile 50:50 v/v and 0.1% formic acid) with a mass spectrometer (Bruker *maXis classic*) equipped with an electrospray ion source in negative mode (flow rate 10 $\mu\text{L}/\text{min}$, source voltage -3.5 kV, sheath gas flow 10 units, capillary temperature 250 °C). The high-resolution mass spectrometer was calibrated prior to measurements with a calibration mixture (Bruker Daltonics). Optical rotation was measured with a Perkin Elmer 341 polarimeter. FT-IR spectra were acquired at 25 °C on a Bruker Tensor 27 IR spectrometer and the data were analyzed adopting Opus 4.2.

All reaction batches were characterized adopting reversed-phase (RP) chromatography using aRP-C18 (3 μm) column (150 x 3 mm ID) from Advanced Chromatography Technologies (ACT) using gradient elution chromatography (mobile phase A: H_2O containing 0.1% (v/v) formic acid, mobile phase B: MeOH containing 0.1% (v/v) formic acid; gradient: 20% B to 100% B in 20 min). The flow rate adopted was 0.4 mL/min at 25 °C, the sample injection volume 2.5 μL , and detection was performed at 214 nm.

The preparative purification and enantioseparation was carried out on a Bischoff Chromatography HPLC system (Bischoff, Leonberg, Germany) equipped with a manual

injector (loop volume=10 ml), a LC-CaDi 22-14 as interface module, a programmable Lambda 1010 UV/VIS detector and two high precision dosing pumps enabling gradient elution. A column (250 x 16 mm ID) packed with 100 Å, 10 µm silica gel modified with *tert*-butylcarbamoylquinidine selector (prototype of Chiralpak QD-AXTM) from Chiral Technologies Europe (Illkirch, France) was employed. The mobile phase composition is specified in the compound characterization. Flow rate was set up to 20 mL/min. The injection volume was up to 5 mL per run and the detection was carried out at 210, 220, 240, and 254 nm.

4.2. General procedure for the synthesis of amido-aminophosphonate derivatives (entry n°1-15):

The aminophosphonic acid (1 eq.; 0.25 M) (commercially available, for suppliers see supporting information, or synthesized according to literature procedure^[54]) and the selected aldehyde (1.5eq) were dissolved in MeOH in a microwave glass vial. Tetra-*n*-butylammoniumhydroxyde (0.25 eq. from 1M methanolic solution) and isocyanide (11 mmol) were sequentially added to this mixture. The microwave reaction vial was sealed, heated and stirred under microwave irradiation at 100 °C for 150 min. In case of the presence of residual unreacted educts, the reaction mixture was removed by filtration (generally constituted by the unreacted aminophosphonic acid). The filtrate was evaporated under reduced pressure and the crude residue was purified by column chromatography or chiral anion exchange chromatography, giving viscous oils or solids as products.

Methyl hydrogen [2-({2-[(2,6-dimethylphenyl)amino]-2-oxo-1-phenylethyl}amino)propane-2-yl]phosphonate (1 Table 3). Prepared from (2-aminopropane-2-yl)phosphonic acid (39 mg, 0.24 mmol). Purification by preparative chromatography on Chiralpak QD-AXTM; $k_1 = 2.82$ (Mobile phase: MeOH/ACN 50/50; v/v containing 25 mM formic acid, apparent pH adjusted in mixture to 4 with NH₄OH). Compound obtained as a sticky solid (yield: 79 mg, 0.21 mmol 82% [a]). An alternative purification procedure consisted of liquid extraction (0.1M HCl / DCM) followed by evaporation under vacuum and crystallization in toluene (yield: 66%[b]). ¹H NMR (400 MHz, CD₃OD, 25°C, TMS): δ = 1.45 (d, 3J_{H,P} = 13.6 Hz, 3 H, CH₃), 1.46 (d, 3J_{H,P} = 13.6 Hz, 3 H, CH₃), 2.06 (bs, 6 H, 2×CH₃), 3.67 (d, 3J_{H,P} = 9.9 Hz, 3 H, OCH₃), 5.24 (bs, 1 H, CH), 7.04 (m, 3 H, Ar-H), 7.40 (m, 3 H, Ar-H), 7.61 (d, 3J_{H,H} = 7.3 Hz) ppm. ¹³C NMR (100 MHz, CD₃OD, 25°C, TMS): δ = 170.2 (C=O), 136.5 (C_q), 132.5 (C_q), 132.3 (C_q), 130.2 (Ar-CH), 129.7 (Ar-CH), 129.2 (Ar-CH), 128.6 (Ar-CH), 61.1 (d, J_{C,P} = 6 Hz, CH), 60.9- 59.4 (J_{C,P} = 143 Hz (CH₃)₂C), 52.3- 52.2 (J_{C,P} = 7 Hz, OCH₃), 23.5 (CH₃), 22.4 (CH₃), 20.4 (Ar-CH₃)

ppm. ^{31}P NMR (162 MHz, CD_3OD , TMS): 18.92 ; FT-IR ν : 3248 3037 2794 1665 1600-1400 1296 cm^{-1} . MS (ESI): m/z 389.2 $[\text{M}-\text{H}]^-$; HRMS (ESI-NM): calcd for $\text{C}_{20}\text{H}_{27}\text{N}_2\text{O}_4\text{P}$: 390.1708 found $[\text{M}-\text{H}]^-$ = 389.1650; $\text{C}_{20}\text{H}_{26}\text{N}_2\text{O}_4\text{P} + \text{Na}$: 412.1533 obsd $[\text{M}-\text{H}]^-$ = 411.1469; Optical rotation: first eluted enantiomer from Chiralpak QD-AX: $[\alpha]_{\text{RT}}$: Na (589nm) 64.2; Hg (578 nm) 67.5; (546 nm) 79.1; (436 nm) 148.1 (c = 1.02 g/100 mL, methanol); second eluted enantiomer: $[\alpha]_{\text{RT}}$: Na (589 nm) -71.5; Hg (578 nm) -73.8; (546 nm) -85.2; (436 nm) -153.7 (c = 1.03 g/100 mL, methanol). The lab book of this compound is UD50 and has been the one I've used most; ULLI for friends.

***N*-{2-[(2,6-dimethylphenyl)amino]-2-oxo-1-[4-(prop-2-en-1-yloxy)phenyl]ethyl}-2-**

[hydroxy(methoxy)phosphoryl]propane-2-aminium formate (2 Table 3). Prepared from (2-aminopropane-2-yl)phosphonic acid (100 mg, 0.64 mmol). Purification by preparative HPLC on Chiralpak QD-AXTM; k_1 = 3.23 (mobile phase: MeOH/ACN 50/50; v/v containing 25 mM formic acid, apparent pH adjusted in mixture to 4 with NH_4OH) Compound isolated as a sticky solid (yield: 138mg, 0.64 mmol 50%). ^1H NMR (400 MHz, CD_3OD , 25°C, TMS): δ 7.6 (d, J = 8.15Hz 2H), 7.1 (m , J = 6Hz, 5H), 6.1 (m, J = 5.4, 1H) 5.7 (s, J , 1H), 5.4 (m, J = 15Hz, 1H), 5.3 (m, J = 9Hz, 1H), 4.6 (dt, J = 5.2, 2H), 3.7 (d, J = 10Hz, 3H), 2.0 (s, J , 6H), 1.5 (m, J = 6Hz, 6H), 1.46-1.37 (m, J = 4.84Hz, 9H), 1.35 (s, J , 3H) ppm. ^{13}C NMR (101 MHz, MeOD, 27°C, TMS) δ 170.2 (C=O), 161.6 (Cq), 137.3 (Cq), 135.0 (Ar-CH), 135.0 (Cq), 131.6 (Ar-CH), 131.6 (Ar-CH), 129.1 (Ar-CH), 128.7 (Cq), 118.1 (CH₂), 116.9 (Ar-CH), 70.2 (CH₂), 62.1 (JC,P=6Hz, CH), 53.0- 52.9 (JC,P=6Hz, OCH₃), 24.0 (CH₃), 22.4 (CH₃), 18.8 (Ar-CH₃) ppm; ^{31}P NMR (162 MHz, CD_3OD , TMS): δ 18.98 ppm; FT-IR ν : 3250, 3200, 3025, 2863, 1667, 1600-1400, 1327 cm^{-1} MS (ESI): m/z 445.1 $[\text{M}-\text{H}]$; HRMS (ESI-NM): calcd for $\text{C}_{23}\text{H}_{31}\text{N}_2\text{O}_5\text{P}$: 446.1971 found $[\text{M}-\text{H}]^-$ = 445.1903 $\text{C}_{23}\text{H}_{30}\text{N}_2\text{O}_5\text{P} + \text{Na}$: 468.1790 found $[\text{M}-\text{H}]^-$ = 467.1724

***N,N,N*-tributylbutan-1-aminium formate - methyl [2-({2-[(2,6-dimethylphenyl)amino]-1-(naphthalen-1-yl)-2-oxoethyl}ammonio)propan-2-yl]phosphonate (3 Table 3).** Prepared from (2-aminopropan-2-yl)phosphonic acid (117 mg, 0.75 mmol). k_1 = 6.68 (mobile phase: MeOH/ACN 50/50; v/v containing 25 mM Formic Acid, apparent pH adjusted in mixture to 4 with NH_4OH) . Purification by preparative HPLC on Chiralpak QD-AXTM. Compound obtained as a sticky solid (yield: 216 mg, 0.49 mmol 66%). ^1H NMR (400 MHz, CD_3OD , 25°C, TMS): δ 7.9 (m, J = 10 Hz 3H), 7.6 (m, J = 7.8Hz 1H), 7.5 (m, J = 7.8Hz 2H), 7.0 (m, J = 3.6 Hz 4H), 5.9 (s, J , 1H), 3.62 (d, J = 9.6Hz, 3H), 2.05 (s, J , 1H), 1.42 (m, J , 6H), 1.5 (m, J = 7.8Hz, 6H) ppm. ^{13}C NMR (101 MHz, MeOD, 27°C, TMS) δ 173.6 (C=O), 137.0 (Cq), 135.8 (Cq) , 132.2 (Cq), 130.3 (Ar-CH), 130.0 (Ar-CH), 129.1 (Ar-CH), 128.4 (Ar-CH), 127.7 (Ar-CH), 127.1 (Ar-CH), 126.5 (Ar-CH), 125.5 (Ar-CH), 58.4- 56.9 (JC,P=152.1 Hz, (CH₃)C), 52.2 (2x CH), 23.5 (J_{C,P}=4 Hz, CH₃), 18.7 (Ar-CH₃) ppm; ^{31}P NMR (162 MHz, CD_3OD , TMS): δ 24.21 ppm; FT-IR

v: 3180, 2970, 2794, 1705, 1600-1400, 1342 cm^{-1} . MS (ESI): m/z 439.2 $[\text{M-H}]^-$; HRMS (ESI-NM): calcd for $\text{C}_{24}\text{H}_{29}\text{N}_2\text{O}_4\text{P}$: 440.1865 found $[\text{M-H}]^-$ = 439.1810; Optical rotation: first eluted enantiomer from Chiralpak QD-AX: $[\alpha]$ RT F1: Na (589nm) 16.6; Hg (578nm) 18.7; (546nm) 21.5, (436nm), 44.7 (c = 1.48 g/100mL, d : 1 dm methanol); second eluted enantiomer: Na (589nm) -17.8; Hg (578nm)-17.8; (546nm) -21.2; (436nm) -36.6 (c = 0.96 g/100mL, d : 1 dm imethanol).

N,N-dibutyl-N-propylbutan-1-aminium formate - methyl (2-([2-(tert-butylamino)-2-oxo-1-phenylethyl]ammonio)propan-2-yl)phosphonate (4 Table 3): Prepared from (2-aminopropan-2-yl)phosphonic acid (125 mg, 0.8 mmol). k_1 = 2.67 (MeOH/ACN 50/50; v/v containing 25 mM Formic Acid, apparent pH adjusted in mixture to 4 with NH_4OH) Chiralpak QD-AXTM. Compound obtained as a sticky solid (yield: 214 mg, 0.44 mmol 80%). ^1H NMR (400 MHz, CD_3OD , 25°C, TMS): δ 7.5 (m, J = 7.45 Hz 2H), 7.4 (m, J = 15.44 Hz, 3H), 5.15 (s, J , 1H) 3.7 (d, 9.83 Hz, 3H), 1.46-1.37 (m, J = 4.84 Hz, 9H), 1.35 (s, J , 3H) ppm; ^{13}C NMR (101 MHz, MeOD, 27°C) δ 175.6 (C=O), 138.0 (Ar-C), 130.1 (Ar-CH), 129.4 (Ar-CH), 62.1 (CH), 58.0 (Cq), 52.4- 52.3 ($J_{\text{C,P}}$ = 7 Hz, CH), 52.3 (Cq), 28.6 (CH_3), 23.4 (CH_3), 21.8 (Ar-CH₃) ppm; ^{31}P NMR (162 MHz, CD_3OD , TMS): δ 21.11 ppm; FT-IR v: 3457, 3002, 2876, 1738, 1600-1400, 1367 cm^{-1} ; MS calcd for $\text{C}_{16}\text{H}_{27}\text{N}_2\text{O}_4\text{P}$ 342.17 found 341.1 $[\text{M-H}]^-$; MS (ESI): m/z 341.2 $[\text{M-H}]^-$; HRMS (ESI-NM): calcd for $\text{C}_{16}\text{H}_{27}\text{N}_2\text{O}_4\text{P}$: 342.1708 found $[\text{M-H}]^-$ = 341.1641

N,N,N-tributylbutan-1-aminium formate - methyl [2-([1-(anthracen-9-yl)-2-[(2,6-dimethylphenyl)amino]-2-oxoethyl]ammonio)propan-2-yl]phosphonate (5 Table 3). Prepared from (2-aminopropan-2-yl)phosphonic acid (104 mg, 0.66 mmol). R_f (k_1) = 6.37 (MeOH/ACN 50/50; v/v containing 25 mM Formic Acid, apparent pH adjusted in mixture to 4 with NH_4OH) Chiralpak QD-AXTM. Compound obtained as a sticky solid (yield: 213 mg, 0.44 mmol 66%). ^1H NMR (400 MHz, CD_3OD , 25°C, TMS): δ 8.80 (d, J = 8.61 Hz 1H), 8.64 (s, 1H), 8.48 (d, J = 8.43 Hz 1H), 8.15 (t, J = 9.50 Hz 2H), 7.73 (t, J = 8.41 Hz 1H), 7.58 (m, 2H), 7.05 (m, 3H), 6.47 (s, 1H), 3.62 (d, 10.33 Hz, 3H), 1.46-1.37 (m, J = 4.84 Hz, 9H), 2.14 (s, 3H), 1.33 (m, 6) ppm; ^{13}C NMR (101 MHz, MeOD, 27°C, TMS) δ 170.9 (C=O), 137.1 (Cq), 136.1 (Cq), 132.3 (Cq), 131.1 (Cq), 129.5 (Ar-CH), 129.3 (Cq), 128.1 (Ar-CH), 127.4 (Ar-CH), 126.9 (Ar-CH), 125.1 (Ar-CH), 59.9- 59.8 ($J_{\text{C,P}}$ = 101 Hz, (CH_3)C), 57.7 (CH), 52.7 (CH_3), 23.8 (CH_3), 23.2 (CH_3), 18.8 (Ar-CH₃) ppm; ^{31}P NMR (162 MHz, CD_3OD , TMS): δ 23.12 ppm; FT-IR v: 3255, 2969, 2873, 1739, 1600-1400 1366 cm^{-1} ; MS (ESI): m/z 489.1 $[\text{M-H}]^-$; HRMS (ESI-NM): calcd for $\text{C}_{28}\text{H}_{31}\text{N}_2\text{O}_4\text{P}$: 490.2021 found $[\text{M-H}]^-$ = 489.1941 $\text{C}_{28}\text{H}_{30}\text{N}_2\text{O}_4\text{P} + \text{Na}$: 512.1846 found $[\text{M-H}]^-$ = 511.1759; $[\alpha]_{\text{D}20}$ F1: Na (589nm) 59.3; Hg (578nm) 64.6; (546nm) 77.8, (436nm) 201.3 (c = 0.57 g/100mL, d : 1 dm in methanol); $[\alpha]_{\text{D}20}$ F2: Na (589nm) -26.3; Hg (578nm) -87.3; (546nm) -102.6; (436nm) -232.9 (c = 0.39 g/100mL, d : 1 dm in methanol).

N,N,N-tributylbutan-1-aminium methyl [1-({1-(anthracen-9-yl)-2-[(2,6-dimethylphenyl)amino]-2-oxoethyl}amino)cyclopentyl]phosphonate (6 Table 3).

Prepared from (1-aminocyclopentyl)phosphonic acid (200 mg, 1.27 mmol). R_f = 0.38 (MeOH/DCM (1/2; v/v) silica flash chromatography. Compound obtained as a red powder (yield: 465 mg, 0.90 mmol 71%). ^1H NMR (400 MHz, CD_3OD , 25°C , TMS): δ 8.6(d, $J=9.2$ Hz 2H), 8.5 (t, $J=5.5$ Hz, 2H), 8.1(t, $J=8.8$ Hz, 2H), 7.6 (m, J , 1H), 7.5 (m, 3H), 7.0(m, 3 H), 6.5 (s, 1H), 3.7(d, 9.6 Hz, 3H) 2.3 (s, J , 3H), 1.6 (m, 1H), 1.4 (m 1H) ppm; ^{13}C NMR (101 MHz, MeOD, 27°C , TMS) δ 176.4 (C=O), 137.2 (Cq), 135.9 (Cq), 133.5 (Cq), 133.2 (Cq), 130.9 (Ar-CH) , 130.5 (Cq), 130.3 (Ar-CH), 129.0 (Ar-CH), 128.2 (Ar-CH), 126.5 (Ar-H), 67.6- 66.1($J_{\text{C,P}}=160$ Hz, $\text{C}(\text{CH}_2)_2$), 57.9 ($J_{\text{C,P}}=7$ Hz, OCH_3), 51.75 (CH), 37.2- 33.9 ($J_{\text{C,P}}=330$ Hz, CH_2) , 24.74 (CH_2), 20.66 (CH_3) ppm; ^{31}P NMR (162 MHz, CD_3OD , TMS): δ 27.88 ppm; FT-IR v: 3457, 3016, 2801, 1739, 1600-1400, 1367 cm^{-1} ; MS (ESI): m/z 515.2 $[\text{M-H}]^-$; HRMS (ESI-NM): calcd for $\text{C}_{30}\text{H}_{33}\text{N}_2\text{O}_4\text{P}$: 516.2178 found $[\text{M-H}]^-$ = 515.2085

N,N,N-tributylbutan-1-aminium methyl [1-({1-(anthracen-9-yl)-2-[(2,6-dimethylphenyl)amino]-2-oxoethyl}amino)cyclopentyl]phosphonate (7 Table 3).

Prepared from [amino(phenyl)methyl]phosphonic acid (90 mg, 0.48 mmol), added of 0.4mL of methanolic tetrabutylammoniumhydroxide solution (1M, 0.4mmol) and sonicated for 5min. The obtained yellowish solution was dried under vacuum, dissolved in 5mL of allyl alcohol and transferred into a 5mL microwave flask To the solution were added: [amino(phenyl)methyl]phosphonic acid (90 mg, 0.48 mmol), 9-Anthracenecarboxaldehyde aldehyde (0.2 g, 0.96mmol) and 2,6-Dimethylphenyl isocyanide (0.2 mg, 1.1mmol). The vial was sealed and the reaction was stirred under microwave irradiation at 100°C for 150min. After this time a brown solution with a precipitate was observed. The supernatant was transferred in a round bottomed flask and purified through chiral anion exchange chromatography. R_f (k_1)= 7.5 (MeOH 100 mM Formic Acid, 50mM ammonium formate) Chiralpak QD-AXTM; Compound obtained as a sticky solid (yield: 180mg, 0.32 mmol 32%). ^1H NMR (600 MHz, MeOD, TMS) δ 8.61 (s, Ar-H), 8.50 (d, $^3J(\text{H,H})=8.73$ Hz, Ar-H), 8.30 (m, Ar-H), 8.21- 8.02 (dd, $^3J(\text{H,H})_1=8$ Hz, $^3J(\text{H,H})_2=46$ Hz, 2H, Ar-H), 7.88 (m, Ar-H), 7.74 (d, $^3J(\text{H,H})=9$ Hz, Ar-H), 7.36- 7.62 (m, 8H, Ar-H), 6.99- 7.16 (m, 4H, Ar-H), 5.81 (s, CH), 5.31 (m, CH), 4.58 - 4.83 (m, CH_2), 3.95 (m, 1H), 3.75 (d, $^3J(\text{H,H})=17$ Hz, CH), 3.7 - 3.6 (m, CH), 2.27 (s, 6H, Ar- CH_3) ppm. ^{13}C NMR (151 MHz, MeOD, TMS) δ 174.3 (C=O), 137.6 (CH-allyl), 137.2 (Cq), 135.6 (Cq), 135.3 (Cq), 133.7 (Cq), 133.5 (Cq), 132.9 (Cq), 131.2 (Ar-CH), 131.0 (Ar-CH) , 130.7 (Ar-CH), 130.4 (Ar-CH), 130.1 (Ar-CH), 129.5 (Ar-CH), 129.2 (Ar-CH), 129.0 (Ar-CH), 128.4 (Ar-CH), 127.9 (Ar-CH), 126.2 (Ar-CH), 125.5 (Ar-CH), 124.4 (Ar-CH), 116.4 (CH-allyl), 66.8, 66.7 ($J_{\text{C,P}}=6$ Hz, CH), 61.9, 60.97 ($J_{\text{C,P}}=158$ Hz, CH-(Ph)), 58.7, 58.6 ($J_{\text{C,P}}=14.5$ Hz,

O-CH) , 19.0 (Ar-CH₃) ppm; ³¹P NMR (162 MHz, CD₃OD, TMS): δ 16.47 ppm. FT-IR ν: 3457, 3016, 2801, 1739, 1600-1400, 1367 cm⁻¹; MS (ESI): *m/z* 563.2 [M-H]⁻; HRMS (ESI-NM): calcd for C₃₀H₃₃N₂O₄P: 564.2178 found [M-H]⁻ = 564.2089

N,N,N-tributylbutan-1-aminium methyl [1-({2-[(2,6-dimethylphenyl)amino]-2-oxo-1-phenylethyl}amino)cyclopentyl]phosphonate (8 Table 3).

Prepared from (1-aminocyclopentyl)phosphonic acid (102 mg, 0.65 mmol). Liquid extraction (0.1M HCl / DCM) followed by evaporation under vacuum and crystallization in Toluene. Compound obtained as a sticky solid (yield: 216 mg, 0.49 mmol 66%). ¹H NMR (400 MHz, CD₃OD, 25°C, TMS): δ 7.7(m, J= 3.8Hz 2H), 7.5 (m , J=2.8Hz, 3H), 7.0 (m , J=7.1Hz, 3H), 6.1 (s, J, 1H), 3.7(d, 9.9 Hz, 3H) 2.0 (s, J, 3H), 1.7 (m, 1H), 1.4 (m, 1H) ppm ¹³C NMR (101 MHz, CDCl₃, 27°C, TMS) δ 168.4 (C=O) , 136.9 (Cq), 135.0 (Cq), 134.4 (Cq), 131.2 (Ar-H), 130.4 (Ar-H), 130.2 (Ar-H), 129.2 (Ar-H), 128.8 (Ar-H) , 71.6- 70.1 (J_{C,P}=151.5 Hz, C(CH₂)₂ , 63.0 (OCH₃), 52.3- 52.2 (J_{C,P}=7 Hz, CH), 35.6- 33.1 (CH₂), 24.8 (CH₂) , 18.2 (Ar-CH₃) ppm; ³¹P NMR (162 MHz, CD₃OD, TMS): δ 24.98 ppm; MS (ESI): *m/z* 415.1 [M-H]⁻; FT-IR 3248, 3037, 2794, 1665, 1600-1400, 1296 cm⁻¹ ; HRMS (ESI-NM): calcd for C₂₂H₂₉N₂O₄P: 416.1865 found [M-H]⁻ = 415.1798 C₂₂H₂₈N₂O₄P + Na: 438.1690 found [M-H]⁻ = 437.1619

N,N,N-tributylbutan-1-aminium methyl [1-({2-[(2,6-dimethylphenyl)amino]-2-oxo-1-phenylethyl}amino)ethyl]phosphonate (Entry n°9 Table n° 3).

Prepared from DL-(1-aminoethyl)phosphonic acid (117 mg, 0.94 mmol). R_f (k₁) = 6.52 (MeOH/ACN 50/50; v/v containing 25 mM Formic Acid, apparent pH adjusted in mixture to 4 with NH₄OH) Chiralpak QD-AX™;.Compound obtained as a sticky solid (yield: 123 mg, 0.33 mmol 34%). ¹H NMR (400 MHz, CD₃OD, 25°C, TMS): δ 7.65 (m, 2H), 7.42 (m, 3H), 6.98(m, 3H), 5.63 (s, 1H), 3.55 (d, J=10.70Hz, 3H), 3.15 (m, 1H), 1.90 (s, broad signal, 1H), 1.44 (q , J=7.41Hz, 3H) ppm; ¹³C NMR (101 MHz, MeOD, 27°C) δ 167.9 (C=O), 137.3 (Cq), 134.7 (Cq), 133.6 (Cq), 132.0 (Ar-H), 131.0 (Ar-H), 130.6 (Ar-H), 129.6 (Ar-H), 129.2 (Ar-H), 63.6 (J_{C,P}=4 Hz, CH), 52.9 (J_{C,P}=6 Hz, CH), 51.8- 50.4 (J_{C,P}= 143 Hz, OCH₃), 18.5, 14.3 (Ar-CH₃) ppm; ³¹P NMR (162 MHz, CD₃OD, TMS): δ 15.5 ppm, FT-IR ν: 3456, 2969, 2794, 1665, 1600-1400, 1296 cm⁻¹; MS (ESI): *m/z* 375.2 [M-H]⁻; HRMS (ESI-NM): calcd for C₁₉H₂₅N₂O₄P Exact Mass: 376.1552: 376.1552 found [M-H]⁻ = 375.1497; C₁₈H₂₃N₂O₄P + Na[M+H]⁺:396.2159 found [M-H]⁻ = 397.2245

N,N,N-tributylbutan-1-aminium methyl [1-({2-[(2,6-dimethylphenyl)amino]-2-oxo-1-phenylethyl}amino)-2-methylpropyl]phosphonate (10 Table 3).

Prepared from DL-(1-amino-2-methylpropyl)phosphonic acid (115 mg, 0.75 mmol). R_f (k₁) = 6.03 (MeOH/ACN 50/50; v/v containing 25 mM Formic Acid, apparent pH adjusted in mixture to 4 with NH₄OH) Chiralpak QD-AX™.Compound obtained as a sticky solid (yield: 197 mg,

0.49 mmol 65%). ¹H NMR (400 MHz, CD₃OD, 25°C, TMS): δ 7.76 (m, 2H), 7.53 (m, 3H), 7.06 (m, 3H), 5.80 (s, 1H), 3.67 (d, J=10.78, 3H), 3.06 (dd, J₁=13.34, J₂=3.72, 1H), 2.46 (m, 1), 2.05 (s, broad signal 6H), 1.22 (s, 6H), ppm; ¹³C NMR (101 MHz, MeOD, 27°C, TMS) δ 166.4 (C=O), 136.1 (Cq), 135.7 (Cq), 132.8 (Cq), 130.4 (Ar-CH), 130.1 (Ar-CH), 129.5 (Ar-CH), 128.2 (Ar-CH), 125.4 (Ar-CH), 64.9 (CH), 63.2- 61.8 (C(CH(CH₃)₂), 51.2- 50.6 (JC, P= 70 Hz, OCH₃), 29.6 (CH(CH₃), 22.9 (CH₃), 21.1 (CH₃), 17.8 (Ar-CH₃), 17.3 (Ar-CH₃) ppm; ³¹P NMR (162 MHz, CD₃OD, TMS): δ 14.35 ppm; FT-IRv: 3456, 2969, 2874, 1740, 1600-1400, 1367 cm⁻¹; MS calcd for C₂₁H₂₉N₂O₄P: 404.44 found (NM) 403.2; HRMS (ESI-NM): calcd for C₂₁H₂₉N₂O₄P: 404.1865 found [M-H]⁻ = 403.1803; C₂₁H₂₉N₂O₄P + Na [M-H]⁻: 426.1690 found [M-H]⁻ = 425.1623

N,N,N-tributylbutan-1-aminium formate - methyl ({[1-(tert-butylamino)-3,3-dimethyl-1-oxohex-5-en-2-yl]ammonio}methyl)phosphonate (11 Table 3) Prepared from (aminomethyl)phosphonic acid (500 mg, 4.50 mmol). The solution was afterwards transferred into a round flask while white precipitate (constituted by the unreacted APA) was allowed to react in the same conditions reported before with another aliquot of aldehyde and isonitrile in TBAH solution for another 150min. The two solutions were combined, evaporated under vacuum and the crude product was purified by chiral chromatography R_f (k₁) = 2.95 (MeOH/ACN 50/50; v/v containing 25 mM Formic Acid, apparent pH adjusted in mixture to 4 with NH₄OH) Chiralpak QD-AXTM; Compound obtained as a sticky solid (yield: 1330 mg, 4.16 mmol 93%). ¹H NMR (400 MHz, CD₃OD, 25°C, TMS): δ 5.90 (m, 1H), 5.15 (m, 2H), 3.80 (s, 1H), 3.63 (d, J= 10.33Hz, 3H), 3.07 (m, 1H), 2.80 (m, 1H), 2.21 (m, 1H), 2.03 (d, J= 16.14Hz, 1H), 1.38 (s, 9H), 1.06 (d, J=7.10 Hz, 6H) ppm; ¹³C NMR (101 MHz, MeOD, 27°C, TMS) δ 167.2 (C=O), 134.5 (CH-Allyl), 119.6 (CH₂-Allyl), 70.3 (JC, P= 4 Hz, CH), 53.0 (C (CH₃)₃), 52.3 (JC, P= 7 Hz, OCH₃), 44.2 (CH₂), 37.4 (CH₂), 28.7 (C(CH₃)₃), 24.8 (Cq), 24.1- 23.3 (JC, P= 70 Hz, CH₂) ppm; ³¹P NMR (162 MHz, CD₃OD, TMS): δ 11.87 ppm; FT-IR v: 3456, 2969, 2794, 1665, 1600-1400, 1296 cm⁻¹; MS (ESI): m/z 375.2 [M-H]⁻; HRMS (ESI-NM): calcd for C₁₉H₂₅N₂O₄P Exact Mass: 376.1552: 376.1552 found [M-H]⁻ = 375.1497; C₁₈H₂₃N₂O₄P + Na[M+H]⁺: 396.2159 found [M-H]⁻ = 397.2245

N,N,N-tributylbutan-1-aminium formate - methyl ({[1-(tert-butylamino)-1-oxododec-11-en-2-yl]ammonio}methyl)phosphonate (12 Table 3). Prepared from (aminomethyl)phosphonic acid (639 mg, 5.77 mmol). R_f (k₁) = 3.78 (MeOH/ACN 50/50; v/v containing 25 mM Formic Acid, apparent pH adjusted in mixture to 4 with NH₄OH) Chiralpak QD-AXTM; Compound obtained as a sticky solid (yield: 1.47 g, 3.9 mmol 68%). ¹H NMR (400 MHz, CD₃OD, 25°C, TMS): δ 5.81 (m, 1H), 4.97 (m, 2H), 3.61 (d, J= 11.11Hz, 2H), 3.36 (s, 1H), 2.98 (m, 2H), 2.06 (m, 2H), 1.37 (m, 23H) ppm ¹³C NMR (101 MHz, MeOD, 27°C, TMS) δ 168.1 (C=O),

140.1 (CH-Allyl), 114.7 (CH₂-Allyl), 62.8 (CH), 52.8 (Cq), 52.3 (OCH₃), 42.5-41.1 (J_{C,P}= 140 Hz, CH₂), 34.8 (CH₂), 31.6 (CH₂), 30.3 (CH₂), 30.1 (CH₂), 28.8 (CH₃), 25.7 (CH₂) ppm; ³¹P NMR (162 MHz, CD₃OD, TMS): δ 11.19 ppm; FT-IR ν: 3470, 3002, 2769, 1661, 1600-1400, 1280 cm⁻¹; MS (ESI): *m/z* 362.2 [M-H]⁻; HRMS (ESI-NM): calcd for C₁₇H₃₅N₂O₄P Exact Mass: 362.2334, found [M-H]⁻ = 361.2338;

Methyl [2-({2-[(2,6-dimethylphenyl)amino]-2-oxo-1-[4-(prop-2-en-1-yloxy)phenyl]ethyl}amino)-3,3-dimethylbutyl]phosphonate (13 Table n° 3)

Prepared from DL-(2-amino-3,3-dimethylbutyl)phosphonic acid (125 mg, 0.69 mmol). R_f (k1) = 1.4 (MeOH/ACN 50/50; v/v containing 25 mM Formic Acid, apparent pH adjusted in mixture to 4 with NH₄OH) Chiralpak QD-AX™; apparent pH adjusted to 4 with NH₄OH. Compound obtained as a sticky solid (yield: 175 mg, 0.37 mmol 43%); ¹H NMR (400 MHz, CD₃OD, 25°C, TMS): δ 7.73 (d, J= 8.83, 2H), 7.06 (m, 5H), 6.07 (m, 1H), 5.74 (s, 1H), 5.41 (dd, J=1.66, 1H), 5.27 (dd, J=1.52, 1H), 4.62 (d, J=5.01, 2H), 3.65 (d, J= 10.63Hz, 3H), 3.23 (m, 1H), 2.06 (s, 6H), 1.93 (s, 1H), 0.89 (s, 9H) ppm; ¹³C NMR (101 MHz, MeOD, 27°C, TMS) δ 161.7 (C=O), 152.1 (Cq), 137.1 (Cq), 134.7 (Cq), 134.5 (CH-Allyl), 132.4 (Ar-CH), 131.4 (Ar-CH), 129.1 (Ar-CH), 128.6 (Ar-CH), 117.8 (CH₂-Allyl), 116.5 (Ar-CH), 69.9 (CH₂), 64.4 (CH), 63.4 (J_{C,P}= 5Hz, CH), 51.8 (J_{C,P}= 6Hz, OCH₃), 35.6- 35.5 (J_{C,P}= 11Hz, CH), 26.6 (CH₃), 18.4 (Ar-CH₃) ppm; ³¹P NMR (162 MHz, CD₃OD, TMS): δ 23.49 ppm; FT-IR ν: 3457, 3016, 2795, 1739, 1600-1400, 1367 cm⁻¹; MS (ESI): *m/z* 487.1 [M-H]⁻; HRMS (ESI-NM): calcd for C₂₆H₃₇N₂O₅P: 488.2440 found [M-H]⁻ = 487.2371

N,N,N-tributylbutan-1-aminium formate - methyl ({[1-(cyclohexylamino)-3,3-dimethyl-1-oxohex-5-en-2-yl]ammonio}methyl)phosphonate (3 Table 4). Prepared from (aminomethyl)phosphonic acid (111 mg, 1.0 mmol). R_f (k1) = 2.82 (MeOH/ACN 50/50; v/v containing 25 mM Formic Acid, apparent pH adjusted in mixture to 4 with NH₄OH) Chiralpak QD-AX™;. Compound obtained as a sticky solid (yield: 317 mg, 0.92 mmol 91.53%). ¹H NMR (400 MHz, CD₃OD, 25°C, TMS): δ 5.87 (m, 1H), 5.17 (dd, J₁=10.88 Hz, J₂=2.17Hz, 2H), 3.73 (m, 1H), 3.57 (d, J=10.33Hz, 3H), 3.04 (m, 1H), 2.91 (m, 1H), 2.25 (d, J=7.06, 2H), 1.96 (m, 3H), 1.71 (m, 4H), 1.32 (m, 4H), 1.09 (d, 6H), ppm; ¹³C NMR (101 MHz, MeOD, 27°C, TMS) δ 167.3 (C=O), 134.5 (CH-Allyl), 119.6 (CH₂-Allyl), 69.7 (CH), 50.3 (CH), 44.3 (CH₂), 37.4 (CH₂), 33.6 (J_{C,P}= 5Hz, CH₂), 26.5 (CH), 26.0 (CH₂), 24.2 (CH), 23.5 (CH₃) ppm; ³¹P NMR (162 MHz, CD₃OD, TMS): δ 12.1 ppm; FT-IR ν: 3526, 2888, 1785, 1377 cm⁻¹; MS calcd for C₂₁H₂₉N₂O₄P: 404.44 found (NM) 403.2; MS (ESI): *m/z* 345.2 [M-H]⁻; HRMS (ESI-NM): calcd for C₁₆H₃₁N₂O₄P: 346.2021 found [M-H]⁻ = 345.1956; C₁₆H₃₀N₂O₄P + Na [M-H]⁻: 368.1919 found [M-H]⁻ = 367.1780

N,N,N-tributylbutan-1-aminium methyl (2-[[1-(cyclohexylamino)-3,3-dimethyl-1-oxohex-5-en-2-yl]amino]ethyl)phosphonate (4 Table 4). Prepared from (aminoethyl)phosphonic acid (100 mg, 0.80 mmol). R_f (k1) = 1.35 (MeOH/ACN 50/50; v/v containing 15 mM Formic Acid, apparent pH adjusted in mixture to 4 with NH_4OH) Chiralpak QD-AXTM. Compound obtained as a sticky solid (yield: 122 mg, 0.34 mmol 42%). ^1H NMR (400 MHz, CD_3OD , 25°C, TMS): δ 5.87 (m, 1H), 5.19 (m, 2H), 3.74 (d, 3H $J=11.60$), 3.66 (s, 1H), 3.31 (m, 2H), 3.19 (m, 1H), 2.28 (m, 3H), 1.88 (m, broad peak, 2H), 1.77 (m, broad peak, 2H), 1.65 (m, broad peak, 2H), 1.32 (m, 5H), 1.10 (d, $J=9.6$, 6H) ppm; ^{13}C NMR (101 MHz, MeOD, 27°C) δ 166.7 (C=O), 134.4 (CH-Allyl), 119.9 (CH_2 -Allyl), 69.2 (CH), 51.7 ($J_{\text{C,P}}=7\text{Hz}$, OCH_3), 50.3 (CH), 44.2 (CH_2), 37.4 (CH_2), 33.6 ($J_{\text{C,P}}=5\text{Hz}$, CH_2), 26.5 (CH), 26.0 (CH_2), 24.2 (CH), 23.7 (CH_3), 23.6 (CH_3) ppm; ^{31}P NMR (162 MHz, CD_3OD , TMS): δ 26.93 ppm; FT-IR ν : 3526, 2888, 1785, 1377 cm^{-1} ; MS (ESI): m/z 359.2 $[\text{M-H}]^-$; HRMS (ESI-NM): calcd for $\text{C}_{17}\text{H}_{33}\text{N}_2\text{O}_4\text{P}$: 360.2178 found $[\text{M-H}]^-$ = 359.2180; $\text{C}_{17}\text{H}_{32}\text{N}_2\text{O}_4\text{P} + \text{Na}$: 382.2003 found $[\text{M-H}]^-$ = 381.1999

N,N,N-tributylbutan-1-aminium formate - methyl (3-[[1-(cyclohexylamino)-3,3-dimethyl-1-oxohex-5-en-2-yl]ammonio]propyl)phosphonate (5 Table 4). Prepared from (aminopropyl)phosphonic acid (100 mg, 0.72 mmol). R_f (k1)= 1.28 (MeOH/ACN 50/50; v/v containing 15 mM Formic Acid, apparent pH adjusted in mixture to 4 with NH_4OH) Chiralpak QD-AXTM. Compound obtained as a sticky solid (yield: 55 mg, 0.15 mmol 20%). ^1H NMR (400 MHz, CD_3OD , 25°C, TMS): δ 5.90 (m, 1H), 5.14 (m, 2H), 3.83 (s, 1H), 3.75 (m, 1H), 3.61 (m, 2H), 3.07 (m, 1H), 2.81 (m, 1H), 2.22 (m, 2H), 1.89 (m, 2H), 1.77 (m, 2H), 1.65 (m, 3H), 1.06 (d, $J=10.77$, 7H), 1.32 (m, 8H) ppm; ^{13}C NMR (101 MHz, MeOD, 27°C) δ 166.16 (C=O), 134.1 (CH-Allyl), 120.1 (CH_2 -Allyl), 69.2 (CH), 52.9- 52.8 ($J_{\text{C,P}}=10\text{Hz}$, OCH_3), 50.5 (CH), 44.2 (CH_2), 43.8 (CH_2), 37.4 (CH_2), 33.6 ($J_{\text{C,P}}=5\text{Hz}$, CH_2), 26.5 (CH), 26.0 (CH_2), 24.1 (CH), 23.9 (CH_3), 23.6 (CH_3) ppm; ^{31}P NMR (162 MHz, CD_3OD , TMS): δ 26.47 ppm; FT-IR 3526, 2888, 1785, 1377 cm^{-1} ; ^1MS (ESI): m/z 373.2 $[\text{M-H}]^-$; FTIR: 3526, 2888, 1785, 1377 cm^{-1} . HRMS (ESI-NM): calcd for $\text{C}_{18}\text{H}_{35}\text{N}_2\text{O}_4\text{P}$: 374.2334 found $[\text{M-H}]^-$ = 373.2270

4.3. Procedure for the hydrolysis of the amido-aminophosphonic acid methyl ester derivatives (1 Table 3):

A solution of purified monomethyl ester (24mg, 0.061mmol) in dry dichloromethane (CH_2Cl_2 , 2.25mL) was sonicated for about 1 minute. Bromotrimethylsilane (BrSiMe_3 , 0.183mmol, 3eq) was added dropwise and the reaction was allowed to react for 15h at 25 °C. After removal of the solvent under reduced pressure methanol (5mL) was added. The solution was heated at 50 °C for 2h and afterwards concentrated under high vacuum to obtain the hydrobromide salt of the respective aminophosphonic acid derivative as yellow solid in quantitative yield.

N,N,N-tributylbutan-1-aminium formate - {[1-(cyclohexylamino)-3,3-dimethyl-1-oxohex-5-en-2-yl]ammonio}acetate (2 Table 4). Prepared from entry n°2 table n°4 (50 mg), following the general procedure Ugi 5C-4CR reported above. The dried crude product was hydrolyzed following the procedure reported above using a larger excess of the reactant Bromotrimethylsilane (6eq.). The dried reaction mixture was purified through chiral anion exchange chromatography. Rf= 1.8 (MeOH/ACN 50/50; v/v containing 25 mM Formic Acid, apparent pH adjusted in mixture to 4 with NH₄OH) Chiralpak QD-AX™. ¹H NMR (400 MHz, CD₃OD, 25°C,TMS): δ 5.88 (m, 1H), 5.15 (m, 2H), 3.70 (m, 2H), 3.55 (d, J=14.65, 1H), 3.19 (d, J=14.64, 1H), 2.24 (m, 2H), 1.87 (m, 2H), 1.76 (m, 2H), 1.65 (m, 1H), 1.30 (m, 6H), 1.09 (d, J=17.09, 6H) ppm; ¹³C NMR (101 MHz, MeOD, 27°C) δ 167.2 (C=O), 134.4 (CH-Allyl), 119.6 (CH₂-Allyl), 70.0 (J_{C,P}= 3Hz, CH), 59.5 (J_{C,P}= 5Hz, OCH₃), 50.4 (CH), 44.2 (CH₂), 43.5 (CH₂), 42.1 (CH₂), 37.4 (CH₂), 33.6 (J_{C,P}= 8Hz, CH₂), 26.5 (CH), 26.0 (CH₂), 24.1 (CH₃), 23.4 (CH₃) ppm; FT-IR ν: 3456, 2969, 2874, 1740, 1367 cm⁻¹. MS (ESI): m/z 295.0 [M-H]⁻; HRMS (ESI-NM): calcd for C₁₆H₂₈N₂O₃: 296.2100 found [M-H]⁻ = 295.2311

[2-({2-[(2,6-dimethylphenyl)amino]-2-oxo-1-phenylethyl}amino)propan-2-yl]phosphonic acid (1 Table 5). Prepared from entry n°1 table n°3 (24mg). The raw product was desalted dissolving it in water (1mL) and capturing it on a reversed-phase C-18 SPE (500mg cartridge) column. The SPE column was first rinsed with MeOH (3 column volumes) and then conditioned with water (3 volumes). Afterwards, the sample was applied. After washing with 2 column volumes of water, the product was eluted using MeOH. The collected fraction was dried under vacuum leading to a white solid (yield: 22mg, 0.059mmol, 94%). ¹H NMR (400 MHz, CD₃OD, 25°C,TMS): δ 7.73 (m, 2H), 7.50 (t, J=3.9Hz, 2H), 7.04 (m, 3H), 6.04 (s, J, 1H), 2.12-1.95 (s, broad, 6H), 1.58 (t, J=13.36Hz, 6H). ¹³C NMR (100 MHz, CD₃OD, 25°C,TMS): δ = 168.2 (C=O), 137.0 (Cq), 134.9 (Cq), 134.3 (Cq), 131.2 (Ar-CH), 130.2 (Ar-CH), 129.7 (Ar-CH), 129.6 (Ar-CH), 128.8 (Ar-CH), 62.3 (d, J_{C,P} = 6 Hz, CH), 59.2, 57.7 (J_{C,P} = 152 Hz (CH₃)₂C), 23.7 (CH₃), 21.7 (CH₃), 19.0 (Ar-CH₃) ppm; ³¹P NMR (162 MHz, CD₃OD, TMS): δ 15.03 ppm; FT-IR ν: 3248, 3037, 2794, 1665, 1600-1400, 1296 cm⁻¹; MS calcd for C₂₀H₂₇N₂O₄P: 376.16 found [M-H]⁻; MS (ESI): m/z 375.1 [M-H]⁻; HRMS (ESI-NM): calcd for C₁₉H₂₅N₂O₄P: 376.1552 found [M-H]⁻ = 375.1493; C₁₉H₂₅N₂O₄P + Na: 398.1377 found [M-H]⁻ = 397.1310

([1-(tert-butylamino)-3,3-dimethyl-1-oxohex-5-en-2-yl]amino)methylphosphonic acid (2 Table 5) ¹H NMR (400 MHz, CD₃OD, 25°C,TMS): δ 5.90 (m, 1H), 5.15 (m, 2H), 3.80 (s, 1H), 3.63 (d, J= 10.33Hz, 3H), 3.07 (m, 1H), 2.80 (m, 1H), 2.21 (m, 1H), 2.03 (d, J= 16.14Hz, 1H), 1.38 (s, 9H), 1.06 (d, J=7.10 Hz, 6H) ppm; ¹³C NMR (101 MHz, MeOD, 27°C, TMS) δ 166.1 (C=O), 134.1 (CH-Allyl), 119.9 (CH₂-Allyl), 70.1 (J_{C,P}= 4 Hz, CH), 53.4 (C (CH₃)₃), 44.1 (CH₂), 37.5 (CH₂), 28.4 (C(CH₃)₃), 24.9 (Cq), 24.0- 23.2 (J_{C,P}= 74 Hz, CH₂) ppm; ³¹P NMR (162 MHz,

CD₃OD, TMS): δ 11.87 ppm; FT-IR ν : 3456, 2969, 2794, 1665, 1600-1400, 1296 cm⁻¹; MS (ESI): m/z 375.2 [M-H]⁻;

([1-(tert-butylamino)-1-oxododec-11-en-2-yl]amino)methyl)phosphonic acid (3 Table 5)
¹H NMR (400 MHz, CD₃OD, 25°C, TMS): δ 5.81 (m, 1H), 4.97 (m, 2H), 3.61 (d, J = 11.1 Hz, 2H), 3.36 (s, 1H), 2.98 (m, 2H), 2.06 (m, 2H), 1.37 (m, 23H) ppm; ¹³C NMR (101 MHz, MeOD, 27°C, TMS) δ 168.6 (C=O), 140.6 (CH-Allyl), 115.4 (CH₂-Allyl), 63.3 (CH), 52.8 (Cq), 42.7-41.3 (J_{C,P} = 140 Hz, CH₂), 34.9 (CH₂), 31.6 (CH₂), 30.3 (CH₂), 30.2 (CH₂), 28.6 (CH₃), 25.5 (CH₂) ppm. ³¹P NMR (162 MHz, CD₃OD, TMS): δ 11.19 ppm; FT-IR ν : 3470, 3002, 2769, 1661, 1600-1400, 1280 cm⁻¹; MS (ESI): m/z 362.2 [M-H]⁻; HRMS (ESI-NM): calcd for C₁₇H₃₅N₂O₄P Exact Mass: 362.2334, found [M-H]⁻ = 361.2338;

5. Acknowledgements

This work was financially supported by the University of Vienna through the interdisciplinary doctoral program: "Initiativkolleg Functional Molecules" (IK I041-N).

6. References

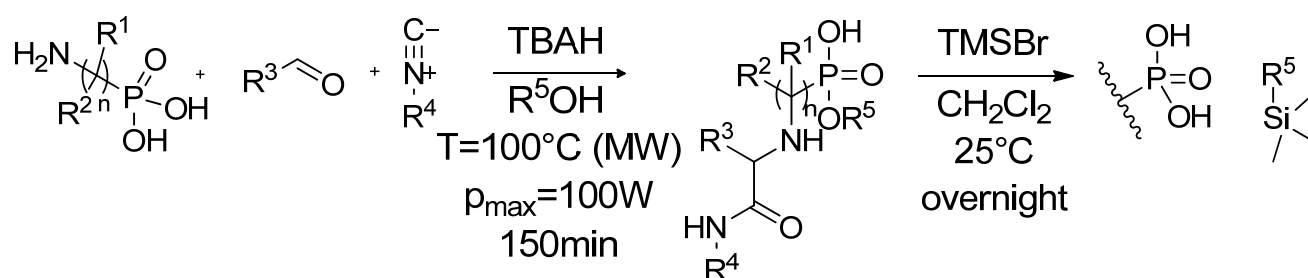
- [1] M. S. Tswett, *Proceedings of the Warsaw Society of Naturalists, Biology Section* **1905**, 14, 20-39.
- [2] L. R. Snyder, J. J. Kirkland, J. W. Dolan, in *Introduction to Modern Liquid Chromatography*, John Wiley & Sons, Inc., **2010**, pp. 2-13.
- [3] A. Vailaya, C. Horváth, *Journal of Chromatography A* **1998**, 829, 1-27.
- [4] F. Švec, Z. Děyl, T. B. Tennikova, in *Journal of Chromatography Library, Vol. Volume 67* (Eds.: T. B. T. František Švec, D. Zdeněk), Elsevier, **2003**, pp. V-VI.
- [5] D. Guilleme, J. Ruta, S. Rudaz, J.-L. Veuthey, *Anal Bioanal Chem* **2010**, 397, 1069-1082.
- [6] F. Švec, J. M. J. Frechet, *Analytical Chemistry* **1992**, 64, 820-822.
- [7] J. Nawrocki, M. Rigney, A. McCormick, P. W. Carr, *Journal of Chromatography A* **1993**, 657, 229-282.
- [8] L. R. Snyder, J. J. Kirkland, J. W. Dolan, in *Introduction to Modern Liquid Chromatography*, John Wiley & Sons, Inc., **2010**, pp. 361-402.
- [9] A. J. Alpert, *J Chromatogr* **1990**, 499, 177-196.
- [10] aA. J. Alpert, *Analytical Chemistry* **2007**, 80, 62-76; bA. E. Karatapanis, Y. C. Fiamegos, C. D. Stalikas, *Journal of Chromatography A* **2011**, 1218, 2871-2879.
- [11] G. Schuster, W. Lindner, *Journal of Chromatography A* **2013**, 1273, 73-94.
- [12] C. Horvath, W. Melander, *Journal of Chromatographic Science* **1977**, 15, 393-404.
- [13] L. Lloyd, J. Kennedy, *Bioseparation* **1999**, 8, 330-331.
- [14] J. Ståhlberg, *Journal of Chromatography A* **1999**, 855, 3-55.
- [15] M. C. Millot, T. Debranché, A. Pantazaki, I. Gherghi, B. Sébille, C. Vidal-Madjar, *Chromatographia* **2003**, 58, 365-373.
- [16] B. Sellergren, K. J. Shea, *Journal of Chromatography A* **1993**, 654, 17-28.

- [17] N. Fontanals, R. M. Marcé, F. Borrull, *Journal of Chromatography A* **2007**, 1152, 14-31.
- [18] F. Progent, M. Taverna, A. Banco, A. Tchapla, C. Smadja, *Journal of Chromatography A* **2006**, 1136, 221-225.
- [19] L. W. McLaughlin, *Chemical Reviews* **1989**, 89, 309-319.
- [20] aW. Bicker, M. Lämmerhofer, T. Keller, R. Schuhmacher, R. Krska, W. Lindner, *Analytical Chemistry* **2006**, 78, 5884-5892; bH. Hinterwirth, M. Lämmerhofer, B. Preinerstorfer, A. Gargano, R. Reischl, W. Bicker, O. Trapp, L. Brecker, W. Lindner, *Journal of Separation Science* **2010**, 33, 3273-3282; cM. Lämmerhofer, R. Nogueira, W. Lindner, *Anal Bioanal Chem* **2011**, 400, 2517-2530; dR. Nogueira, M. Lämmerhofer, W. Lindner, *Journal of Chromatography A* **2005**, 1089, 158-169.
- [21] M. Lämmerhofer, *Journal of Chromatography A* **2010**, 1217, 814-856.
- [22] aS. Topiol, M. Sabio, *Journal of the American Chemical Society* **1989**, 111, 4109-4110; bT. D. Booth, D. Wahnnon, I. W. Wainer, *Chirality* **1997**, 9, 96-98.
- [23] L. R. Snyder, J. J. Kirkland, J. W. Dolan, in *Introduction to Modern Liquid Chromatography*, John Wiley & Sons, Inc., **2010**, pp. 665-724.
- [24] S. L. Cui, X. F. Lin, Y. G. Wang, *J. Org. Chem.* **2005**, 70, 2866-2869.
- [25] M. Laemmerhofer, W. Lindner, *Liquid chromatographic enantiomer separation and chiral recognition by cinchona alkaloid-derived enantioselective separation materials*, Vol. 46, **2008**.
- [26] aM. Lämmerhofer, W. Lindner, *Journal of Chromatography A* **1996**, 741, 33-48; bJ. Olšovská, M. Flieger, F. Bachechi, A. Messina, M. Sinibaldi, *Chirality* **1999**, 11, 291-300.
- [27] C. V. Hoffmann, M. Laemmerhofer, W. Lindner, *Journal of Chromatography A* **2007**, 1161, 242-251.
- [28] C. V. Hoffmann, R. Pell, M. Lämmerhofer, W. Lindner, *Analytical Chemistry* **2008**, 80, 8780-8789.
- [29] C. Rosini, C. Bertucci, D. Pini, P. Altemura, P. Salvadori, *Chromatographia* **1987**, 24, 671-676.
- [30] A. Mandl, L. Nicoletti, M. Lämmerhofer, W. Lindner, *Journal of Chromatography A* **1999**, 858, 1-11.
- [31] aC. Hulme, *Multicomponent Reactions* **2005**, 311-341; bC. C. Musonda, D. Taylor, J. Lehman, J. Gut, P. J. Rosenthal, K. Chibale, *Bioorganic & Medicinal Chemistry Letters* **2004**, 14, 3901-3905; cC. Musonda Chitalu, D. Taylor, J. Lehman, J. Gut, J. Rosenthal Philip, K. Chibale, *Bioorg Med Chem Lett* **2004**, 14, 3901-3905; dW. Wang, A. Domling, *Journal of Combinatorial Chemistry* **2009**, 11, 403-409; eC. Hulme, V. Gore, *Current Medicinal Chemistry* **2003**, 10, 51-80; fG. Miao, R. Lan, C. Le, Y. Kan, S. Kandasamy, V. Joshi, L. Yu, *Abstracts of Papers, 231st ACS National Meeting, Atlanta, GA, United States, March 26-30, 2006* **2006**, ORGN-310; gG. Miao, Y. Kan, C. Le, V. Joshi, R. Qiu, L. Yu, C. Baldino, *Abstracts of Papers, 229th ACS National Meeting, San Diego, CA, United States, March 13-17, 2005* **2005**, ORGN-061; hP. A. Tempest, *Current Opinion in Drug Discovery & Development* **2005**, 8, 776-788; iA. Dömling, I. Ugi, *Angewandte Chemie International Edition* **2000**, 39, 3168-3210.
- [32] A. Gautier, *Ann.Chim. (Paris)* **1869**, 17, 218.
- [33] W. Lieke, *Justus Liebigs Ann. Chem.* **1859**, 316.
- [34] A. Arizpe, F. J. Sayago, A. I. Jiménez, M. Ordóñez, C. Cativiela, *European Journal of Organic Chemistry* **2011**, 2011, 3074-3081.
- [35] aG. Skorna, I. Ugi, *Angewandte Chemie International Edition in English* **1977**, 16, 259-260; bH. Eckert, B. Forster, *Angewandte Chemie International Edition in English* **1987**, 26, 894-895.
- [36] aM. Passerini, *Gazzetta Chimica Italiana* **1921**, 51, 121; bM. Passerini, *Gazzetta Chimica Italiana* **1921**, 51, 181.
- [37] L. Banfi, A. Basso, G. Guanti, R. Riva, in *Multicomponent Reactions*, Wiley-VCH Verlag GmbH & Co. KGaA, **2005**, pp. 1-32.

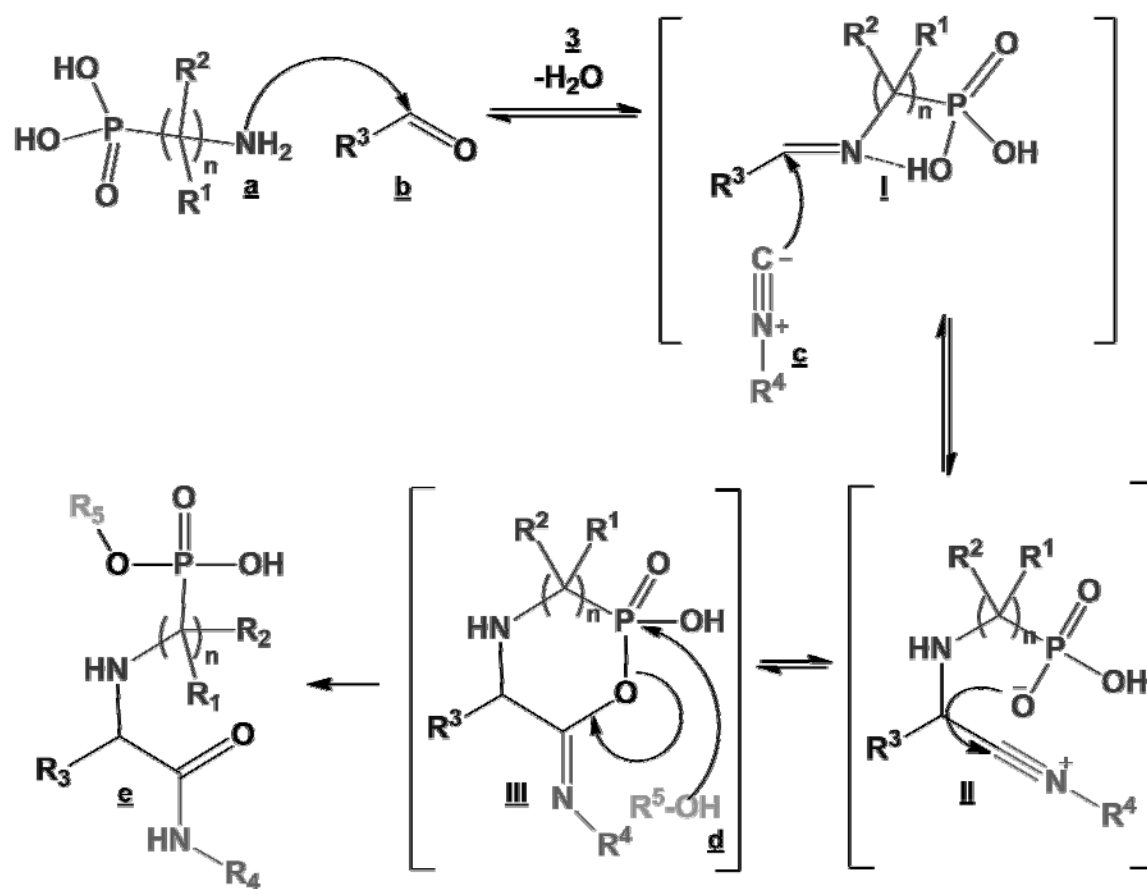
- [38] N. Cheron, R. Ramozzi, L. El Kaim, L. Grimaud, P. Fleurat-Lessard, *The Journal of Organic Chemistry* **2012**.
- [39] al. Ugi, A. Demharter, W. Hörl, T. Schmid, *Tetrahedron* **1996**, 52, 11657-11664; bA. Demharter, W. Hörl, E. Herdtweck, I. Ugi, *Angewandte Chemie International Edition in English* **1996**, 35, 173-175.
- [40] al. Ugi, C. Steinbrückner, *Chemische Berichte* **1961**, 94, 734-742; bH. P. Isenring, W. Hofheinz, *Synthesis* **1981**, 1981, 385-387.
- [41] J. J. Chen, A. Golebiowski, S. R. Klopfenstein, L. West, *Tetrahedron Letters* **2002**, 43, 4083-4085.
- [42] aH. R. Hudson, V. P. Kukhar, *Aminophosphonic and aminophosphinic acids: chemistry and biological activity*, Wiley, **2000**; bW. Liu, C. J. Rogers, A. J. Fisher, M. D. Toney, *Biochemistry* **2002**, 41, 12320-12328.
- [43] aH. Braeuner-Osborne, J. Egebjerg, E. Nielsen, U. Madsen, P. Krosgaard-Larsen, *Journal of Medicinal Chemistry* **2000**, 43, 2609-2645; bA. Mucha, P. Kafarski, Ł. Berlicki, *Journal of Medicinal Chemistry* **2011**, 54, 5955-5980.
- [44] aJ. R. Morphy, N. R. A. Beeley, B. A. Boyce, J. Leonard, B. Mason, A. Millican, K. Millar, J. P. Oconnell, J. Porter, *Bioorganic & Medicinal Chemistry Letters* **1994**, 4, 2747-2752; bI. Kraicheva, A. Bogomilova, I. Tsacheva, G. Momekov, K. Troev, *Eur J Med Chem* **2009**, 44, 3363-3367; cP. Kafarski, B. Lejczak, *Phosphorus Sulfur* **1991**, 63, 193-215; dR. Grzywa, J. Oleksyszyn, G. S. Salvesen, M. Drag, *Bioorg Med Chem Lett* **2010**, 20, 2497-2499; eR. Grzywa, A. M. Sokol, M. Sieńczyk, M. Radziszewicz, B. Kościółek, M. P. Carty, J. Oleksyszyn, *Bioorganic & Medicinal Chemistry* **2010**, 18, 2930-2936.
- [45] C. Selvam, C. Goudet, N. Oueslati, J. P. Pin, F. C. Acher, *J Med Chem* **2007**, 50, 4656-4664.
- [46] E. M. Wallace, J. A. Moliterni, M. A. Moskal, A. D. Neubert, N. Marcopulos, L. B. Stamford, A. J. Trapani, P. Savage, M. Chou, A. Y. Jeng, *J Med Chem* **1998**, 41, 1513-1523.
- [47] aJ. Beck, S. Gharbi, A. Herteg-Fernea, L. Vercheval, C. Bebrone, P. Lassaux, A. Zervosen, J. Marchand-Brynaert, *European Journal of Organic Chemistry* **2009**, 2009, 85-97; bS. Yang, X.-W. Gao, C.-L. Diao, B.-A. Song, L.-H. Jin, G.-F. Xu, G.-P. Zhang, W. Wang, D.-Y. Hu, W. Xue, X. Zhou, P. Lu, *Chinese Journal of Chemistry* **2006**, 24, 1581-1588.
- [48] H. C. Manning, T. Goebel, J. N. Marx, D. J. Bornhop, *Org Lett* **2002**, 4, 1075-1078.
- [49] aC. Kalinski, M. Umkehrer, L. Weber, J. Kolb, C. Burdack, G. Ross, *Molecular Diversity* **2010**, 14, 513-522; bH. Bienaymé, C. Hulme, G. Odon, P. Schmitt, *Chemistry – A European Journal* **2000**, 6, 3321-3329.
- [50] A. Basso, L. Banfi, R. Riva, G. Guanti, *Tetrahedron Letters* **2004**, 45, 587-590.
- [51] H. M. Hügel, *Molecules* **2009**, 14, 4936-4972.
- [52] C. O. Kappe, B. Pieber, D. Dallinger, *Angewandte Chemie International Edition* **2013**, 52, 1088-1094.
- [53] S. De Lombaert, M. D. Erion, J. Tan, L. Blanchard, L. El-Chehabi, R. D. Ghai, Y. Sakane, C. Berry, A. J. Trapani, *J. Med. Chem.* **1994**, 37, 498-511.
- [54] F. Hammerschmidt, M. Hanbauer, *J. Org. Chem.* **2000**, 65, 6121-6131.
- [55] G. Auger, J. van Heijenoort, D. Blanot, C. Deprun, *Journal für Praktische Chemie/Chemiker-Zeitung* **1995**, 337, 351-357.
- [56] A. Mucha, P. Kafarski, L. Berlicki, *Journal of medicinal chemistry* **2011**, 54, 5955-5980.
- [57] aF. Hammerschmidt, Y.-F. Li, *Tetrahedron* **1994**, 50, 10253-10264; bF. Hammerschmidt, F. Wuggenig, *Tetrahedron: Asymmetry* **1999**, 10, 1709-1721; cU. Schmidt, H. W. Krause, G. Oehme, M. Michalik, C. Fischer, *Chirality* **1998**, 10, 564-572; dA. Woschek, W. Lindner, F. Hammerschmidt, *Advanced Synthesis & Catalysis* **2003**, 345, 1287-1298; eF. Wuggenig, A. Schweifer, K. Mereiter, F. Hammerschmidt, *European Journal of Organic Chemistry* **2011**, 1870-1879.
- [58] F. Hammerschmidt, H. Voellenkle, *Liebigs Ann. Chem.* **1989**, 577-583.

- [59] C. Fischer, U. Schmidt, T. Dwars, G. Oehme, *Journal of Chromatography A* **1999**, 845, 273-283.
- [60] aW. H. Pirkle, J. A. Burke, *Journal of Chromatography A* **1992**, 598, 159-167; bW. H. Pirkle, L. Jonathan Brice, S. Caccamese, G. Principato, S. Failla, *Journal of Chromatography A* **1996**, 721, 241-246; cW. H. Pirkle, L. Jonathan Brice, T. S. Widlanski, J. Roestamadj, *Tetrahedron: Asymmetry* **1996**, 7, 2173-2176.
- [61] aE. Zarbl, M. Lammerhofer, F. Hammerschmidt, F. Wuggenig, M. Hanbauer, N. M. Maier, L. Sajovic, W. Lindner, *Analytica Chimica Acta* **2000**, 404, 169-177; bM. Lämmerhofer, D. Hebenstreit, E. Gavioli, W. Lindner, A. Mucha, P. Kafarski, P. Wieczorek, *Tetrahedron: Asymmetry* **2003**, 14, 2557-2565.
- [62] F. Wuggenig, A. Schweifer, K. Mereiter, F. Hammerschmidt, *European Journal of Organic Chemistry*, 2011, 1870-1879.
- [63] C. V. Hoffmann, R. Reischl, N. M. Maier, M. Lämmerhofer, W. Lindner, *Journal of Chromatography A* **2009**, 1216, 1147-1156.
- [64] aC. V. Hoffmann, R. Reischl, N. M. Maier, M. Lämmerhofer, W. Lindner, *Journal of Chromatography A* **2009**, 1216, 1157-1166; bR. Pell, S. Sić, W. Lindner, *Journal of Chromatography A* **2012**; cS. Wernisch, W. Lindner, *Journal of Chromatography A* **2012**.
- [65] aC. V. Hoffmann, R. Reischl, N. M. Maier, M. Lammerhofer, W. Lindner, *Journal of chromatography. A* **2009**, 1216, 1157-1166; bC. V. Hoffmann, R. Reischl, N. M. Maier, M. Lammerhofer, W. Lindner, *Journal of chromatography. A* **2009**, 1216, 1147-1156; cR. Pell, S. Sic, W. Lindner, *Journal of chromatography. A* **2012**, 1269, 287-296; dR. Pell, S. Sić, W. Lindner, *Journal of Chromatography A* **2012**, 1269, 287-296; eS. Wernisch, R. Pell, W. Lindner, *Journal of Separation Science* **2012**, 35, 1560-1572.
- [66] N. M. Maier, S. Schefzick, G. M. Lombardo, M. Feliz, K. Rissanen, W. Lindner, K. B. Lipkowitz, *Journal of the American Chemical Society* **2002**, 124, 8611-8629.
- [67] **!!! INVALID CITATION !!!**
- [68] al. Kraicheva, A. Bogomilova, I. Tsacheva, G. Momekov, K. Troev, *European Journal of Medicinal Chemistry* **2009**, 44, 3363-3367; bP. Kafarski, B. Lejczak, *Phosphorus Sulfur* **1991**, 63, 193-215; cR. Grzywa, J. Oleksyszyn, G. S. Salvesen, M. Drag, *Bioorg Med Chem Lett* **2010**, 20, 2497-2499.
- [69] C. Selvam, C. Goudet, N. Oueslati, J.-P. Pin, F. C. Acher, *Journal of Medicinal Chemistry* **2007**, 50, 4656-4664.
- [70] Y. Xu, K. Yan, B. Song, G. Xu, S. Yang, W. Xue, D. Hu, P. Lu, G. Ouyang, L. Jin, Z. Chen, *Molecules* **2006**, 11, 666-676.
- [71] H. C. Manning, T. Goebel, J. N. Marx, D. J. Bornhop, *Organic Letters* **2002**, 4, 1075-1078.
- [72] A. F. G. Gargano, M. Lämmerhofer, W. Lindner, **xx**.
- [73] M. Lämmerhofer, E. Zarbl, W. Lindner, B. P. Simov, F. Hammerschmidt, *ELECTROPHORESIS* **2001**, 22, 1182-1187.
- [74] A. F. G. Gargano, Kohout M. , Macíková P., Lämmerhofer M. , Lindner W, *Analytical and Bioanalytical Chemistry* **2013**, *In print*.
- [75] Peter G. M. Wuts, T. W. Greene, **2008**.
- [76] aC. Czerwenka, M. Lämmerhofer, W. Lindner, *Journal of Separation Science* **2003**, 26, 1499-1508; bC. Czerwenka, M. M. Zhang, H. Kählig, N. M. Maier, K. B. Lipkowitz, W. Lindner, *The Journal of Organic Chemistry* **2003**, 68, 8315-8327.
- [77] M. Lämmerhofer, P. Franco, W. Lindner, *Journal of Separation Science* **2006**, 29, 1486-1496.

7. Figure captions:



Scheme 1: Reaction scheme and conditions



Scheme 2: Postulated reaction mechanism

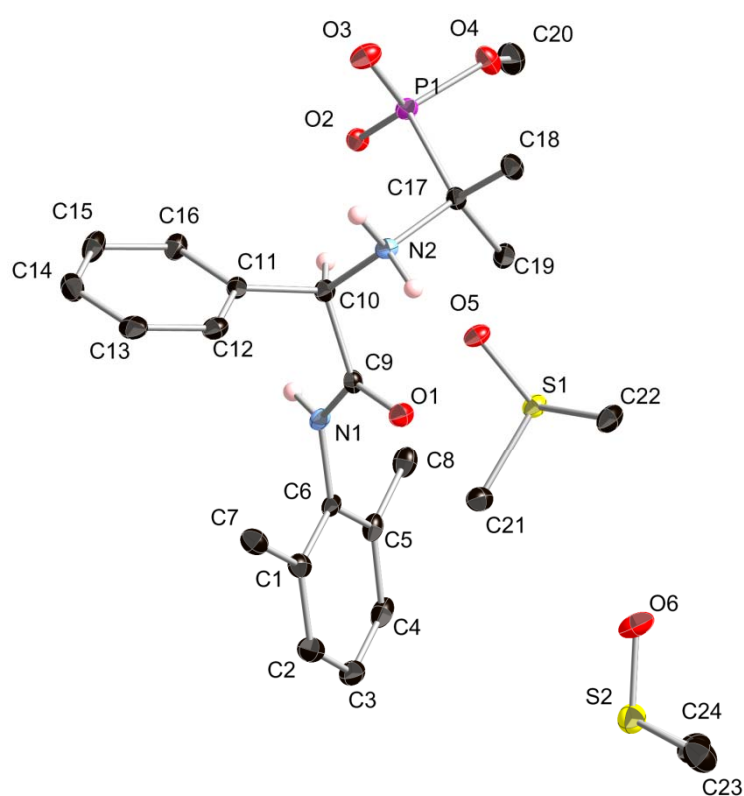


Figure 1: Crystallographic structure of **1** *Table 3*. Thermal ellipsoids drawn at the 35% probability level, selected hydrogens omitted for clarity. Experimental details reported in the experimental section.

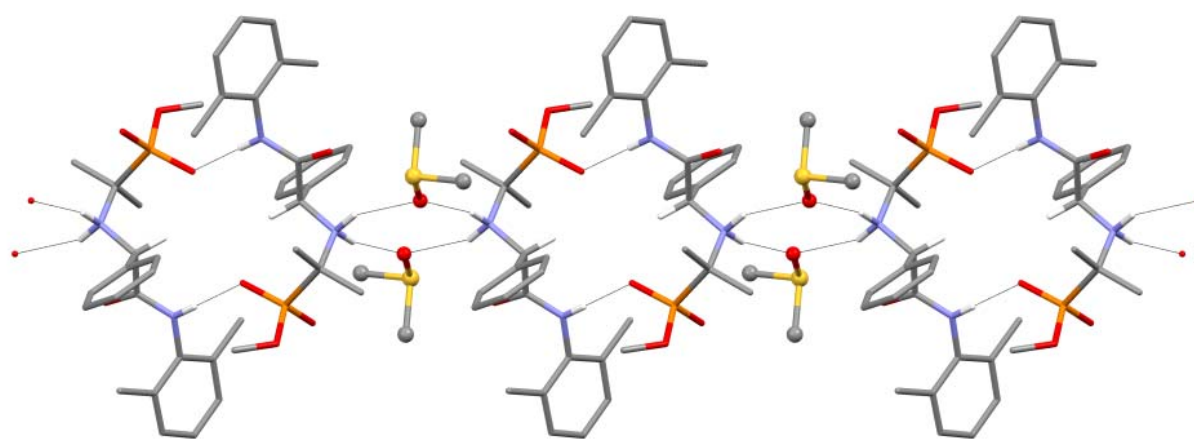
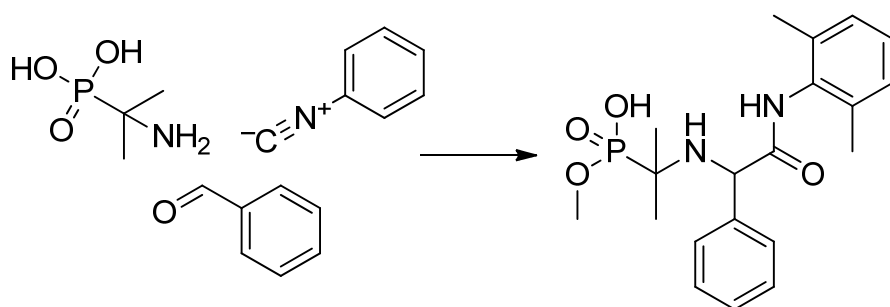


Figure 2: Crystallographic structure **1** *Table 3:* Formation of hydrogen bonded chains extend along the b axis.

Table 1. Optimization of reaction conditions. All the reactions were carried out with 2-amino-2-propane phosphonic acid (0.2 mmol), benzaldehyde (0.3mmol), 2,6-dimethylisocyanide (0.3mmol) in the indicated solvent (2mL)



Entry	Solvent	T [°C]	Time [min]	MW [W]	Yield [%] ^[a]
1	MeOH	-30 to 0	2 days ^[b]	- [c]	0
2	MeOH	0	2 days ^[b]	- [c]	0
3	MeOH	25	2 days ^[b]	- [c]	0
4	MeOH	40	2 days ^[b]	- [c]	20
5	MeOH	50	2 days ^[b]	- [c]	35
6	DCM	100	30	100	0
7	Toluene	100	30	100	0
8	DMSO	100	30	100	0
9	MeOH	50	90	100	28
10	MeOH	75	90	125	33
11	MeOH	100	30	100	38
12	MeOH	100	90	100	42
13	MeOH	100	90	50	42
14	MeOH	100	90	150	41
15	MeOH	100	150	100	45
16	MeOH	125	90	100	37
17	MeOH	150	90	100	2

^[a] Determined through calibrated (RP) LC-MS analysis

^[b] Conventional heating

Table 2. Effect of ion-pairing agent and its concentration on the Ugi-5C-4CR ^[a]

All the reactions were carried out with the same educts and the same concentrations as in Table 1 in MeOH (2 mL) for 150 min at 100°C with maximum MW of 100 W

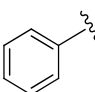
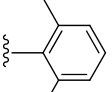
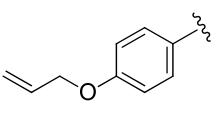
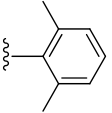
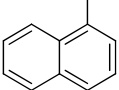
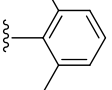
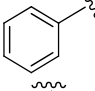
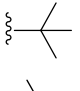
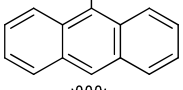
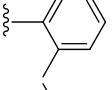
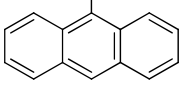
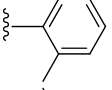
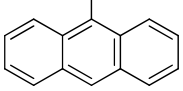
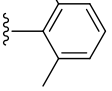
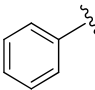
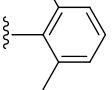
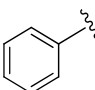
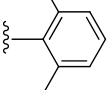
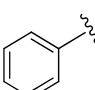
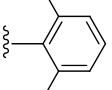

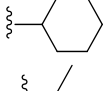
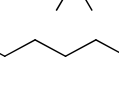
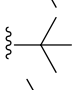
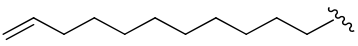
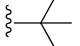
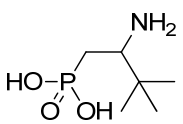
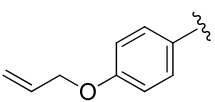
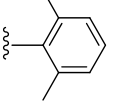
Entry	Ion pairing agent	Mol eq ^[a]	Yield [%] ^[b]
1	-		45
2	CH ₃ COOH	0.5	2
3	HCl	0.5	0
4	TFA	0.5	0
5	NaOH	0.5	16
6	Hünig Base	0.5	21
7	TBAH ^[c]	0.1	58
8	TBAH ^[c]	0.3	71
9	TBAH ^[c]	0.5	79
10	TBAH ^[c]	1.0	6

^[a] Rel. to APA

^[b] Determined by calibrated RPLC-MS analysis

^[c] TBAH, tetra-n-butylammonium hydroxyide

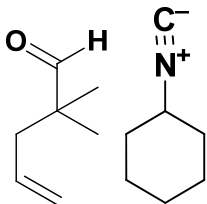
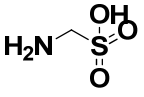
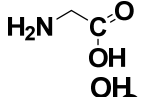
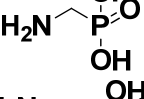
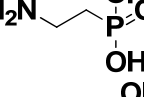
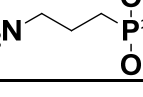
Table 3 : Ugi-5C-4CR reaction yields for reaction in MeOH with different APAs, aldehydes and isocyanides (compound numbers refer to products)

Product No	Aminophosphonic acid	Aldehyde (R ³)	Isocyanide (R ⁴)	Yield [%] ^[a]
1	R ¹ , R ² = CH ₃			71 ^[b] 66 ^[c]
2	R ¹ , R ² = CH ₃			50 ^[c]
3	R ¹ , R ² = CH ₃			66 ^[c]
4	R ¹ , R ² = CH ₃			80 ^[c]
5	R ¹ , R ² = CH ₃			66 ^[c]
6	R ¹ = -(CH ₂) ₄ -			71 ^[d]
7	R ¹ = Ph, R ² = H			32 ^{[c][e]}
8	R ¹ = -(CH ₂) ₄ -			66 ^[c]
9	R ¹ = CH ₃ , R ² = H			34 ^[c]
10	R ¹ = CH(CH ₃) ₂ , R ² = H			55 ^[c]
11	R ¹ = R ² = H			92 ^[c]
12	R ¹ = R ² = H			93 ^[c]
13	R ¹ = R ² = H			68 ^[c]
14				43 ^[c]

^[a] Isolated yield based on starting aminophosphonic acid^[b] Liquid extraction (0.1M HCl / DCM) followed by evaporation under vacuum and crystallization in toluene^[c] Chiral anion-exchange chromatography with CHIRALPAK QN-AXTM column, mobile phase compositions are reported in the compound characterization section^[d] Silica flash chromatography with DCM/MeOH (2:1; v/v) as mobile phase

^[e] Reaction performed in allyl alcohol

Table 4 : Influence of the type and length of the amino acid component on the reaction yield

Reaction mixture	Amino Acid	Compound n°	Yield*[%]
		15	0***
		16	21 ^[b]
		17	92 ^[b]
		18	42 ^[b]
		19	20 ^[b]

SUPPORTING INFORMATION INDEX:

Section S1: Materials

Section S2: Chromatographic conditions for synthesis optimization

Section S3: Chiral chromatographic enantioseparation

Section S4: Optimization of methyl ester hydrolysis conditions

Section S5: X-Ray crystallography of entry n°1 Table n°3

Section S6: VCD investigation over single enantiomers entry n°1 Table n°3

Section S7: NMR spectrum

Figure N1: ^1H spectrum of entry n°1 *Table n°3* purified through crystallization (a) and ^1H (b), ^{13}C (c), ^{31}P (d) spectrum of the same entry purified through CHIRALPAK QD-AXTM in the absence of TBAH in the reaction mixture, ^1H spectrum of a synthesis batch purified through CHIRALPAK QD-AXTM in the presence of TBAH (e).

SECTION S1: MATERIALS

(2-aminopropan-2-yl)phosphonic acid, (1-aminocyclopentyl)phosphonic acid, (1-aminoethyl)phosphonic acid, from [amino(phenyl)methyl]phosphonic acid, (aminoethyl)phosphonic acid, (aminopropyl) phosphonic acid were of a purity grade of at least 97% and supplied by Acros Organics (Geel, Belgium). (Aminomethyl) phosphonic acid 98% was bought through epsilon chimie (Brest-Guipavas, France). (1-amino-2-methylpropyl)phosphonic acid and (2-amino-3,3-dimethylbutyl)phosphonic acid were synthesized according to literature procedure ^[54].

Benzaldehyde, 4-allyloxy benzaldehyde, 1-naphthaldehyde, anthracene-9-carbaldehyde, 2,2-dimethylpent-4-enal, 10-undecylenic aldehyde, 2,6-dimethylphenyl isocyanide, cyclohexyl isocyanide, *t*-butyl isocyanide, glycine, (aminomethyl) sulfonic acid, were of a purity grade of at least 90% and obtained from Sigma-Aldrich (Vienna, Austria).

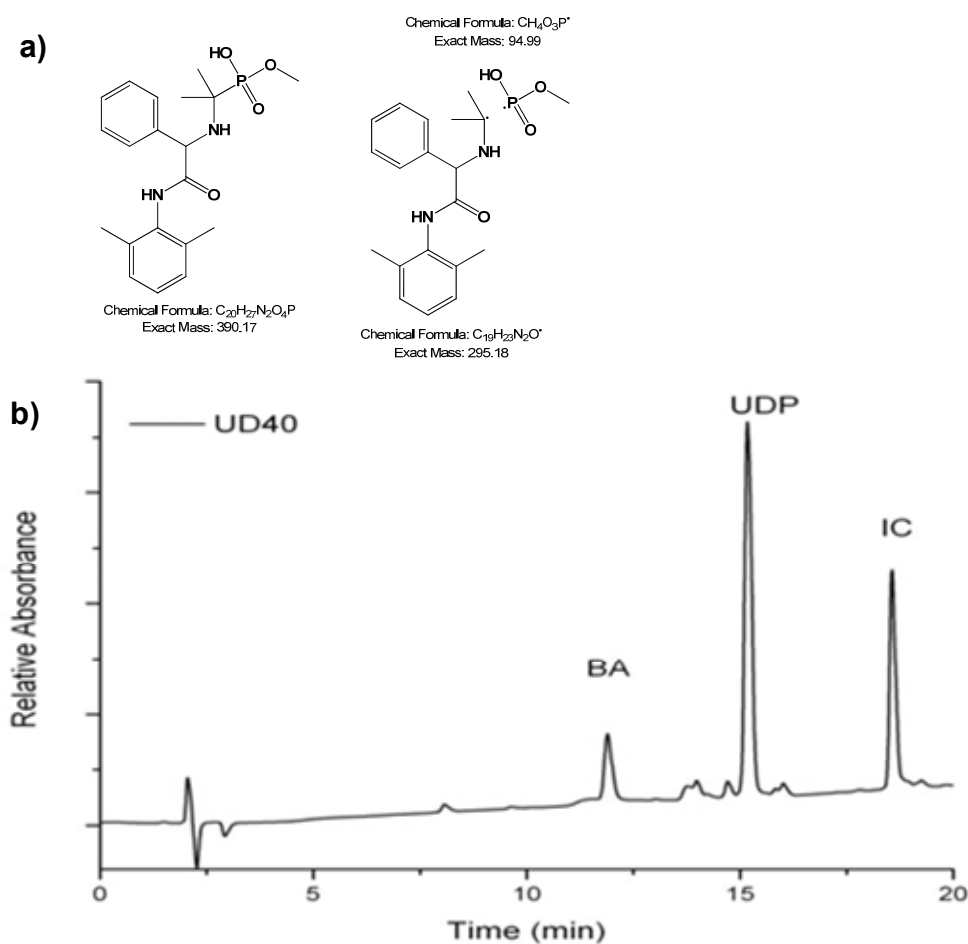
Tetrabutylammonium hydroxide (technical grade 25% in MeOH), bromotrimethyl silane, formic acid (FA) were of a purity grade of at least 97% and purchased from Fluka (Sigma-Aldrich).

Acetonitrile (ACN) and Methanol (MeOH) chromatography grade (VWR, Vienna, Austria), Acetic acid (Fluka, for HPLC, $\geq 98.0\%$), Ammonium Acetate (Fluka, for HPLC, $\geq 98.0\%$), Formic Acid (Fluka, for HPLC, $\geq 98.0\%$), Ammonium Acetate (Fluka, for HPLC, $\geq 98.0\%$) as well as distilled water filtered through a Milli-Pore (Milli-Q) water purification system (18.2 M Ω quality) were used for the preparation of the mobile phases.

SECTION S2: CHROMATOGRAPHIC CONDITIONS FOR SYNTHESIS OPTIMIZATION

All reaction batches were characterized adopting reversed-phase (RP) chromatography by RP-C18 (3 μ m, 3x150 mm column from Advanced Chromatography Technologies (ACT) using gradient elution chromatography (mobile phase A: H₂O 0.1% formic acid, mobile phase B: MeOH 0.1% formic acid; gradient: 20% B to 100% B in 20 min). The flow rate adopted was 0.4 mL/min at 25 °C, the sample injection volume 2.5 μ L, detection was performed at 214 nm and in alternate mode (cycles of positive and negative MS) using an ion-trap MS (Fig. S1)

In order to evaluate the results from the synthesis optimization in a quick manner, without purifying each batch we experimentally determined the linear relationship presented between the chromatographic peak area and the compound quantity (calibration curve, Fig. S2).



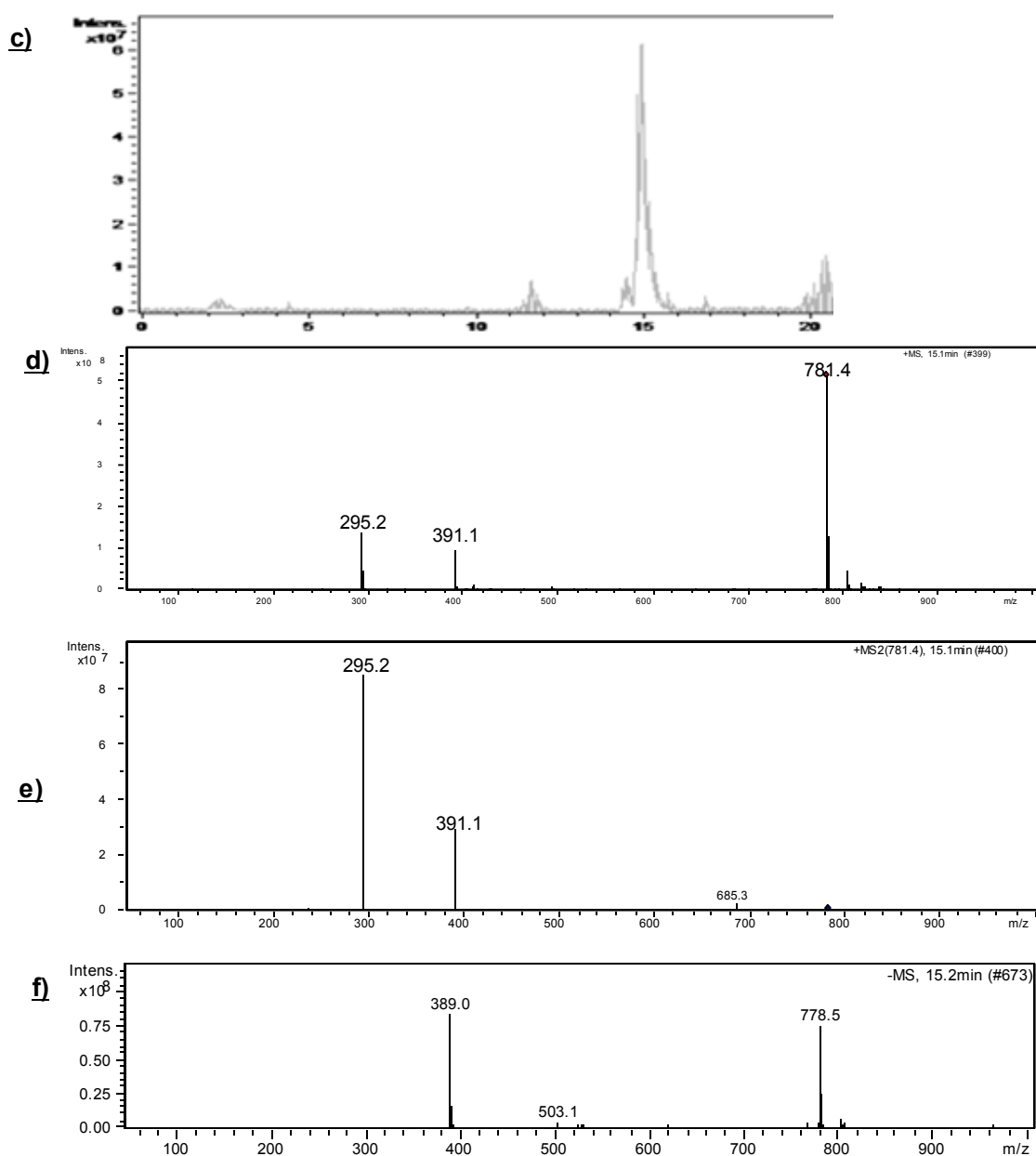


Figure S1: **a)** Chemical structure, Mw and fragmentation of entry n°1 *table 1,2 and 3*, used as target compound during the synthesis optimization. **b)** RP-LC chromatogram of the crude product of entry n°9 *table n°2* (BA= benzaldehyde, IC= 2,5 dimethyl phenyl isonitrile, UDP= product code). **c)** TIC (50-1000 m/z) of the RP analysis of the crude product of entry n°9 *table n°2*. **d)** Ms spectrum in positive mode of product peak (UDP, time= 15 min), the compound in the ESI generate dimers. **e)** MS/MS of the dimer of product dimer (781), resulting in the MS of the product. **f)** Ms spectrum in negative mode of product peak (UDP, time= 15 min).

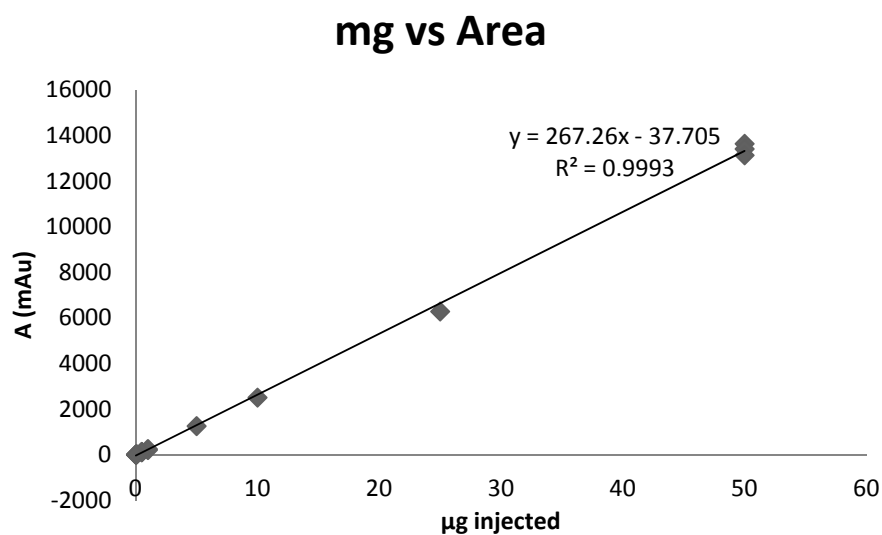


Figure S2

Calibration curve between µg injected of entry n°1 *table 1,2 and 3* (in the range between 0.02 and 50µg) of and A detected. The curve was used during the synthesis optimization to estimate the yield of a certain product batch.

Section S3: Chiral chromatographic enantioseparation

Entry n°1-5 and 7-15 of *table n°3*, as well as the compounds reported in *table n°4* were purified adopting a weak chiral anion exchanger (CHIRALPAK QD-AX™).

In *fig. S3* we reported the hypothesized interaction mechanism between selector and selectand and in *fig. S4* an example of the chiral enantioseparation of entry n° 5 *table n°3*.

Using chiral anion exchange chromatography coupled with MS detection we investigated the influence of the chirality of the starting Aminophosphonic acid in terms of diastereomeric excess of the product (*table S1, S2 and fig. S5,S6*). We observed a small influence on the conformation of the newly generated chiral center given by the use of chiral acidic educts (entry n°1-3 *table S1*). Interestingly when more bulky residues are adopted (entry n°3-4 *table S1*) the diastereomeric excess was similarly influenced.

The chromatographic conditions for such analysis were:

MP: 98% MeOH 2% AcOH 0.5g Ammonium Acetate (V=1L); SP: Chiral anion exchanger Chiralpak QN-AX™, 150 x 4 mm ID packed $\lambda = 254\text{nm}$, flow rate: 1mL/min, Inj:5 μL .

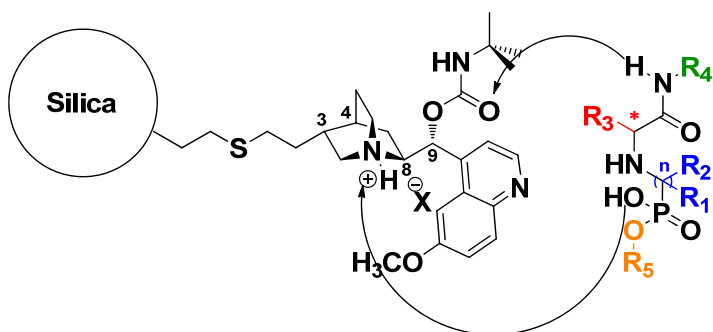


Figure S3: Representation of the hypothesized interaction mechanism between the chiral SP CHIRALPAK QN/QD AX and the amido-aminophosphonate structure generated from the reported synthetic approach.

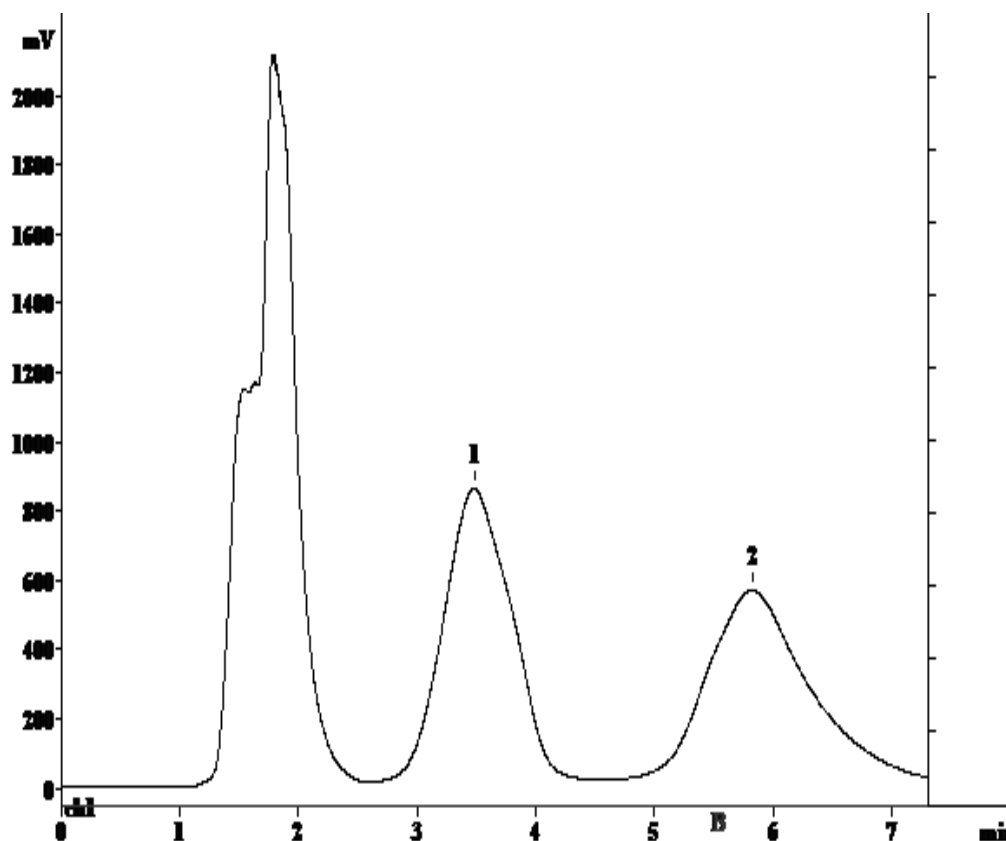


Figure S4: Chromatogram of preparative enantioseparation of entry n° 5 *table n°3*.
Chromatographic conditions MP: 100% MeOH 75mM FA app pH adj to 4 (NH₄OH)
SP: Chiral anion exchanger Chiralpak QD-AX™, 250 x 16 mm ID packed with 100 Å , 10 μm silica gel . λ= 310nm , flow rate: 15mL/min , Inj:1mL (25 mg).

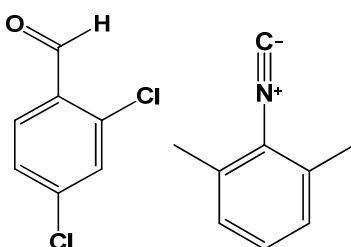
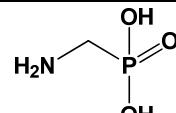
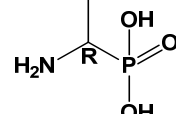
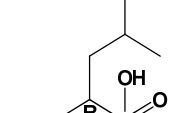
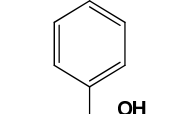
Reaction mixture	Entry	Solvent	APA	d.e. [%], R as starting educt	d.e. [%] racemic educt
	1	MeOH		-	0
	2	MeOH		27	0
	3	MeOH		33	10
	4	MeOH		-	32

Table S1: Influence of the chirality of the starting Aminophosphonic acid in terms of diastereomeric excess of the aminophosphonate product.

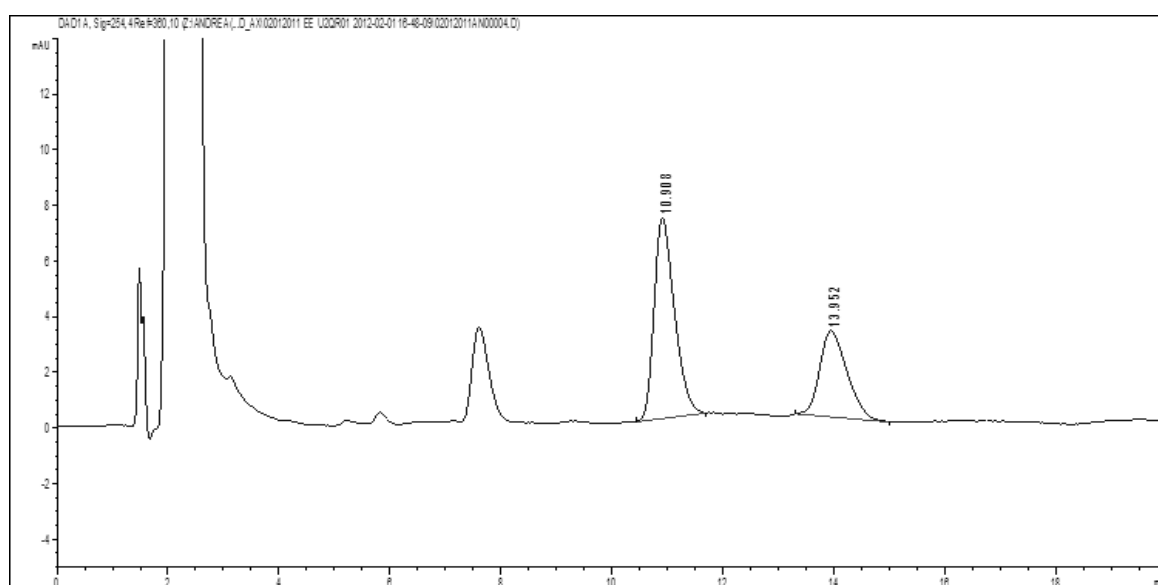


Figure S6: Example of the determination of the diastereomeric excess of compound entry n°3 *table S1*.

#	Time	Area	Area%	d.e %
1	10.908	183.6	66.52	33%
2	13.952	92.4	33.47	

Table S2: Example of the determination of the diastereomeric excess of compound entry n°3 *table S1*.

Section S4: Optimization of hydrolysis procedure

In order to ensure the possibility of generating a phosphonic acid derivative from the obtained phosphonate compound we investigated several hydrolysis approaches (*Fig. S7 Table S3*). Phosphonic acid monoesters are commonly transformed into the corresponding acids by adopting acidic or basic media, like aqueous HCl or NaOH ^[55]. Such conditions were not sufficient to hydrolyze our target compound (entry n°1 *table n°1*). Therefore other methods had to be selected; amongst those provided by literature, reports employing Trimethylsilylbromide (TMSBr) seemed the most promising one. This result was confirmed by our findings, reporting quantitative yield in the case of the reaction in DCM (*Fig. S8*). The optimized reaction protocol was also tested on one isolated enantiomer and no racemization was observed (*Fig. S9*).

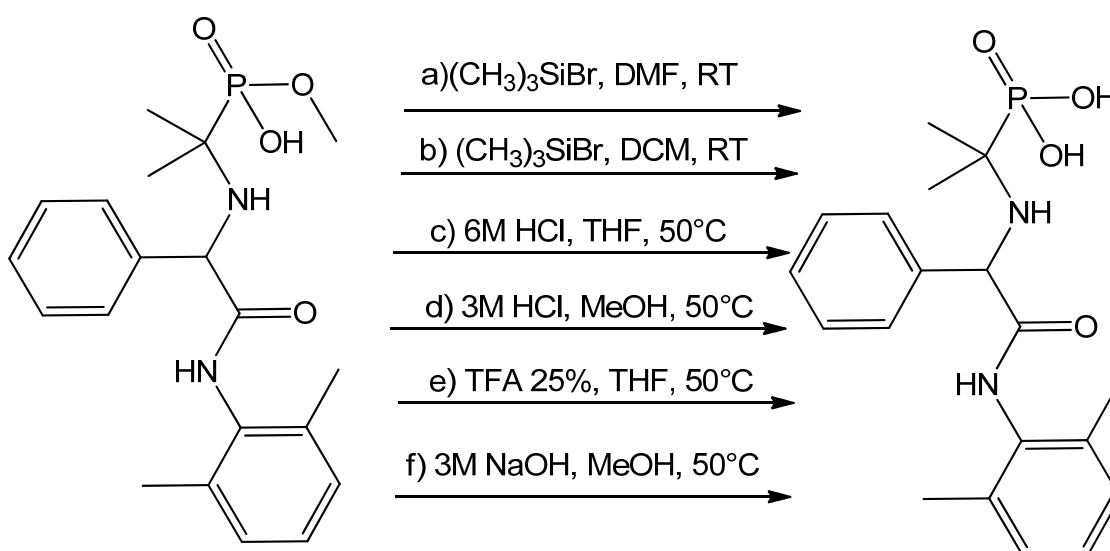


Figure S7: Optimization of hydrolysis procedure

Table S3: All the reaction were performed starting from 2mg of entry 1 *Table n°1* and left to react overnight

	% free acid	% Methyl ester
a	40	60
b	100	0
c	40	60
d	23	77
e	4	96
f	4	96

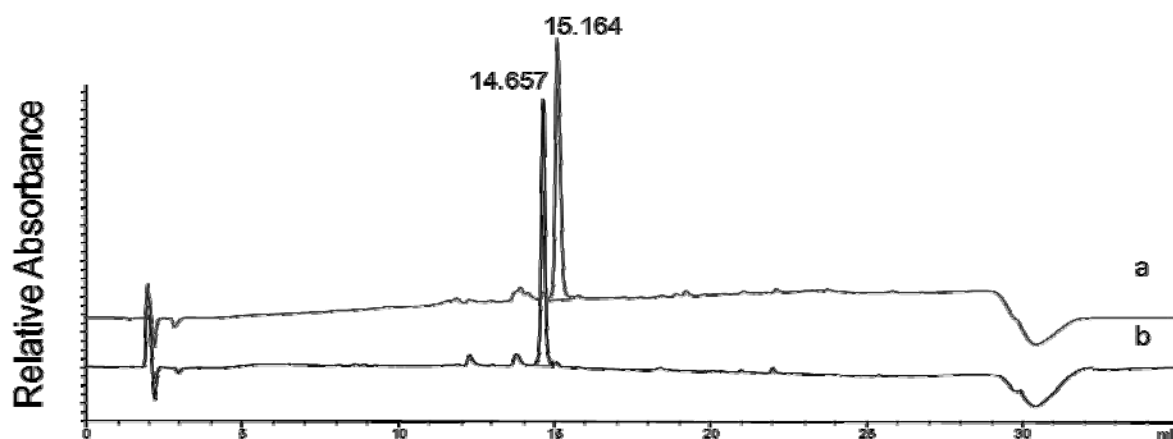


Figure S8: Overlay of RP chromatogram of entry n°1(a, red trace) *Table n°1* it's hydrolyzed form (entry n°16, b, blue trace).

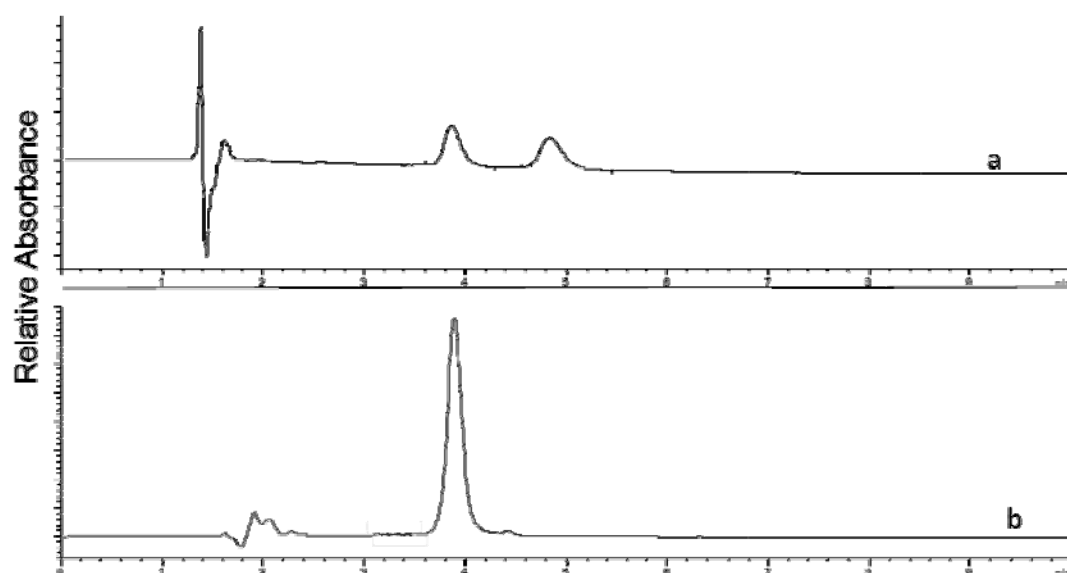


Figure S9: Overlay of chiral anion exchange analysis of hydrolysis reaction performed on racemic entry n°1 *Table n°1* (a, blue trace), and the same procedure done on the enantiomerically rich compound (b, red trace, initial ee before and after hydrolysis=98%)

Section S5: X-Ray crystallography of entry n°1 Table n°3



X-Ray Diffraction

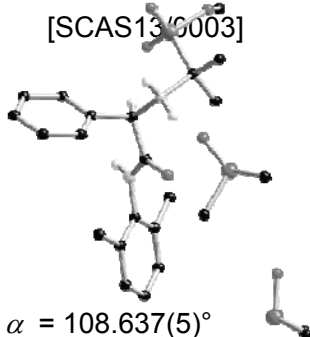
Chemistry - University of Southampton

Dr Mark E Light

light@soton.ac.uk

0230599429

Table S4. Crystal data and structure refinement details.

Identification code	2013scas0005	[SCAS130003]
(AZ13676820)		
Empirical formula	$C_{24}H_{39}N_2O_6PS_2$ $C_{20}H_{27}N_2O_4P, 2(C_2H_6OS)$	
Formula weight	546.66	
Temperature	100(2) K	
Wavelength	0.71073 Å	
Crystal system	Triclinic	
Space group	$P\bar{1}$	
Unit cell dimensions	$a = 9.373(3)$ Å $b = 12.019(4)$ Å $c = 13.078(4)$ Å	$\alpha = 108.637(5)^\circ$ $\beta = 95.801(6)^\circ$ $\gamma = 95.605(4)^\circ$
Volume	$1375.7(7)$ Å ³	
Z	2	
Density (calculated)	1.320 Mg / m ³	
Absorption coefficient	0.292 mm ⁻¹	
$F(000)$	584	
Crystal	Platelet; Colourless	
Crystal size	$0.100 \times 0.030 \times 0.010$ mm ³	
θ range for data collection	2.969 – 26.371°	
Index ranges	$-11 \leq h \leq 11, -15 \leq k \leq 15, -16 \leq l \leq 16$	
Reflections collected	20014	
Independent reflections	5617 [$R_{int} = 0.0820$]	
Completeness to $\theta = 25.242^\circ$	99.7 %	
Absorption correction	Semi-empirical from equivalents	
Max. and min. transmission	1.000 and 0.821	
Refinement method	Full-matrix least-squares on F^2	
Data / restraints / parameters	5617 / 0 / 337	
Goodness-of-fit on F^2	1.093	
Final R indices [$F^2 > 2\sigma(F^2)$]	$R1 = 0.0691, wR2 = 0.1179$	
R indices (all data)	$R1 = 0.1056, wR2 = 0.1320$	
Largest diff. peak and hole	0.434 and -0.439 e Å ⁻³	

Materials and Methods

Diffraction: *Rigaku AFC12* goniometer equipped with an enhanced sensitivity (HG) *Saturn724+* detector mounted at the window of an *FR-E+ SuperBright* molybdenum rotating anode generator with HF *Varimax* optics (100 μ m focus). **Cell determination, Data collection, Data reduction and cell refinement & Absorption correction:** CrystalClear-SM Expert 2.0 r7 (Rigaku, 2011) , **Structure solution:** SHELXS97 (Sheldrick, G.M. (2008). *Acta Cryst.* **A64**, 112-122). **Structure refinement:** SHELXL2012 (G. M. Sheldrick (2012), University of Göttingen, Germany). **Graphics:** CrystalMaker: a crystal and molecular structures program for Mac and Windows. CrystalMaker Software Ltd, Oxford, England (www.crystallmaker.com)

Special details: All hydrogen atoms were clearly identified in the difference map, C-H were then placed in calculated positions and refined using a riding model, N-H were freely refined.

Structure Quality: Grade **B**, slightly high R_1 & R_{int} values due to thin crystals.

Room temperature Cell (300K): Cell determined at 300K: $a = 9.504(37)$, $b = 12.129(52)$, $c = 13.321(55)$, $\alpha = 108.346(83)$, $\beta = 96.052(72)$, $\gamma = 95.623(82)$

Table S5. Atomic coordinates [$\times 10^4$], equivalent isotropic displacement parameters [$\text{\AA}^2 \times 10^3$] and site occupancy factors. U_{eq} is defined as one third of the trace of the orthogonalized U^{ij} tensor.

Atom	<i>x</i>	<i>y</i>	<i>z</i>	U_{eq}	<i>S.o.f.</i>
P1	−119(1)	2441(1)	11952(1)	19(1)	1
O1	−2050(2)	2194(2)	8113(2)	21(1)	1
O2	−16(2)	1157(2)	11398(2)	19(1)	1
O3	1221(2)	3306(2)	12395(2)	28(1)	1
O4	−1097(3)	2567(2)	12917(2)	26(1)	1
N1	−1484(3)	318(2)	7771(2)	19(1)	1
N2	−427(3)	3058(2)	10092(2)	17(1)	1
C1	−2156(4)	122(3)	5845(3)	21(1)	1
C2	−3085(4)	−432(3)	4868(3)	26(1)	1
C3	−4235(4)	−1278(3)	4793(3)	29(1)	1
C4	−4475(4)	−1601(3)	5694(3)	27(1)	1
C5	−3581(4)	−1073(3)	6696(3)	22(1)	1
C6	−2428(3)	−212(3)	6751(3)	17(1)	1
C7	−907(4)	1035(3)	5907(3)	26(1)	1
C8	−3838(4)	−1442(3)	7673(3)	28(1)	1
C9	−1336(4)	1477(3)	8342(3)	18(1)	1
C10	−142(3)	1880(3)	9337(3)	18(1)	1
C11	1345(4)	1957(3)	8979(3)	18(1)	1
C12	1718(4)	2656(3)	8350(3)	23(1)	1
C13	3062(4)	2668(3)	7994(3)	27(1)	1
C14	4036(4)	1966(3)	8251(3)	31(1)	1
C15	3670(4)	1273(3)	8881(3)	29(1)	1
C16	2327(4)	1269(3)	9244(3)	22(1)	1
C17	−1272(4)	2998(3)	11032(3)	18(1)	1
C18	−1488(4)	4273(3)	11625(3)	23(1)	1
C19	−2720(3)	2215(3)	10557(3)	22(1)	1
C20	−1860(4)	1549(3)	13076(3)	34(1)	1
S1	−3236(1)	4577(1)	8726(1)	21(1)	1
O5	−1701(2)	4967(2)	9334(2)	21(1)	1
C21	−3078(4)	4195(3)	7319(3)	24(1)	1
C22	−4025(4)	5899(3)	8851(3)	28(1)	1
S2	−6946(1)	4189(1)	5257(1)	33(1)	1
O6	−6257(3)	4632(2)	6429(2)	44(1)	1
C23	−7843(5)	5339(3)	5052(3)	41(1)	1
C24	−8531(4)	3214(3)	5200(3)	37(1)	1

Table S6. Bond lengths [Å] and angles [°].

P1–O3	1.486(2)	C9–N1–C6	122.9(3)
P1–O2	1.498(2)	C10–N2–C17	115.6(2)
P1–O4	1.610(2)	C2–C1–C6	117.8(3)
P1–C17	1.859(3)	C2–C1–C7	120.3(3)
O1–C9	1.232(4)	C6–C1–C7	121.9(3)
O4–C20	1.440(4)	C3–C2–C1	121.2(3)
N1–C9	1.339(4)	C2–C3–C4	120.0(3)
N1–C6	1.440(4)	C3–C4–C5	121.3(3)
N2–C10	1.512(4)	C6–C5–C4	117.6(3)
N2–C17	1.545(4)	C6–C5–C8	121.4(3)
C1–C2	1.398(4)	C4–C5–C8	121.0(3)
C1–C6	1.406(4)	C5–C6–C1	122.1(3)
C1–C7	1.501(5)	C5–C6–N1	118.1(3)
C2–C3	1.380(5)	C1–C6–N1	119.8(3)
C3–C4	1.385(5)	O1–C9–N1	125.0(3)
C4–C5	1.402(5)	O1–C9–C10	120.8(3)
C5–C6	1.400(4)	N1–C9–C10	114.2(3)
C5–C8	1.513(5)	N2–C10–C11	112.1(3)
C9–C10	1.542(4)	N2–C10–C9	107.7(3)
C10–C11	1.518(4)	C11–C10–C9	110.6(3)
C11–C16	1.385(4)	C16–C11–C12	119.5(3)
C11–C12	1.396(5)	C16–C11–C10	118.7(3)
C12–C13	1.388(5)	C12–C11–C10	121.8(3)
C13–C14	1.388(5)	C13–C12–C11	120.5(3)
C14–C15	1.389(5)	C12–C13–C14	119.8(3)
C15–C16	1.389(5)	C13–C14–C15	119.8(4)
C17–C19	1.523(4)	C16–C15–C14	120.3(3)
C17–C18	1.525(4)	C11–C16–C15	120.1(3)
S1–O5	1.524(2)	C19–C17–C18	111.0(3)
S1–C21	1.774(3)	C19–C17–N2	109.2(3)
S1–C22	1.785(3)	C18–C17–N2	105.3(2)
S2–O6	1.504(3)	C19–C17–P1	113.1(2)
S2–C23	1.763(4)	C18–C17–P1	110.0(2)
S2–C24	1.780(4)	N2–C17–P1	107.9(2)
O3–P1–O2	119.94(14)	O5–S1–C21	106.30(15)
O3–P1–O4	108.07(14)	O5–S1–C22	106.43(14)
O2–P1–O4	109.36(13)	C21–S1–C22	96.86(17)
O3–P1–C17	107.67(14)	O6–S2–C23	106.31(18)
O2–P1–C17	109.70(14)	O6–S2–C24	105.72(18)
O4–P1–C17	100.32(14)	C23–S2–C24	96.59(19)
C20–O4–P1	122.0(2)		

Symmetry transformations used to generate equivalent atoms:

Table S7. Anisotropic displacement parameters [$\text{\AA}^2 \times 10^3$]. The anisotropic displacement factor exponent takes the form: $-2\pi^2 [h^2 a^{*2} U^{11} + \dots + 2 h k a^* b^* U^{12}]$.

Atom	U^{11}	U^{22}	U^{33}	U^{23}	U^{13}	U^{12}
P1	21(1)	18(1)	19(1)	8(1)	1(1)	6(1)
O1	23(1)	16(1)	24(1)	6(1)	0(1)	6(1)
O2	24(1)	16(1)	20(1)	7(1)	3(1)	8(1)
O3	25(1)	25(1)	32(1)	13(1)	-7(1)	-1(1)
O4	36(2)	23(1)	25(1)	11(1)	13(1)	10(1)
N1	19(2)	17(2)	21(2)	8(1)	-1(1)	6(1)
N2	17(2)	16(2)	18(2)	7(1)	-1(1)	3(1)
C1	24(2)	18(2)	22(2)	5(1)	4(2)	6(2)
C2	32(2)	24(2)	24(2)	7(2)	2(2)	7(2)
C3	28(2)	26(2)	26(2)	0(2)	-2(2)	8(2)
C4	17(2)	19(2)	40(2)	3(2)	0(2)	3(2)
C5	16(2)	18(2)	31(2)	8(2)	5(2)	4(2)
C6	15(2)	13(2)	21(2)	2(1)	-1(1)	6(1)
C7	34(2)	23(2)	23(2)	9(2)	6(2)	5(2)
C8	21(2)	24(2)	39(2)	11(2)	6(2)	2(2)
C9	16(2)	20(2)	20(2)	8(1)	6(1)	5(2)
C10	18(2)	15(2)	20(2)	5(1)	2(1)	5(1)
C11	16(2)	16(2)	19(2)	0(1)	1(1)	3(1)
C12	21(2)	23(2)	22(2)	6(2)	-2(2)	1(2)
C13	23(2)	29(2)	23(2)	6(2)	-1(2)	-7(2)
C14	20(2)	32(2)	29(2)	-5(2)	6(2)	-3(2)
C15	20(2)	18(2)	43(2)	0(2)	-1(2)	7(2)
C16	19(2)	15(2)	29(2)	3(2)	2(2)	2(2)
C17	18(2)	19(2)	18(2)	7(1)	5(1)	5(2)
C18	29(2)	22(2)	23(2)	9(2)	8(2)	11(2)
C19	18(2)	26(2)	25(2)	10(2)	4(2)	6(2)
C20	35(2)	36(2)	35(2)	14(2)	13(2)	3(2)
S1	18(1)	19(1)	24(1)	6(1)	-1(1)	1(1)
O5	16(1)	21(1)	25(1)	8(1)	-5(1)	-2(1)
C21	28(2)	20(2)	24(2)	5(2)	0(2)	5(2)
C22	24(2)	19(2)	36(2)	2(2)	-5(2)	9(2)
S2	31(1)	32(1)	35(1)	9(1)	4(1)	6(1)
O6	33(2)	56(2)	37(2)	12(1)	-13(1)	2(1)
C23	55(3)	32(2)	37(2)	10(2)	12(2)	11(2)
C24	34(2)	34(2)	41(2)	13(2)	-5(2)	4(2)

Table S8. Hydrogen coordinates [$\times 10^4$] and isotropic displacement parameters [$\text{\AA}^2 \times 10^3$].

Atom	<i>x</i>	<i>y</i>	<i>z</i>	<i>U</i> _{eq}	<i>S.o.f.</i>
H1A	−1040(40)	−120(30)	8010(30)	22(10)	1
H1B	470(40)	3590(30)	10360(30)	49(12)	1
H1C	−980(40)	3400(30)	9700(30)	21(9)	1
H2	−2922	−223	4243	32	1
H3	−4861	−1638	4124	35	1
H4	−5260	−2193	5631	33	1
H7A	−679	940	5171	39	1
H7B	−61	932	6355	39	1
H7C	−1168	1830	6234	39	1
H8A	−3973	−747	8279	42	1
H8B	−3001	−1786	7889	42	1
H8C	−4706	−2031	7483	42	1
H10	−207	1287	9726	21	1
H12	1046	3127	8165	28	1
H13	3316	3154	7575	32	1
H14	4950	1959	7996	37	1
H15	4340	800	9065	35	1
H16	2082	794	9675	26	1
H18A	−2041	4577	11120	35	1
H18B	−543	4764	11898	35	1
H18C	−2020	4297	12238	35	1
H19A	−3301	2239	11144	33	1
H19B	−2554	1398	10197	33	1
H19C	−3237	2505	10025	33	1
H20A	−2724	1242	12528	52	1
H20B	−2149	1780	13806	52	1
H20C	−1227	934	13001	52	1
H21A	−2447	4828	7199	37	1
H21B	−4038	4093	6901	37	1
H21C	−2661	3453	7080	37	1
H22A	−4148	6285	9613	43	1
H22B	−4971	5700	8394	43	1
H22C	−3389	6438	8615	43	1
H23A	−8412	5637	5646	62	1
H23B	−8488	5035	4356	62	1
H23C	−7127	5984	5040	62	1
H24A	−8253	2502	5333	55	1
H24B	−9106	2989	4478	55	1
H24C	−9107	3614	5757	55	1

Table S9. Hydrogen bonds [\AA and $^\circ$].

$D-H\cdots A$	$d(D-H)$	$d(H\cdots A)$	$d(D\cdots A)$	$\angle(DHA)$
$N1-H1A\cdots O2^i$	0.81(3)	1.96(3)	2.778(4)	179(4)
$N2-H1B\cdots O5^{ii}$	0.96(4)	1.89(4)	2.794(4)	155(3)
$N2-H1C\cdots O1$	0.91(3)	2.18(3)	2.696(4)	115(2)
$N2-H1C\cdots O5$	0.91(3)	2.23(3)	3.070(3)	153(3)

Symmetry transformations used to generate equivalent atoms:

(i) $-x, -y, -z+2$ (ii) $-x, -y+1, -z+2$

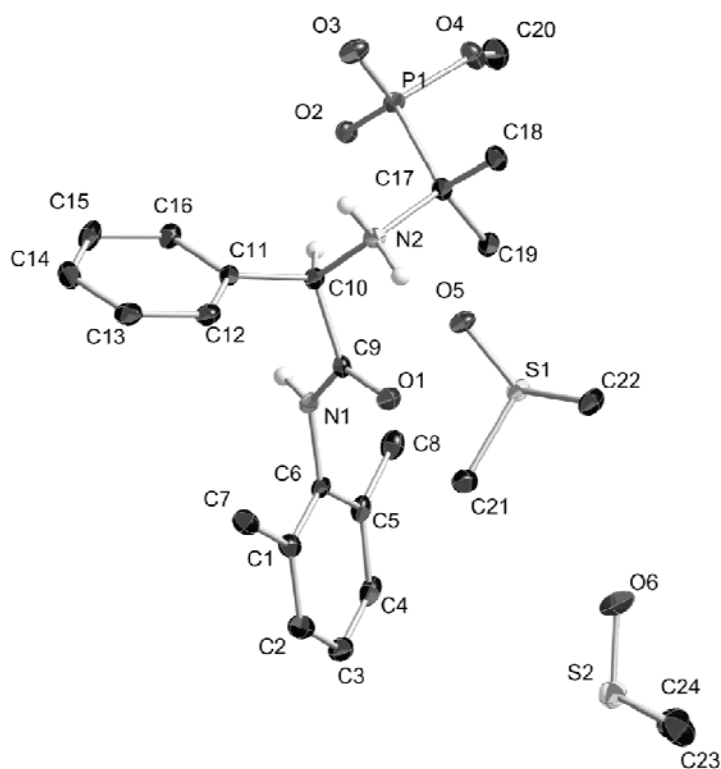


Figure S10: Thermal ellipsoids drawn at the 35% probability level, selected hydrogens omitted for clarity.

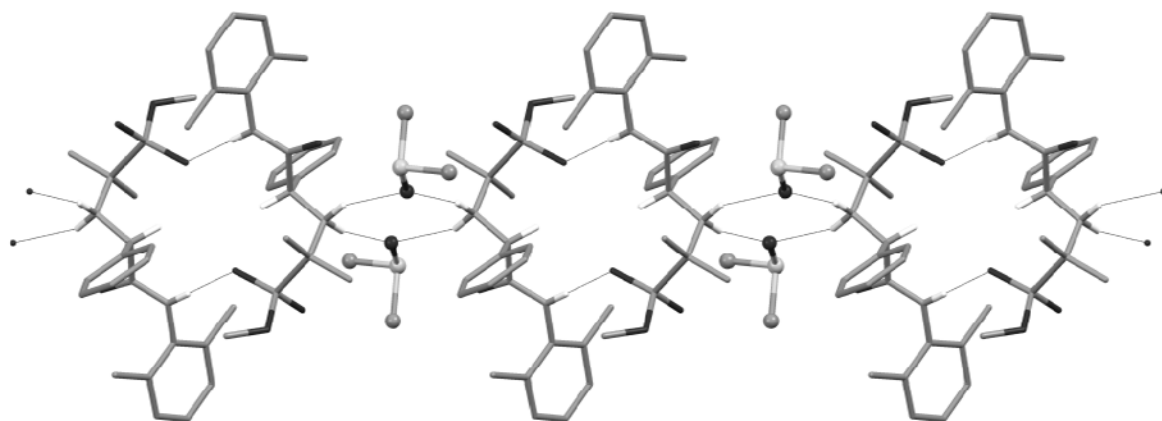


Figure S11: Hydrogen bonded chains extend along the b axis

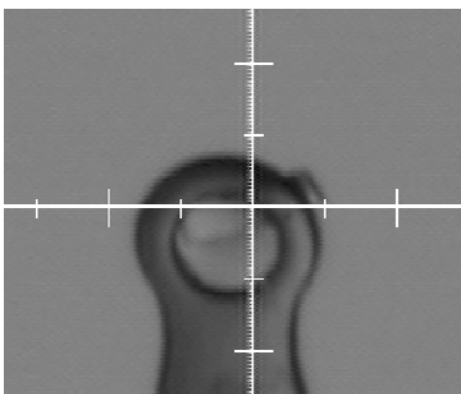


Figure S12: Crystal image

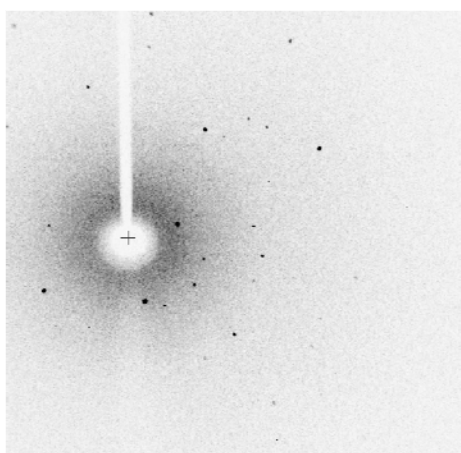


Figure S13: Representative diffraction frame

Section S6: VCD investigation over single enantiomers entry n°1 Table n°3

Entry n°1 of Table 3 was enantiomerically separated adopting a CHIRALPAK QN-AX column under polar organic mode as previously described in section S2 (Figure S14). The isolated fractions (F1 and F2) were characterized for their purity having ee% of 99% (F1) and 74% (F2) respectively (Figure S15 and 16). A desalting step was applied: each fraction was dissolved in water + 0.1% Formic acid and separately captured on a reversed-phase C-18 SPE (500mg cartridge) column. The SPE column was first rinsed with MeOH (3 column volumes) and then conditioned with water (3 volumes). Afterwards, the sample was applied. After washing with 2 column volumes of water, the product was eluted using MeOH. The collected fractions were dried under vacuum leading to a white solid.

The desalted fractions were analyzed by VCD spectrometry and compared to their calculated spectra. Fraction 1 was assigned as R enantiomer and Fraction 2 presented areas of overlap with the S enantiomer, however probably due to the lower enantiomeric purity of this fraction the assignment was not unequivocal (Figure S16 to S23).

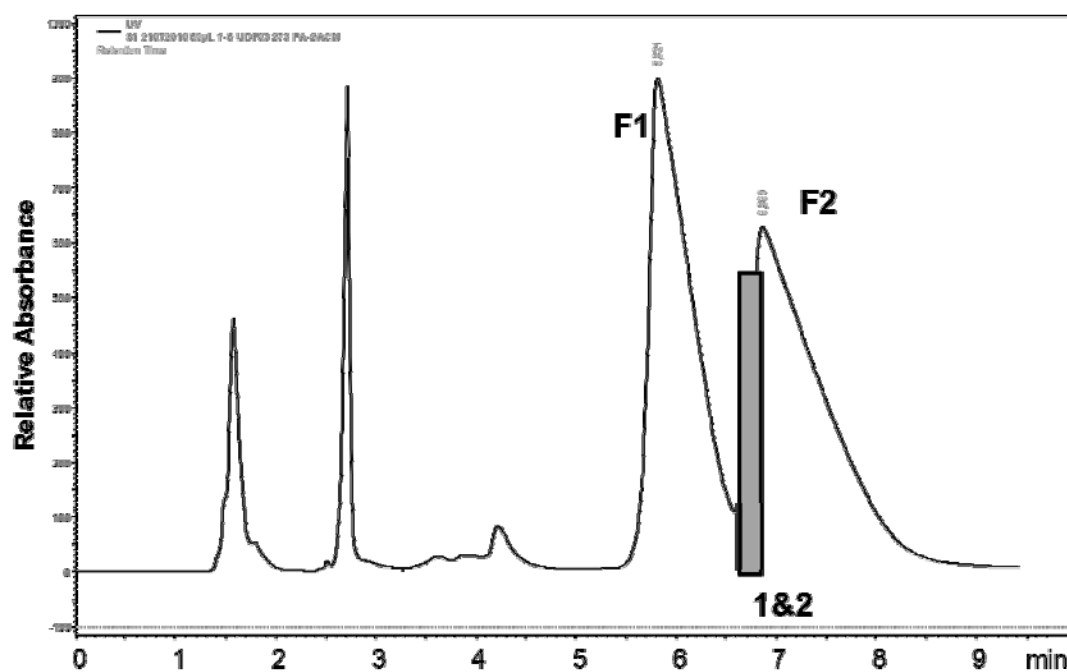


Figure S14: Semipreparative separation of entry n°1 Table 3 on CHIRALPAK QN-AX. Injection of 1 mg compound (100 μ L of 10mg/mL solution in MeOH 0.5%FA solution). Mobile phase MeOH 33mM formic acid 5mM ammonium acetate. α = 1,16, λ =273nm.

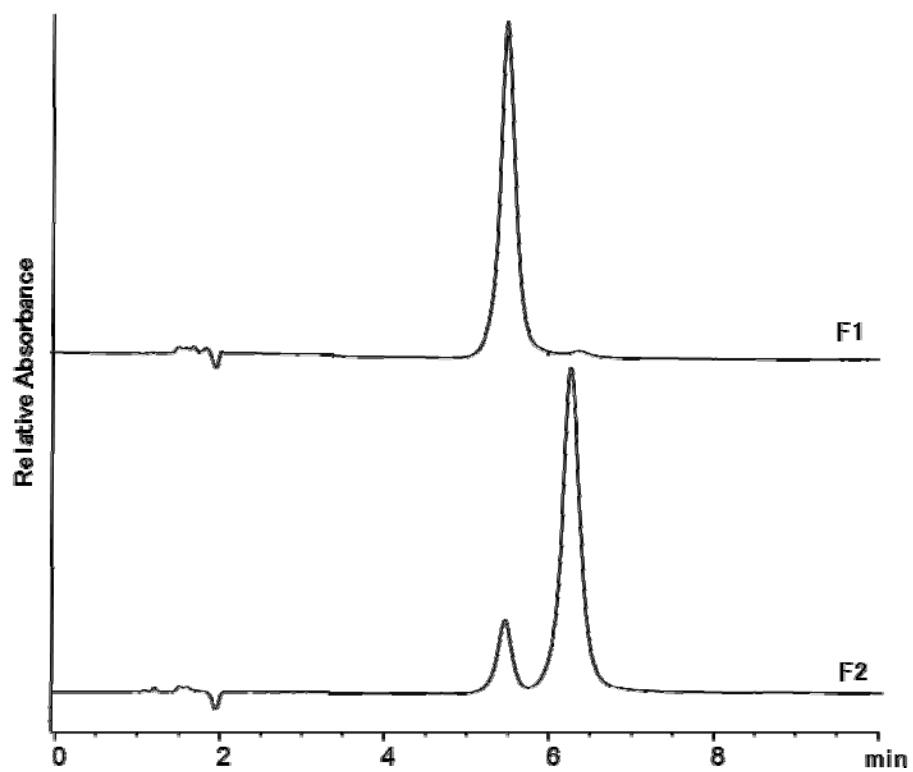


Figure S15: Determination of enantiomeric excess (ee%) of collected fractions. F1 ee=99%, F2: A%=13-87% ee=74%. Separation performed on a CHIRALPAK QN AX column. Mobile phase MeOH/ CAN 50/50 v/v 175mM acetic acid, 4mM ammonium acetate

VCD analysis: Materials and Methods

Computational Spectral Simulations: A Monte Carlo molecular mechanics search for low energy geometries was conducted for the structures outlined in Figure 1. The *Maestro* graphical interface (Schrödinger Inc.) was used to generate starting coordinates for conformers. All conformers within 5 kcal/mole of the lowest energy conformer were used as starting points for density functional theory (DFT) minimizations within *Gaussian09*.

Optimized structures, harmonic vibrational frequencies/intensities, VCD rotational strengths, and free energies at STP (including zero-point energies) were determined for each conformer. In these calculations, the functional B3LYP and the basis set 6-31G* were used. Simulations of infrared and VCD spectra for each conformation were generated using an in-house built program to fit Lorentzian line shapes (12 cm⁻¹ line width) to the computed spectra thereby allowing direct comparisons between simulated and experimental spectra.

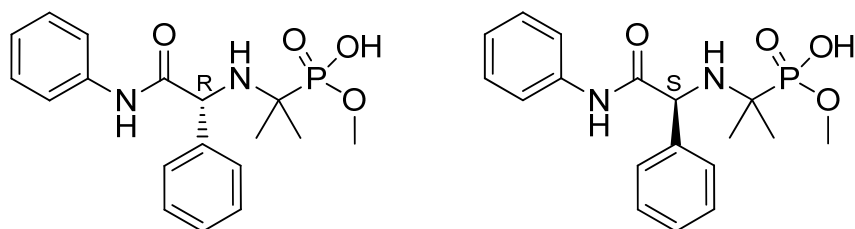


Figure S16. Chemical structure adopted for the VCD calculation

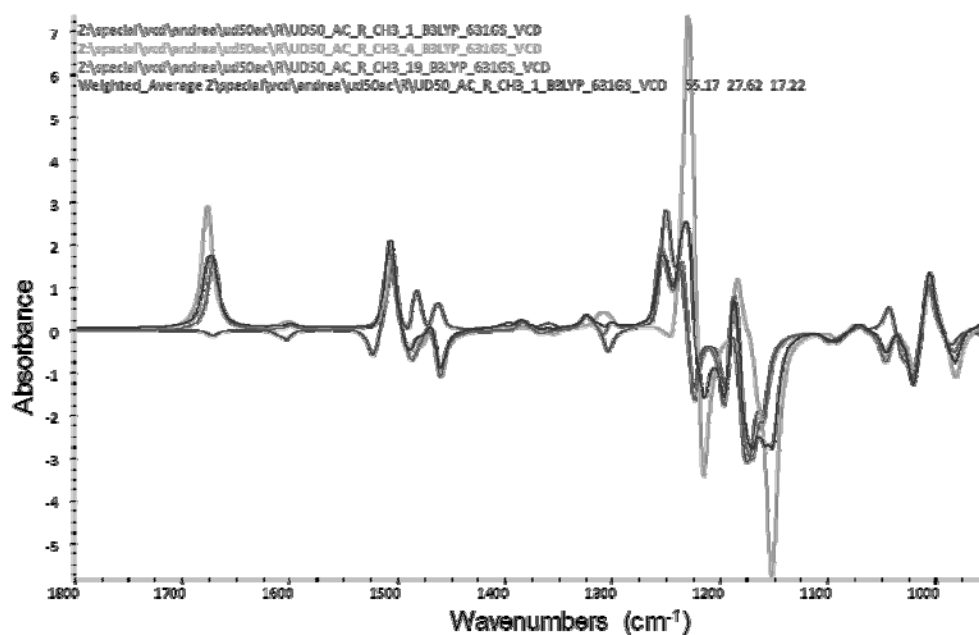


Figure S18: VCD spectra of the three conformations of lowest energy and the average spectrum according to Boltzmann distribution of these conformations for the **R** enantiomer: Their relative energies and distribution are listed in the table S9.

Table S9: Simulation of conformations for the **R** enantiomer.

Sample Name	Include ?	Hartrees	Kcal/mol	Relative Kcal	Population	Distribution	Area	Area 2	NRE
Z:\special\vcd\andrea\ud50ac\R\UD50_AC_R_CH3_19_B3LYP_631GS_VCD	Y	-1490.56...	-935346...	0.00	1.000000	55.17	16.08	-93.10	2653.47
Z:\special\vcd\andrea\ud50ac\R\UD50_AC_R_CH3_4_B3LYP_631GS_VCD	Y	-1490.56...	-935346...	0.41	0.500609	27.62	52.54	-66.51	2678.44
Z:\special\vcd\andrea\ud50ac\R\UD50_AC_R_CH3_1_B3LYP_631GS_VCD	Y	-1490.56...	-935346...	0.69	0.312089	17.22	33.27	-69.98	2663.99
Z:\special\vcd\andrea\ud50ac\R\UD50_AC_R_CH3_36_B3LYP_631GS_VCD	N	-1490.56...	-935341...	5.64	0.000073	00.00	17.42	12.09	2605.75
Z:\special\vcd\andrea\ud50ac\R\UD50_AC_R_CH3_18_B3LYP_631GS_VCD	N	-1490.56...	-935344...	2.54	0.013752	00.00	-27.93	10.31	2646.20
Z:\special\vcd\andrea\ud50ac\R\UD50_AC_R_CH3_34_B3LYP_631GS_VCD	N	-1490.56...	-935341...	5.64	0.000073	00.00	17.41	12.05	2605.73
Z:\special\vcd\andrea\ud50ac\R\UD50_AC_R_CH3_15_B3LYP_631GS_VCD	N	-1490.56...	-935344...	2.54	0.013752	00.00	-27.82	10.30	2646.18
Z:\special\vcd\andrea\ud50ac\R\UD50_AC_R_CH3_29_B3LYP_631GS_VCD	N	-1490.56...	-935341...	5.61	0.000077	00.00	9.05	-38.04	2645.83
Z:\special\vcd\andrea\ud50ac\R\UD50_AC_R_CH3_30_B3LYP_631GS_VCD	N	-1490.56...	-935341...	5.08	0.000189	00.00	45.09	8.90	2640.42
Z:\special\vcd\andrea\ud50ac\R\UD50_AC_R_CH3_26_B3LYP_631GS_VCD	N	-1490.56...	-935344...	2.15	0.026558	00.00	-10.66	116.04	2680.03
Z:\special\vcd\andrea\ud50ac\R\UD50_AC_R_CH3_27_B3LYP_631GS_VCD	N	-1490.56...	-935344...	2.16	0.026114	00.00	-10.66	116.01	2680.06
Z:\special\vcd\andrea\ud50ac\R\UD50_AC_R_CH3_7_B3LYP_631GS_VCD	N	-1490.56...	-935344...	2.37	0.018321	00.00	-3.42	19.67	2653.03
Z:\special\vcd\andrea\ud50ac\R\UD50_AC_R_CH3_6_B3LYP_631GS_VCD	N	-1490.56...	-935344...	2.37	0.018321	00.00	-3.29	19.19	2653.04
Z:\special\vcd\andrea\ud50ac\R\UD50_AC_R_CH3_13_B3LYP_631GS_VCD	N	-1490.56...	-935341...	5.61	0.000077	00.00	-5.68	-40.49	2643.72
Z:\special\vcd\andrea\ud50ac\R\UD50_AC_R_CH3_14_B3LYP_631GS_VCD	N	-1490.56...	-935344...	2.44	0.016280	00.00	15.53	90.84	2668.51
Z:\special\vcd\andrea\ud50ac\R\UD50_AC_R_CH3_25_B3LYP_631GS_VCD	N	-1490.56...	-935341...	5.62	0.000076	00.00	-5.64	-40.58	2643.79
Z:\special\vcd\andrea\ud50ac\R\UD50_AC_R_CH3_17_B3LYP_631GS_VCD	N	-1490.56...	-935344...	2.54	0.013752	00.00	-27.92	10.35	2646.20
Z:\special\vcd\andrea\ud50ac\R\UD50_AC_R_CH3_16_B3LYP_631GS_VCD	N	-1490.56...	-935344...	2.54	0.013752	00.00	-27.87	10.33	2646.18
Z:\special\vcd\andrea\ud50ac\R\UD50_AC_R_CH3_10_B3LYP_631GS_VCD	N	-1490.56...	-935344...	2.44	0.016280	00.00	15.68	90.59	2668.55
Z:\special\vcd\andrea\ud50ac\R\UD50_AC_R_CH3_31_B3LYP_631GS_VCD	N	-1490.56...	-935343...	3.70	0.001942	00.00	37.72	23.76	2642.89
Z:\special\vcd\andrea\ud50ac\R\UD50_AC_R_CH3_12_B3LYP_631GS_VCD	N	-1490.56...	-935344...	2.54	0.013752	00.00	-27.84	10.34	2646.19
Z:\special\vcd\andrea\ud50ac\R\UD50_AC_R_CH3_35_B3LYP_631GS_VCD	N	-1490.56...	-935343...	3.55	0.002501	00.00	22.74	11.21	2663.55
Z:\special\vcd\andrea\ud50ac\R\UD50_AC_R_CH3_32_B3LYP_631GS_VCD	N	-1490.56...	-935343...	3.70	0.001942	00.00	37.70	23.68	2642.87
Z:\special\vcd\andrea\ud50ac\R\UD50_AC_R_CH3_24_B3LYP_631GS_VCD	N	-1490.56...	-935343...	3.54	0.002543	00.00	22.75	11.22	2663.54
Z:\special\vcd\andrea\ud50ac\R\UD50_AC_R_CH3_33_B3LYP_631GS_VCD	N	-1490.56...	-935343...	3.56	0.002459	00.00	22.75	11.50	2663.57

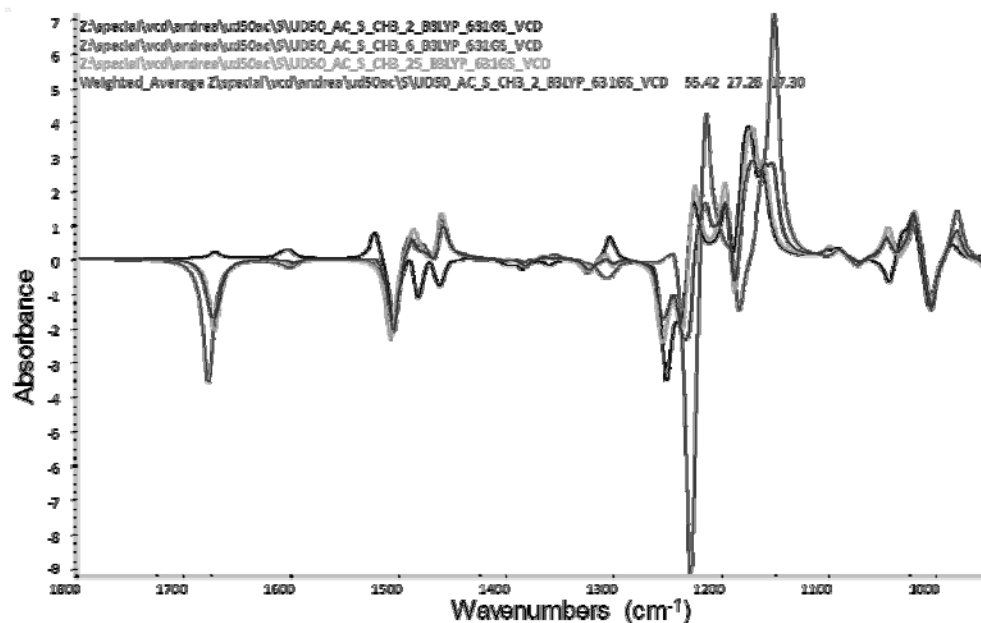


Figure S19: VCD spectra of the three conformations of lowest energy and the average spectrum according to Boltzmann distribution of these conformations for the **The S** enantiomer:. Their relative energies and distribution are listed in the table below.

TableS10: Simulation of conformations for the **S** enantiomer.

Sample Name	Include ?	Hartrees	Kcal/mol	Relative Kcal	Population	Distribution	Area	Area 2	NRE
Z:\special\vcd\andrea\ud50ac\S\UD50_AC_S_CH3_25_B3LYP_631GS_VCD	Y	-1490.56...	-935346...	0.00	1.000000	55.42	-15.96	92.96	2653.43
Z:\special\vcd\andrea\ud50ac\S\UD50_AC_S_CH3_6_B3LYP_631GS_VCD	Y	-1490.56...	-935346...	0.42	0.492231	27.28	-52.63	65.61	2678.49
Z:\special\vcd\andrea\ud50ac\S\UD50_AC_S_CH3_2_B3LYP_631GS_VCD	Y	-1490.56...	-935346...	0.69	0.312089	17.30	-33.20	69.98	2664.00
Z:\special\vcd\andrea\ud50ac\S\UD50_AC_S_CH3_36_B3LYP_631GS_VCD	N	-1490.56...	-935341...	5.65	0.000072	00.00	-17.44	-12.10	2605.75
Z:\special\vcd\andrea\ud50ac\S\UD50_AC_S_CH3_20_B3LYP_631GS_VCD	N	-1490.56...	-935344...	2.55	0.013522	00.00	27.87	-10.35	2646.20
Z:\special\vcd\andrea\ud50ac\S\UD50_AC_S_CH3_34_B3LYP_631GS_VCD	N	-1490.56...	-935341...	5.65	0.000072	00.00	-17.41	-12.05	2605.73
Z:\special\vcd\andrea\ud50ac\S\UD50_AC_S_CH3_21_B3LYP_631GS_VCD	N	-1490.56...	-935344...	2.55	0.013522	00.00	27.91	-10.37	2646.21
Z:\special\vcd\andrea\ud50ac\S\UD50_AC_S_CH3_1_B3LYP_631GS_VCD	N	-1490.55...	-935338...	7.81	0.000002	00.00	20.51	108.31	2638.98
Z:\special\vcd\andrea\ud50ac\S\UD50_AC_S_CH3_33_B3LYP_631GS_VCD	N	-1490.56...	-935341...	5.65	0.000072	00.00	-17.41	-12.05	2605.73
Z:\special\vcd\andrea\ud50ac\S\UD50_AC_S_CH3_30_B3LYP_631GS_VCD	N	-1490.56...	-935341...	5.09	0.000186	00.00	-45.21	-8.88	2640.40
Z:\special\vcd\andrea\ud50ac\S\UD50_AC_S_CH3_27_B3LYP_631GS_VCD	N	-1490.56...	-935344...	2.13	0.027470	00.00	11.70	-117.15	2679.97
Z:\special\vcd\andrea\ud50ac\S\UD50_AC_S_CH3_14_B3LYP_631GS_VCD	N	-1490.56...	-935344...	2.38	0.018015	00.00	3.33	-19.46	2653.04
Z:\special\vcd\andrea\ud50ac\S\UD50_AC_S_CH3_7_B3LYP_631GS_VCD	N	-1490.56...	-935344...	2.38	0.018015	00.00	3.30	-19.19	2653.04
Z:\special\vcd\andrea\ud50ac\S\UD50_AC_S_CH3_29_B3LYP_631GS_VCD	N	-1490.56...	-935341...	5.62	0.000076	00.00	-9.06	38.04	2645.83
Z:\special\vcd\andrea\ud50ac\S\UD50_AC_S_CH3_12_B3LYP_631GS_VCD	N	-1490.56...	-935344...	2.45	0.016007	00.00	-15.68	-90.59	2668.55
Z:\special\vcd\andrea\ud50ac\S\UD50_AC_S_CH3_32_B3LYP_631GS_VCD	N	-1490.56...	-935341...	5.65	0.000072	00.00	-17.41	-12.05	2605.73
Z:\special\vcd\andrea\ud50ac\S\UD50_AC_S_CH3_16_B3LYP_631GS_VCD	N	-1490.56...	-935344...	2.45	0.016007	00.00	-15.52	-90.82	2668.51
Z:\special\vcd\andrea\ud50ac\S\UD50_AC_S_CH3_22_B3LYP_631GS_VCD	N	-1490.56...	-935344...	2.55	0.013522	00.00	27.93	-10.31	2646.21
Z:\special\vcd\andrea\ud50ac\S\UD50_AC_S_CH3_8_B3LYP_631GS_VCD	N	-1490.56...	-935344...	2.38	0.018015	00.00	3.30	-19.19	2653.04
Z:\special\vcd\andrea\ud50ac\S\UD50_AC_S_CH3_15_B3LYP_631GS_VCD	N	-1490.56...	-935341...	5.62	0.000076	00.00	5.68	40.49	2643.72
Z:\special\vcd\andrea\ud50ac\S\UD50_AC_S_CH3_18_B3LYP_631GS_VCD	N	-1490.56...	-935344...	2.55	0.013522	00.00	27.86	-10.30	2646.19
Z:\special\vcd\andrea\ud50ac\S\UD50_AC_S_CH3_17_B3LYP_631GS_VCD	N	-1490.56...	-935344...	2.54	0.013752	00.00	27.83	-10.29	2646.19
Z:\special\vcd\andrea\ud50ac\S\UD50_AC_S_CH3_26_B3LYP_631GS_VCD	N	-1490.56...	-935343...	3.71	0.001909	00.00	-37.73	-23.78	2642.88
Z:\special\vcd\andrea\ud50ac\S\UD50_AC_S_CH3_28_B3LYP_631GS_VCD	N	-1490.56...	-935343...	3.56	0.002459	00.00	-22.73	-11.18	2663.52
Z:\special\vcd\andrea\ud50ac\S\UD50_AC_S_CH3_31_B3LYP_631GS_VCD	N	-1490.56...	-935343...	3.56	0.002459	00.00	-22.80	-11.58	2663.56

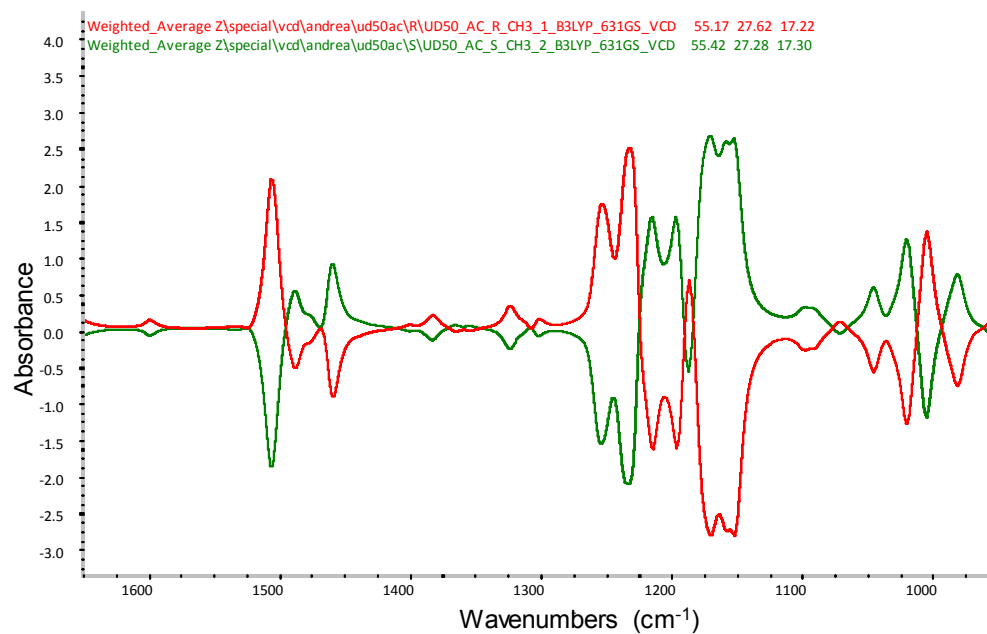


Figure S20: Overlay for simulated spectra of R (red) and S (green) enantiomer

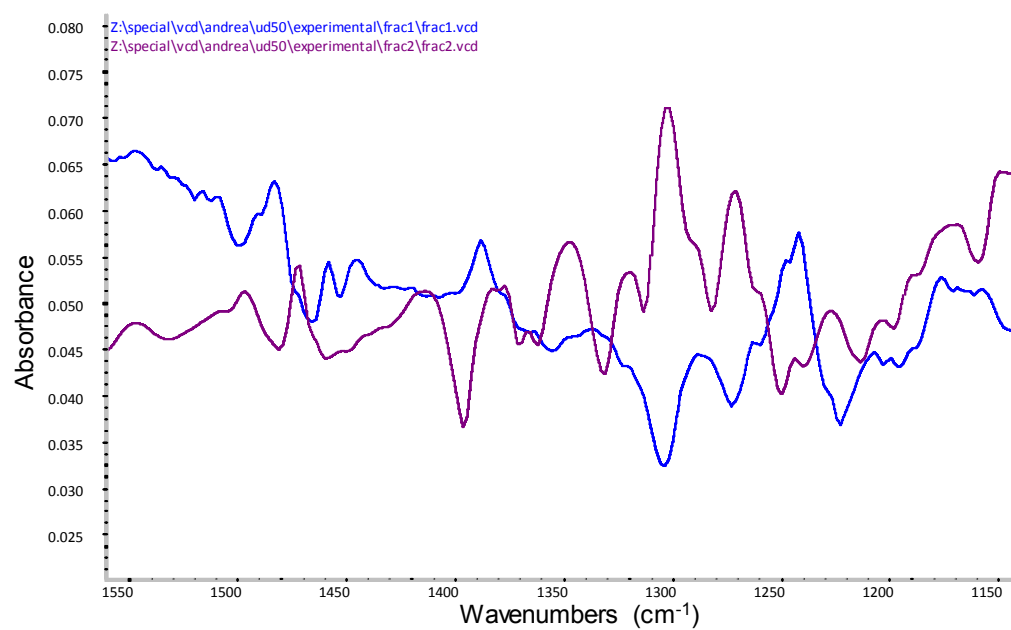


Figure S21: Overlay of the experimental VCD spectra from fraction 1 (blue) and 2 (violet).

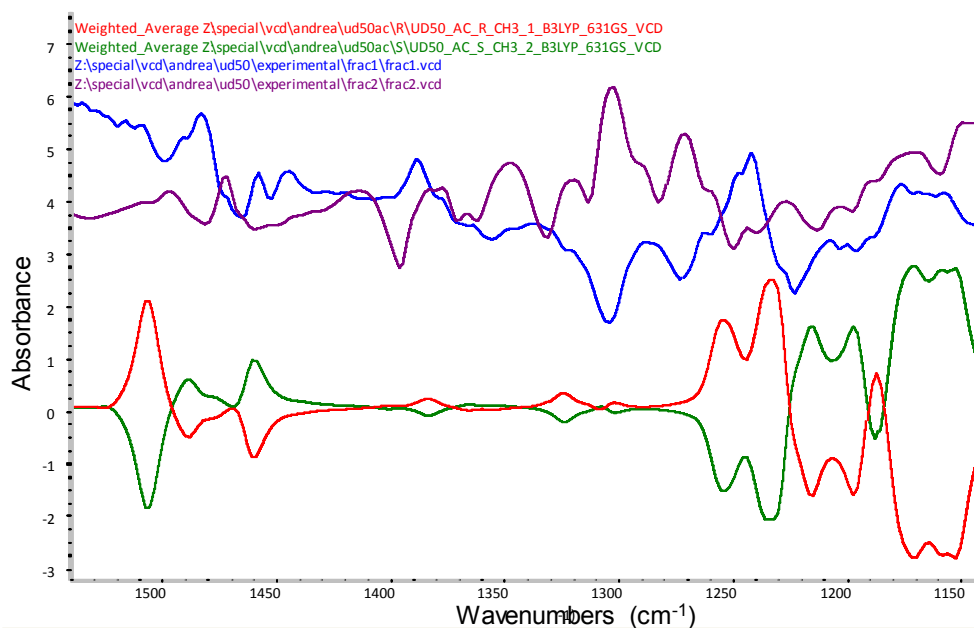


Figure S22: Overlay of experimental calculated VCD spectra.

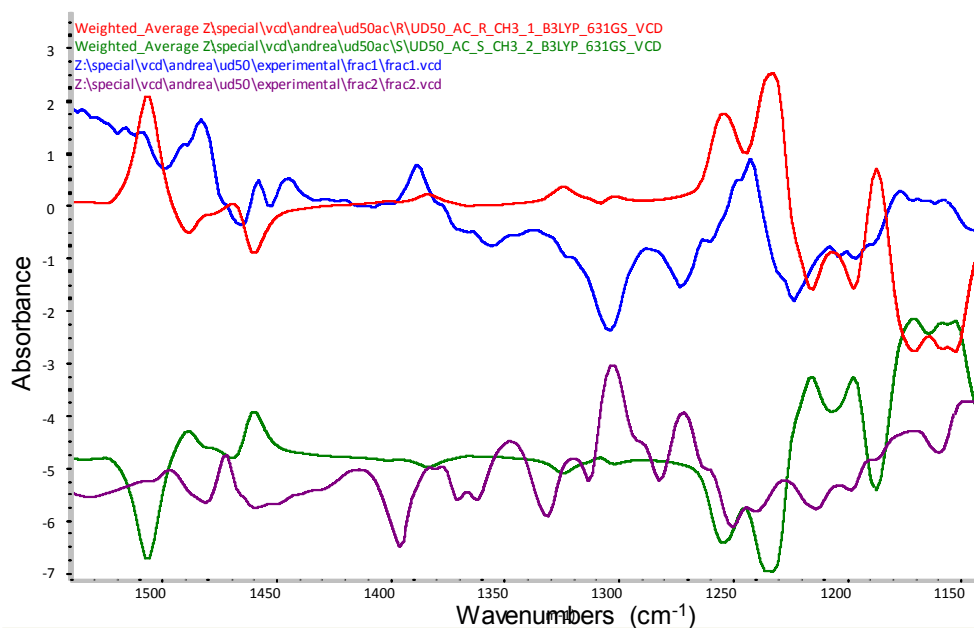


Figure S23: Assignment of the isolated enantiomer respect to the simulated spectra. Fraction 1 could be assigned to the R enantiomer (blue trace experimental, red trace from calculations); fraction 2 could not be unequivocally assigned as S although partial fitting was observed (violet trace experimental, green trace from calculations).

SECTION S9: NMRs SPECTRA

(the spectra of compound 1 table 1 is reported as example of the NMR spectra of the compound lybrary, the complete supporting information is available at: https://www.dropbox.com/s/wb0ju3ta13u7m33/Supporting_Info_AndreaGargano_UGIAPAMCR.docx

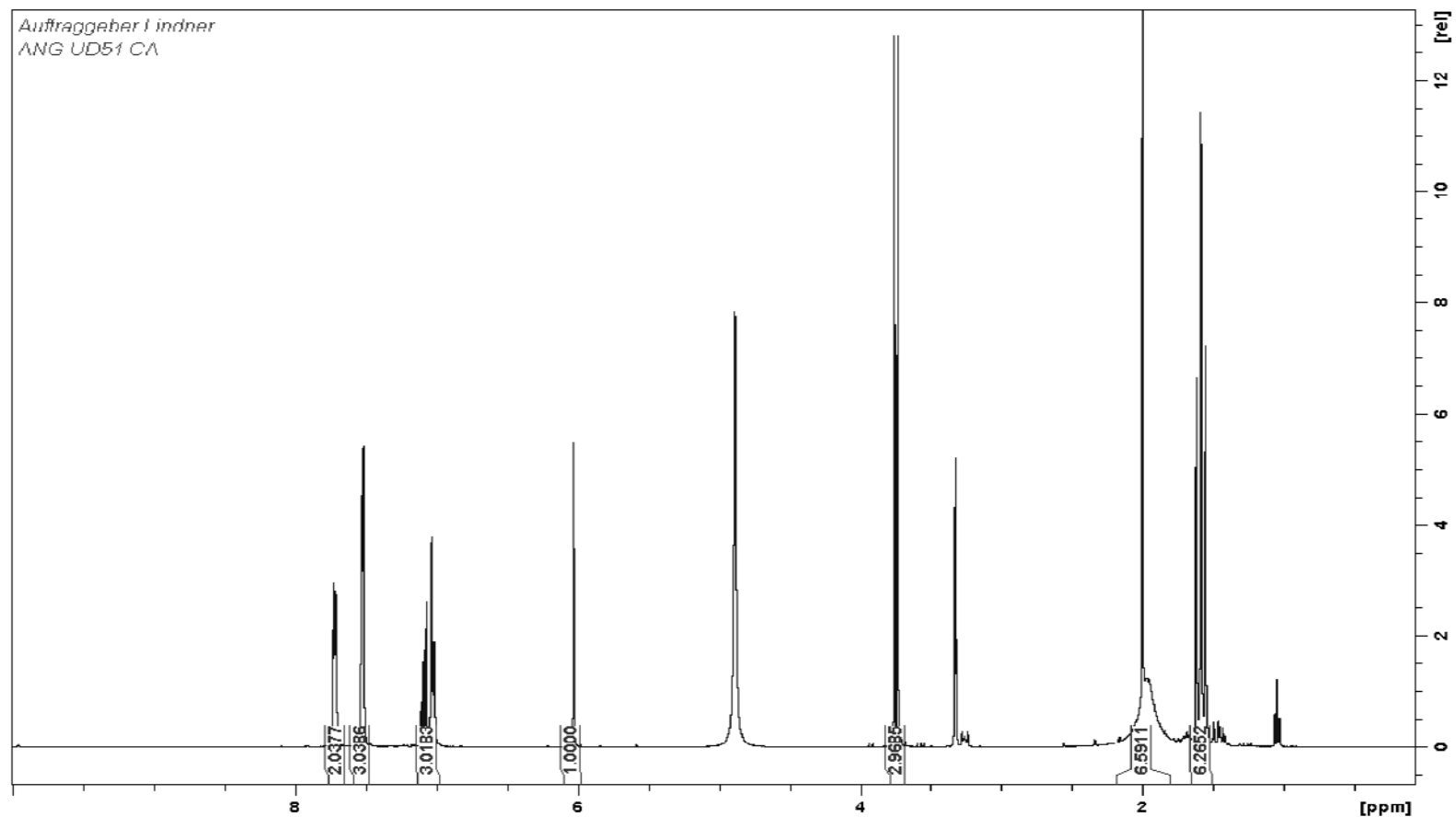
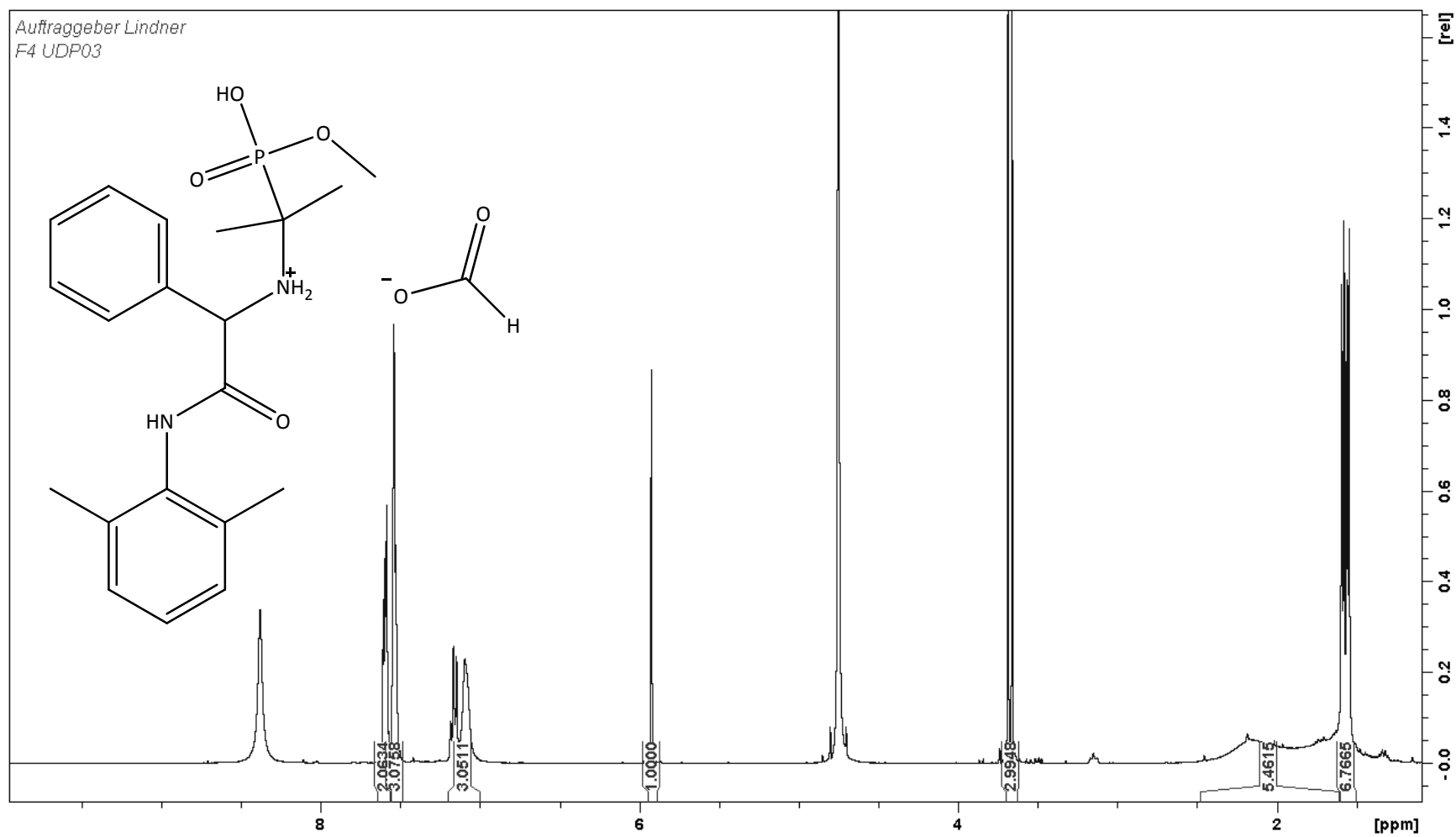
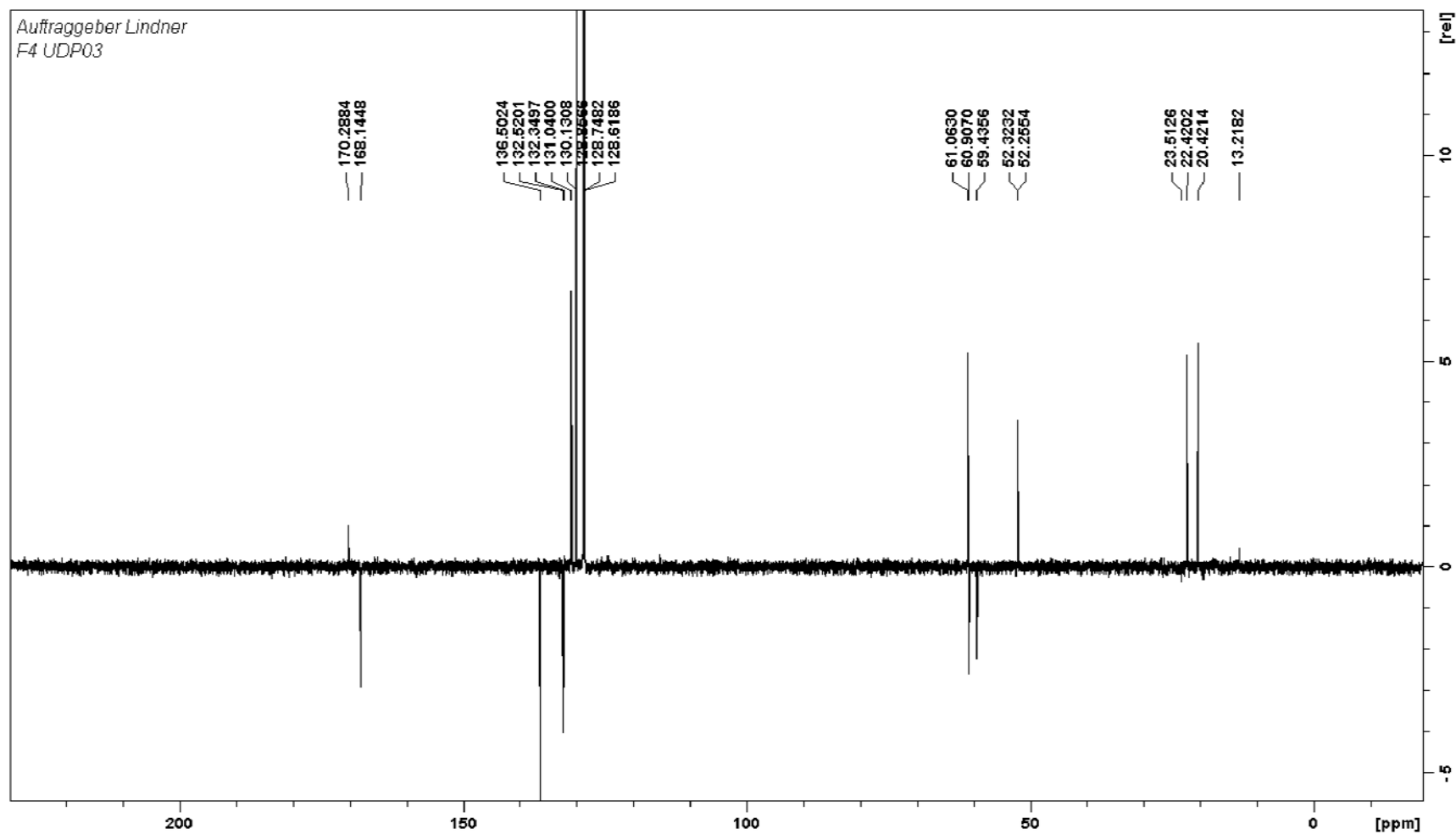


Figure S8 (a)

^1H -NMR spectrum in CD_3OD of entry n°1 table n°3

**Figure S8 (b)**

^1H -NMR spectrum in CD_3OD of entry n°**1** *table n°3* purified through chiral anion exchange chromatography

**Figure S8 (c)**

^{13}C -NMR spectrum in CD_3OD of entry n°1 table n°3

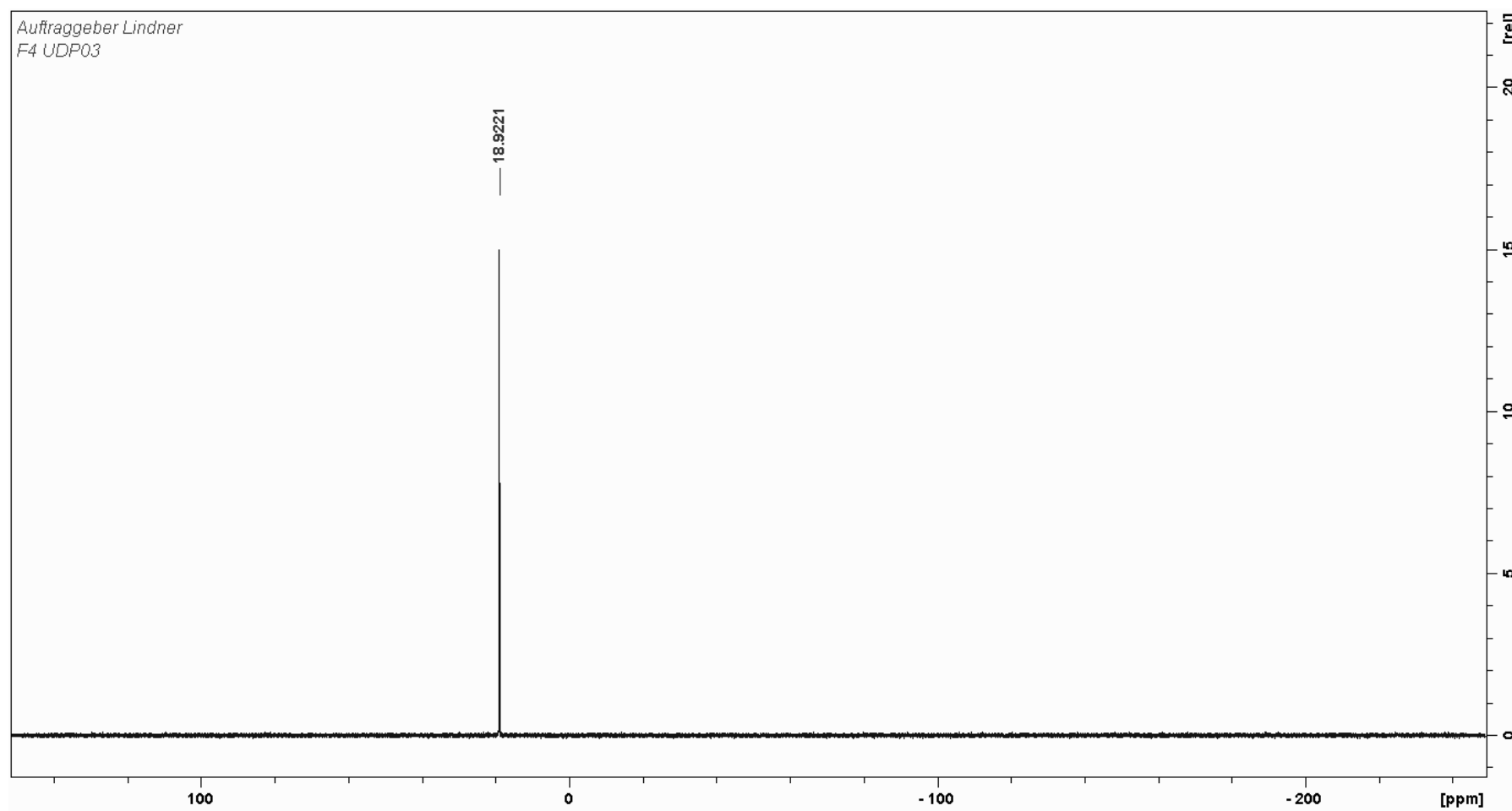
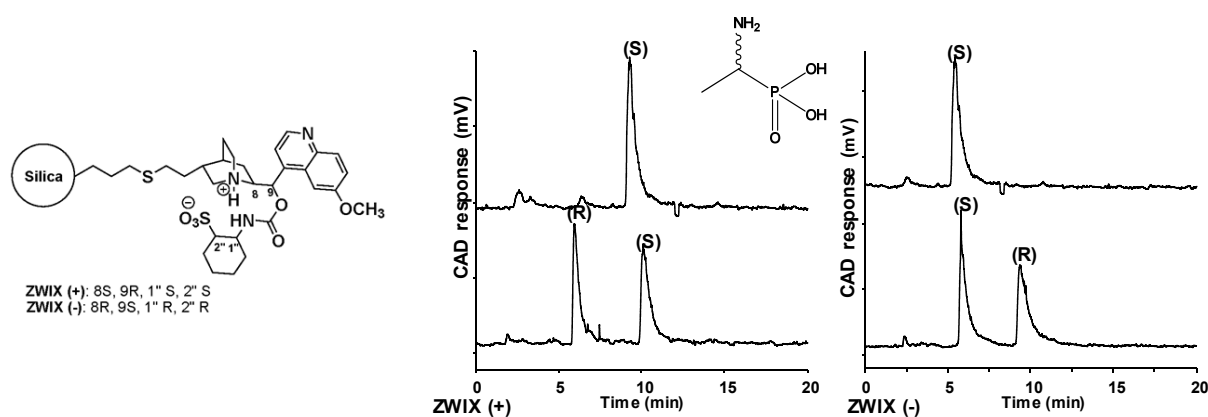


Figure S8 (d)

^{31}P -NMR spectrum in CD_3OD of entry **1** table n°3

Manuscript 2



Graphical abstract:

Direct high-performance liquid chromatographic enantioseparation of free α , β and γ -aminophosphonic acids employing cinchona-based chiral zwitterionic ion-exchangers

Direct high-performance liquid chromatographic enantioseparation of free α , β and γ -aminophosphonic acids employing cinchona-based chiral zwitterionic ion-exchangers

Andrea F.G. Gargano¹, Michal Kohout^{1,2}, Pavla Macíková^{1,3}, Michael Lämmerhofer^{1,4}, Wolfgang Lindner^{1*}

¹ *Department of Analytical Chemistry, University of Vienna, Waehringer Strasse 38, 1090 Vienna, Austria*

² *Current address: Department of Organic Chemistry, Institute of Chemical Technology, Technicka 5, CZ-16628, Prague, Czech Republic*

³ *Current address: Regional Centre of Advanced Technologies and Materials, Department of Analytical Chemistry, Faculty of Science, Palacky University, 17. listopadu 1192/12, 77146 Olomouc, Czech Republic*

⁴ *Current address: Institute of Pharmaceutical Sciences, University of Tübingen, Auf der Morgenstelle 8, 72076 Tübingen, Germany*

*wolfgang.lindner@univie.ac.at

T +43 1 4277 52300

F +43 1 4277 9523

michael.laemmerhofer@uni-tuebingen.de

Institute of Pharmaceutical Sciences

University of Tübingen

Auf der Morgenstelle 8

72076 Tübingen, Germany

T +49 7071 29 78793

F +49 7071 29 4565

Abstract

In the present contribution we report a chiral HPLC enantioseparation method for free α , β , γ -aminophosphonic acids, amino hydroxy phosphonic acids and aromatic aminophosphinic acids with different substitution patterns. The enantioseparation of these novel synthons was achieved by means of HPLC on CHIRALPAK ZWIX (+) and (-) (cinchona-based chiral zwitterionic ion-exchangers) under polar organic chromatographic elution conditions. Mobile phase characteristics like acid-to-base ratio, type of counterion and solvent composition were systematically varied in order to investigate their effect on the separation performance and achieve optimal separation conditions for the set of analytes. Under the optimized conditions, 32 out of 37 studied racemic aminophosphonic acids reached baseline separation employing a single generic mass spectrometry-compatible mobile phase, with reversal of elution order using (+) and (-) columns.

Keywords

HPLC, Cinchona chiral zwitterionic ion-exchanger, Enantiomer separation, Chiral stationary phases, Aminophosphonic acids, Aminophosphinic acids.

1. Introduction

Amino acids (AAs) play a key role in nature, constituting the structural units of peptides, proteins and enzymes. Aminophosphonic acids (APAs) can very efficiently act as biomimetics, representing phosphorus analogues of AAs, competing with them at the active site of enzymes^[42a] and cell receptors^[56]. Their unique characteristics render this class of compounds of considerable biological and pharmacological interest, with applications as antitumor^[44a-d], neuroactive^[44c, 45], antihypertensive^[44c, 46], antimicrobial^[44c, 47], herbicidal^[42a, 44c] and imaging agents^[48].

Biological activity is mostly observed for one enantiomer and, therefore, utilization strictly relies on the enantiomeric purity of these chiral compounds. Several concepts for the preparation of such chiral chemical entities with high enantiomeric excess (ee) have been reported to date^[54, 57]. In contrast, there are only a few enantioselective analytical methods currently available for chiral phosphonic acids, which might be useful for the study of stereochemical pathways of stereoselective reactions and for the determination of the enantiomeric purity of the final products. Most often, indirect ³¹P-NMR methods, based on different complexation induced shifts (CIS) of signals of diastereomeric complexes with a chiral solvating agent, are used for these purposes^[57a, 58]. While several reports have been published on different enantioselective HPLC methods for the ester analogues of phosphonic and amino phosphonic acids, e.g., using cellulose or amylose based chiral stationary phases (CSPs)^[59] or 'Pirkle-type' CSPs^[60], publications dealing with the direct enantioseparation of amino phosphonic acids with underivatized phosphonic acid are scarce. In a previous paper, we demonstrated the separation of *N*-derivatized amino phosphonic and phosphinic acids by HPLC on quinine-derived chiral anion exchangers^[61]. In this contribution we focus on direct enantioseparation of underivatized aminophosphonic and aminophosphinic acids on recently commercialized quinine and quinidine-based zwitterionic chiral stationary phases CHIRALPAK ZWIX (+) and ZWIX (-)TM, respectively. The optimization of flow rate, temperature, mobile phase compositions and buffer system is discussed and enantioseparation of a pool of 44 amino acids including aminophosphonic, phosphinic, carboxylic, and sulfonic acid with a single mobile phase is reported.

2. Experimental

1. Materials

HPLC solvents methanol (MeOH) and acetonitrile (ACN) were of HPLC-grade quality and purchased from Sigma-Aldrich (Vienna, Austria) and Merck (Darmstadt, Germany). Millipore grade water was obtained from an in-house Millipore system (resistivity: 18.2 M Ω x cm at 25 °C). Formic acid (FA), 7N ammonia solution in MeOH, acetic acid (AA), propionic acid (PA), β -alanine (β -Ala) were of analytical grade from Sigma–Aldrich (Vienna, Austria).

Racemic mixtures and/or enantiomerically pure analytes employed in this study were either commercially available (Across organics, Belgium) or synthesized according to established procedures ^{[62] [57d]}. About 1 mg of the analytes were dissolved initially in 100 μ L of DMSO and then diluted with 900 μ L of mobile phase. The injected sample volume was 5 μ L.

2. Apparatus and chromatography

HPLC experiments were carried out using an 1100 series LC system from Agilent Technologies (Agilent, Waldbronn, Germany) equipped with a binary gradient pump, autosampler, vacuum degasser, temperature-controlled column compartment, diode array detector for the detection of aromatic samples and Charged Aerosol Detector (CAD) from Thermo Fisher Scientific (Sunnyvale, CA, USA) for non-aromatic species. In order to reduce the baseline noise of the CAD detector under reduced flow rate (0.93 and 0.66 mm/s), the gas flow was reduced from 35 psi to 30 psi. The data were processed with Agilent ChemStation software version Rev. B.01.03.

The chiral stationary phases adopted for the study were CHIRALPAK ZWIX (+) and (-)TM (150×3 mm I.D., 3 μ m particle size) from Chiral Technologies Europe (Illkirch, France) based on *trans*-(1''S, 2''S)-N-[[[(8S, 9R)-6'-methoxycinchonan-9-yl)oxy]carbonyl]-2-2''-aminocyclohexanesulfonic acid and *trans*-(1''R, 2''R)-N-[[[(8R, 9S)-6'-methoxycinchonan-9-yl)oxy]carbonyl]-2-2''-aminocyclohexanesulfonic acid, respectively ^[28, 63].

In the mobile phase study the chromatographic parameters if not specified differently were: flow rate 1.33 mm/s (0.55 mL/min), injection of 5 μ L, detection at 258 nm. The dead time (t_0) was determined after each modification of chromatographic parameters by three injections of acetone.

The mobile phase for the enantioseparation of the aminophosphonic acid reported in *table 1* was MeOH containing 200 mM formic acid and 50 mM ammonia. Other conditions were as follows: flow rate, 0.93 mm/s; temperature, 15 °C.

3. Results and Discussion

The present contribution describes the enantioseparation of free (non-protected) aminophosphonic acids (APAs) on novel cinchona-based chiral zwitterionic ion-exchangers commercialized under the name CHIRALPAK ZWIX (+)TM and (-)TM. The chemical structure of these CSPs is depicted in *Fig. 1*. Note that the chiral selectors in CHIRLAPAK ZWIX(+) and (-) are diastereomeric, but experimentally show pseudo-enantiomeric behavior, inter alia a reversed elution order for aminophosphonic acids enantiomers in most cases. The selectors were immobilized onto thiopropyl-modified silica gel employing thiol-ene click chemistry, generating brush type stationary phases ^[28, 63-64].

The enantirecognition properties of the cinchona-based ZWIX CSPs towards unprotected amino carboxylic and aminosulfonic acids have been described in previous contributions ^[63-64, 64c, 65]. However, no investigations have been performed so far towards the phosphonic and phosphinic acid analogues. Using these low molecular weight CSPs we could baseline separate ($R_s \geq 1.5$) 32 out of 37 compounds (**1-36** and **44**) of the investigated aminophosphonic acid analyte set with a single MS compatible mobile phase.

3.1. Optimization of chromatographic parameters

In order to achieve the best separation performance, separation conditions were optimized using the ZWIX (-) that had proven lower enantiodiscriminating properties in our preliminary experiments. In order to fulfill the scope we selected two α -aminophosphonic acids: ([amino(phenyl)methyl]phosphonic acid **13**, [1-amino-3-(phenylthio)propyl]phosphonic acid **25**) and one γ -aminophosphonic acid: (3-amino-2-(4-chlorophenyl)propyl)phosphonic acid, phaclofen, **38**) (see *Fig. 2a*) to study the influence of different chromatographic parameters on the enantioseparation.

3.2. Effect of counterion type and of acid-to-base ratio

Similarly to anion exchange (AX) mode, in chiral zwitterionic ion-exchange (ZWIX) chromatography long range electrostatic interactions between oppositely charged atoms of chiral selector (SO) and zwitterionic selectand (SA) constitute the initial dominant type of driving forces for the SA approach towards the chiral selector. Subsequently, directional H-bond mediated ionic interactions can orient the zwitterionic SA at the chiral zwitterionic selector resulting eventually in a chiral recognition process ^[26a, 63, 66].

In such type of chromatography the proton activity of the mobile phase influences the ionization status of both species and therefore the strength of their interaction. As a consequence the ion exchange process will be affected by the strength, concentration and ratio of the acidic and the basic additives. Therefore all these parameters have to be considered in the phase of optimization of the buffer system.

Previously published data on chiral enantioseparation on such stationary phases reported a weak dependency of separation parameters by variation of the type of base ^[64a]. Therefore, in our optimization we employed ammonia throughout as base component in the eluent and focused our study on the effect given by the type of the acidic component of the mobile phase. Furthermore, we evaluated the possibility of the use of a zwitterionic buffer (β -alanine).

As starting test conditions we adopted an acid to base ratio of 3:1, which was previously identified as a successful operation mode for ZWIX CSPs, using 150 mM of the acidic component and 50 mM of NH_3 in MeOH ^[64a]. Employing such composition, we studied the effect of the strength and different chain length (i.e. distinct lipophilicity and acidity) of an acidic additive (formic, acetic and propionic acid). *Fig. 2* summarizes the findings, comparing the effects of such variation on selectivity and resolution. Separation factors for α -aminophosphonic acid were slightly higher with acetic acid than propionic acid, but dropped significantly with formic acid (FA). The trend was different for compound **38**, which showed the highest enantioselectivity with formic acid and the lowest with acetic acid. However, the gain in enantioselectivity for α -aminophosphonic acid with acetic and propionic acid as compared to formic acid was unfavorably outbalanced by the loss in efficiency. We observed in general a negative trend in terms of separation efficiency when formic acid was substituted by acetic acid or propionic acid. The reason for such phenomena could be ascribed to the lower acidity of acids with longer aliphatic chains and therefore with their less pronounced counter ion properties.

As a compromise between the length and strength of the acidic additive, we decided to test a zwitterionic additive, namely β -alanine. Due to solubility reasons, it was necessary to add an excess of FA (100 mM) in order to obtain a clear 50 mM methanolic solution of β -alanine. The resulting mobile phase had an acid to base ratio of 3:1. Under such conditions we did not observe an improvement of the separation performances, however the possibility of using such zwitterionic buffer offer a further confirmation of a zwitterionic SA-SO interaction.

In addition to the variation of the type of buffer components it was also of interest to study the effect of the ratio of formic acid and ammonia on the retention characteristics. This parameter determines the proton activity of the mobile phase and therefore the charge state and interaction strength between SAs and SO. Altogether we tested five methanolic mobile phases containing 50 mM of basic additive (ammonia) with acidic component (formic acid) in a molar ratio between 1:5 and 2:1. The obtained results are summarized in *Fig. 3*. We observed a nearly constant retention factor in acidic mobile phases (ratio 1-5 to 1-1), once more confirming the double charge interaction between SA and SO. While the retention dropped significantly in basic media (ratio 2-1) as consequence of the reduced protonation of the quinuclidine ring. The resolution values showed their maximum in the acidic range (at 1-

5 or 1-4 ratio) but dropped significantly under neutral or basic conditions (1-1, 2-1). This result suggests that a modification of the proton activity of the medium could influence the spatial vicinity of the two charged units of the CSP (intramolecular counterions). The closer vicinity of these moieties in a strongly acidic media (due to a higher charge of the quinuclidine ring) would influence the spatial interactions between SA-SO resulting in differences in the chiral recognition.

In final experiments we investigated the dependence of the retention on the ionic strength at constant acid-to-base ratio. In accordance to an ion-exchange retention mechanism, higher retention factors were observed when mobile phases with lower buffer concentration were adopted. However, we did not observe significant differences in terms of selectivity and efficiency (data not shown) and therefore we selected a higher buffer concentration (200 mM formic acid – 50 mM ammonia) as final optimized eluent in order to reduce the analysis time. Generally, the trends with regards to effects of mobile phase additives on enantioseparation largely reflected those previously described for AAs ^[64a]. The stronger acidity of the aminophosphonic acid as SAs solely leads to minor shifts in optima of the resulting optimized mobile phase.

3.3. *Effect of solvent composition, temperature and flow rate*

As previously investigated, the tested Cinchona zwitterionic chiral ion-exchangers afforded the best results in polar organic mode ^[67]. However, in order to further tune the performance of this chromatographic method, we investigated the effect of the bulk solvent composition. First, we tested eluent systems based on MeOH (polar protic solvent) with a formic acid/ammonia ratio of 3 -1 and increasing content of ACN (polar aprotic solvent). Findings for the chromatographic parameters k_1 , α , R_s on the variation of the bulk solvent composition are depicted in *Fig. 4*. As expected, an increase in the ACN content increases retention times due to the reduced solvation power of such system. However, such modification does not significantly enhance separation properties. Furthermore, we tested the effect of the addition of small percentage (1-5%) of water in the elution media with various compositions (MeOH/ACN, 50/50 (data not shown) or 75/25; v/v), but no beneficial effect was observed for such three components mobile phase systems (*Fig. 5*).

Summarizing our findings we can conclude that mobile phases based solely on MeOH as bulk solvent offers the best performances.

In order to further improve the separation efficiency we tested the influence of flow rate (from 1.33 to 0.66 mm/s) and temperature (from 15 to 55 °C) on the separation (results summarized in *Fig. 6*). An analysis of the data from the temperature study reveals that retention factors and resolution are decreasing with increasing temperature (enthalpically driven retention process). A low temperature of 15 °C is favorable in terms of resolution. With regards to the flow rate, increased plate heights at faster flow velocities deteriorates

resolutions and thus low flow rates such as 0.66 mm/s would be preferred. However, due to an increased analysis times at such slow flow rates we selected a flow rate of 0.93 mm/s as optimum.

To summarize, the selected chromatographic parameters for the separation of the analytes reported in *Table 1* are: MeOH containing 200 mM formic acid and 50 mM ammonium as mobile phase. This generic eluent was run at a flow rate of 0.93 mm/s at a column temperature of 15 °C and provided sufficient separations for most of the target aminophosphonic acid compounds tested.

3.4. Elements of chiral recognition and structure-enantioselectivity relationships

The developed chromatographic method allowed us to baseline separate ($R_s \geq 1.5$) 32 from the pool of 37 aminophosphonic acid with above specified generic eluent, demonstrating once more the good enantioselectivity properties of such CSPs towards free aminophosphonic and phosphinic acids besides earlier reported amino carboxylic and sulfonic acids. The chromatographic data for all the tested aminoacids are summarized in *Table 1*.

Recently published papers investigated the enantioselectivity mechanism of cinchona based zwitterionic ion-exchangers studying the influence of structural modification of the SO together with the variation of the amphoteric SA species ^[67]. The simultaneous ionic interactions between the protonated base and dissociated acid of the SA towards the dissociated sulfonic group and protonated quinuclidine nitrogen of the SO are the dominating forces in the retention process. Ionic forces are not spatially oriented and have to be supported by oriented intermolecular SO-SA interactions in order to establish a different affinity towards one of the SA enantiomers. In the present case, both of the ionic interactions are, however, mediated via a H-bond which provides these interactions of directional character. Together with these elements the cinchona-based zwitterionic CSPs present geometrically and conformationally oriented interaction sites such as the carbamate group (H-bonding) and the quinoline ring ($\pi-\pi$). These elements together or separately constitute the elements of chiral recognition of the CSP which can lead to chiral discrimination between the enantiomers of the zwitterionic analytes.

The CHIRALPAK ZWIX(+) and (-) are based on quinine (QN) and quinidine (QD), respectively, coupled with 2-aminocyclohexylsulfonic acid (*S,S* and *R,R* respectively). These CSPs are, as mentioned above, considered as pseudoenantiomeric CSPs, and thus behave like enantiomers, although they are actually diastereomers. As a consequence this means that by changing from QN- to QD-based CSP the elution order of the SA enantiomers is switched (*Fig. 7*) ^[67]. In the present study the property of the reversal of the elution order of

aminophosphonic acid between (+) and (-) could not be extensively explored due to the lack of enantiomerically pure standards. However, with the available enantiomerically pure standards we observed reversal of elution order in analogy to what has been reported for amino carboxylic and amino sulfonic acids ^[67].

In *Fig. 8* we present a comparison between the enantioseparation performances (in terms of selectivity and resolution) for the tested ZWIX (+) and (-) CSPs. Except for some particular cases (e.g compounds **20** and **44**) we observed similar enantioselectivity properties for the two pseudo-enantiomeric CSPs (*Fig. 8a*). However, as can be seen in *Fig. 8b*, QD-based CSP (ZWIX (-)) generally offered lower separation efficiency and thus lower resolution. Although our analyte set was limited and it is hard to derive general conclusions, we observed a better enantioresolving power of the ZWIX (+) column for α -aminophosphonic acid, while the ZWIX (-) was better for γ -type aminophosphonic acid. Such phenomenon is most probably related to the diastereomeric nature of the selectors and their different conformations.

The heterogeneity, in terms of structural elements, of the analyte portfolio allowed us to evaluate the influence of various structural motifs on enantioselectivity, which may give therefore a deeper insight into the enantiorecognition process for such zwitterionic species. Generally, elongation of the alkyl side chain of the aminophosphonic acid resulted in increased retention and enhanced enantioselectivities (entries **1**, **2**, **9**, **10**, **11**). Similar effect was observed for branched aliphatic side chains (entries **3**, **7**). Introduction of polar thiol, sulfide or sulfone groups in the side chain (entries **4-6**) led to an increase of retention times, with the sulfone derivative (entry **6**) having the strongest influence. We assume that such behavior could be caused by additional hydrogen bond formation, although enantioselectivity is not significantly enhanced.

Comparing aliphatic and aromatic α -substituents of the same carbon chain length (entries **12** and **13**), the aliphatic one offered lower retention and enhanced enantioselectivity. This observation was further supported by better enantioselectivity and resolution achieved for entry **18** in comparison to entry **17**. These results indicate that in this particular case repulsive interactions may take place between the selector system and the bulky groups of respective aminophosphonic acids thus playing a more significant role in chiral recognition than potentially active attractive π - π interactions.

The introduction of a second α substituent results in higher steric hindrance which reduces the strength of the SO-SA interaction (lower retention factor) (compare entries **7/8** for aliphatic side chain and **13/14** as well as **19/20** for aromatic side chain). In case of aliphatic aminophosphonic acid this disturbs chiral distinction and leads to a worse separation (**7/8**). On the contrary, for the aromatic aminophosphonic acid (entries **13/14**, **19/20**) enantioselectivity gets improved. It is worth to note that increasing bulkiness of the alkyl

substituent at the stereogenic center yields increased enantioseparation factors in case of β -aminophosphonic acid as well (cf. entries **26,27**).

The enantioseparation of β -amino- α -hydroxy phosphonic acids was generally lower than in case of α -amino phosphonic acids. No chiral recognition was observed under given conditions for β -amino- α -hydroxy phosphonic acid derivatives bearing only hydrogen or aliphatic substituents (entries **28-30**). We found that a substitution with aromatic moieties (entries **31-34**) supports chiral recognition. With increasing size of the aromatic ring α -values increase, however, substitutions of hydrogens of the aromatic moiety by a methyl group was rather disturbing. In principle, the reason for poor performance of ZWIX CSPs towards these species is due to the presence of the α -hydroxyl group that apparently disturbs the chiral recognition mechanism, while other aliphatic β -amino phosphonic acids (e.g. **26, 27**) are well separated.

Monoprotic acids such as phosphinic acids (**41, 42**) and sulphonic acids (**43**) were separated with excellent selectivity and resolution; probably due to lack of the competing second acidic group (*Fig 9*). As a special class we chose cyclic secondary α -aminophosphonic acids. In both cases (entry **35, 40**) enantioseparation was not observed under given conditions, even though the compounds were well retained. We assume that this behavior could be caused by pronounced rigidity of these substrates which led to conformationally stable species that could not specifically interact with the SO. However, since the corresponding carboxylic acid analogs are well resolved, one may argue that these secondary amino phosphonic acid compounds just need a specific optimization.

4. Conclusion

In the present contribution we report the first direct HPLC enantioseparation of non-protected aminophosphonic acids on recently developed zwitterionic CSPs (Chiralpak ZWIX (+) and ZWIX (-)TM) based on cinchona alkaloid scaffold.

By variation of the chromatographic parameters we investigated the contribution of the mobile phase to the enantiorecognition of such zwitterionic analytes, finding optimum conditions under which most of the investigated APAs were successfully enantioseparated. We found that these diprotic acidic analytes (APAs) require in comparison to amino acids or peptides ^[65e] more acidic mobile phases, however, the character of the optimal buffer salt remained the same. In concord with this result, the use of zwitterionic buffer did not improve the general performance of the ZWIX CSPs.

Chiral recognition facilitated by cinchona-based CSPs is usually supported by strong π - π interactions of quinoline ring of the selector and an aromatic moiety of the analyte ^[66]. We documented that repulsive interactions of bulky aliphatic functionalities and, in the same time, their van der Waals interactions can strongly enhance chiral recognition properties of the novel zwitterionic CSPs.

We have shown that recently commercialized chiral stationary phases CHIRALPAK ZWIX (+) and ZWIX (-)TM can be employed for direct enantioseparation of free aminophosphonic and aminophosphinic acids in polar organic mode.

5. Acknowledgement

This work was financially supported by the University of Vienna through the interdisciplinary doctoral program: "Initiativkolleg Functional Molecules" (IK I041-N). Authors would like to thank Dr. Jan Pícha (Institute of Organic Chemistry and Biochemistry, AS CR) and Prof. Friedrich Hammerschmidt (Institute of Organic Chemistry, University of Vienna) for providing several samples of aminophosphonic acids. We are further grateful to the Operational Program Research and Development for Innovations - European Regional Development Fund (project CZ.1.05/2.1.00/03.0058) and the project of Palacký University in Olomouc PRF_2012_020 for the financial support.

6. Figure Caption

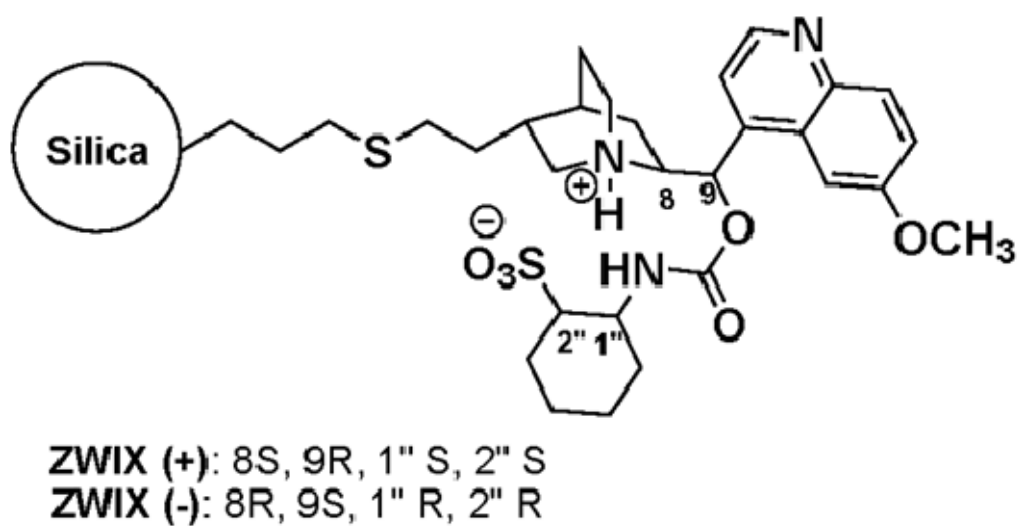
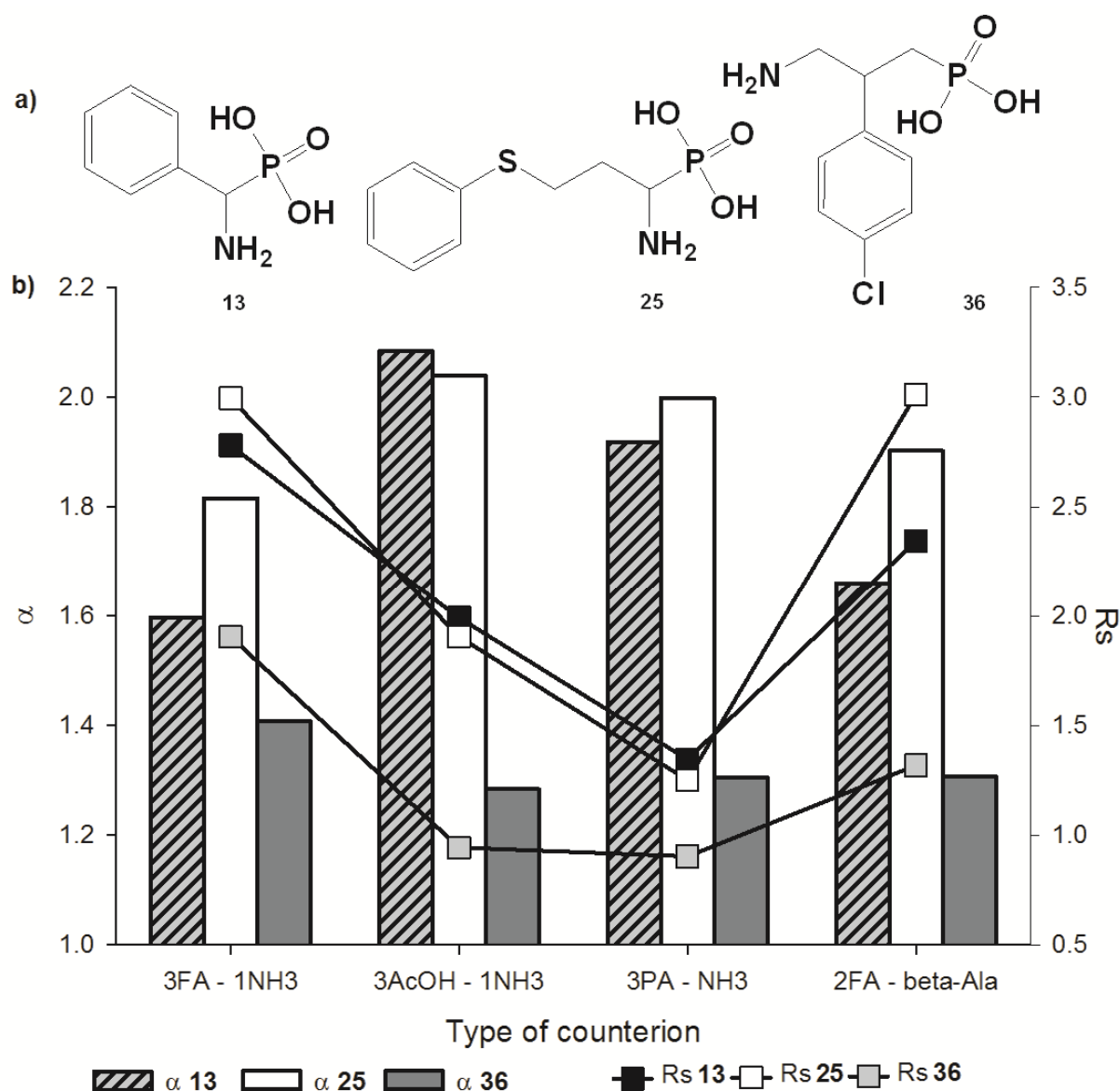
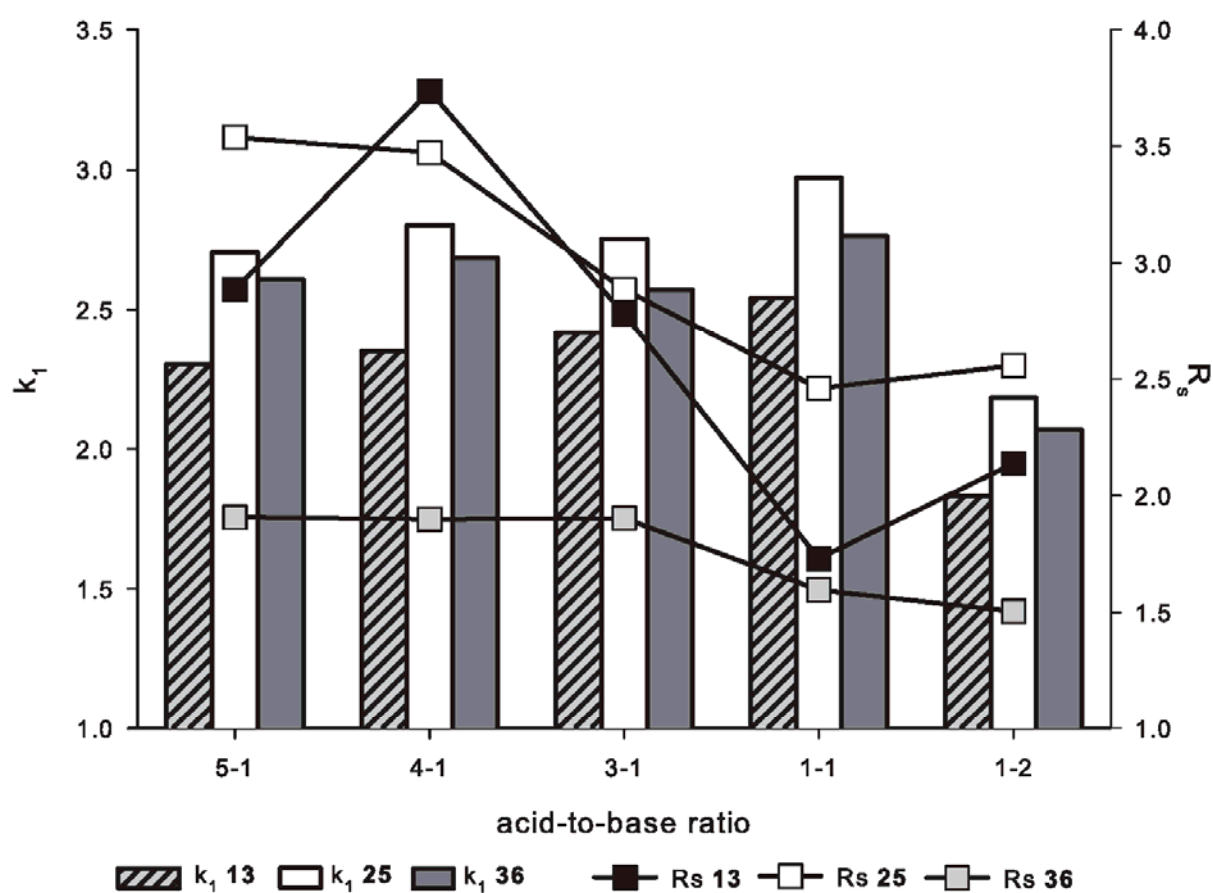


Fig.1.

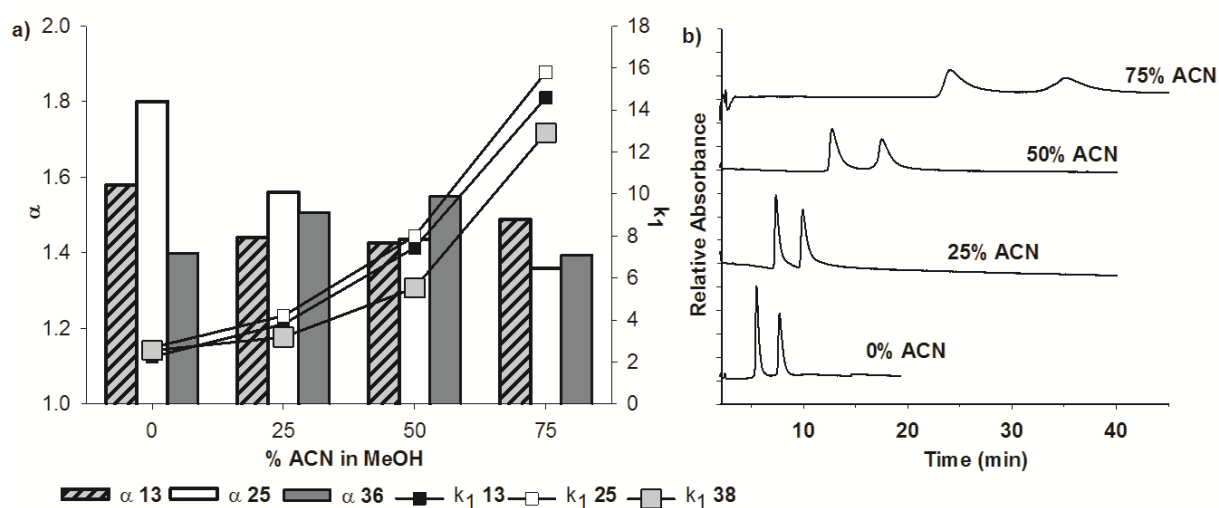
Chemical structures of the commercially available chiral zwitterionic stationary phases ZWIX(+) and ZWIX (-)TM

**Fig.2.**

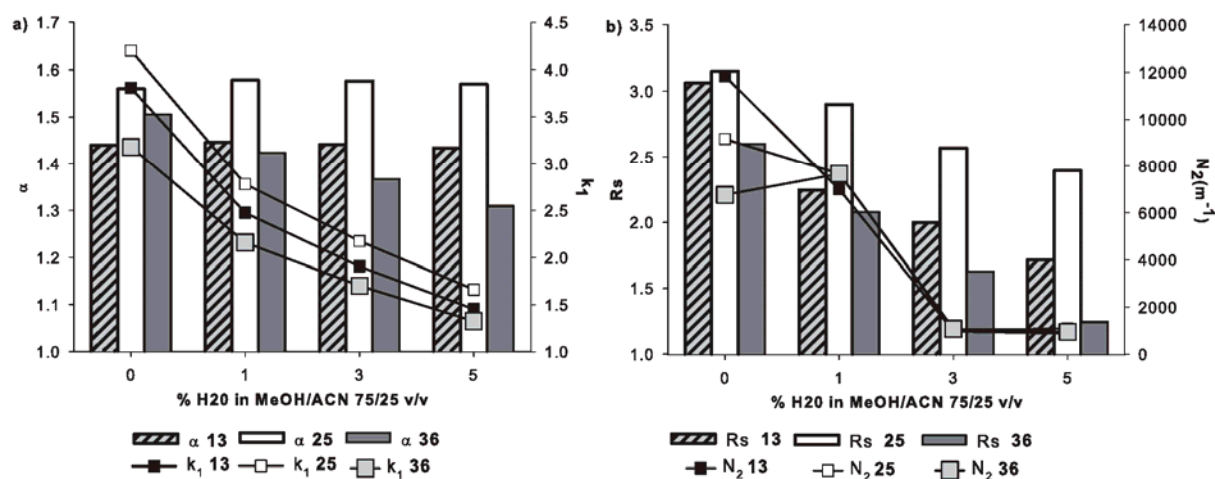
a) Chemical structure of the compounds adopted for the mobile phase optimization. b) Influence of buffer type of the mobile phase on enantioselectivity and resolution. FA – NH₃, formic acid/Ammonia; AcOH - NH₃, acetic acid - ammonia; PA – NH₃, propionic acid – ammonia, acid to base given as molar ratios (150/50 mM for FA, AcOH, PA FA - beta-alanine, 100/50 mM). Chromatographic parameters as specified in material and methods section.

**Fig.3.**

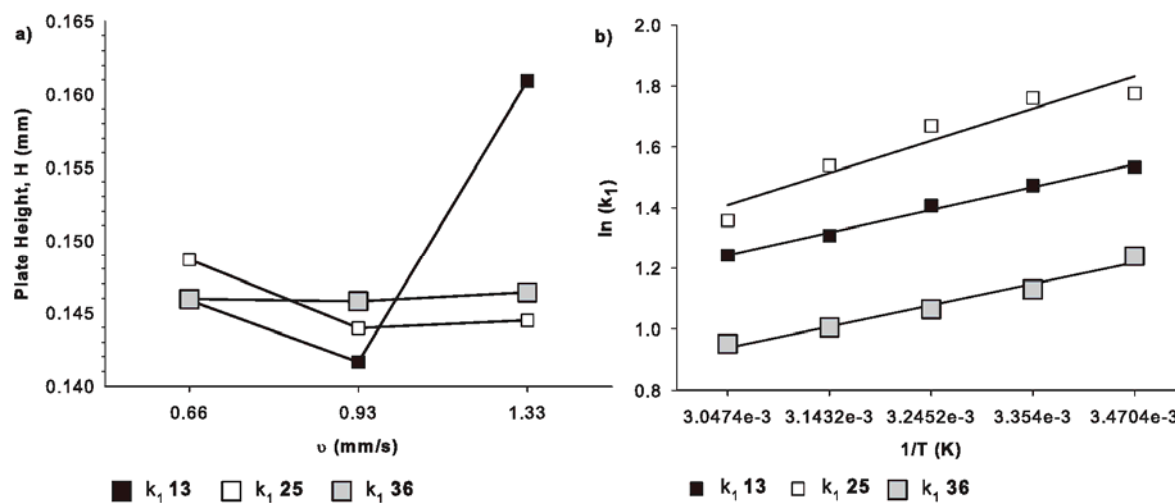
Effect of the acid to base ratio in the mobile phase on the capacity factor and resolution. Mobile phases composed of formic acid/ ammonia, acid to base given as molar ratios 250/ 50 mM (5-1), 200/ 50 mM (4-1), 150/ 50 mM (3-1), 50/ 50 mM (1-1), 50/ 100 mM (1-2). Chromatographic parameters as specified in material and methods section.

**Fig.4.**

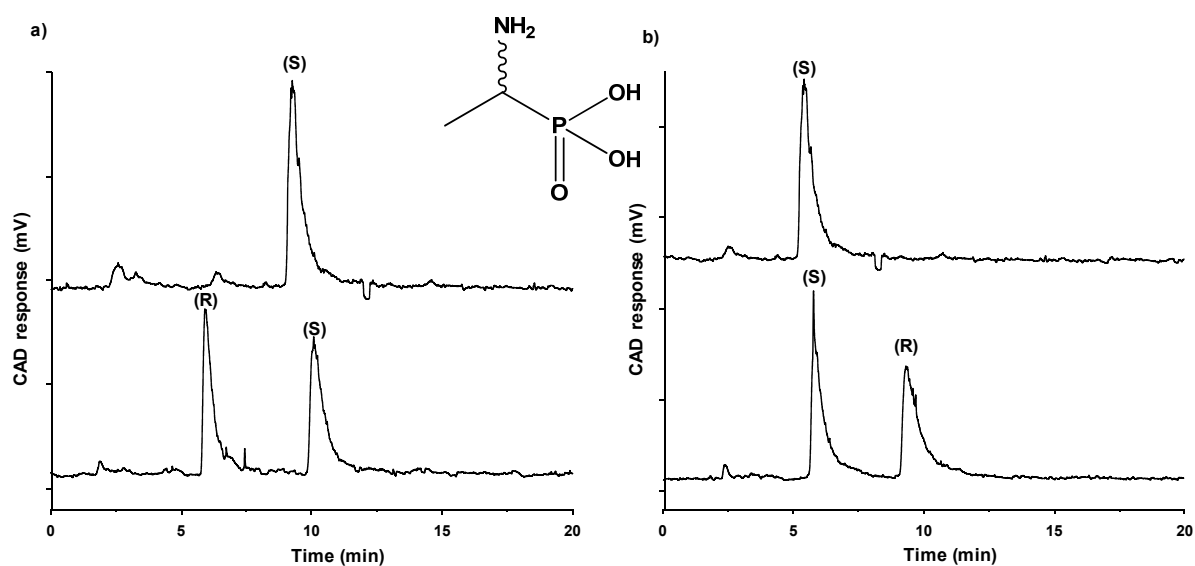
Influence of ACN and MeOH as bulk eluent solvent for on Chiralpak ZWIX (-)TM (a) on enantioselectivity and retention, and (b) chromatographic profiles ($\lambda = 254$ nm) of **13**. Mobile phase composed of 200 mM formic acid and 50 mM ammonia in ACN-MeOH mixtures (v/v). For conditions see materials and methods section.

**Fig.5.**

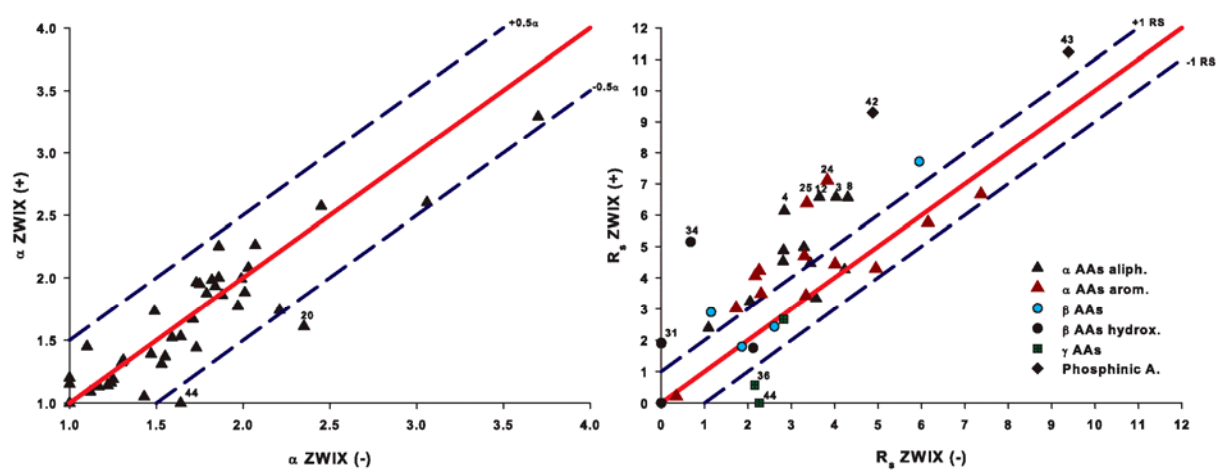
Influence of small percentages of water in the eluent composed of 200 mM formic acid and 50 mM ammonia in MeOH/ACN (75:25; v/v) on retention and selectivity (a) as well as resolution and plate numbers (b). For conditions see materials and methods section.

**Fig.6.**

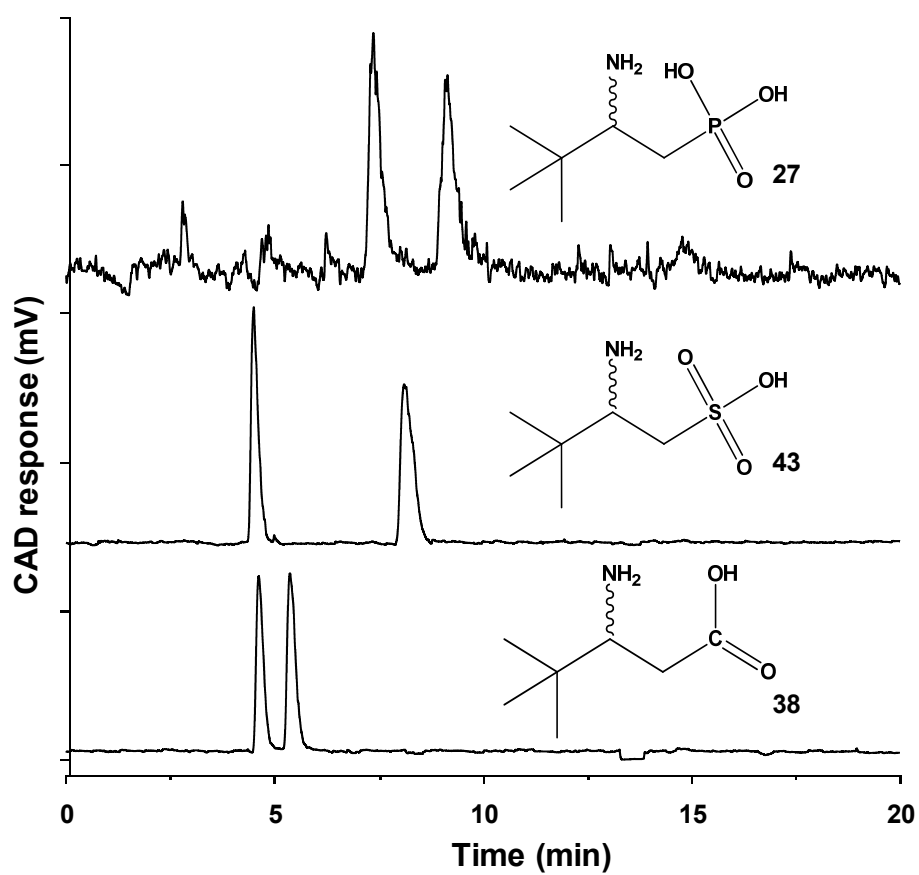
Influence of temperature (a) and linear flow rate (b) and on retention and resolution. For conditions see materials and methods section.

**Fig.7.**

Reversed elution order of compound **1** on Chiralpak ZWIX(+) (a) and (-) (b). For conditions see materials and methods section.

**Fig.8.**

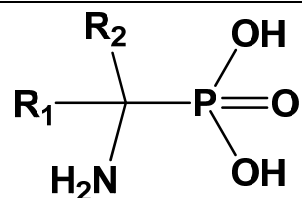
Comparison of enantioselectivity a) and resolution b) performances of Chiralpak ZWIX(+) versus (-) with respect to the analyte set reported in *table 1* (for conditions see materials and methods section).

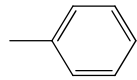
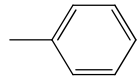
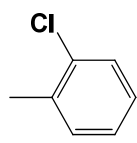
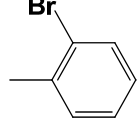
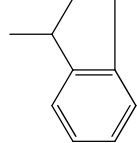
**Fig.9.**

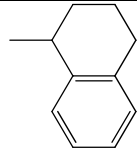
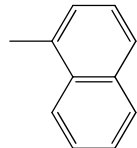
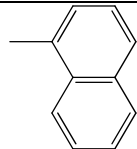
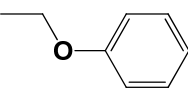
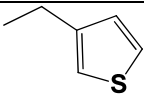
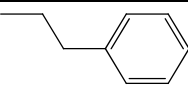
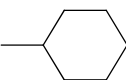
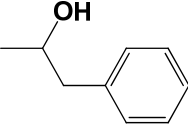
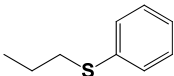
Effect of acidic functionality in zwitterionic analytes on enantioseparation (for conditions see materials and methods section).

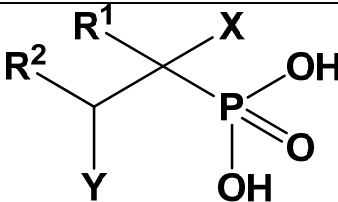
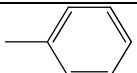
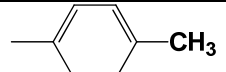
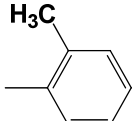
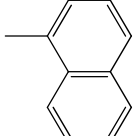
Table 1.

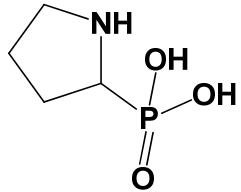
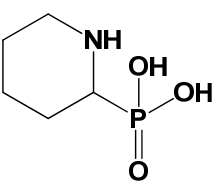
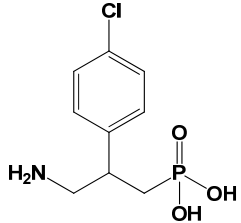
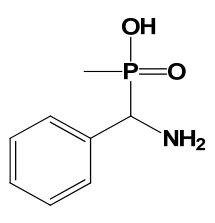
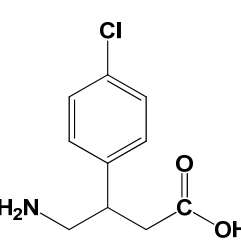
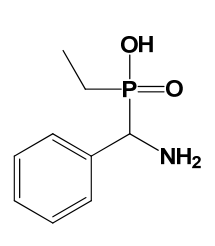
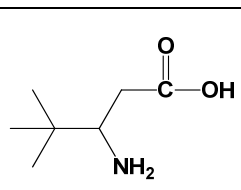
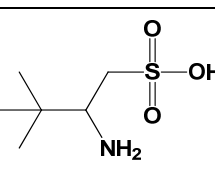
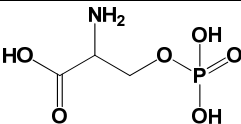
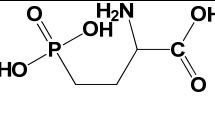
Structures, retention factor, selectivity and resolution of α , β , γ -aminophosphonic , aminophosphinic, amino sulfonic and carboxylic acids investigated in the present study. e.o., elution order (configuration of first eluted enantiomer). For conditions see materials and methods section.



N	R ₁	R ₂	k ₁		α	R _s	e. o.	N	R ₁	R ₂	k ₁		α	R _s	e. o.
<u>1</u>	-H	-CH ₃	Z+	1.89	1.77	3.33	R	<u>13</u>	-H		Z+	3.82	1.52	4.43	R
			Z-	1.72	1.97	3.57	S				Z-	2.73	1.59	4.01	S
<u>2</u>	-H	-CH ₂ CH ₃	Z+	1.90	1.99	4.47	n.d.	<u>14</u>	-CH ₃		Z+	2.39	1.74	6.66	n.d.
			Z-	1.62	1.99	3.44	n.d.				Z-	1.54	2.21	7.37	n.d.
<u>3</u>	-H	-CH(CH ₃) ₂	Z+	1.97	2.08	6.57	R	<u>15</u>	-H		Z+	2.33	1.67	4.69	n.d.
			Z-	1.86	2.03	4.03	S				Z-	1.67	1.71	3.30	n.d.
<u>4</u>	-H	-(CH ₂) ₂ SH	Z+	2.88	1.98	6.13	n.d.	<u>16</u>	-H		Z+	2.69	1.53	4.23	n.d.
			Z-	2.25	1.82	2.84	n.d.				Z-	1.81	1.64	2.26	n.d.
<u>5</u>	-H	-(CH ₂) ₂ SCH ₃	Z+	2.37	1.93	3.23	R	<u>17</u>	-CH ₃		Z+	2.09	1.39	3.47	R
			Z-	2.22	1.84	2.05	S				Z-	1.38	1.47	2.30	S

<u>6</u>	-H	-(CH ₂) ₂ SO ₂ CH ₃	Z+	4.85	1.88	4.26	n.d.	<u>18</u>	-CH ₃		Z+	2.58	1.44	4.29	R
			Z-	4.08	2.01	4.23	n.d.				Z-	1.66	1.73	4.95	R
<u>7</u>	-H	-CH ₂ CH(CH ₃) ₂	Z+	1.68	2.25	6.56	R	<u>19</u>	-H		Z+	7.12	1.37	3.41	R
			Z-	1.78	1.86	4.30	S				Z-	4.79	1.55	3.34	S
<u>8</u>	-CH ₃	-CH ₂ CH(CH ₃) ₂	Z+	1.03	1.32	2.39	n.d.	<u>20</u>	-CH ₃		Z+	4.01	1.61	5.76	R
			Z-	0.99	1.30	1.09	n.d.				Z-	2.30	2.35	6.15	S
<u>9</u>	-H	-(CH ₂) ₃ CH ₃	Z+	1.80	2.00	4.52	n.d.	<u>21</u>	-H		Z+	1.75	1.73	4.05	n.d.
			Z-	1.63	1.86	2.81	n.d.				Z-	1.73	1.49	2.17	n.d.
<u>10</u>	-H	-(CH ₂) ₄ CH ₃	Z+	1.89	1.95	4.88	n.d.	<u>22</u>	-H		Z+	2.86	1.09	0.20	n.d.
			Z-	1.76	1.75	2.82	n.d.				Z-	3.53	1.12	0.35	n.d.
<u>11</u>	-H	-(CH ₂) ₅ CH ₃	Z+	1.96	1.96	4.98	n.d.	<u>23</u>	-H		Z+	2.83	1.87	7.10	n.d.
			Z-	1.86	1.73	3.29	n.d.				Z-	2.72	1.79	3.83	n.d.
<u>12</u>	-H		Z+	2.32	2.26	6.57	S	<u>24</u>	-H		Z+	2.48	1.13	3.02	n.d.
			Z-	2.27	2.07	3.65	R				Z-	1.62	1.17	1.73	n.d.
								<u>25</u>	-H		Z+	3.46	1.86	6.38	n.d.
											Z-	3.50	1.88	3.36	n.d.

												
					Z+				Z-			
No	X	Y	R ₁	R ₂	k ₁	α	R _s	e.o.	k ₁	α	R _s	e.o.
<u>26</u>	-H	-NH ₂	-H	CH(CH ₃) ₂	4.85	1.16	1.79	n.d.	3.41	1.24	1.86	n.d.
<u>27</u>	-H	-NH ₂	-H	C(CH ₃) ₃	2.34	1.34	2.89	n.d.	1.68	1.31	1.15	n.d.
<u>28</u>	-OH	-NH ₂	-H	-H	2.01	1.00	-	n.d.	1.70	1.00	-	n.d.
<u>29</u>	-OH	-NH ₂	-H	-CH(CH ₃) ₂	5.36	1.00	-	n.d.	4.30	1.00	-	n.d.
<u>30</u>	-OH	-NH ₂	-H	-CH(CH ₃)(CH ₂ CH ₃)	3.91	1.00	-	n.d.	2.58	1.00	-	n.d.
<u>31</u>	-OH	-NH ₂	-H		8.76	1.20	1.89	n.d.	5.41	1.00	-	n.d.
<u>32</u>	-OH	-NH ₂	-H		9.63	1.15	1.91	n.d.	5.63	1.00	-	n.d.
<u>33</u>	-OH	-NH ₂	-H		7.81	1.14	1.75	n.d.	4.47	1.22	2.12	n.d.
<u>34</u>	-OH	-NH ₂	-H		13.30	1.45	5.15	n.d.	8.12	1.10	0.68	n.d.

OTHER STRUCTURES													
No		k ₁		α	R _s	e.o.	No		k ₁		α	R _s	e.o.
<u>35</u>		Z+	1.76	-	-	n.d.	<u>40</u>		Z+	1.93	-	-	n.d.
		Z-	1.54	-	-	n.d.			Z-	1.75	-	-	n.d.
<u>36</u>		Z+	5.74	1.05	0.57	n.d.	<u>41</u>		Z+	0.64	3.29	11.23	n.d.
		Z-	3.27	1.43	2.16	n.d.			Z-	0.53	3.70	9.39	n.d.
<u>37</u>		Z+	2.10	1.19	2.66	n.d.	<u>42</u>		Z+	1.03	2.60	9.30	n.d.
		Z-	1.60	1.25	2.82	n.d.			Z-	0.76	3.06	4.88	n.d.
<u>38</u>		Z+	1.10	1.31	2.43	n.d.	<u>43</u>		Z+	1.05	2.57	7.71	n.d.
		Z-	0.94	1.53	2.61	n.d.			Z-	0.79	2.45	5.95	n.d.
<u>39</u>		Z+	-	-	-	n.d.	<u>44</u>		Z+	2.12	1.00	-	n.d.
		Z-	-	-	-	n.d.			Z-	1.81	1.64	2.26	n.d.

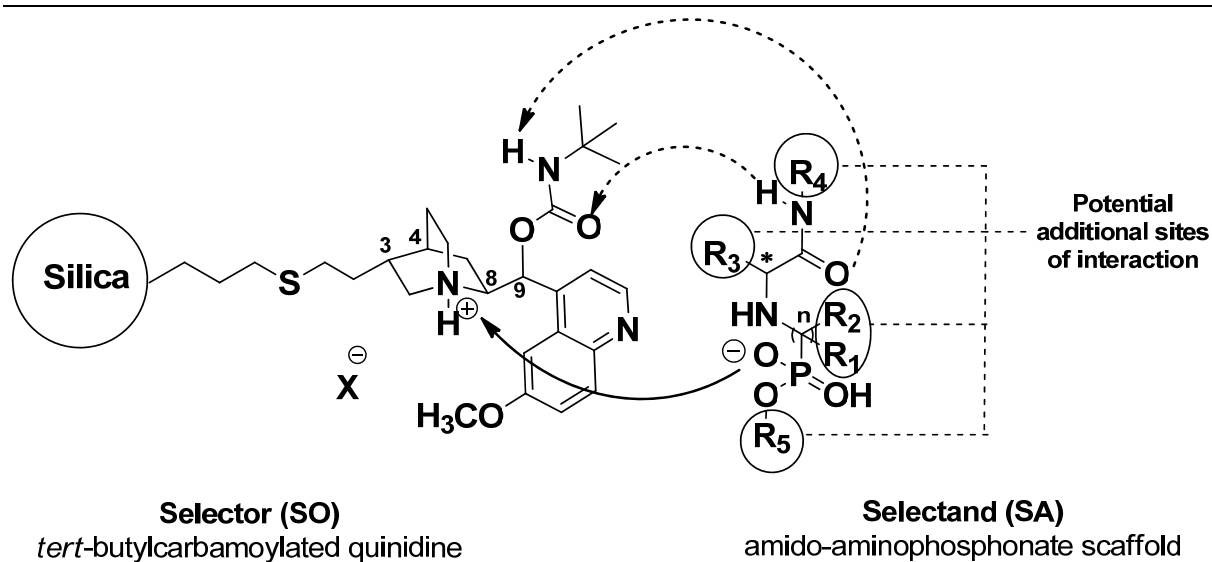
References

1. Hudson HR, Kukhar VP (2000) Aminophosphonic and aminophosphinic acids: chemistry and biological activity. Wiley,
2. Mucha A, Kafarski P, Berlicki L (2011) Remarkable potential of the alpha-aminophosphonate/phosphinate structural motif in medicinal chemistry. *J Med Chem* 54 (17):5955-5980. doi:10.1021/jm200587f
3. Morphy JR, Beeley NRA, Boyce BA, Leonard J, Mason B, Millican A, Millar K, Oconnell JP, Porter J (1994) Potent and Selective Inhibitors of Gelatinase-A .2. Carboxylic and Phosphonic Acid-Derivatives. *Bioorganic & Medicinal Chemistry Letters* 4 (23):2747-2752. doi:10.1016/S0960-894x(01)80588-6
4. Kraicheva I, Bogomilova A, Tsacheva I, Momekov G, Troev K (2009) Synthesis, NMR characterization and in vitro antitumor evaluation of new aminophosphonic acid diesters. *Eur J Med Chem* 44 (8):3363-3367. doi:10.1016/j.ejmech.2009.03.017
5. Kafarski P, Lejczak B (1991) Biological Activity of Aminophosphonic Acids. *Phosphorus Sulfur* 63 (1-2):193-215. doi:10.1080/10426509108029443
6. Grzywa R, Oleksyszyn J, Salvesen GS, Drag M (2010) Identification of very potent inhibitor of human aminopeptidase N (CD13). *Bioorg Med Chem Lett* 20 (8):2497-2499. doi:10.1016/j.bmcl.2010.02.111
7. Selvam C, Goudet C, Oueslati N, Pin JP, Acher FC (2007) L-(+)-2-Amino-4-thiophosphonobutyric acid (L-thioAP4), a new potent agonist of group III metabotropic glutamate receptors: increased distal acidity affords enhanced potency. *J Med Chem* 50 (19):4656-4664. doi:10.1021/jm070400y
8. Wallace EM, Moliterni JA, Moskal MA, Neubert AD, Marcopulos N, Stamford LB, Trapani AJ, Savage P, Chou M, Jeng AY (1998) Design and synthesis of potent, selective inhibitors of endothelin-converting enzyme. *J Med Chem* 41 (9):1513-1523. doi:10.1021/jm970787c
9. Beck J, Gharbi S, Herteg-Ferneu A, Vercheval L, Bebrone C, Lassaux P, Zervosen A, Marchand-Brynaert J (2009) Aminophosphonic Acids and Aminobis(phosphonic acids) as Potential Inhibitors of Penicillin-Binding Proteins. *European Journal of Organic Chemistry* 2009 (1):85-97. doi:10.1002/ejoc.200800812
10. Yang S, Gao X-W, Diao C-L, Song B-A, Jin L-H, Xu G-F, Zhang G-P, Wang W, Hu D-Y, Xue W, Zhou X, Lu P (2006) Synthesis and Antifungal Activity of Novel Chiral α -Aminophosphonates Containing Fluorine Moiety. *Chinese Journal of Chemistry* 24 (11):1581-1588. doi:10.1002/cjoc.200690296
11. Manning HC, Goebel T, Marx JN, Bornhop DJ (2002) Facile, efficient conjugation of a trifunctional lanthanide chelate to a peripheral benzodiazepine receptor ligand. *Org Lett* 4 (7):1075-1078. doi:10.1021/ol017155b
12. Hammerschmidt F, Hanbauer M (2000) Transformation of arylmethalamines into alpha-aminophosphonic acids via metalated phosphoramidates: Rearrangement of partly configurationally stable N-phosphorylated alpha-aminocarbanions. *J Org Chem* 65 (19):6121-6131. doi:10.1021/jo000585f
13. Hammerschmidt F, Li Y-F (1994) Determination of absolute configuration of α -hydroxyphosphonates by ^{31}P NMR spectroscopy of corresponding Mosher esters. *Tetrahedron* 50 (Copyright (C) 2012 American Chemical Society (ACS). All Rights Reserved.):10253-10264. doi:10.1016/s0040-4020(01)81758-0
14. Hammerschmidt F, Wuggenig F (1999) Enzymes in organic chemistry. Part 9: Chemo-enzymatic synthesis of phosphonic acid analogues of L-valine, L-leucine, L-isoleucine, L-methionine and L- α -aminobutyric acid of high enantiomeric excess. *Tetrahedron: Asymmetry* 10 (Copyright (C) 2012 American Chemical Society (ACS). All Rights Reserved.):1709-1721. doi:10.1016/s0957-4166(99)00152-4

15. Schmidt U, Krause HW, Oehme G, Michalik M, Fischer C (1998) Enantioselective synthesis of α -aminophosphonic acid derivatives by hydrogenation. *Chirality* 10 (Copyright (C) 2012 American Chemical Society (ACS). All Rights Reserved.):564-572. doi:10.1002/(sici)1520-636x(1998)10:7<564::aid-chir3>3.0.co;2-2
16. Woschek A, Lindner W, Hammerschmidt F (2003) Enzymes in Organic Chemistry, 11:[1] Hydrolase-Catalyzed Resolution of α - and β -Hydroxyphosphonates and Synthesis of Chiral, Non-Racemic β -Aminophosphonic Acids. *Advanced Synthesis & Catalysis* 345 (12):1287-1298. doi:10.1002/adsc.200303135
17. Wuggenig F, Schweifer A, Mereiter K, Hammerschmidt F (2011) Chemoenzymatic Synthesis of Phosphonic Acid Analogues of L-Lysine, L-Proline, L-Ornithine, and L-Pipecolic Acid of 99 % ee – Assignment of Absolute Configuration to (–)-Proline. *European Journal of Organic Chemistry* (10):1870-1879. doi:10.1002/ejoc.201001501
18. Hammerschmidt F, Voellenkle H (1989) Absolute configuration of (2-amino-1-hydroxyethyl)phosphonic acid from *Acanthamoeba castellanii* (Neff). Preparation of phosphonic acid analogs of (+)- and (–)-serine. *Liebigs Ann Chem* (Copyright (C) 2012 American Chemical Society (ACS). All Rights Reserved.):577-583
19. Fischer C, Schmidt U, Dwars T, Oehme G (1999) Enantiomeric resolution of derivatives of α -aminophosphonic and α -aminophosphinic acids by high-performance liquid chromatography and capillary electrophoresis. *Journal of Chromatography A* 845 (1–2):273-283. doi:10.1016/s0021-9673(99)00487-2
20. Pirkle WH, Burke JA (1992) Separation of the enantiomers of the 3,5-dinitrobenzamide derivatives of α -amino phosphonates on four chiral stationary phases. *Journal of Chromatography A* 598 (2):159-167. doi:[http://dx.doi.org/10.1016/0021-9673\(92\)85044-T](http://dx.doi.org/10.1016/0021-9673(92)85044-T)
21. Pirkle WH, Jonathan Brice L, Caccamese S, Principato G, Failla S (1996) Facile separation of the enantiomers of diethyl N-(aryl)-1-amino-1-arylmethanephosphonates on a rationally designed chiral stationary phase. *Journal of Chromatography A* 721 (2):241-246. doi:[http://dx.doi.org/10.1016/0021-9673\(95\)00844-6](http://dx.doi.org/10.1016/0021-9673(95)00844-6)
22. Pirkle WH, Jonathan Brice L, Widlanski TS, Roestamadji J (1996) Resolution and determination of the enantiomeric purity and absolute configurations of α -aryl- α -hydroxymethanephosphonates. *Tetrahedron: Asymmetry* 7 (8):2173-2176. doi:[http://dx.doi.org/10.1016/0957-4166\(96\)00263-7](http://dx.doi.org/10.1016/0957-4166(96)00263-7)
23. Zarbl E, Lämmerhofer M, Hammerschmidt F, Wuggenig F, Hanbauer M, Maier NM, Sajovic L, Lindner W (2000) Direct liquid chromatographic enantioseparation of chiral α - and β -aminophosphonic acids employing quinine-derived chiral anion exchangers: determination of enantiomeric excess and verification of absolute configuration. *Anal Chim Acta* 404 (2):169-177. doi:10.1016/s0003-2670(99)00700-x
24. Lämmerhofer M, Hebenstreit D, Gavioli E, Lindner W, Mucha A, Kafarski P, Wieczorek P (2003) High-performance liquid chromatographic enantiomer separation and determination of absolute configurations of phosphonic acid analogues of dipeptides and their α -aminophosphonic acid precursors. *Tetrahedron: Asymmetry* 14 (17):2557-2565. doi:10.1016/s0957-4166(03)00537-8
25. Hoffmann CV, Reischl R, Maier NM, Lämmerhofer M, Lindner W (2009) Stationary phase-related investigations of quinine-based zwitterionic chiral stationary phases operated in anion-, cation-, and zwitterion-exchange modes. *Journal of Chromatography A* 1216 (7):1147-1156. doi:10.1016/j.chroma.2008.12.045
26. Hoffmann CV, Pell R, Lämmerhofer M, Lindner W (2008) Synergistic Effects on Enantioselectivity of Zwitterionic Chiral Stationary Phases for Separations of Chiral Acids, Bases, and Amino Acids by HPLC. *Analytical Chemistry* 80 (22):8780-8789. doi:10.1021/ac801384f
27. Hoffmann CV, Reischl R, Maier NM, Lämmerhofer M, Lindner W (2009) Investigations of mobile phase contributions to enantioselective anion- and zwitterion-exchange modes on quinine-based zwitterionic chiral stationary phases. *Journal of Chromatography A* 1216 (7):1157-1166. doi:10.1016/j.chroma.2008.12.044
28. Pell R, Sić S, Lindner W (2012) Mechanistic investigations of cinchona alkaloid-based zwitterionic chiral stationary phases. *Journal of Chromatography A* (Article in press). doi:10.1016/j.chroma.2012.08.006

29. Wernisch S, Lindner W (2012) Versatility of Cinchona-based zwitterionic chiral stationary phases: Enantiomer and diastereomer separations of non-protected oligopeptides utilizing a multi-modal chiral recognition mechanism. *Journal of Chromatography A* (0). doi:10.1016/j.chroma.2012.06.094
30. Hoffmann CV, Reischl R, Maier NM, Lammerhofer M, Lindner W (2009) Investigations of mobile phase contributions to enantioselective anion- and zwitterion-exchange modes on quinine-based zwitterionic chiral stationary phases. *Journal of chromatography A* 1216 (7):1157-1166. doi:10.1016/j.chroma.2008.12.044
31. Hoffmann CV, Reischl R, Maier NM, Lammerhofer M, Lindner W (2009) Stationary phase-related investigations of quinine-based zwitterionic chiral stationary phases operated in anion-, cation-, and zwitterion-exchange modes. *Journal of chromatography A* 1216 (7):1147-1156. doi:10.1016/j.chroma.2008.12.045
32. Pell R, Sic S, Lindner W (2012) Mechanistic investigations of cinchona alkaloid-based zwitterionic chiral stationary phases. *Journal of chromatography A* 1269:287-296. doi:10.1016/j.chroma.2012.08.006
33. Pell R, Sić S, Lindner W (2012) Mechanistic investigations of cinchona alkaloid-based zwitterionic chiral stationary phases. *Journal of Chromatography A* 1269:287-296. doi:10.1016/j.chroma.2012.08.006
34. Wernisch S, Pell R, Lindner W (2012) Increments to chiral recognition facilitating enantiomer separations of chiral acids, bases, and ampholytes using Cinchona-based zwitterion exchanger chiral stationary phases. *Journal of Separation Science* 35 (13):1560-1572. doi:10.1002/jssc.201200103
35. Lämmerhofer M, Lindner W (1996) Quinine and quinidine derivatives as chiral selectors I. Brush type chiral stationary phases for high-performance liquid chromatography based on cinchonan carbamates and their application as chiral anion exchangers. *Journal of Chromatography A* 741 (1):33-48. doi:10.1016/0021-9673(96)00137-9
36. Maier NM, Schefzick S, Lombardo GM, Feliz M, Rissanen K, Lindner W, Lipkowitz KB (2002) Elucidation of the Chiral Recognition Mechanism of Cinchona Alkaloid Carbamate-type Receptors for 3,5-Dinitrobenzoyl Amino Acids. *Journal of the American Chemical Society* 124 (29):8611-8629. doi:10.1021/ja020203i

Manuscript 3



Graphical abstract:

Enantioseparation of chiral amido-aminophosphonate scaffolds from a novel Ugi multi-component Reaction by liquid chromatography on quinidine-based chiral anion exchangers

Enantioseparation of chiral amido-aminophosphonate scaffolds from a novel Ugi multi-component Reaction by liquid chromatography on quinidine-based chiral anion exchangers

Andrea F.G. Gargano¹, Wolfgang Lindner¹, Michael Lämmerhofer^{2*}

¹ *Department of Analytical Chemistry, University of Vienna, Waehringer Strasse 38, 1090 Vienna, Austria*

² *Institute of Pharmaceutical Sciences, University of Tübingen, Auf der Morgenstelle 8, 72076 Tübingen, Germany*

*michael.laemmerhofer@uni-tuebingen.de

Institute of Pharmaceutical Sciences

University of Tübingen

Auf der Morgenstelle 8

72076 Tübingen, Germany

T +49 7071 29 78793

F +49 7071 29 4565

Keywords

HPLC, carbamoylated Cinchona stationary phases, Enantiomer separation, Aminophosphonic acids, Aminophosphonate, Ugi multi-component reaction.

Abstract

In the present work a novel Ugi multicomponent reaction (MCR) was used to generate zwitterionic chromatographic selectors with capability for application for mixed-mode chromatography featuring complementary selectivities in reversed-phase (RP) and hydrophilic interaction liquid chromatography (HILIC) modes. Aminophosphonate zwitterionic chromatographic molecules were synthesized adopting a single one pot microwave assisted three-component UGI-MCR synthesis and after purification were immobilized by thiol-ene click chemistry on silica beads. Chromatographic characteristics of these stationary phases were evaluated by variation of experimental conditions for a selected set of diverse analytes with neutral, acidic, basic and zwitterionic character. Interestingly multimodal separation capabilities were found for the novel selectors (i.e. columns can be operated both in HILIC and in RP mode with good selectivity and efficiency). They were further investigated comparatively to structurally related commercially available mixed mode, HILIC and RP columns. The resultant chromatographic data were analyzed by Principal Component Analysis (PCA). PCA clearly revealed that the new reversed-phase/zwitterionic ion-exchangers (RP/ZWIX) are complementary to common RP, HILIC and mixed-mode phases on the market and could be a promising alternative in impurity profiling and 2D-HPLC concepts. Moreover, the adopted synthetic approach offers the capability to generate chemical diversity simply by the variation of the starting aldehyde, aminophosphonic acid and or isonitrile components. This unique characteristics offers great possibility for the design of novel selectors for mixed mode chromatography like RP/ZWIX, HILIC, affinity and chiral chromatography.

1. Introduction

Aminophosphonic acids represent a particular class of amino acids in which the carboxylic group is replaced by a phosphonic acid function. Due to their structural similarity such molecules can act as antagonists of amino acids affecting a variety of physiological processes. This characteristic renders aminophosphonic acids of considerable biological and pharmacological interest. The applications of this class of molecules are reported as antitumor^[42a, 44a, 44e, 68], neuroactive^[42a, 68b, 69], antihypertensive^[42a, 46, 68b], antimicrobial^[42a, 47a, 68b, 70], herbicidal^[42a, 68b] and imaging agents^[42a, 71].

We recently developed a novel synthetic approach to further functionalize these bioactive molecules using combinatorial chemistry^[72]. Adopting a novel Ugi five-center four-component reaction (U-5C-4CR)^[39a] we could generate racemic phosphopeptide-like structures by the mean of a one pot reaction.

It is well established that usually only one of the enantiomers exerts physiological activity. Thus, the development of a simple and versatile method for the enantioseparation of these structures is strongly desirable. In this context, carbamoylated cinchona-derived stationary phases had previously demonstrated good enantioselectivity properties for protected aminophosphonic acid^[61, 73]. Similarly we reported a chromatographic method based on zwitterionic carbamoylated cinchonane-based ion-exchangers for unprotected aminophosphonic acids^[74]. We therefore investigated the enantioseparation of these novel amido-aminophosphonate structures adopting quinidine carbamate based stationary phases under chiral anion exchange conditions. The developed method offers the important advantage of obtaining by a single step both chemically and (when this is possible) enantiomerically pure compounds. Moreover, thanks to the capability of the synthetic approach to generate chemical diversity we could obtain a heterogeneous analyte set that allowed us to evaluate the influence of various structural motifs on enantioselectivity. Such elements disclose structure-enantioselectivity relationships which are useful for gaining insight into molecular recognition mechanisms and for the application of this method to other structurally related analytes.

2. Experimental

2.1. Materials

HPLC solvents methanol (MeOH) and acetonitrile (ACN) were of HPLC-grade quality and purchased from Sigma-Aldrich (Vienna, Austria) and Merck (Darmstadt, Germany). Formic acid (FA), 7N ammonia solution in MeOH, acetic acid (AA) were of analytical grade from Sigma-Aldrich (Vienna, Austria). DL Leucine and DL-Phospholeucine were purchased from Across Organics (Gel, Belgium) and N-FMOC protected α -amino acids were prepared according to literature procedure ^[75]. (2-Aminopropane-2-yl)phosphonic acid, (1-aminocyclopentyl)phosphonic acid, (1-aminoethyl)phosphonic acid, [amino(phenyl)methyl]phosphonic acid, (2-aminoethyl) phosphonic acid, (3-aminopropyl) phosphonic acid were of a purity grade of at least 97% and supplied by Acros Organics. (Aminomethyl) phosphonic acid 98% was obtained from Epsilon Chimie (Brest-Guipavas, France). The remaining aminophosphonic acid educts were synthesized according to literature procedures ^[54]. Aldehydes and isocyanides were of a purity grade of at least 95% and supplied by Sigma Aldrich (Vienna, Austria). Tetra-n-butylammonium hydroxide (TBAH) (technical grade 25% in MeOH) and bromotrimethyl silane were purchased from Fluka (Sigma-Aldrich).

3.1. Analytes synthesis

The analytes adopted for this study were synthesized by a modification of a recently published synthetic protocol ^[72] starting from aminophosphonic acid, aldehyde and isonitrile in alcohol as solvent. Briefly, the aminophosphonic acid, aldehyde and isonitrile (about 1 mg of each component) were weighted in an HPLC vial, tetra-n-butyl ammonium hydroxide (TBAH) (1M methanolic solution, 10 μ L) was added and diluted with MeOH (500 μ L). In the case of compounds no. **2**, **3**, **4** TBAH was added to the aminophosphonic acid and subsequently the MeOH from the ion-pair reagent solution was removed by evaporation under nitrogen (20 min). Then, the corresponding alcohol (isopropanol for **2**, allyl alcohol for **3**, and benzylalcohol for **4**) was added (500 μ L). The vials containing the reaction mixture were sealed and shaken for 16h at 50°C and used without further workup. In the case of compounds no. **39** and **40**, after completion of the reaction a hydrolysis procedure was applied ^[46, 53]. Briefly, the reaction mixture was dried under nitrogen and sonicated for about 1 minute in DCM (500 μ L). Bromotrimethylsilane (BrSiMe₃, 20 μ L) was added dropwise and the reaction was allowed to react for 15h at RT. After removal of the solvent using nitrogen flow, methanol (500 μ L) was added. The solution was heated at 50 °C for 2h. All the reaction

batches were analyzed with by RPLC-MS, in order to verify the presence of the product compound in the reaction mixture.

3.2. Apparatus and chromatography

HPLC–ESI-MS experiments were performed on an Agilent 1100 series LC/MSD ion-trap (IT) system (Waldbronn, Germany). The HPLC system was equipped with a binary gradient pump, autosampler, vacuum degasser and a temperature-controlled column compartment (Agilent, Waldbronn, Germany). The reaction mixtures after synthesis were analyzed by RPLC-MS via electrospray ionization interface using an ACE C-18 column (5 μ m particle size, C18, 100 Å, 150 mm \times 3.0 mm I.D.). The mobile phase consisted of HPLC-grade water containing 0.1% formic acid (A) and methanol containing 0.1% formic acid (B). The analyses were performed with a 20 minute gradient: 20-100% mobile phase B. The flow rate was 0.93 mm s⁻¹ (0.4 mL min⁻¹) and the injection of 2 μ L of the sample was performed with needle wash. The m/z scans were performed in negative mode from m/z 50 to 1000 with a scan rate of 13.000 m/z s⁻¹ and a maximal accumulation time of 300 ms. The chiral stationary phase adopted for the study was Chiralpak QD-AXTM (150 x 3 mm I.D., 5 μ m particle size) from Chiral Technologies Europe (Illkirch, France) based on *tert*-butylcarbamoylquinidine (8R, 9S). If not differently specified, the chromatographic parameters were as follows: flow rate, 1.33 mm s⁻¹; injection, 2 μ L; detection, UV at 254 nm. For the determination of the dead volume it was monitored the elution time of acetone (average of three injections). The identification of compounds in *Table 3* was performed by extracted ion chromatograms of the corresponding analyte masses from the total ion current analysis. The mobile phase adopted for the analysis of the compounds in *Table 1* was MeOH/ACN (50/50; v/v) containing 180 mM acetic acid with the apprent pH of the mixture adjusted to 5 with ammonia.

3. Results and discussion

3.2.1. *Quinidine carbamate stationary phase as purification tool for amido-aminophosphonate products from UgiMulti-Component Reactions*

The present contribution describes a straightforward purification and enantioseparation method for novel amido-aminophosphonate chiral scaffolds obtained by Ugi-five-center four-component reactions (U-5C-4CR) adopting cinchona-based chiral anion-exchangers. In *Fig. 1* is reported the reaction scheme for the synthesis: the aminophosphonic acid condenses together with aldehyde and isocyanide reactants in alcohol to generate peptide-like amino phosphonic acid derivatives. Adopting a multi-component reaction approach molecules carrying the same structural motif can be differently substituted under the same reaction conditions using different reactants ^[72]. The capability of generating molecules with a high degree of chemical heterogeneity is a characteristic feature that makes these synthetic approaches an important tool in the quest of drug discovery.

In particular, the above described U-5C-4CR with aminophosphonic acids as bifunctional acid and base component is characterized by fast kinetics and high yields when it is run in its microwave version. However traditional heating also demonstrated to be effective ^[72]. In the present study, for sake of simplicity we selected the latter approach and opted for an analytical scale synthesis. Reactions were performed in HPLC vials that were reacted for 16h at 50°C under shaking. The reaction mixtures were then characterized by RPLC-MS to check the presence of the desired product and subsequently analyzed via chiral anion-exchange chromatography.

Typically, reaction mixtures from combinatorial chemistry present a high level of chemical complexity (i.e. educts, product(s) and side product(s) that possess similar properties). When applicable ion-exchange chromatography offers the important advantage of selectively retain charged species and is therefore a useful tool to reduce the sample complexity. In particular, cinchona carbamate based stationary phases combine the robustness and purification advantages of anion-exchange chromatography with enantiodiscriminating properties. Aldehydes, isonitriles and aminophosphonic acids educts are scarcely retained or elute within the dead volume when analyzed with these anion-exchangers in polar organic mode. The first two educts are neutral and therefore are not undergoing ionic interaction with the selector unless their residual groups are charged. Aminophosphonic acids are generally scarcely retained due to their zwitterionic nature. The amido-aminophosphonates products, on the other hand, are also zwitterionic but feature other interactive sites such as amide groups and aromatic moieties which allow concerted simultaneous ionic with H-bond and/or aromatic interactions as illustrated in *Fig. 2* [20-22]. As a result, amido-aminophosphonates can be separated by their educts and depending on their substitution pattern, simultaneously

enantioseparated (see supporting information for an example of a typical elution profile of raw reaction mixture).

In the course of the investigation, we explored the effect of the mobile phase composition on the retention and chiral recognition process. Moreover, thanks to the heterogeneity of structural elements that such a combinatorial chemistry approach offered, we could evaluate the influence of various structural motifs on enantioselectivity.

3.2.2. *Mobile phase influence*

In ion-exchange chromatography the mobile phase characteristics influence the solvation and ionization status of both selector and selectand and therefore the strength of their interaction. As consequence the interaction process will be affected by the strength (acidity/basicity), the concentration and ratio of the acidic and basic additives composing the buffer as well as by the characteristic of the bulk solvent and the mobile phase temperature. The impact of mobile phase variation on retention and enantioseparation parameters was evaluated using compound **7** as test substance. The results are summarized in *Fig 3* and *4*.

3.1. *Effect of counter-ion concentration and bulk solvent composition*

In *Fig. 3a* is reported the dependency of retention factor, selectivity and resolution with respect to the counterion (FA) concentration in MeOH/ACN-based mobile phases. The dependency of the retention factor on the concentration of counterion demonstrates that the interaction is driven by an anion-exchange principle (higher buffer concentration results in lower retention, the linear trendline for the double logarithmic plot of retention factors versus counterion concentration is in support of the anion-exchange process, see supporting information). In the studied buffer range (12.5 - 100 mM FA concentration) the enantioselectivity appear to be marginally influenced by the buffer concentration, while the resolution increased thanks to an increase of the theoretical plate number (data not shown) at lower buffer concentrations (*Fig. 3a*).

An increase in the amount of ACN reduces the polarity and the proton activity of the media leading to a modification of the balance between interaction forces in the retention process. Comparing mobile phases with 50% of ACN with respect to the one based on 100% MeOH, we observed similar enantioselectivities but higher resolution values for the former (*Fig. 3b*). It is worth to mention that such a modification of the mobile phase conditions modulated also the retention of aldehyde educts as well as of side products (data not shown). In order to avoid interferences from too strong retention, such mobile phases with elevated ACN-content should, therefore, be applied with care and mainly be adopted for analytical characterization while MeOH-based eluents are certainly of advantage for purification purposes.

3.2. Influence of apparent pH and type of counter ion

The acidity of the eluent is decisive for ionization state of both selector and selectand and is thus a very important parameter for optimization. We therefore studied the variation of the chromatographic parameters in dependence of the apparent pH in the range between 3 and 7. As discussed above, the selectands possess low pKa and pI (for calculations see supporting information) and are therefore charged within the studied pH range. The retention increase between apparent pH 3 and 6 can be mainly attributed to altered analyte ionization i.e. increasing phosphonic acid dissociation while above pH 6 the drop in retention reflects the reduction of the anion-exchange capacity due to diminution of the effective charge of the CSP. Higher α -values and improved efficiencies at low pH result in improved resolution at more acidic conditions.

As last parameter connected to the nature of the buffer system, we compared formic and acetic acid as acidic additive (*Fig.3d*). The lower acidity of acetic acid results in higher retention values yet does not seem to alter significantly enantioselectivity and resolution values. In the prospective of applying the optimized mobile phase system to a heterogeneous set of analytes we tested these two counterion additives also for the separation of compounds **6**, **28**, **33**. Under additive concentrations, yielding similar retention factors acetic acid mobile phases offered better enantioseparation parameters (data reported in the supporting information).

3.3. Effect of temperature and thermodynamic aspects

For the investigation of the effect of temperature, compound **6**, **28**, **33** and, for comparison, also Fmoc-protected Leucine (Leu) and Phospholeucine (P-Leu) were separated with a mobile phase composition of MeOH/ACN (50/50; v/v) containing 50 mM formic acid (apparent pH adjusted with ammonia to 4) at different temperatures (288, 298, 308, 318, 328 K). Comparison of the retention factors and selectivity values indicated that all recorded values decreased with increasing temperature. The best performances were observed at subambient temperature (288K) However, the gain was not significant for analytes characterized by low enantioselectivity and resolution (**1** and **33**) and seemed to be prominent mainly for well resolved analytes (**28**, Fmoc-Leu, Fmoc-P-Leu, data reported in the supporting information). We therefore kept 298K as temperature for further separations (data extracted by the evaluation of the van't Hoff plots like $\Delta(\Delta H)$; $\Delta(\Delta S)$; $\Delta(\Delta G)$ are available in the supporting information).

As conclusion of the mobile phase study, MeOH/ACN (50/50; v/v) was selected as bulk solvent and acetic acid served as buffer system (180 mM apparent pH 5, adjusted with

ammonia). Such mobile phase is suitable for analytical purposes, but for preparative scale separations formic acid based mobile phases are preferred due to their higher buffer volatility that avoid the necessity of a desalting process. For the same reason, a low ACN content should be preferred in order to reduce the possibility of educts co-elution as mentioned above.

3.4. Elements of chiral recognition and structure-enantioselectivity relationships

In order to investigate the contribution of different residues in the common amido-aminophosphonate scaffold we systematically varied the components of the reaction mixture, namely the alcohol, aminophosphonic acid, aldehyde and isocyanide. By this multi-component reaction approach we could obtain a chemically diverse analyte portfolio characterized by distinct structural elements of the phosphonate scaffold. Their thorough analysis in terms of retention and enantioselectivity may give a deeper insight into the enantiorecognition process for such species and be helpful for the application of this method to structurally related species.

To ensure correct peak assignment the chromatograms of the reaction mixtures were monitored with MS detection, extracting the EICs of the products of interest. The obtained results in terms of retention, enantioselectivity and resolution are summarized in *Table 1*.

3.4.1. Modification of the alcohol educts

Table 1a presents analytes obtained from the same educts mixture in presence of different alcohols (methanol, 2-propanol, allyl alcohol, benzyl alcohol). Despite the limited number of entries reported in this investigation, it is evident that the modification of the ester site does not introduce elements promoting enantioselective interaction. On the contrary, it can be concluded that, except in the case of the *isopropyl group* (**2**), bigger residues just add an increment of retention, but disturb the chiral recognition process.

3.4.2. Modification of the aminophosphonic acid educt

The variation of the aminophosphonic acid component has a marked influence on the chromatographic separation process (*Table 2a, b*). There is a strong dependence of the retention and enantiorecognition on the atomic distance between ammonium and phosphonate site. Comparing **1**, **5** and **6** (and also **10** to **15**) it becomes evident that all chromatographic parameters decline from α - over β - to γ -amino-phosphonate compounds. The elongation of the amino phosphonic acid educt changes the distance between the primary acidic interaction site and the supportive amide (H-donor and acceptor group). This

results in a spatial displacement of amide and carbamate moieties upon primary ionic interaction and does not allow simultaneous geometrically and conformationally oriented H-bonding interactions. Eventually, this leads to retention decrease and ultimately of enantioselectivity. The same phenomenon and trend has been observed for N-acyl protected dipeptide, tripeptide and tetrapeptide. Retention and separation factors drop for these solutes in the same order ^[76].

Generally, the introduction of additional residues in the amino acid portion appears to be an element that gives higher structural rigidity to the selectand and at the same time can tentatively insert further spatially oriented interaction points with the selector. With introduction of alkyl substituents at R₁ of the amino phosphonic acid educt, enantiodiscrimination (R_s) increases with steric bulkiness in the order hydrogen (**1**) < methyl (**9**) < cyclohexyl (**13**) < *isopropyl* (**10**) < *isobutyl* (**11**) < phenyl (**14**) (Fig. 5). This order correlates with steric descriptors such as the Taft's parameter and clearly indicates that steric interactions are involved ^[77]. This holds for both pairs of enantiomers. The introduction of a second α substituent (R₂) appears to result in steric hindrance which reduces the strength of the SO-SA interactions (lower retention factor) and furthermore decreases enantioselectivity.

3.4.3. Variation of the aldehyde educts

Generation of molecular diversity via the R₃ substituent is an attractive feature due to the huge variety of aldehyde which are commercially available. Effects observed by variation of this residue are reported in *Table 3*. Separation factors appear to be larger for bulky alkyl than n-alkyl substituents (**17** vs. **18**) and increase with extension of aromatic ring system (**1**, **28**, **31**). It can be assumed that oriented π - π interactions with the quinoline of the selector are driving this effect. Generally, comparing electron-rich (π acidic) and electron-poor (π basic) aromatic systems the latter present higher retention on the CSP (compare entry **19-23**, **27** to **24-26**, **30**) but not necessarily larger separation factors. For both electron-rich and electron-poor systems especially ortho, but also para positions are preferred in terms of enantiorecognition (cf 19-21. 24 vs 25).

Increasing the aromaticity of the aldehyde educts strengthen SA-SO interactions (*Fig. 6*). In particular, the anthracene residue (**31**) furnished exceptional enantioseparation values (α = 1.82).

3.4.4. Variation of the isocyanide (isonitrile)

Due to limited commercial availability of these synthons, only few distinct isocyanides were tested in this study and the results are summarized in *Table 4*. From this preliminary data set, it can be derived that bulky R₄ residues are favorable (**1** and **33**), probably because they

stereoselectively shield the access to the amide for H-bonding for one of the two enantiomers. The result shows that respect to the 2,5 dimethyl phenyl residue (**1**) Neither more extended aromatic (**36**, **37**), aliphatic (**34**), H-acceptor (**35**) or basic (**38**) substituents are capable of providing larger separation factors. Therefore, we can conclude that at this site the presence of a sterically demanding group, tentatively incorporated in a rigid aromatic system, is the best substitution combination to achieve good enantiodiscriminating properties in our SA-SO system.

3.4.5. Multiple component modifications

Additionally, we compared the separation properties of carboxy, mono-methylphosphonate and phosphonic acid analogues (*Table 5*). Carboxylic acids with respect to their phosphonate analogues demonstrated lower strength of interaction with the CSP (compare **1** to **39**) but higher chiral separation factors. Under the adopted separation conditions, it was not possible to directly compare phosphonate and phosphonic acids (obtained by hydrolysis of the methyl phosphonic acid ester) due to the higher acidity of phosphonic acid and stronger retention which results from higher effective charge. We therefore used a previously published method to analyze such compounds ^[61a]. Under these conditions, we observed a stronger retention and better enantioseparation properties of the phosphonic acids with respect to its mono-methyl phosphonate analogue. Although a direct comparison of the three acids with one mobile phase was not achieved, it can be deduced that the presence of the methyl ester residue partially disturb the orientation of the molecule on the CSP. This effect can also justify the better enantioseparation properties given by the carboxylic type of acids.

It is worthwhile to mention that by combination of particular aforementioned residues can result in synergistic effects and lead to greatly enhanced α -values. This was of particular interest because this study was supposed to lead to new chiral selectors by adopting the reciprocity principle of chiral recognition. Infact, the combined introduction of an athracene residue (via aldehyde component) and a phenyl group (via aminophosphonic acid educt) dramatically enhanced the separation parameters of the corresponding product (see *Table 3*, **43** and **44**). This result indicates both an increment in the rigidity of the structure combined with additional π - π interactions with the quinoline ring of the selector. No difference in chromatographic parameters was observed when in such a system methyl ester substituent was replaced by an allyl group (**43** vs. **44**). Compound **44** was immobilized in enantiomerically pure form on silica gel affording a new interesting zwitterionic chiral stationary phase (results reported elsewhere).

4. Conclusion

Chiral anion-exchange chromatography on a quinidine carbamate stationary phase proved to be a suitable chromatographic method for the purification and enantioseparation of phosphonic acid pseudopeptides generated by Ugi-MCR. By variation of the chromatographic parameters, we investigated the contribution of the mobile phase to the enantiorecognition of such zwitterionic analytes, finding optimum conditions in polar organic mobile phases based on acetic acid as counterion.

From the analysis of a heterogeneous analyte set we can conclude that the chiral recognition process is generally supported both by the presence of π - π bonding sites as well as by sterically demanding residues in the selectand structure. However, their influence is strictly connected to their distance with respect to the chiral center and the acidic site.

The new compounds are will be tested as potentially bioactive compounds. Individual enantiomers constitute interesting new chiral selectors for enantiomer separation of basic compounds which will be reported elsewhere.

5. Acknowledgements

This work was financially supported by the University of Vienna through the interdisciplinary doctoral program: "Initiativkolleg Functional Molecules" (IK I041-N). Authors would like to thank Prof. Friedrich Hammerschmidt (Institute of Organic Chemistry, University of Vienna) for providing several samples of aminophosphonic acids.

6. Reference

- [1] J.R. Morphy, N.R.A. Beeley, B.A. Boyce, J. Leonard, B. Mason, A. Millican, K. Millar, J.P. Oconnell, J. Porter, *Bioorg Med Chem Lett*, 4 (1994) 2747-2752.
- [2] I. Kraicheva, A. Bogomilova, I. Tsacheva, G. Momekov, K. Troev, *European Journal of Medicinal Chemistry*, 44 (2009) 3363-3367.
- [3] P. Kafarski, B. Lejczak, *Phosphorus Sulfur*, 63 (1991) 193-215.
- [4] R. Grzywa, J. Oleksyszyn, G.S. Salvesen, M. Drag, *Bioorg Med Chem Lett*, 20 (2010) 2497-2499.
- [5] R. Grzywa, A.M. Sokol, M. Sieńczyk, M. Radziszewicz, B. Kościółek, M.P. Carty, J. Oleksyszyn, *Bioorganic & Medicinal Chemistry*, 18 (2010) 2930-2936.
- [6] H.R. Hudson, V.P. Kukhar, *Aminophosphonic and aminophosphinic acids: chemistry and biological activity*, Wiley, 2000.
- [7] C. Selvam, C. Goudet, N. Oueslati, J.-P. Pin, F.C. Acher, *Journal of Medicinal Chemistry*, 50 (2007) 4656-4664.
- [8] E.M. Wallace, J.A. Moliterni, M.A. Moskal, A.D. Neubert, N. Marcopulos, L.B. Stamford, A.J. Trapani, P. Savage, M. Chou, A.Y. Jeng, *J Med Chem*, 41 (1998) 1513-1523.
- [9] J. Beck, S. Gharbi, A. Herteg-Fernea, L. Vercheval, C. Bebrone, P. Lassaux, A. Zervosen, J. Marchand-Brynaert, *European Journal of Organic Chemistry*, 2009 (2009) 85-97.
- [10] S. Yang, X.-W. Gao, C.-L. Diao, B.-A. Song, L.-H. Jin, G.-F. Xu, G.-P. Zhang, W. Wang, D.-Y. Hu, W. Xue, X. Zhou, P. Lu, *Chinese Journal of Chemistry*, 24 (2006) 1581-1588.
- [11] H.C. Manning, T. Goebel, J.N. Marx, D.J. Bornhop, *Organic Letters*, 4 (2002) 1075-1078.
- [12] A.F.G. Gargano, M. Lämmerhofer, W. Lindner, (xx).
- [13] I. Ugi, A. Demharter, W. Hörl, T. Schmid, *Tetrahedron*, 52 (1996) 11657-11664.
- [14] E. Zarbl, M. Lammerhofer, F. Hammerschmidt, F. Wuggenig, M. Hanbauer, N.M. Maier, L. Sajovic, W. Lindner, *Anal. Chim. Acta*, 404 (2000) 169-177.
- [15] M. Lämmerhofer, D. Hebenstreit, E. Gavioli, W. Lindner, A. Mucha, P. Kafarski, P. Wieczorek, *Tetrahedron: Asymmetry*, 14 (2003) 2557-2565.
- [16] M. Lämmerhofer, E. Zarbl, W. Lindner, B.P. Simov, F. Hammerschmidt, *ELECTROPHORESIS*, 22 (2001) 1182-1187.
- [17] A.F.G. Gargano, Kohout M. , Macíková P., Lämmerhofer M. , Lindner W, *Analytical and Bioanalytical Chemistry*, In print (2013).
- [18] Peter G. M. Wuts, T.W. Greene, (2008).
- [19] F. Hammerschmidt, M. Hanbauer, *J. Org. Chem.*, 65 (2000) 6121-6131.

- [20] S. De Lombaert, M.D. Erion, J. Tan, L. Blanchard, L. El-Chehabi, R.D. Ghai, Y. Sakane, C. Berry, A.J. Trapani, *J. Med. Chem.*, 37 (1994) 498-511.
- [21] C. Czerwenka, M. Lämmerhofer, W. Lindner, *Journal of Separation Science*, 26 (2003) 1499-1508.
- [22] C. Czerwenka, M.M. Zhang, H. Kählig, N.M. Maier, K.B. Lipkowitz, W. Lindner, *The Journal of Organic Chemistry*, 68 (2003) 8315-8327.
- [23] M. Lämmerhofer, P. Franco, W. Lindner, *Journal of Separation Science*, 29 (2006) 1486-1496.

7. Figure caption

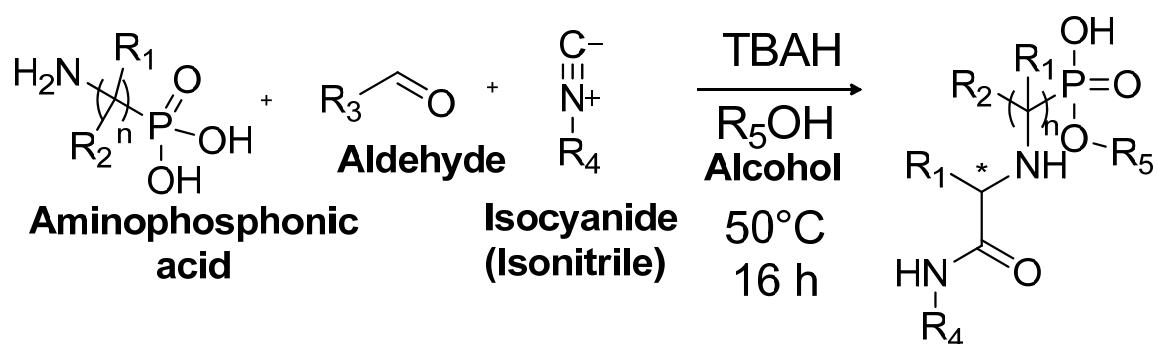


Fig 1: Reaction scheme of the Ugi multi-component reaction adopted to produce the amido-aminophosphonate compounds of this study ^[72].

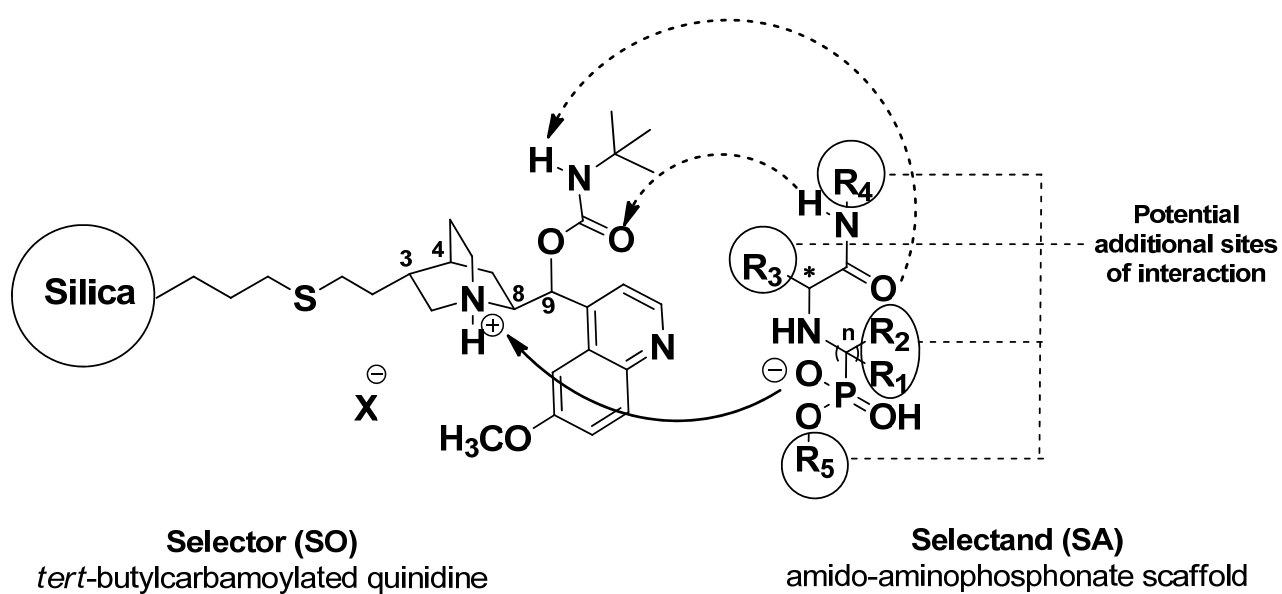


Fig 2: Interactions between CHIRALPAK QD-AX™ selector based on quinidine (8R, 9S) carbamate and the scaffold of the amido-aminophosphonates used in this study.

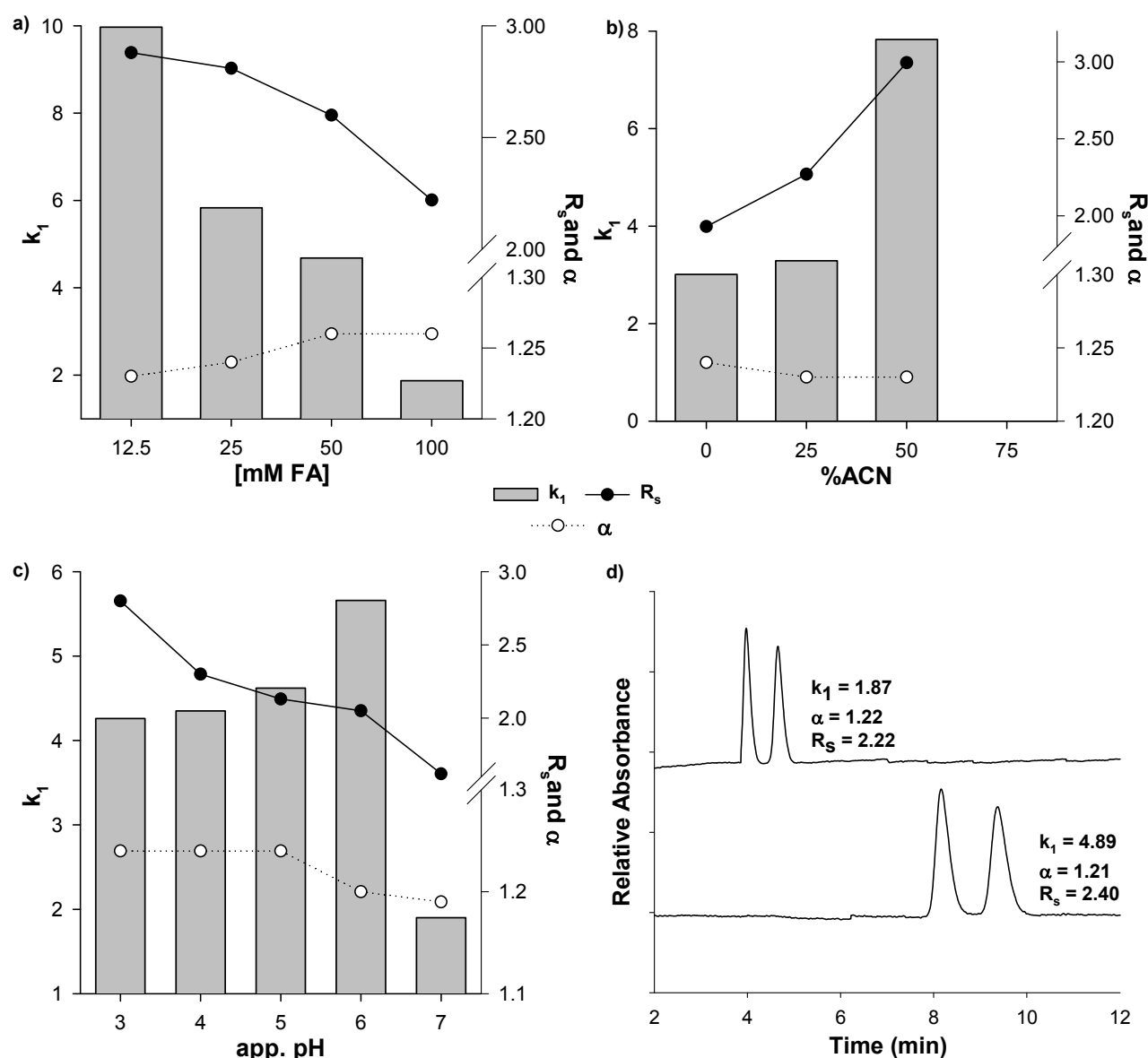


Fig. 3: Mobile phase influence on retention factor (k_1 ; grey columns) and enantioseparation parameters (α , open symbols; R_s closed symbols) of compound **1**: a) Counterion concentration, MP: MeOH/ACN (50/50; v/v) formic acid concentration of 12.5, 25, 50 and 100 mM respectively, apparent pH adjusted to 4 with ammonium hydroxide. b) % of ACN as bulk solvent, methanolic based MP with different % of ACN (25, 50, 75 % v/v) formic acid concentration of 15 mM, apparent pH adjusted to 4. c) apparent pH, MP: MeOH/ACN (50/50; v/v) formic acid concentration of 30 mM. d) type of counterion, MP: MeOH/ACN (50/50; v/v) formic acid and acetic acid concentration of 100 mM, apparent pH adjusted to 5. SP: Chiralpak QD-AX™ 3x150 mm, linear flow velocity of 1.33 mm/s, sample injection volume 5 μ L.

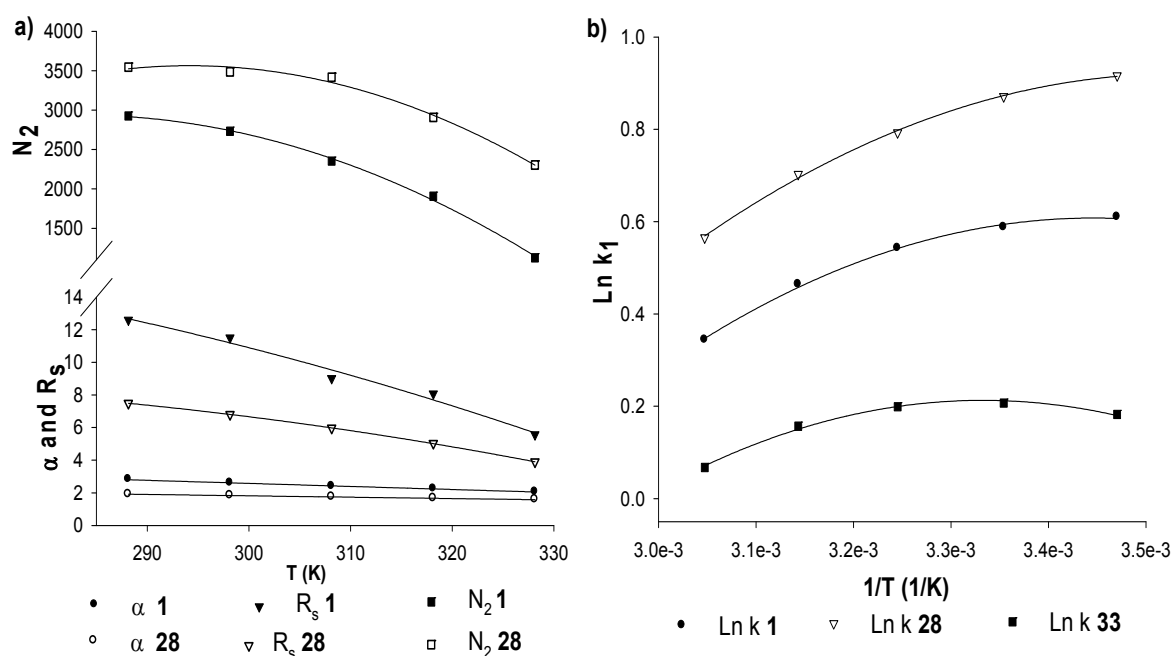
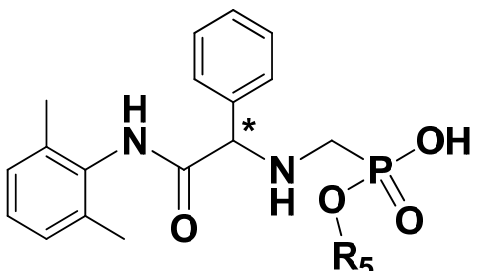


Fig. 4 a) Dependence of resolution, separation factor, and theoretical plate number of the second eluted enantiomer on temperature for compound **1** and **28**. b) Non linear van't Hoff plots of the retention factors for compounds **1**, **28**, **33**. Chromatographic conditions: stationary phase: Chiralpak QD-AX™ 150x4 mm I.D.; mobile phase: MeOH/ACN (50:50; v/v), 50 mM formic acid apparent pH adjusted to 4 with ammonia; flow-rate: 1 mL min⁻¹; detection UV:254 nm; ?.

Table 1: Summary of chromatographic data of amido-aminophosphonate compounds obtained by variation of the alcohol educt. Chromatographic conditions: stationary phase: Chiralpak QD-AX™ (150x3 mm I.D.); mobile phase: MeOH/ACN (50:50; v/v), 180mM acetic acid apparent pH adjusted to 5 with ammonia: flow-rate: 1.33 mm s⁻¹ (0.55 mL min⁻¹); ESI-MS detection in EIC; V_{inj}= 2 µL; T=298 K.



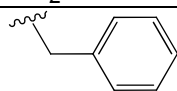
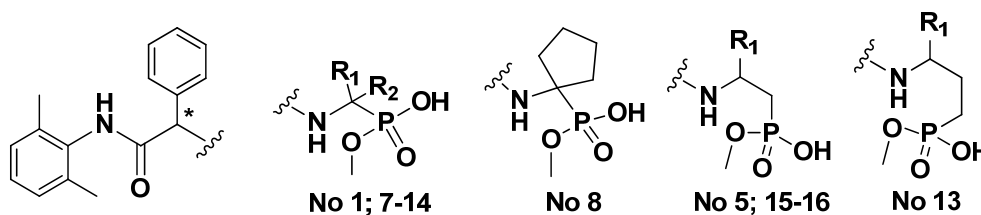
No	R ₅	k ₁	A	R _s
1	-CH ₃	2.18	1.11	1.84
2	-CH(CH ₃) ₂	1.60	1.12	1.85
3	-CH ₂ -CH=CH ₂	2.78	1.03	0.57
4		2.95	1	-

Table 2: Summary of chromatographic data of amido-aminophosphonate compounds obtained by variation of a single reaction component viz. aminophosphonic acid component: a) achiral b) chiral educts. For chromatographic conditions see *Table 2*.

a)



No	R ₁	R ₂	k ₁	α	Rs
1	-H	-H	2.18	1.11	1.84
5	-H	-	1.00	1.11	0.78
6	-H	-	0.66	1	0
7	-CH ₃	-CH ₃	2.34	1.15	2.45
8	-(CH ₂) ₄ -	-	2.39	1.15	2.25

b)

No	R ₁	R ₂	k ₁	α _{1/2}	Rs _{1/2}	K ₃	α _{3/4}	Rs _{3/4}
9	-CH ₃	-H	4.37	1.23	3.23	4.37	1.23	3.23
10	-CH(CH ₃) ₂	-H	3.83	1.59	9.89	4.29	1.53	6.34
11	-CH ₂ CH(CH ₃) ₂	-H	3.46	1.73	9.54	4.12	1.76	9.09
12	-CH ₂ CH(CH ₃) ₂	-CH ₃	1.51	1.42	4.49	1.54	1.42	4.54
13		-H	3.46	1.78	7.51	4.59	1.5	7.20
14		-H	25.08	1.41	25.64	30.07	1.33	15.73
15	-CH(CH ₃) ₂	-	0.65	2.27	2.00	0.75	2.37	3.07
16	-C(CH ₃) ₃	-	0.82	1.08	1.82	0.82	1.08	1.82

Table 3: Summary of chromatographic data of amido-aminophosphonate compounds obtained by variation of the aldehyde component. For chromatographic conditions see *Table 2*.

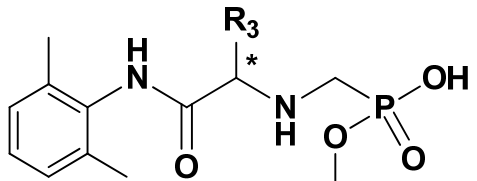
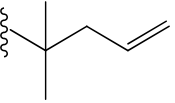
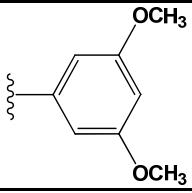
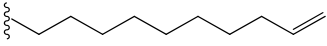
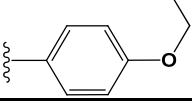
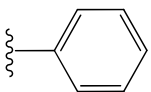
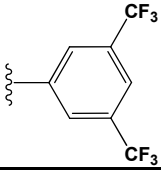
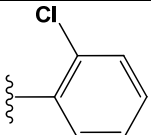
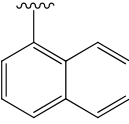
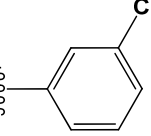
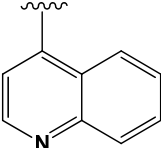
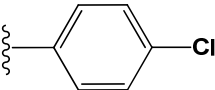
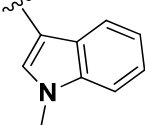
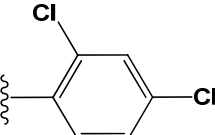
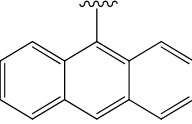
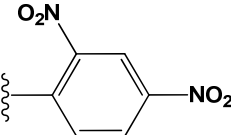
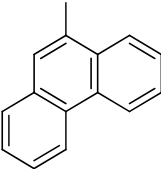
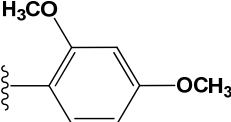
									
No	R ₃	k ₁	α	R _s	No	R ₃	k ₁	α	R _s
17		0.39	1.14	1.23	25		2.02	1.01	0.2
18		5.93	1	-	26		1.91	1.28	1.87
1		2.18	1.11	1.84	27		10.90	1	-
19		6.94	1.18	1.45	28		4.78	1.5	6.57
20		9.91	1.08	0.77	29		16.41	1.11	2.06
21		9.88	1.08	1.39	30		1.78	1.08	0.94
22		10.90	1.14	1.64	31		24.31	1.82	9.48
23		11.66	1.14	2.14	32		20.61	1.31	4.17
24		1.83	1.15	2.29					

Table 4: Summary of chromatographic data of amido-aminophosphonate compounds obtained by variation of the isonitrile educt. For chromatographic conditions see *Table 2*.

No	R ₄	k ₁	α	R _s
33	-C(CH ₃) ₃	1.48	1.1	1.59
34		3.76	1	-
35		0.32	1	-
1		2.18	1.11	1.84
36		8.49	1.07	1.24
37		10.57	1.05	0.75
38		0.35	1	-

Table 5: Summary of chromatographic data of amido-aminophosphonate compounds obtained by simultaneous variation of : a) aldehyde and amino acid b) aldehyde, aminophosphonic acid and alcohol educts. For chromatographic conditions see *Table 2*.

a)

No 41

No	R ₁	R ₃	R ₅	k ₁	α	Rs
39	-H			2.10 t ₀ ⁱ	2.10 t ₀ ⁱ	4.89 t ₀ ⁱ
1	-H			2.18 0.87 ⁱ	1.11 1.22 ⁱ	1.84 1.23 ⁱ
40	-H			- 2.35 ⁱ	- 1.41 ⁱ	- 2.79 ⁱ
41	-(CH ₂) ₄ -			14.66	2.06	12.88

b)

No	R ₁	R ₅	k ₁	α _{1/2}	Rs _{1/2}	K ₃	α _{3/4}	Rs _{3/4}
42	-CH ₂ CH(CH ₃) ₂	-CH ₃	9.56	1.72	10.55	9.25	1.66	8.36
43		-CH ₃	23.27	2.23	17.41	34.64	2.05	15.46
44		-CH ₂ -CH=CH ₂	23.27	2.23	17.41	34.64	2.05	15.46

ⁱ MP conditions: 80% methanol and 20% of a 50 mM aqueous phosphate buffer (Na₂HPO₄). The pH of the mixture was adjusted with phosphoric acid to the apparent pH_a = 5.6. The flow rate was 1 ml min⁻¹, and the column temperature was 25°C.

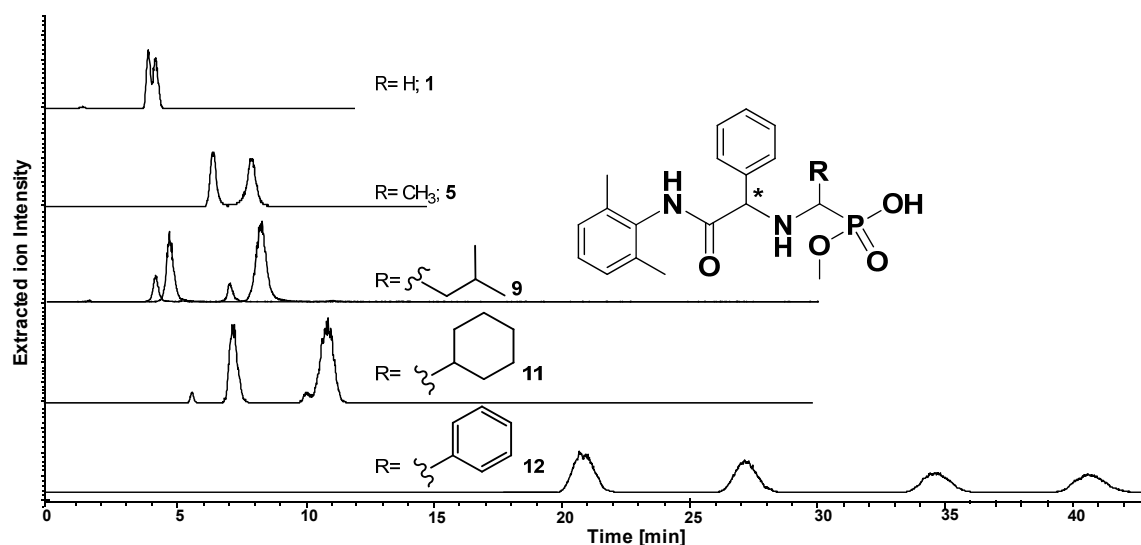


Fig. 5: Overlay of chiral anion-exchange LC-MS analysis of the raw reaction mixtures of compounds **1**, **5**, **9**, **11**, **12** reported in *Table 1*. Chromatograms are reported as EIC: **1** = *m/z* 361, **5** = *m/z* 375, **9** = *m/z* 417, **11** = *m/z* 443, **12** = *m/z* 437. **9** is a non-racemic mixture prepared by mixing reaction mixtures obtained from enantiomerically pure aminophosphonic acids, peak 1 and 3 from *R*-educt, 2 and 4 from *S*-educt. **11** is the product from *S*-enantiomer of a 95% ee aminophosphonic acid educt, peak 1 and 3 from *R*-form, 2 and 4 from *S*-enantiomer. For conditions refer to table 1.

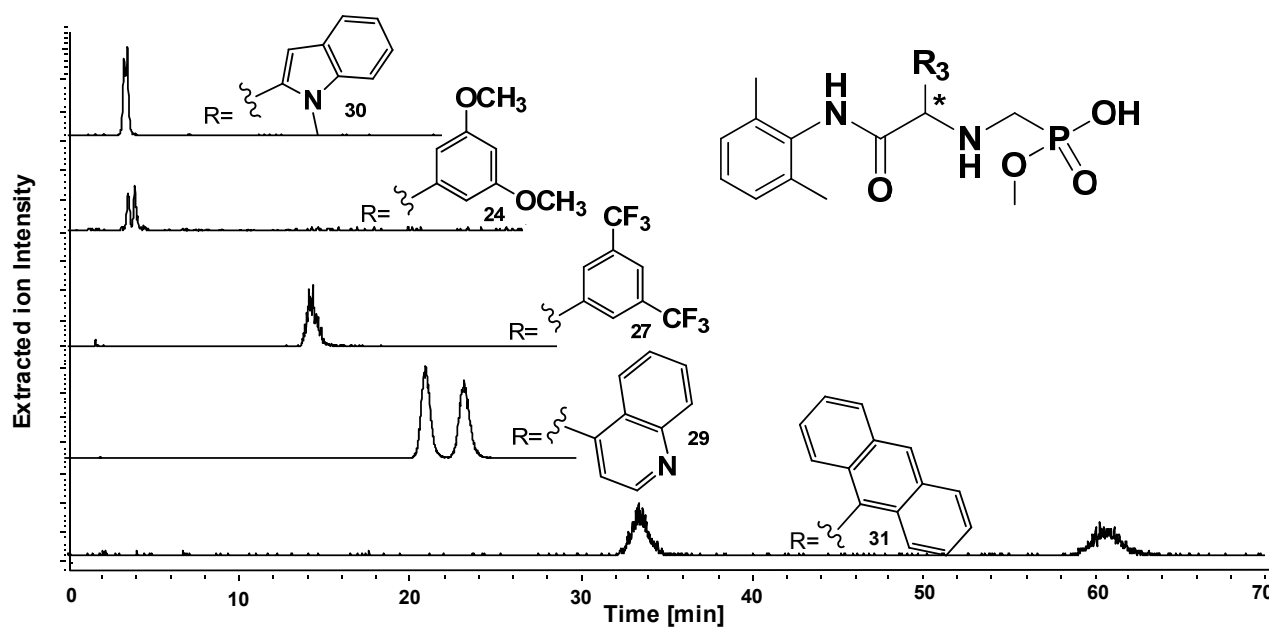


Fig 6: Overlay of chiral anion-exchange analysis by LC-MS of the reaction mixtures of compounds **30**, **24**, **27**, **29**, **31** reported in *Table 3*. Chromatograms are reported as EIC: **30** = m/z 414, **24** = m/z 421, **27** = m/z 412, **29** = m/z 499, **31** = m/z 461. For conditions refer to table 1.

Supporting information

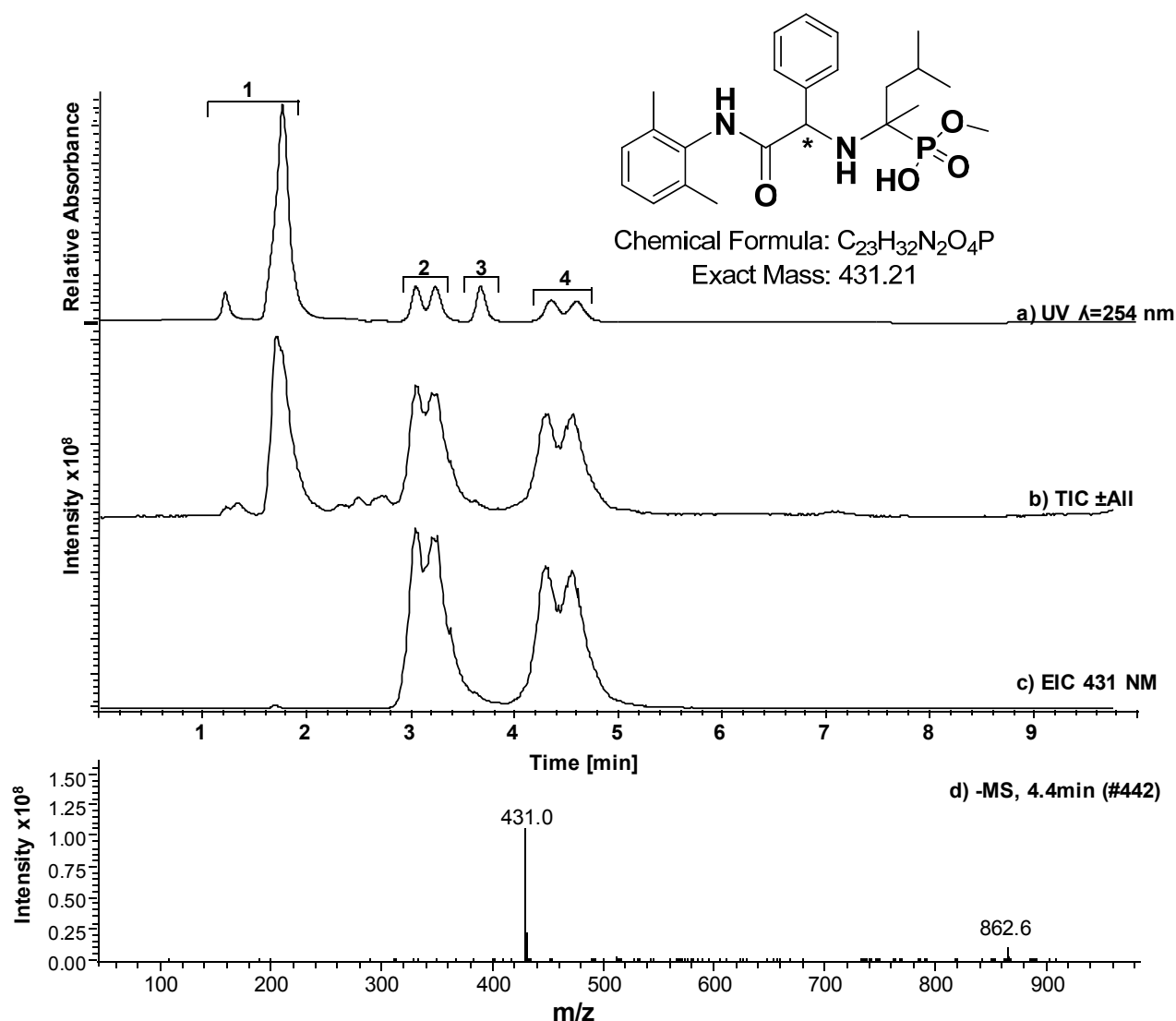


Fig. S1: Chromatograms of a reaction mixture with distinct detection schemes: a) UV ($\lambda=254$ nm) b) MS (total ion current), c) extracted ion chromatogram, and d) spectrum obtained by the injection of the reaction mixture of compound **10**. In the UV chromatogram a) peak 1 represents the elution of the reaction educts, 2 and 4 are the 4 stereoisomers of the product and peak number 5 is an acidic side-product. The mass of m/z 862.6 is given by the formation of dimers during the ionization process. Mobile phase conditions as specified in table 1.

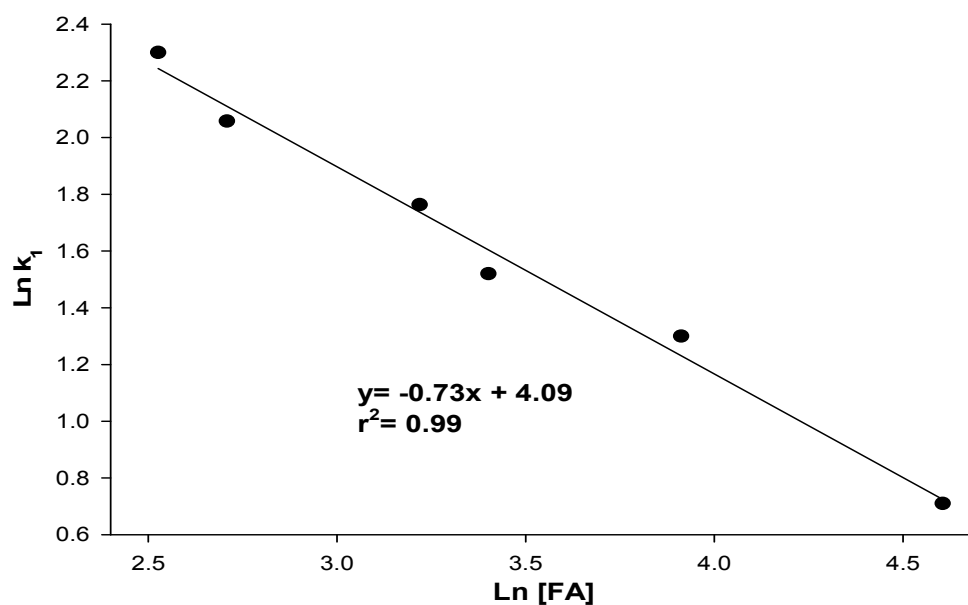


Fig. S2 Linear dependency of logarithms of retention factor of **1** versus logarithm of the concentration of the counterion. For conditions refer to figure 3a.

Table S1: Calculated pI and pKa values of **1 - 44**. Calculations performed with ChemAxon software on chemicalize.org

No	pI	pKa1	pKa2	pKa R
1	3.54	-0.28	7.35	
2	3.51	-0.33	7.35	
3	3.53	-0.29	7.35	
4	3.55	-0.26	7.35	
5	3.56	-0.22	7.44	
6	3.59	-0.36	7.53	
7	3.73	-0.33	7.78	
8	3.7	-0.37	7.76	
9	3.69	-0.32	7.7	
10	3.72	-0.36	7.79	
11	3.78	-0.32	7.87	
12	3.21	-0.42	6.85	
13	5.46	1.41	9.08	
14	5.67	1.41	9.49	
15	4.6	1.3	9.03	
16	5.26	1.92	8.57	
17	4.62	-0.28	8.29	
18	4.57	-0.28	8.18	
19	3.21	-0.26	6.69	
20	3.46	-0.28	7.19	
21	3.47	-0.28	7.22	

No	pI	pKa1	pKa2	pKa R
22	3.19	-0.34	6.71	
23	3.05	0.95	5.14	
24	3.16	-0.26	6.58	
25	3.82	-0.28	7.93	
26	3.54	-0.36	7.44	
27	3.38	-0.28	7.04	
28	3.59	-0.36	7.54	
29	5.09	-0.28	7.49	2.7
30	5.35	-0.29	7.99	3.13
31	3.82	-0.28	7.93	
32	3.71	-0.28	7.71	
33	3.59	-0.36	7.54	
34	3.54	-0.28	7.36	
35	3.59	-0.36	7.54	
36	3.5	-0.36	7.36	0.49
37	3.52	-0.28	7.32	
38	6.8	-0.36	7.55	5.75
39	5.1	3.26	6.94	
40	2.62	-0.65	5.87	8.06
41	4.59	-0.37	8.34	
42	4.61	-0.36	8.37	
44	3.5	-0.44	7.43	

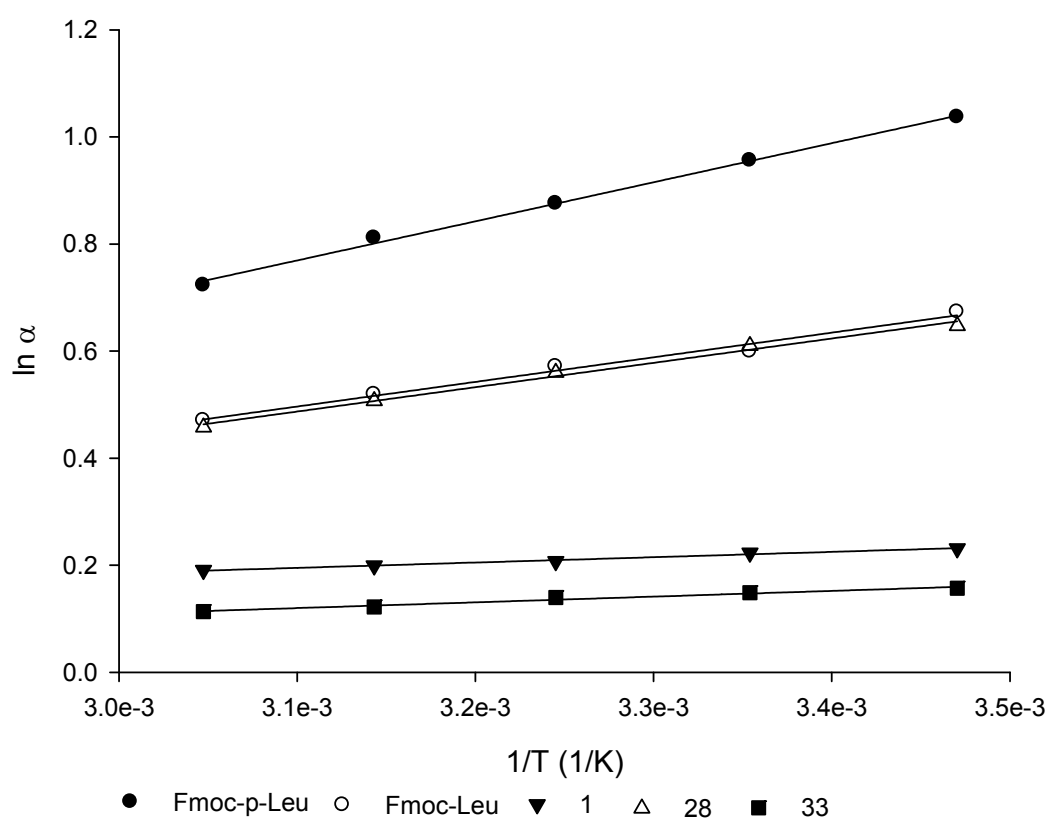


Fig. S3 Linear dependency of logarithms of selectivity factor of **Fmoc-P-Leu**, **Fmoc-Leu**, **1**, **28**, **33** versus $1/T$ ($1/K$). For conditions, refer to figure 4.

Table S2: Retention factors, enantioselectivity parameters and thermodynamic quantities of the enantiomer separation of Fmoc-protected Leucine, Fmoc-Phospholeucine and compounds **1**, **28** and **33** on Chiralpak QD-AX™^a. Data derived by graphical analysis of Figure S3.

SA	k_1	k_2	α	$-\Delta\Delta H^\circ$ (kJ/mol)	$-T\Delta\Delta S^\circ$ (kJ/mol)	$-\Delta\Delta G^{298}$ (kJ/mol)	Q^b
Fmoc-P-Leu	8.32	22	2.6	0.73	1.49	2.22	1.64
Fmoc-Leu	2	3.6	1.82	0.46	0.93	1.39	1.66
1	1.8	2.3	1.22	0.10	0.11	0.21	2.93
28	2.39	4.4	1.84	0.45	0.92	1.37	1.65
33	1.23	1.4	1.16	0.11	0.21	0.32	1.69

^a for chromatographic conditions see Fig.4.

^b $Q = \frac{\Delta\Delta H}{(\Delta\Delta S \cdot 298K)}$

Table S3: Comparison of the enantioselectivity parameters obtained by mobile phases based on formic acid and acetic acid as acidic buffer components. Mobile phases adjusted to pH 5 with ammonia

SA	MeOH/ACN 50/50 v/v					
	50 mM FA pH _a 5			180 mM AcOH pH _a 5		
	k_1	α	R_s	k_1	α	R_s
1	1.80	1.20	2.25	1.86	1.15	2.45
28	2.39	1.63	6.02	2.45	1.5	6.57
33	1.23	1.16	1.27	1.14	1.1	1.59

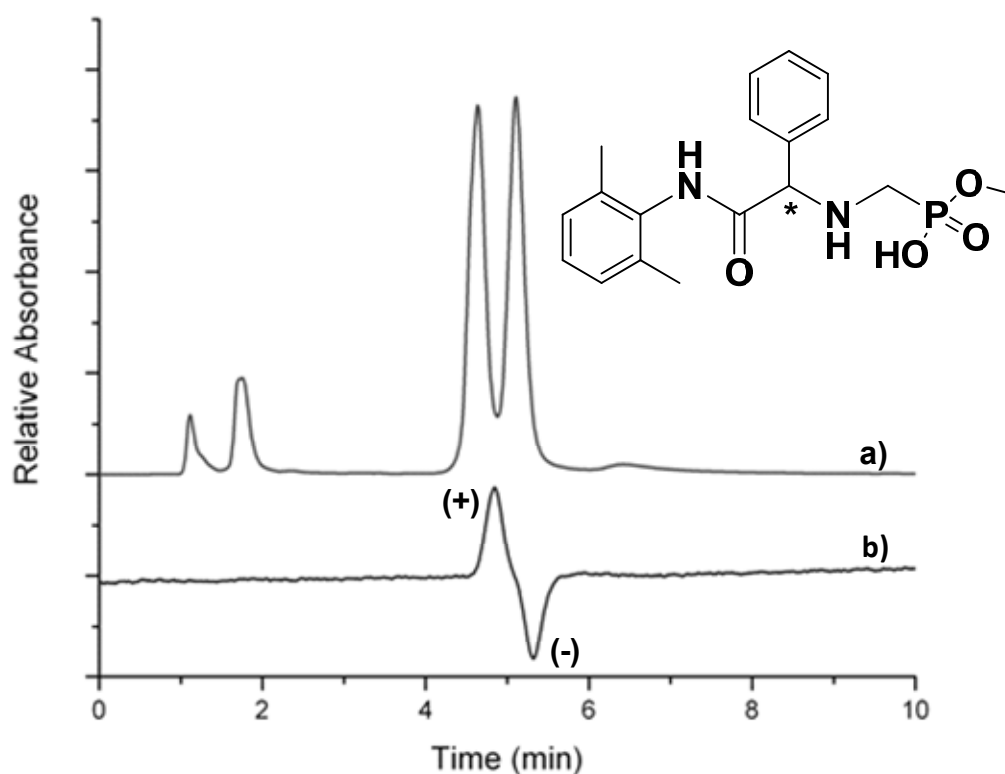
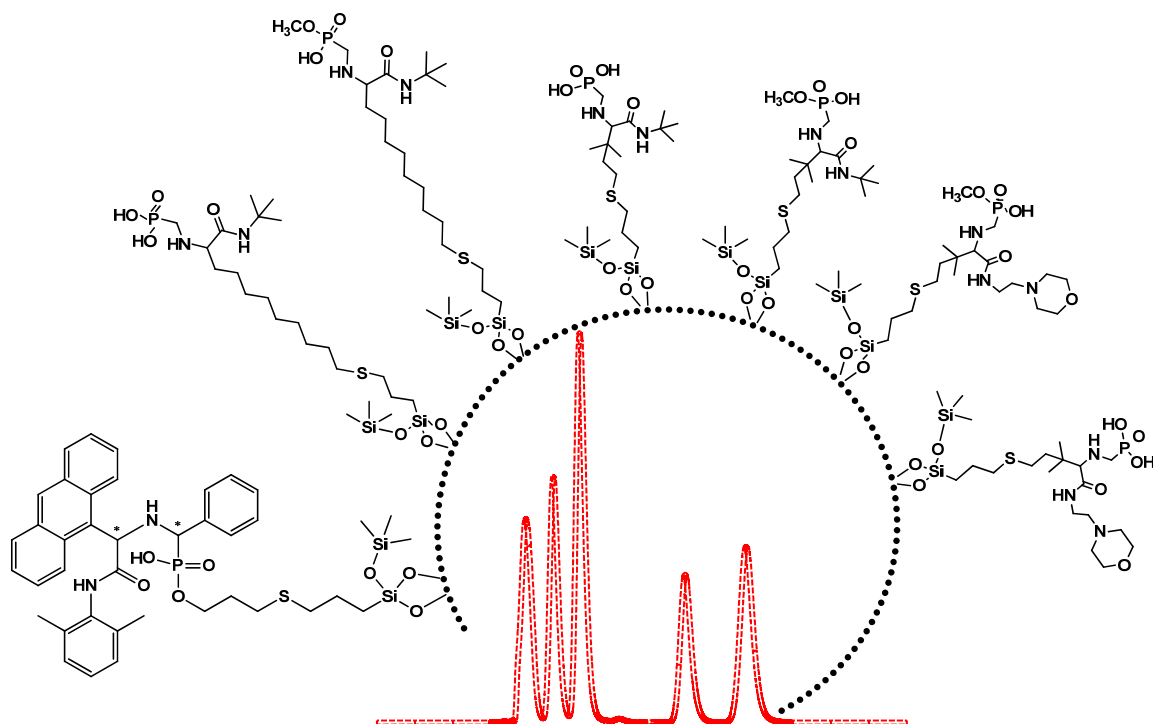


Figure S3: Chromatographic enantioseparation of **1** (purified by crystallization as reported in ^[72]) on Chiralpak QD-AX™. a) $\lambda = 254$ nm, b) Optical rotation detector (Jasco OR-990 optical rotation detector (Jasco, Groß-Umstadt, Germany)). Mobile phase conditions as reported in table 1.

Manuscript 4



Graphical abstract

Mixed mode chromatography with zwitterionic phosphopeptidomimetic selectors from Ugi multicomponent reaction

Mixed mode chromatography with zwitterionic phosphopeptidomimetic selectors from Ugi multicomponent reaction

Andrea F.G. Gargano¹, T. Leek², Wolfgang Lindner¹, Michael Lämmerhofer^{3*}

¹ *Department of Analytical Chemistry, University of Vienna, Waehringer Strasse 38, 1090 Vienna, Austria*

³ *AstraZeneca R&D Mölndal, Pepparedsleden 1 Mölndal, SE-431 83 , Sweden*

² *Institute of Pharmaceutical Sciences, University of Tübingen, Auf der Morgenstelle 8, 72076 Tübingen, Germany*

[*michael.laemmerhofer@uni-tuebingen.de](mailto:michael.laemmerhofer@uni-tuebingen.de)

Institute of Pharmaceutical Sciences

University of Tübingen

Auf der Morgenstelle 8

72076 Tübingen, Germany

T +49 7071 29 78793

F +49 7071 29 4565

Keywords

HPLC , Mixed mode chromatography, Ugi multicomponent reaction, Aminophosphonic acids, Aminophosphonate, HILIC.

Abstract

In the present contribution a novel Ugi multicomponent reaction (MCR) was used to generate zwitterionic chromatographic selectors with capability for application for mixed-mode chromatography featuring complementary selectivities in reversed-phase (RP) and hydrophilic interaction liquid chromatography (HILIC) modes. Aminophosphonate zwitterionic chromatographic molecules were synthesized adopting a single one pot microwave assisted three-component UGI-MCR synthesis and after purification were immobilized by thiol-ene click chemistry on silica beads. Chromatographic characteristics of these stationary phases were evaluated by variation of experimental conditions for a selected set of diverse analytes with neutral, acidic, basic and zwitterionic character. Interestingly multimodal separation capabilities were found for the novel selectors (i.e. columns can be operated both in HILIC and in RP mode with good selectivity and efficiency). They were further investigated comparatively to structurally related commercially available mixed mode, HILIC and RP columns. The resultant chromatographic data were analyzed by Principal Component Analysis (PCA). PCA clearly revealed that the new reversed-phase/zwitterionic ion-exchangers (RP/ZWIX) are complementary to common RP, HILIC and mixed-mode phases on the market and could be a promising alternative in impurity profiling and 2D-HPLC concepts. Moreover, the adopted synthetic approach offers the capability to generate chemical diversity simply by the variation of the starting aldehyde, aminophosphonic acid and or isonitrile components. This unique characteristics offers great possibility for the design of novel selectors for mixed mode chromatography like RP/ZWIX, HILIC, affinity and chiral chromatography.

1. Introduction

The analysis of biomolecules from biomatrices by means of reversed-phase chromatography-mass spectrometry (RPC-MS) can be problematic because of the weak retention properties offered by this technique towards highly polar molecules. Therefore, for analytes of biological interest such as metabolites or physiological intermediates alternatives to bare RPC have been introduced such as the addition of an ion pair to the mobile phase (IPC) or the use of hydrophilic interaction chromatography (HILIC). However, both the methods suffer from limitations such as ion suppression in MS detection for IPC or lack of retentivity of HILIC for lipophilic compounds. In this context the use of mixed-mode columns, offering combined orthogonal separation principles (e.g. RP-WAX) results in novel selectivity profiles that allow the differentiation of the analytes on the basis of various different characteristics rather than just hydrophobicity [1]. The application of this chemistry is known in solid-phase extraction materials [2] and capillary electrochromatography [3]. This approach in LC has become more popular recently. In mixed-mode liquid chromatography different separation principles such as RP and size exclusion [4], size exclusion and cation-exchange [5], RP and HILIC [6-8], RP and anion-exchange [9, 10], RP and cation-exchange [11] have been combined on a single stationary phase to form mixed-mode phases. Such materials also offer greater flexibility in method development and are thus powerful tools when RPLC fails.

Herein, we present the use of amido-aminophosphonate derivatives obtained by Ugi reaction as novel reversed-phase/zwitterionic ion-exchangers (RP/ZWIX). These materials demonstrated reversed-phase (RP), hydrophilic interaction liquid chromatography (HILIC) and ion exchange chromatography (IEX) increments tunable by modification of the elution conditions. This study analyzes the selectivity properties in dependence of the mobile phase composition, demonstrates the applicability of such materials for typical RP and HILIC separations and compares the results obtained towards commercially available columns commonly employed.

2. Materials and methods

2.1. *Materials*

HPLC solvents methanol (MeOH) and acetonitrile (ACN) were of HPLC-grade quality and purchased from Sigma-Aldrich (Vienna, Austria) and Merck (Darmstadt, Germany). Millipore grade water was obtained from an in-house Millipore system (resistivity: 18.2 M Ω x cm at 25 °C). Formic acid (FA), 7N ammonia solution in MeOH and acetic acid (AA) were of analytical grade from Sigma–Aldrich (Vienna, Austria).

The test compounds (butylbenzene, pentylbenzene, caffeine, theobromine, theophylline, adenosine, cytidine, guanosine, thymidine, uridine, ascorbic acid, nicotinic acid, pyridoxine, riboflavin, thiamine) were supplied by Sigma-Aldrich. O,O-Diethyl thiophosphate (DETP) was prepared by hydrolyzation of O,O-diethyl chlorothiophosphate (from Aldrich) in a mixture of ACN/ water (3:1, v/v) in the presence of an equimolar amount of triethylamine. N-tert-Butoxycarbonyl-prolyl-phenylalanine (Boc-Pro-Phe) was purchased from Bachem (Buchs, Switzerland).

2.2. *Synthesis of the amido-aminophosphonate selectors*

The general procedure for the synthesis of the zwitterionic amido-aminophosphonate selectors was reported in [12]. Briefly, the selected aldehyde (1 eq) and the 1-aminomethyl phosphonic acid (1 eq.) were dissolved in MeOH (0.25M) in a microwave glass vial. Tetra-n-butylammoniumhydroxyde (0.25 eq. from 1M methanolic solution) and isocyanide (1 eq) were sequentially added to this mixture. The microwave reaction vial was sealed, heated and stirred under microwave irradiation at 100 °C for 150 min. In case of the presence of residual unreacted educts, the reaction mixture was filtered. The filtrate containing the reaction product was transferred into a round flask, while the white precipitate (constituted by the unreacted aminophosphonic acid) was allowed to react in the same conditions reported before with another aliquot of aldehyde and isonitrile in TBAH solution for another 150 min (below the quantities of aldehyde and isocyanide are given as total amount adopted over the two synthesis cycles). The filtrate was evaporated under reduced pressure and the crude residue was purified by column chromatography or chiral anion exchange chromatography, giving viscous oils or solids as products

Methyl (([1-(tert-butylamino)-3,3-dimethyl-1-oxohex-5-en-2-yl]ammonio)methyl)phosphonate (SO 1, SP 1): Prepared from (1-aminomethyl)phosphonic acid (4.50 mmol), 2,2-dimethyl-4-pentenal (9 mmol over the two synthesis cycles) and tert-butyl isocyanide (9 mmol over the two synthesis cycles). The pooled reaction product was purified by HPLC using Chiralpak QD-AX as column (10 μ m particles, 250 x 2.5 cm ID). $k = 2.95$ (MeOH/ACN 50/50; v/v containing 25 mM formic acid, apparent pH adjusted in mixture to 4 with NH_4OH). Compound obtained from a single fraction (not enantioseparated) as a sticky solid (yield: 1330 mg, 4.16 mmol 93%). ^1H NMR (400 MHz, CD_3OD , 25°C , TMS): δ 5.90 (m, 1H), 5.15 (m, 2H), 3.80 (s, 1H), 3.63 (d, $J = 10.33\text{Hz}$, 3H), 3.07 (m, 1H), 2.80 (m, 1H), 2.21 (m, 1H), 2.03 (d, $J = 16.14\text{Hz}$, 1H), 1.38 (s, 9H), 1.06 (d, $J = 7.10\text{ Hz}$, 6H) ppm; ^{13}C NMR (101 MHz, MeOD, 27°C , TMS) δ 167.2 (C=O), 134.5 (CH-Allyl), 119.6 (CH₂-Allyl), 70.3 (JC,P= 4 Hz, CH), 53.0 (C (CH₃)₃, 52.3 (JC,P= 7 Hz, OCH₃), 44.2 (CH₂), 37.4 (CH₂), 28.7 (C(CH₃)₃), 24.8 (Cq), 24.1- 23.3 (JC,P= 70 Hz, CH₂) ppm; ^{31}P NMR (162 MHz, CD_3OD , TMS): δ 11.87 ppm; FT-IR ν : 3456, 2969, 2794, 1665, 1600-1400, 1296 cm^{-1} ; MS (ESI): m/z 375.2 $[\text{M-H}]^-$;

Methyl ([2,2-dimethyl-1-([2-(morpholin-4-yl)ethyl] ammonio)methyl)phosphonate (SO 3; SP 3): Prepared from (1-aminomethyl)phosphonic acid (639 mg, 5.77 mmol), 2,2-dimethyl-4-pentenal (9 mmol), and 2-morpholinoethyl isocyanide(9 mmol), purified by liquid/liquid extraction (3 X 0.1M HCl / DCM) followed by evaporation under vacuum ^1H NMR (400 MHz, MeOD, 27°C) δ 5.79 – 6.01 (m, 1H), 5.02 – 5.15 (m, 2H), 3.70 (dd, 7H), 3.6 – 3.65 (m, 3H), 3.36 – 3.43 (m, 3H), 3.33 (dt, 2H), 2.73 (dt, 1H), 2.83 (s, 1H), 2.56 – 2.62 (m, 1H), 2.05 – 2.31 (m, 2H), 0.98 (dd, 6H) ppm. ^{13}C NMR (101 MHz, MeOD, 27°C) δ 175.7, 136.7, 118.6, 74.2, 68.3, 59.9 - 59.1, 55.0, 47.4, 37.1, 25.4, 25.2, 24.8, 14.4 ppm. ^{31}P NMR (162 MHz, MeOD, 27°C) δ 22.02 ppm. MS (ESI): m/z 376.3 $[\text{M-H}]^-$

Methyl (([1-(tert-butylamino)-1-oxododec-11-en-2-yl]ammonio)methyl)phosphonate (SO 5; SP 5). Prepared from (1- aminomethyl)phosphonic acid (639 mg, 5.77 mmol). Purified by HPLC with Chiralpak QD-AX. $k_1 = 3.78$ (MeOH/ACN 50/50; v/v containing 25 mM formic acid, apparent pH adjusted in mixture to 4 with NH_4OH). Compound obtained from a single fraction (not enantioseparated) as a sticky solid (yield: 1.47 g, 3.9 mmol 68%). ^1H NMR (400 MHz, CD_3OD , 25°C , TMS): δ 5.81 (m, 1H), 4.97 (m, 2H), 3.61 (d, $J = 11.11\text{Hz}$, 2H), 3.36 (s, 1H), 2.98 (m, 2H), 2.06 (m, 2H), 1.37 (m, 23H) ppm ^{13}C NMR (101 MHz, MeOD, 27°C , TMS) δ 168.1 (C=O), 140.1 (CH-Allyl), 114.7 (CH₂-Allyl), 62.8 (CH), 52.8 (Cq), 52.3 (OCH₃) , 42.5-41.1 (JC,P= 140 Hz, CH₂), 34.8 (CH₂), 31.6 (CH₂), 30.3 (CH₂), 30.1 (CH₂), 28.8 (CH₃), 25.7 (CH₂) ppm; ^{31}P NMR (162 MHz, CD_3OD , TMS): δ 11.19 ppm; MS (ESI): m/z 362.2 $[\text{M-H}]^-$;

Procedure for the hydrolysis of the amido-aminophosphonic acid methyl ester derivatives [12-14],. A solution of purified monomethyl ester (0.7mmol) in dry dichloromethane (CH_2Cl_2 , 20mL) was sonicated for about 1 minute. Bromotrimethylsilane (BrSiMe_3 , 5eq) was added dropwise and the reaction was allowed to react overnight at 25 °C. After removal of the solvent under reduced pressure methanol (10mL) was added. The solution was heated at 50 °C for 2h and concentrated under high vacuum to obtain the hydrobromide salt of the respective aminophosphonic acid derivative as yellow solid in quantitative yield.

{{[1-(tert-butylamino)-3,3-dimethyl-1-oxohex-5-en-2-yl]amino}methyl}phosphonic acid (SO 2; SP2): ^1H NMR (400 MHz, CD_3OD , 25°C, TMS): δ 5.90 (m, 1H), 5.15 (m, 2H), 3.80 (s, 1H), 3.63 (d, $J = 10.33\text{Hz}$, 3H), 3.07 (m, 1H), 2.80 (m, 1H), 2.21 (m, 1H), 2.03 (d, $J = 16.14\text{Hz}$, 1H), 1.38 (s, 9H), 1.06 (d, $J = 7.10\text{ Hz}$, 6H) ppm; ^{13}C NMR (101 MHz, MeOD, 27°C, TMS) δ 166.1 (C=O), 134.1 (CH-Allyl), 119.9 (CH_2 -Allyl), 70.1 ($J_{\text{C,P}} = 4\text{ Hz}$, CH), 53.4 (C(CH_3)₃), 44.1 (CH_2), 37.5 (CH_2), 28.4 (C(CH_3)₃), 24.9 (Cq), 24.0- 23.2 ($J_{\text{C,P}} = 74\text{ Hz}$, CH_2) ppm; ^{31}P NMR (162 MHz, CD_3OD , TMS): δ 11.87 ppm; ; MS (ESI): m/z 375.2 [M-H]⁻;

{{[2,2-dimethyl-1-{{[2-(morpholin-4-yl)ethyl]carbamoyl}pent-4-en-1-yl]amino}methyl}phosphonic acid (SO 4; SP4): ^1H NMR (400 MHz, MeOD, 27°C) δ 5.11 (dd, 2H), 5.81 (ddt, 1H), 3.82 – 3.99 (m, 7H), 3.53 – 3.61 (m, 2H), 3.43 (tdd, 4H), 3.21 – 3.22 (m, 2H), 2.02 – 2.29 (m, 2H), 0.96 – 1.1 (m, 6H) ppm. ^{13}C NMR (101 MHz, MeOD, 27°C) δ 169.7, 134.4, 120.7, 70.4, 65.3, 60.0, 38.5, 34.9, 25.2, 24.7, 23.7, 21.1, 14.3 ppm. ^{31}P NMR (162 MHz, MeOD, 27°C) δ 9.37 ppm. MS (ESI): m/z 365.2 [M-H]⁻

{{[1-(tert-butylamino)-1-oxododec-11-en-2-yl]amino}methyl}phosphonic acid (SO 6 SP6): ^1H NMR (400 MHz, CD_3OD , 25°C, TMS): δ 5.81 (m, 1H), 4.97 (m, 2H), 3.61 (d, $J = 11.11\text{Hz}$, 2H), 3.36 (s, 1H), 2.98 (m, 2H), 2.06 (m, 2H), 1.37 (m, 23H) ppm; ^{13}C NMR (101 MHz, MeOD, 27°C, TMS) δ 168.6 (C=O), 140.6 (CH-Allyl), 115.4 (CH_2 -Allyl), 63.3 (CH), 52.8 (Cq), 42.7-41.3 ($J_{\text{C,P}} = 140\text{ Hz}$, CH_2), 34.9 (CH_2), 31.6 (CH_2), 30.3 (CH_2), 30.2 (CH_2), 28.6 (CH_3), 25.5 (CH_2) ppm. ^{31}P NMR (162 MHz, CD_3OD , TMS): δ 11.19 ppm; MS (ESI): m/z 362.2 [M-H]⁻

2.3. *Selector immobilization (covalent bonding) to silica*

Daisogel silica gel (120 Å, 5 µm) was thio-propyl modified according a previously reported synthetic approach [15], followed by endcapping of free silanol groups with Bis-trimethylsilylacetamid. The calculated thiolcoverage was 0.64 mmol/g as determined by sulfur elemental analysis (4.96% C, 1.20% H, 2.11% S). Oven-dried thio-propyl silica gel (2.20 g), was suspended in methanol (10 ml) and SO (0.89 mmol) dissolved in methanol (5 ml) as well as α,α' -azobisisobutyronitrile (30 mg, 0.18 mmol) were added. The suspension was stirred under reflux for 6 h. After filtration the silica gel was washed with methanol (3 × 20 ml), diethylether (2 × 20 ml), and dried in vacuo at 60°C to yield the new SPs. The SO coverage was calculated from the phosphorus and nitrogen content obtained by elemental analysis (data reported in *Table 1*). The obtained materials were slurry packed into stainless steel columns (150 mm × 4 mm I.D.) using MeOH/2-propanol (90/10; v/v) as slurry solvent.

2.4. *Chromatographic methods*

2.4.1. *Apparatus and chromatography*

HPLC experiments were carried out using an 1100 series LC system from Agilent Technologies (Agilent, Waldbronn, Germany) equipped with a binary gradient pump, autosampler, vacuum degasser, temperature-controlled column compartment, diode array detector for the detection of aromatic samples. The data were processed with Agilent ChemStation software version Rev. B.01.03.

2.4.2. *Stationary phases*

The retention characteristics of the new zwitterionic phosphopeptidomimetic stationary phases were comparatively evaluated in comparison two commercial RP, HILIC and mixed-mode stationary phases. Details about the employed columns can be found in ref. [16]. Additionally, a few other columns were included such as the C-Chocolate column (4x 150mm, 3µm 120 Å silica material) (synthesized as reported in [17]), Nucleodur (Macherey & Nagel, 4x 150 mm, 5µm 100 Å) and PC-HILIC (Shiseido, 4x 150 mm, 5µm 100 Å).

2.4.3. *Mobile phase influence on retention process and repeatability study*

All the studies on mobile phase effects were performed with SP1. The chromatographic conditions are reported in *Figure 4* and *5*. Analytes were dissolved in ACN/ water (90/10; v/v) in a concentration of 0.5 mg/mL. In the repeatability study (*Figure 5*) chromatogram f) was obtained after 100 injections.

2.4.4. *HILIC test conditions*

The mobile phase for the HILIC test mixture was composed of ACN/ammonium acetate buffer (95:5 v/v) for the xanthins test and (90:10 v/v) for the nucleosides and vitamins tests, respectively, and the total buffer concentration was 5 mM. The eluent pH was unadjusted and had an apparent pH of about 8. The flow rate was adjusted to the same linear velocity ($u = 1.7$ mm/s). The test mixtures are specified in *Figure 6* and the concentration was about 1 mg/mL for each compound dissolved in ACN/50mM ammonium acetate (90/10; v/v). Samples were prepared in ACN/H₂O (50/50; v/v), the injection volume of the sample was 5 μ L, column temperature 25°C and the detection wavelength was set to 220 nm. Toluene was used as void volume marker

2.4.5. *RP test conditions*

The mobile phase for the RP-HPLC test run was composed of a mixture of ACN and water (40:60, v/v) containing in total 0.29% (v/v) glacial acetic acid ($C_{tot} = 50$ mM). The pH of the mixture was adjusted to pH 6 with ammonia. The flow rate was adjusted to an equivalent linear flow velocity u of 1.7 mm/s in order to have comparable conditions for columns of different dimensions. The test mixture consisted of butylbenzene, pentylbenzene, DETP, and Boc-Pro-Phe (dissolved in the mobile phase each at a concentration of 0.8 mg/mL). Analyte structures are reported in *Figure 6*. Samples were prepared in ACN/H₂O (50/50; v/v), uracil was employed as void volume marker. The injection volume of the sample was 5 μ L. The column was thermostated at 25°C and the detection wavelength was set to 220 nm.

3. Results and discussion

In the present contribution, we report the chromatographic evaluation of novel amido-aminophosphonates mixed mode stationary phases for LC. These zwitterionic selectors were obtained by a Ugi multicomponent reaction [12] (*Figure 1*) which allows straightforward introduction of functional moieties and binding increments, respectively, via residues of educts and thus flexible adjustment of the selectivity of the stationary phase. We illustrate this concept by the investigation of the retention properties of these novel mixed-mode phases in HILIC and RP-type elution modes and study the dependence of the retention properties on mobile phase composition and structural variations of the selector scaffold.

3.1. *Synthesis of amido-aminophosphonate chromatographic selectors*

Figure 2 depicts the reaction scheme for the synthesis. The aminophosphonic acid condenses together with aldehyde and isocyanide educts in alcohol to generate peptide-like amino phosphonic acid derivatives. Adopting a multi-component reaction approach molecules carrying the same structural motif can be differently substituted under the same reaction conditions using different reactants. In this study, we adopted two different aldehydes and isocyanides in combination with (1-aminomethyl) phosphonic acid using methanol as solvent. A part of the obtained amido-aminophosphonate selectors were subsequently hydrolyzed obtaining a total pool of 6 selectors possessing different acidity and lipophilicity characteristics. The selectors were then immobilized onto thiopropyl-modified silica gel employing thiol-ene click chemistry, generating brush type stationary phases. Elemental analysis data and derived surface coverages for the produced stationary phases are reported in *Table 1*. Although the same conditions were adopted for the immobilization of phosphonate and phosphonic acid selectors the latter resulted in phases having lower surface coverage with respect to their methyl ester derivatives, probably as a consequence of the higher acidity and the consequently stronger electrostatic repulsion interaction with the residual silica silanols of the thiolated phase.

3.2. *Impact of mobile phase variables on retention*

As depicted in *Figure 1* the selectors reported in this study present potentially reversed-phase, ion-exchange, hydrogen-bonding and ion-exclusion retention increments. It is therefore hypothesized that the retention characteristics are derived by a complex interplay

of different retention contributions. In order to study in more details the influence on retention and derive information on the interactions responsible for generating retention we investigated nature and amount of organic modifier, salt concentration and w_pH of the aqueous eluent fraction and column temperature. The study was conducted using SP1 and the analyte set shown in *Figure 3*. The results are summarized in *Figure 4* and described below.

3.2.1. *Variation of modifier content*

The effect of the ACN fraction in the hydro-organic eluent was studied in a range of 5–95% v/v. *Figure 4a* exemplifies the findings for adenine with a mobile phase composed of acetonitrile/20 mM ammonium acetate ($w_pH = 7$). The analyte experienced markedly increased retention at higher amounts of ACN (>60%), a result that indicates the presence of a HILIC-type retention mechanism as expected. On the other hand, we observed a significant RP-like retention at low fractions of ACN (< 20%), resulting in a U-shaped retention curve with respect to the organic modifier content. This result clearly demonstrates the presence of a dual retention mechanism of the present zwitterionic phosphopeptidomimetic stationary phase, in which reversed-phase (at low organic modifier content) and hydrophilic interaction (at high modifier content) mechanisms are prevalent in dependence of the content of organic modifier.

3.2.2. *Variation of salt concentration at fixed w_pH value*

Variation of the salt concentration of mobile phases composed of ACN/ ammonium acetate buffer 90/10 ($w_pH = 7$) resulted in different retention depending on the solute characteristics, demonstrating the importance of ionic interactions in the retention process in the case of ionic analytes. The retention of neutral or non-ionized polar compounds such as adenine and guanine were not influenced by the buffer concentration (slope = 0; *Figure 4b*). In contrast, the corresponding plots of hydroxybenzoic acid and tyramine showed slopes with opposite signs. In the case of the basic compound tyramine an inverse linear relationship was observed between $\ln k$ and $\ln C$, indicating the importance of cation exchange contribution in the retention process. In contrast, the retention increase observed for the acidic compound 4-hydroxybenzoic acid when the ammonium acetate concentration is increased indicates that repulsive ionic interactions are active. Higher ionic strength causes a thinner double layer around the solute ion and the surface-bound ion (i.e. the ion-exchange site) and thus a lower potential. This of course weakens the actual electrostatic repulsion between positively charged ion-exchanger and positively charged acid analyte.

Therefore, it can be concluded that the weak anion exchange properties of the selector, given by the secondary amino residue are outbalanced by the strong phosphonic acid residue under the studied conditions. This results in retention properties similar to a mixed mode RP/cation-exchange phase. In line with this, the zwitterionic solute Tyr behaves more like an acidic compound under given conditions and thus shows a slightly positive slope, i.e. slightly excessive repulsive electrostatic interactions.

3.2.3. *Variation of w_pH at fixed salt concentration*

The charged status of both the analytes and the stationary phase are influencing the strength of ionic, hydrophobic and hydrophilic interactions. The isoelectric point of the zwitterionic selector has been calculated to be around 4.6. Residual silanols probably cause a further shift of the pI to even more acidic. Thus, the hydrophilicity of the ligand increases between pH 4 and 8 from log D of about -1.1 to about - 2.7 and the dissociation and hence the hydrophilicity of the residual silanols gradually increase between pH 4 and 6 as well giving the selector more hydrophilic nature in the pH range between 6 and 8. *Figure 4c* reveals the change of retention factors with w_pH of the eluent and it appears that the shift towards more acidic conditions leads to a decrease in the charge state of the stationary phase (the graph of variation of calculated log D in dependence of pH is reported in the supporting information). The behavior of the basic tyramine can be explained by the change in the dissociation state of the solute which gradually decreases its dissociation when the w_pH is increased. This results in weaker cation exchange interactions and reduced retention at higher pH. The decrease of the retention of the acidic test solute 4-hydroxybenzoic acid upon pH increase can be rationalized by stronger repulsive electrostatic interaction by the more negatively charged selector under such conditions. The zwitterionic tyrosine follows more or less the trends of the basic and acidic test solutes but shows a stronger effect indicating the combined effect of decrease of cation exchange interaction between acidic selector and cationic analyte as well as strengthening of repulsive electrostatic interactions between selector and carboxylic acid moiety of the solute as the pH is increased. 4-Hydroxybenzylalcohol as neutral solute shows a minor effect but retention is slightly decreased at higher pH as well which can be explained by minor dissociation of the phenolic hydroxyl group once the pH is increased. Overall, pH effects can be quite complex and hard to interpret because of the interplay between dissociation states of the various ionizable groups at the ligand, the support, the solutes as well as the buffer constituents.

3.2.4. *Variation of temperature*

Temperature effects were studied in the range of 15–55°C (*Figure 4d*). Retention of non-charged compounds decreased at higher temperatures, tantamount to negative retention enthalpies. Linear van't Hoff plots were observed for all 3 investigated compounds indicating that the retention mechanism does not change over the investigated temperature range.

3.2.5. *Repeatability study and phosphonate ester stability*

In order to investigate the stability of the ester residue under the chromatographic conditions we analyzed the repeatability of the separation performance and peak parameters for a mixture of nucleobases over 100 injections as reported in *Figure 5*. If the methyl phosphonate ester gets hydrolyzed under chromatographic conditions, retention factors should significantly change over time. If this is not the case, sufficient stability would be indicated by this test. In fact, only a very small RSD% (0.45% for 5, guanine) for retention time was observed after 100 injections on column. This proves the chemical stability of the zwitterionic selectors under chromatographic conditions. Moreover, to assess the possible hydrolysis we kept a solution of selector SO1 at 60°C in MeOH and no signs of bis-methyl ester formation were determined by RPLC-MS (data not shown).

3.3. *Characterization of novel mixed mode columns under HILIC elution mode*

To get a more defined idea of the structural elements responsible for retention we have undertaken comparative HILIC tests using three different test mixtures as previously published in [16] for all the produced selectors and stationary phases, respectively. For comparison also thiopropyl silica and a traditional RP material (Synergy Fusion RP) were tested. The test mixtures contained nucleosides (adenosine, cytidine, guanosine, thymidine, and uridine, test set 1), xanthins (caffeine, theobromine, and theophylline; test set 2), and the last one water-soluble vitamins (ascorbic acid, nicotinic acid, pyridoxine, riboflavin, thiamine; test set 3). All analytes were frequently employed solutes to test HILIC columns. Their structures are depicted in Fig. 6 and the chromatographic results are reported in *Figure 8 and 9* and *Table 3,4 and 5*.

Generally, we can conclude that neither the RP column nor the thiopropyl modified silica are demonstrating relevant HILIC properties. By a comparison of the phosphonic/phosphonate phases with respect to the unmodified thiopropyl silica (*Table 3 ,4 ,5*) shows that the

chemical surface of thiopropyl silica is *per se* not capable of generating retention under HILIC conditions and the immobilization of the amido-aminophosphonic/phosphonate compounds leads to the establishment of HILIC like chromatographic properties.

As reported in *Figure 8* none of the amido-aminophosphonate columns displayed the elution order expected from their hydrophilicity as derived by the log D values (reported in *Table 2*: adenosine 1, thymidine 2, uridine 3, guanosine 4, cytidine 5). We observed that compounds with higher hydrogen-donor/acceptor numbers are stronger retained than expected from the log D values leading to the altered elution orders: thymidine (2) < adenosine (1) < uridine (3) < cytidine (5) < guanosine (4). This elution order was observed for all the columns with SP 1-6 except for SP 2 (for which it was perturbed probably due to the low ligand coverage) and has to be ascribed to the mixed mode character of the stationary phases as previously reported in [16].

Baseline separation of all the nucleosides was obtained just in the case of SP1 and the worst separation properties were offered by its phosphonic acid derivative (SP2). The reason for the lower performance of this stationary phase is certainly related to the lower surface coverage with less than half of selector bound per m² compared to its methyl ester equivalent. As a consequence, retention characteristics of the unmodified thiopropyl residues gets prevalent which has poor HILIC capabilities but instead a significant hydrophobic character as discussed in the RP characterization. Although similarly low coverages were obtained in the case of SP4, the presence of the additional charged morpholino group can compensate for this effect. In fact, contributions from linker and support of surfaces incompletely covered with selectors complicate the understanding of the true nature of HILIC interaction principles of various ligands as described by several authors [18].

It appears that the similar behavior of the columns for this analyte set is significantly driven by the H-bonding amide and that the distance between amide groups of the ligand and the residual unmodified thiol groups can influence the retention. This hypothesis is supported by the higher strength of interaction registered for SP5 and 6, which were anchored via a longer spacer (C 10 instead of C5 present in the other SPs).

Figure 9 illustrates the resultant chromatograms for the xanthins. It is evident that a HILIC mode separation is realized on all of the stationary phases. Once again the elution order for all the columns does not follow the decrease in the calculated log D (caffeine > theophylline > theobromine). The inversion of the elution of the dimethyl xanthine derivatives (theobromine > theophylline) cannot be ascribed to the establishment of stronger additional ionic interaction. The slightly more acidic theophylline ($pK_{a, \text{theophylline}} = 8.6$) should be more repulsed with respect to the more basic theobromine ($pK_{a, \text{theobromine}} = 9.9$).

Next, a mixture of water soluble vitamins was analyzed. Reported retention characteristics are highly dependent on the selector and analyte structure which are not explainable only on the basis of a partitioning mechanism (*Table 5*). To some extent, this is not surprising because this test sample contains ionic constituents. In particular the variation of the retention of thiamine, nicotinic and ascorbic acid correlate strongly with the calculated isoelectric point of the selectand. All the selectors carrying a phosphonic acid residue (SP2, 4, 6) exhibited stronger interactions towards thiamine and higher repulsion for acidic analytes with respect to their methyl ester derivatives (SP1, 3, 5), clearly demonstrating the presence of Coulombic interactions under the studied conditions. In addition, the substitution of the lipophilic tert-butyl residue at the amide site (present in SP1,2 and 5, 6) with a basic morpholino residue drastically changed the retention properties of the material. In both SP 3 and 4 the observed retention factor for thiamine was more than 7 time lower than for their equivalents SP 1 and 2, respectively. Similarly, retention factors of ascorbic and nicotinic acid, which were eluted before t_0 with SP1,2 (characterized by negative values for retention factors) due to electrostatic repulsion interactions could be retained i.e. retention factors shifted towards positive values. This result clearly reflects the more balanced charge characteristics offered by the two morpholino-decorated selectors.

3.4. Characterization by RP-type elution mode

In order to elucidate the hydrophobic interaction capability and reversed-phase character of the zwitterionic phosphopeptidomimetic stationary phases we tested the newly produced column set under typical RP conditions adopting ACN and water (40:60, v/v) based mobile phases with 50 mM ammonium acetate as buffer and counterions, adjusted to pH 6. The data obtained by this study are reported in *Figure 10* and *Table 6* and display the applicability of the newly developed selector in reversed phase mode, confirming the hypothesized mixed mode retention mechanism.

In order to analyze the obtained results in terms of hydrophobicity increments, we compared the results to a reference RP column (Synergi Fusion RP). A closer look to the hydrophobic selectivity, measured by the methylene selectivity between butyl and pentyl benzene reveals that the newly developed phases although hydrophilic in their nature still enable separation of solutes merely based on lipophilicity differences ($\alpha\text{CH}_2 = 1.8$ for Synergi Fusion RP and between 1.3 and 1.5 for SP1-6).

Looking at the structural elements of the different selectors, the introduction of a longer alkyl chain at the aldehyde site resulted in enhanced retention and selectivity properties (SP5,6 with respect to 1,2). The substitution of the tert-butyl group with a morpholino group (SP1,2 vs SP3,4) was accompanied by a decrease of the hydrophobic retention and performance properties.

In addition to the examined absolute hydrophobicity and hydrophobic selectivity, the ion exchange character was evaluated by taking into account the retention of DETP and Boc-Pro-Phe. Repulsion or elution with t_0 were observed for SP1,2 and 5,6 while once analyzed with SP3-4 both the analytes were retained and separated, demonstrating once again the zwitterionic character of such phases.

3.5. *Principal component analysis (PCA)*

In *Figure 11* is reported the result of a PCA analysis obtained by processing the retention factors of the novel amido-aminophosphonate columns SP1-6 and literature data [16] for the analyte test set adopted for both the HILIC and RP test. This statistical projection procedure clusters in the score plot the columns of similar character, while the ones being most dissimilar are farthest away from each other in the 2-D plot of PC1 and PC2 (*Fig. 11a*). The values given in parenthesis on the axis description refer to the percentage of variance in the data set explained by the corresponding component and latent variable, respectively.

The score plot of *Fig. 11a* reveals that SP 1-6 are clustered in a region where no other stationary phase is located. These phases are different from the commercial zwitterionic HILIC phases like ZIC-HILIC and PC-HILIC and are orthogonal to Synergy Fusion RP, (commercial) mixed-mode anion-exchangers, and in particular the thiol-modified stationary phase used for the immobilization of the selector. The stationary phases occupy an area in the chemical space of the tested stationary phases which is unoccupied by all the other tested SPs and makes the currently investigated zwitterionic phases to a unique set of columns. The loadings plot in *Figure 11b*) clearly indicate which of the compounds are responsible for the clustering of the columns presented in *Figure 11a*). This clearly demonstrates that the newly developed zwitterionic phosphopeptidomimetics-based stationary phases are complementary to many common phases used in HILIC and RP. Although a significant portion of thiol groups did not react and still constitute the backbone of the stationary phase, the retention characteristics of the novel phases are distant from the original SH modified silica.

Their properties appear to be far away from classical HILIC (zwitterionic, amide, bio, amine etc) phases as well as from reversed phase materials and the other analyzed mixed mode materials.

4. Concluding remarks

A set of novel RP/ZWIX stationary phases was generated by immobilization of amido-aminophosphonate derivatives obtained by Ugi reaction onto thiopropyl silica. Such phases combining alkyl groups with ion exchange moieties represented by mono methyl phosphonate or phosphonic acid or as well as secondary amine and tertiary amine (SP3, 4) combined with polar embedded amide and sulfide groups exhibited typical multimodal retention capabilities. We evaluated the retention properties of such phases in dependence of the mobile phase composition using SP1 as model column and a set of analytes with diverse lipophilicity and charge properties in order to have an insight on the separation properties of the materials. As conclusive study the novel SP were chromatographically evaluated under HILIC elution modes (i.e., ACN-rich hydroorganic eluents) as well as RP conditions (i.e., employing aqueous-rich hydroorganic eluents). The results obtained were analyzed on the basis of the different structural elements inserted in the molecular scaffold. Complementary retention profiles distinct to common HILIC and RPLC phases were found. The RP/ZWIX phases hold therefore considerable promise to be useful as complementary stationary phases in impurity profiling and 2D-HPLC.

5. Acknowledgement

This work was financially supported by the University of Vienna through the interdisciplinary doctoral program: "Initiativkolleg Functional Molecules" (IK I041-N).

A. Figure caption

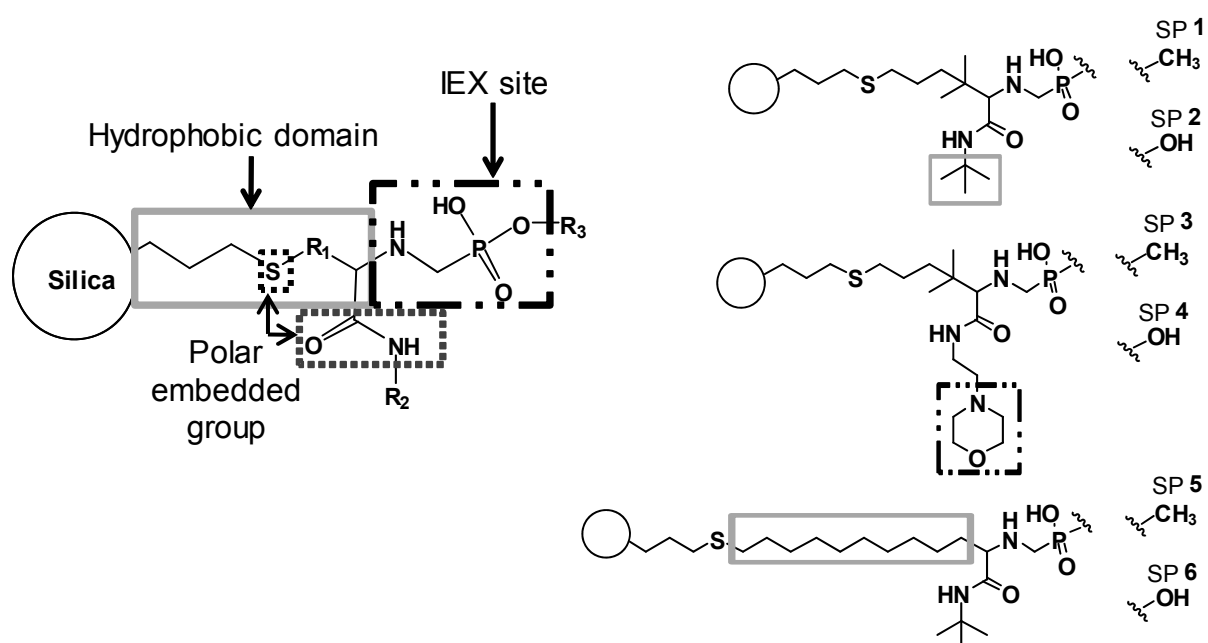


Figure 1: Structure of mixed-mode reversed-phase/zwitterionic ion-exchange (RP/ZWIX) stationary phase synthesized by Ugi MCR [19].

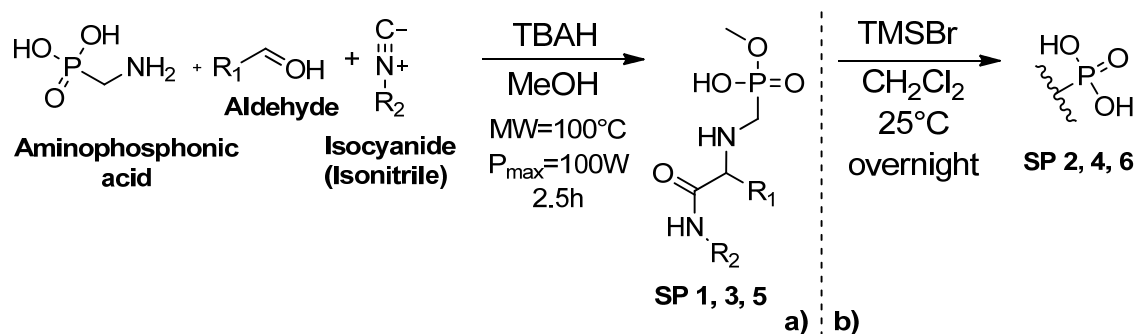


Figure 2. a) Reaction scheme of the aminophosphonic acid based Ugi 5 center 4 components reaction (Ugi 5C-4CR) adopted to synthesize the selectors of this study (SP1, 3, 5). b) Reaction conditions for the hydrolysis process of the mono methyl phosphonates (SP 2, 4, 6). [19]

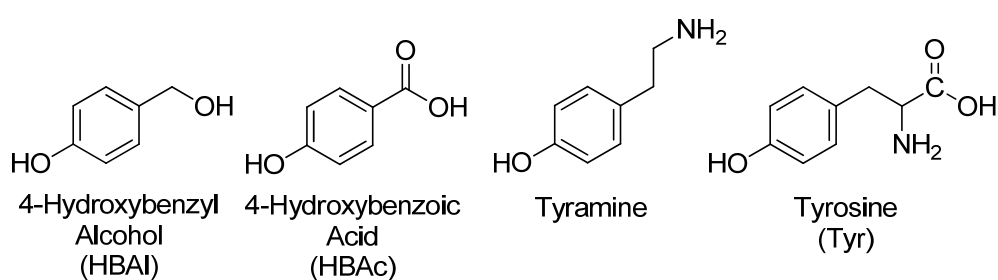


Figure 3: Chemical structure of the analytes adopted for the study on the influence of the mobile phase characteristics on retention (adenosine, cytidine and adenine are reported in Figure 5).

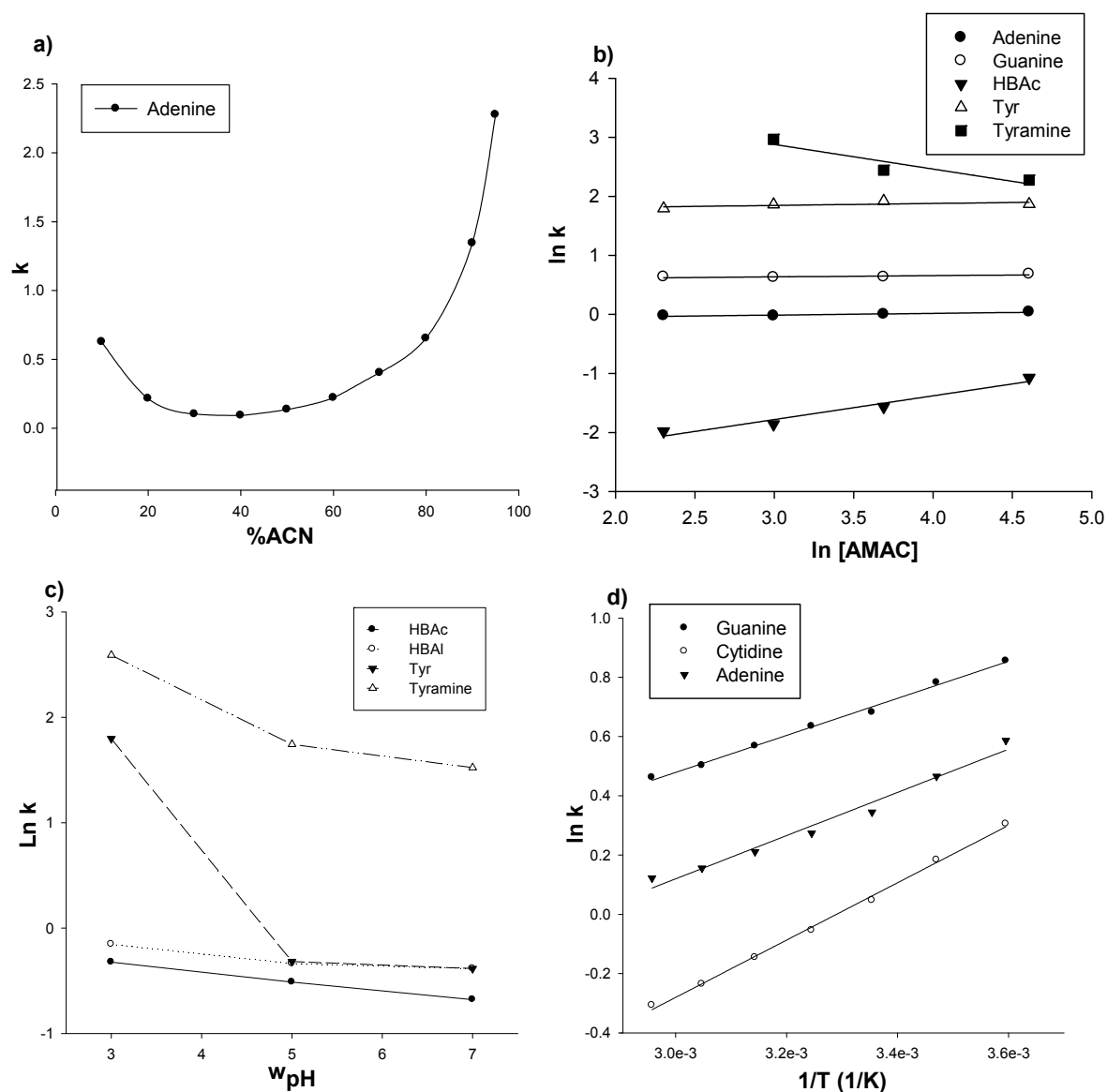


Figure 4: Mobile phase influence on retention process on SP1: a) variation of retention factor of adenine in dependence of the % of ACN. MP: 20 mM Ammonium acetate (AMAC) / ACN. b) Dependency of logarithms of retention factor versus logarithm of the concentration of the buffer salt and counterions, respectively. MP: ACN / ammonium acetate (5, 10, 20, 50, 100 mM) (90/10; v/v). c) Dependency of retention factors on the pH of the aqueous medium. MP: ACN/ 20 mM ammonium acetate (90/10; v/v). d) Linear van't Hoff plots of $\ln k$ vs. inverse of temperature in K. MP: ACN/ 40 mM ammonium acetate buffer (85/25; v/v). Flow rate 1.33 mm/s (1 mL/min), detection at 220 nm, temperature of 25°C if not stated differently and injection volume of 5 μ L.

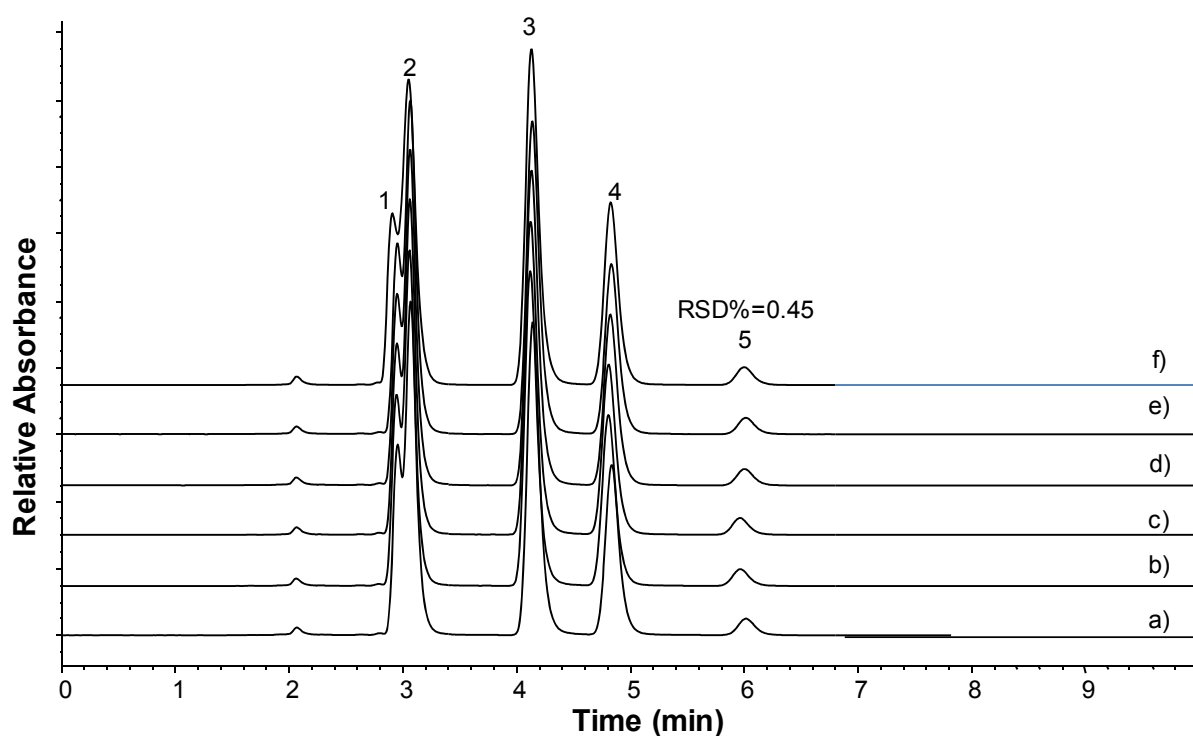


Figure 5: Repetability and stability test for SP1. Consecutive injection of a mixture consisting of 1 Thymine, 2 Uracil, 3 Adenine, 4 Cytidine and 5 Guanine and to marker (toluene) on SP1. Chromatograms recorded from injections 1 to 5 (a-e) and after 100 injections (f). Value of relative standard deviation % (RSD%) calculated for guanine. MP: ACN/ 20 mM ammonium acetate buffer (85/15; v/v). For other conditions refer to the materials and methods section.

Table 1: Selector coverage and calculated isoelectric point, log P/log D value for the mixed mode selectors of this study.

	%C	%N	%P	Sel. amt. [$\mu\text{mol}/\text{m}^2$]	pI ^c	Log D (pH 6)	Log D (pH 8)
In house dev. MM columns							
SP1	9.08	0.78	0.79	0.83	4.61	0.82	0.90
SP2	6.25	0.32	0.41	0.29	2.79	1.37	-3.40
SP3	8.21	0.68	0.54	0.58	7.17	0.75	0.56
SP4	6.53	0.55	0.37	0.39	6.27	-3.25	0.41
SP5	11.14	0.83	0.86	0.92	4.57	0.92	0.97
SP6	8.93	0.57	0.56	0.60	2.94	1.07	1.84
Reference columns							
SH mod	4.96	-	-	2.17	-	0.99	0.99
Phenomenex Synergi 4 μ Fusion-RP 80	12.00	-	-	-	-	-	-

1. Surface area: 320 m²/g, Particle size: 5 μm , column dimension: 4 x 150 mm
2. SH mod, thiopropyl-modified silica used for the immobilization of the ligands
3. pI, isoelectric point of zwitterionic selectors as calculated by ACD

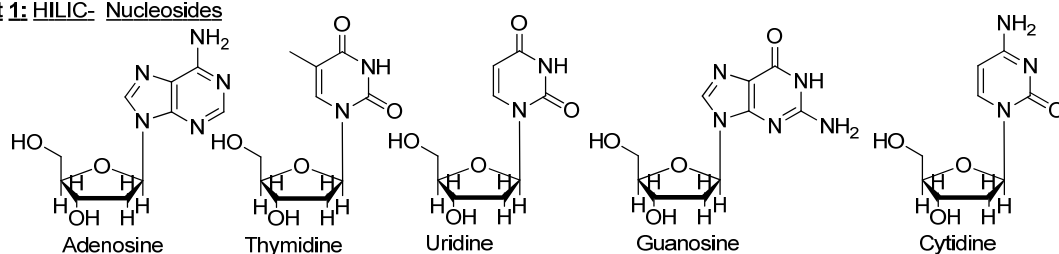
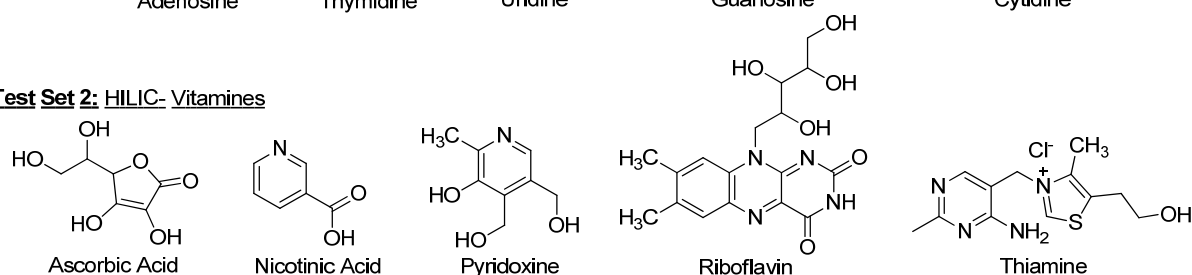
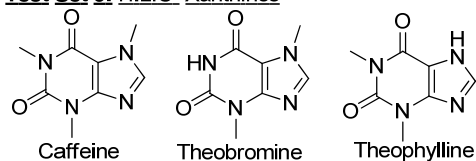
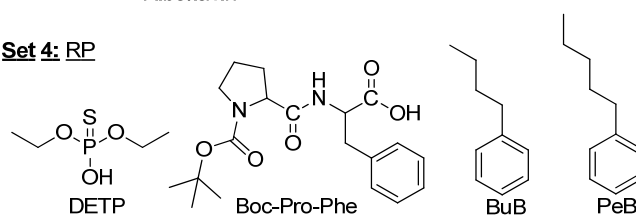
Test Set 1: HILIC- Nucleosides**Test Set 2: HILIC- Vitamines****Test Set 3: HILIC- Xanthines****Test Set 4: RP**

Figure 6: Chemical formula of the different test series of compounds used in the characterization of the column performances and comparison towards other in-house produced or commercially available columns. Compounds numbered in accordance to their log D at the studied pH, characteristics reported in the supporting information.

Table 2. Analyte characteristics

	Substance:	Mol. Formula	MW [g/mol]	log D ^{b)}	log P ^{b)}	log P \pm ^{b)}	
Nucleosides	Thymidine	C ₁₀ H ₁₄ N ₂ O ₅	242.23	-1.13	-1.11	0.49	(pH _a 7.9)
	Cytidine	C ₉ H ₁₃ N ₃ O ₅	243.22	-1.93	-1.94	0.45	
	Adenosine	C ₁₀ H ₁₃ N ₅ O ₄	267.25	-1.02	-1.02	0.51	
	Guanosine	C ₁₀ H ₁₃ N ₅ O ₅	283.25	-1.74	-1.72	0.57	
	Uridine	C ₉ H ₁₂ N ₂ O ₆	244.20	-1.76	-1.61	0.44	
Vitamines	Riboflavin (B ₂)	C ₁₇ H ₂₀ N ₄ O ₆	376.37	-4.01	-2.02	0.98	(pH _a 7.9)
	Ascorbic acid (C)	C ₆ H ₈ O ₆	176.13	-5.62	-2.41	0.45	
	Thiamine*HCl (B ₁)	C ₁₂ H ₁₈ Cl ₂ N ₄ OS	337.27	-1.61	-1.61	0.66	
	Pyridoxine (B ₆)	C ₈ H ₁₁ NO ₃	169.18	-1.39	-1.1	0.25	
	Nicotinic acid (B ₃)	C ₆ H ₅ NO ₂	123.11	-2.98	0.15	0.34	
Xanthines	Caffeine	C ₈ H ₁₀ N ₄ O ₂	194.19	-0.13	-0.13	0.37	(pH _a 8.1)
	Theobromine	C ₇ H ₈ N ₄ O ₂	180.17	-0.73	-0.72	0.55	
	Theophylline	C ₇ H ₈ N ₄ O ₂	180.17	-0.29	-0.17	0.31	
RP test	Boc-Phe-Pro	C ₁₉ H ₂₆ N ₂ O ₅	362.42	-0.48	2.31	0.42	(pH _a 6)
	DETP	C ₄ H ₁₁ O ₃ PS	170.17	-1.25	1.34	0.38	
	BuB	C ₁₀ H ₁₄	134.22	3.82	3.82	0.31	
	PeB	C ₁₁ H ₁₆	148.24	4.26	4.26	0.35	

a) Calculated via chemicalize.org

b) Calculated with ACD/chemsketch

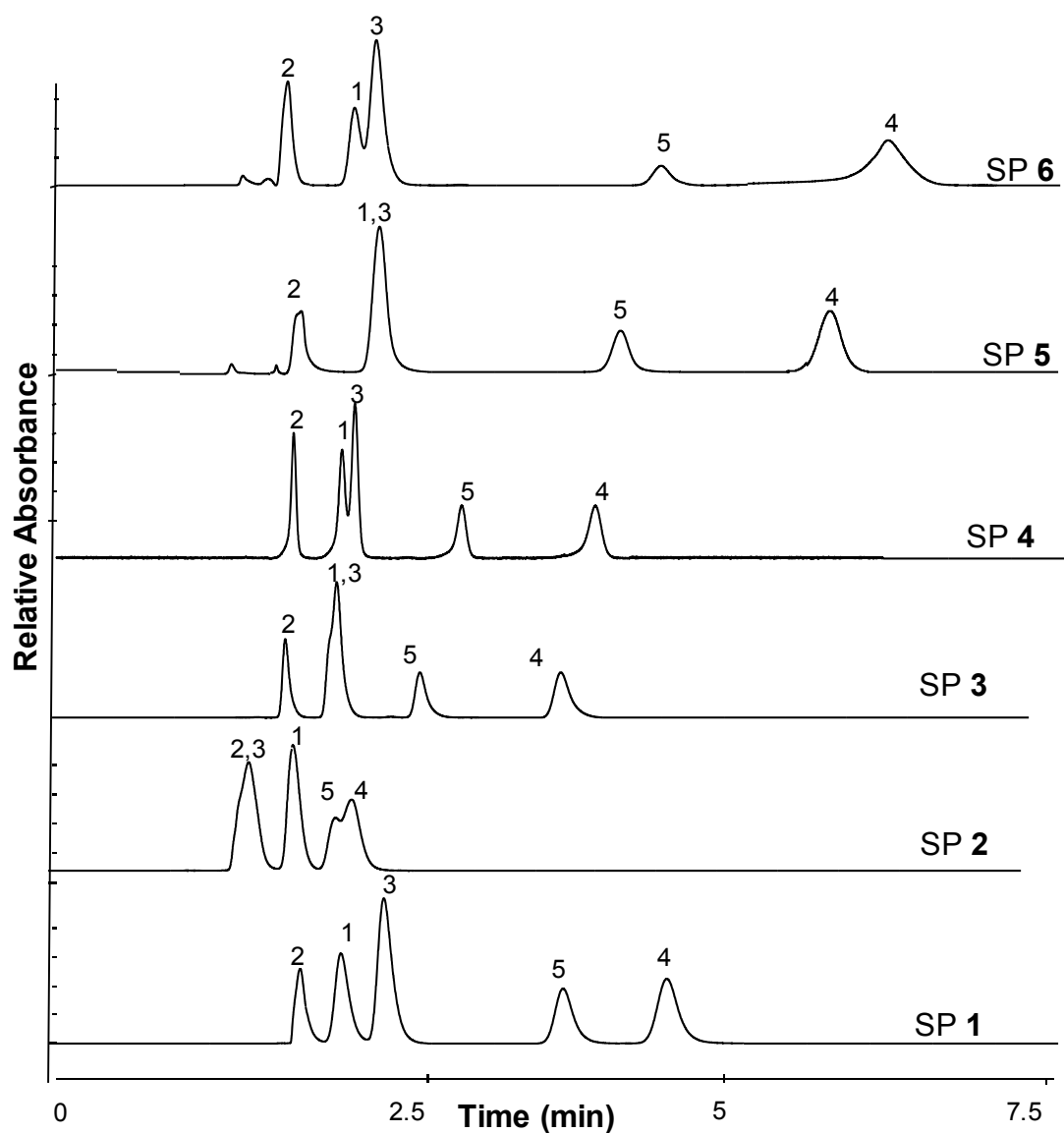


Figure 8: Separation of Test set 1 (nucleosides) on the novel amido-aminophosphonate based SP 1-6. 1, adenosine; 2, thymidine; 3, uridine; 4, guanosine; 5, cytidine. (Note, numbering corresponds to the elution order as expected from log D values). For conditions refer to the materials and methods section.

Table 3. Chromatographic results for the HILIC test for test set 1

	$k_{\text{thymidine}}$	$k_{\text{adenosine}}$	k_{uridine}	k_{cytidine}	$k_{\text{guanosine}}$
In-house developed MM columns					
SP1	0.38	0.88	0.63	1.87	2.44
SP2	0.14	0.40	0.14	0.64	0.64
SP3	0.36	0.66	0.62	1.15	1.96
SP4	0.24	0.56	0.49	1.11	1.79
SP5	0.36	0.66	0.66	1.15	1.97
SP6	0.33	0.67	0.60	1.26	2.01
Reference columns					
SH mod	with t_0	0.11	with t_0	0.15	0.15
Synergi Fusion-RP (Phenomenex)	with t_0	0.04	with t_0	0.16	0.04

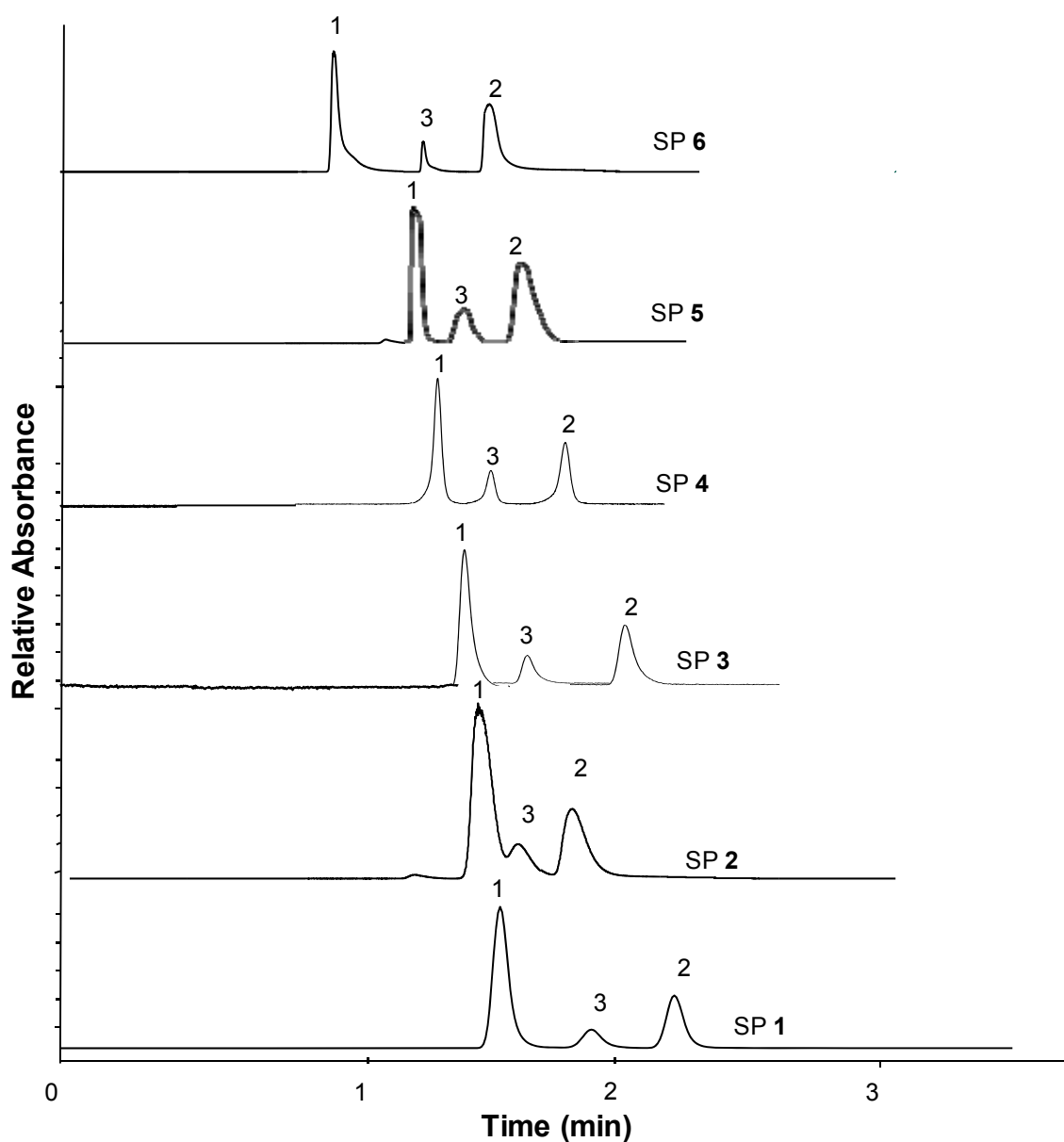


Figure 9: Separation of test set 3 (Xanthines) on the novel amido-aminophosphonate based SP 1-6. For conditions refer to the materials and methods section. 1, caffeine; 2, theophylline; 3, theobromine. (Note, numbering corresponds to the elution order as expected from log D values).

Table 4. Chromatographic results for the HILIC test for test set

	k_{caffeine}	$k_{\text{theobromine}}$	$k_{\text{theophylline}}$
In-house developed MM columns			
SP1	0.19	0.38	0.55
SP2	0.21	0.33	0.48
SP3	0.06	0.21	0.37
SP4	0.06	0.18	0.35
SP5	0.00	0.17	0.44
SP6	0.01	0.30	0.56
Reference columns			
SH mod	with t_0	with t_0	with t_0
Synergi Fusion-RP (Phenomenex)	with t_0	with t_0	with t_0

^{a)} Conditions see Experimental

Table 5. Chromatographic results for the HILIC test for test set 2.

	k_{thiamine}	$k_{\text{pyridoxine}}$	$k_{\text{riboflavine}}$	$k_{\text{ascorbic acid}}$	$k_{\text{nicotinic acid}}$
In-house developed MM columns					
SP1	58.44	0.83	1.24	-0.10	0.00
SP2	78.24	0.42	0.42	-0.13	-0.13
SP3	7.89	0.49	0.98	0.19	0.52
SP4	9.86	0.69	1.27	0.06	0.40
SP5	30.31	0.52	1.5	0.16	0.00
SP6	43.51	0.58	1.58	0.15	-0.11
Reference columns					
SH mod	0.3	0.21	0.099	-0.18	with t_0
Synergi Fusion-RP (Phenomenex)	14.94	0.11	with t_0	with t_0	0.44

^{a)} Conditions see Experimental

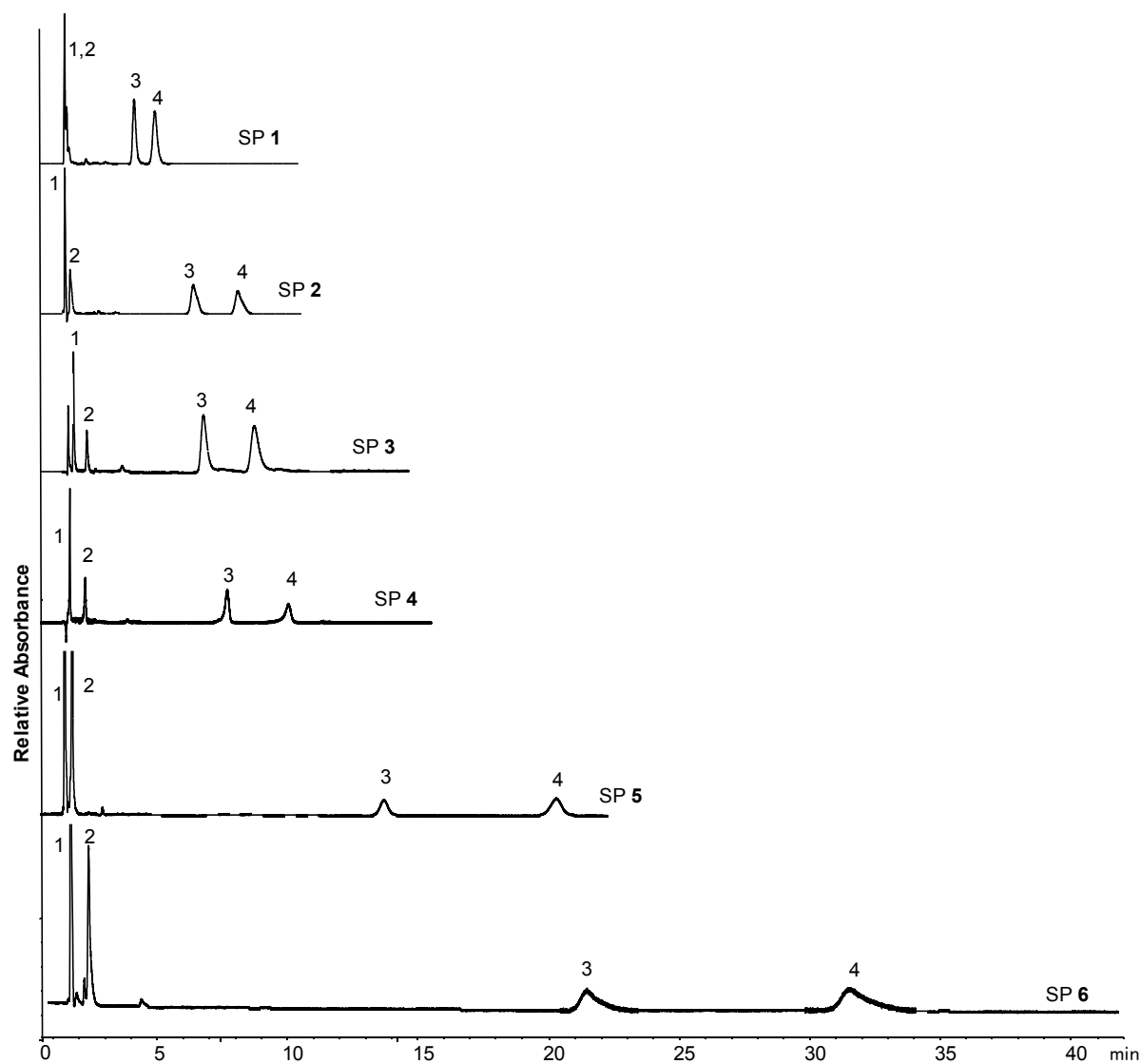


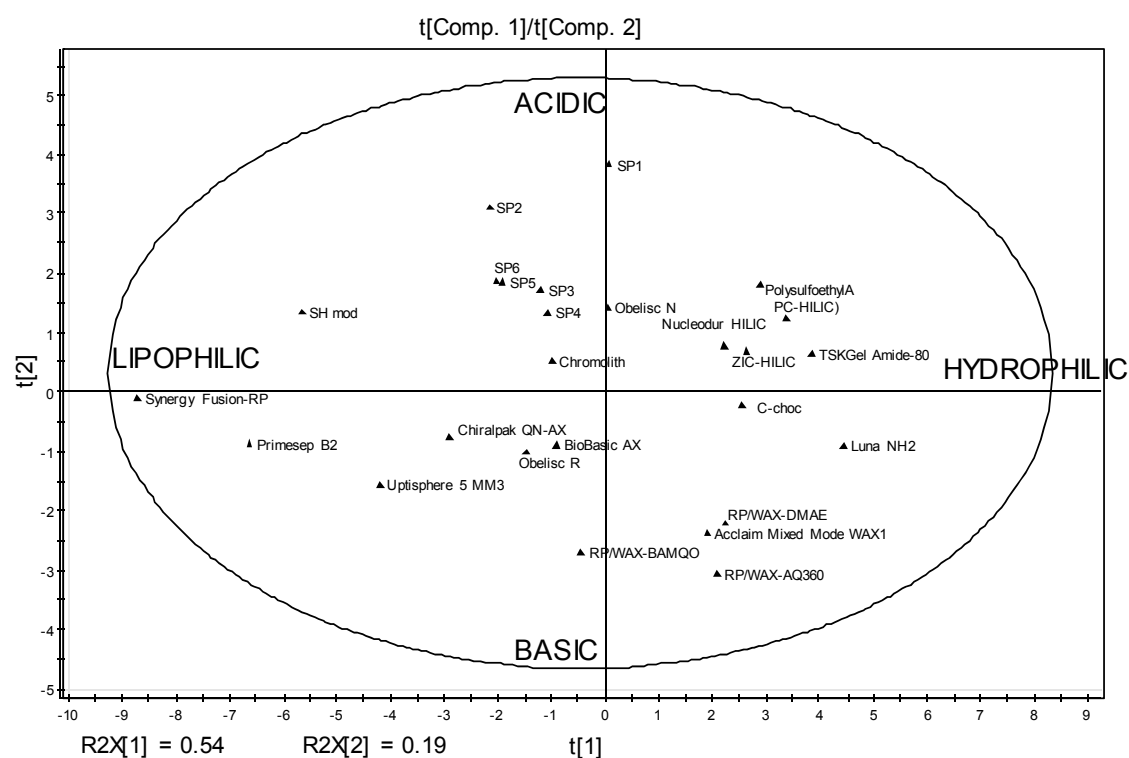
Figure 10: Separation of test set 4 (RP mixture) on the novel amido-aminophosphonate based SP 1-6. 1, DETP; 2, Boc-Pro-Phe; 3, butylbenzene; 4, pentylbenzene. For conditions refer to the materials and methods section.

Table 6. Chromatographic results for the RP test set 4

	k_{BuB}	k_{PeB}	k_{DETP}	$k_{\text{BocProPhe}}$	α_{CH2}
In-house developed MM columns					
SP1	2.04	2.69	-0.20	-0.13	1.32
SP2	3.79	5.17	-0.20	0.00	1.36
SP3	4.56	6.30	0.17	0.60	1.38
SP4	4.79	6.63	0.03	0.46	1.38
SP5	9.96	15.12	-0.23	0.01	1.52
SP6	16.56	24.84	-0.20	0.12	1.50
Reference columns					
SH mod	5.02	6.33	with t_0	with t_0	1.26
Synergi Fusion-RP (Phenomenex)	24.17	43.28	with t_0	0.06	1.79

^{a)} Conditions see Experimental, all measurements at pH 6.0

a)



b)

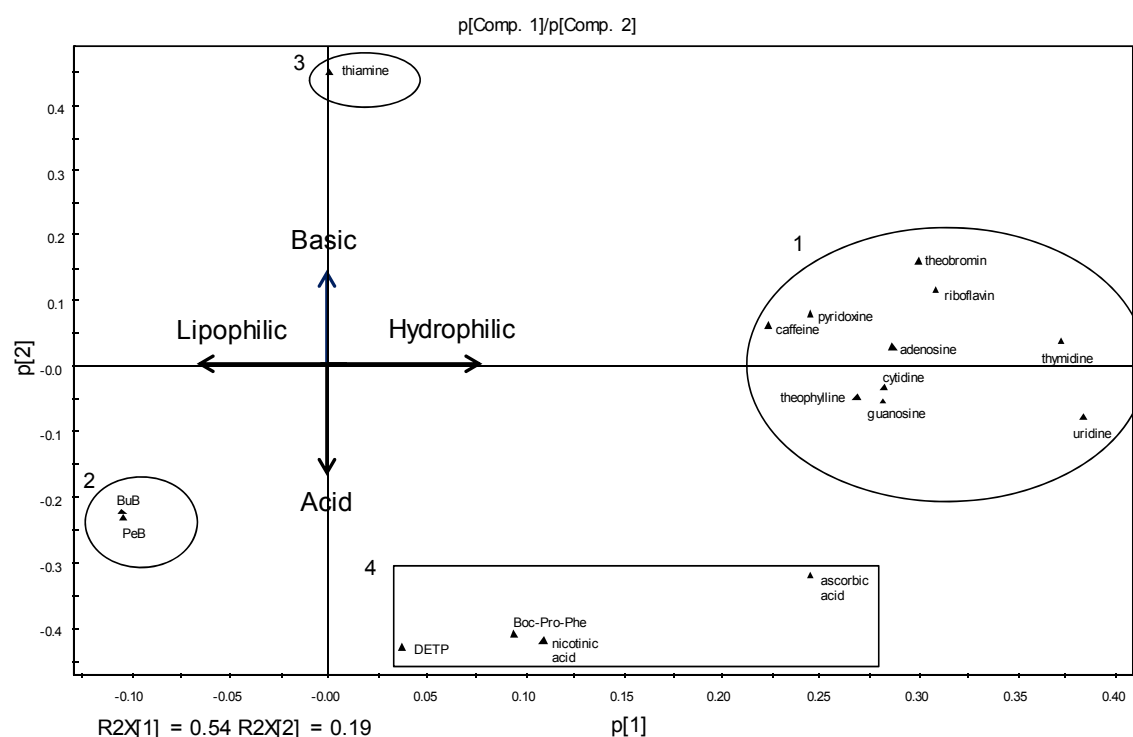


Figure 11: Principal component analysis derived from retention factors of test sets 1-4 under HILIC and RP conditions, respectively., a) loadings plot b) Score plot. For conditions refer to the materials and methods section. The full summary of retention factor values are included in the supporting information.

B. References

1. Lämmerhofer, M., R. Nogueira, and W. Lindner, *Multi-modal applicability of a reversed-phase/weak-anion exchange material in reversed-phase, anion-exchange, ion-exclusion, hydrophilic interaction and hydrophobic interaction chromatography modes*. Analytical and Bioanalytical Chemistry, 2011. **400**(8): p. 2517-2530.
2. Fontanals, N., R.M. Marcé, and F. Borrull, *New materials in sorptive extraction techniques for polar compounds*. Journal of Chromatography A, 2007. **1152**(1–2): p. 14-31.
3. Progent, F., et al., *Chromatographic behaviour of peptides on a mixed-mode stationary phase with an embedded charged group by capillary electrochromatography and high-performance liquid chromatography*. Journal of Chromatography A, 2006. **1136**(2): p. 221-225.
4. Hagestam, I.H. and T.C. Pinkerton, *Internal surface reversed-phase silica supports for liquid chromatography*. Analytical Chemistry, 1985. **57**(8): p. 1757-1763.
5. Rbeida, O., et al., *Fully automated LC method for the determination of sotalol in human plasma using restricted access material with cation exchange properties for sample clean-up*. Journal of Pharmaceutical and Biomedical Analysis, 2003. **32**(4–5): p. 829-838.
6. Liu, X. and C. Pohl, *New hydrophilic interaction/reversed-phase mixed-mode stationary phase and its application for analysis of nonionic ethoxylated surfactants*. Journal of Chromatography A, 2008. **1191**(1–2): p. 83-89.
7. Jandera, P., et al., *Polymethacrylate monolithic and hybrid particle-monolithic columns for reversed-phase and hydrophilic interaction capillary liquid chromatography*. Journal of Chromatography A, 2010. **1217**(1): p. 22-33.
8. Urban, J., et al., *Preparation and characterization of polymethacrylate monolithic capillary columns with dual hydrophilic interaction reversed-phase retention mechanism for polar compounds*. Journal of Separation Science, 2009. **32**(15-16): p. 2530-2543.
9. Bischoff, R. and L.W. McLaughlin, *Chemically synthesized hydrophobic anion-exchange high-performance liquid chromatography supports used for oligonucleotide resolution by mixed mode chromatography*. Journal of Chromatography A, 1983. **270**(0): p. 117-126.
10. Nogueira, R., M. Lämmerhofer, and W. Lindner, *Alternative high-performance liquid chromatographic peptide separation and purification concept using a new mixed-mode reversed-phase/weak anion-exchange type stationary phase*. Journal of Chromatography A, 2005. **1089**(1–2): p. 158-169.
11. Mant, C.T. and R.S. Hodges, *Mixed-mode hydrophilic interaction/cation-exchange chromatography: Separation of complex mixtures of peptides of varying charge and hydrophobicity*. Journal of Separation Science, 2008. **31**(9): p. 1573-1584.
12. Gargano, A.F.G., M. Lämmerhofer, and W. Lindner, *Manuscript 1*. 2013.
13. Wallace, E.M., et al., *Design and synthesis of potent, selective inhibitors of endothelin-converting enzyme*. J Med Chem, 1998. **41**(9): p. 1513-23.
14. De Lombaert, S., et al., *N-Phosphonomethyl Dipeptides and Their Phosphonate Prodrugs, a New Generation of Neutral Endopeptidase (NEP, EC 3.4.24.11) Inhibitors*. J. Med. Chem., 1994. **37**(4): p. 498-511.
15. Dabre, R., et al., *Statistical optimization of the silylation reaction of a mercaptosilane with silanol groups on the surface of silica gel*. Journal of Chromatography A, 2009. **1216**(16): p. 3473-3479.
16. Lämmerhofer, M., et al., *Mixed-mode ion-exchangers and their comparative chromatographic characterization in reversed-phase and hydrophilic interaction chromatography elution modes*. Journal of Separation Science, 2008. **31**(14): p. 2572-2588.
17. Schuster, G. and W. Lindner, *Chocolate HILIC phases: development and characterization of novel saccharide-based stationary phases by applying non-enzymatic browning (Maillard*

- reaction) on amino-modified silica surfaces. *Analytical and Bioanalytical Chemistry*, 2011. **400**(8): p. 2539-2554.
18. Schuster, G. and W. Lindner, *Comparative characterization of hydrophilic interaction liquid chromatography columns by linear solvation energy relationships*. *Journal of Chromatography A*, 2013. **1273**(0): p. 73-94.
 19. Gargano, A.F.G., W. Lindner, and M. Lämmerhofer, *Manuscript 1*. 2013.

C.

Supporting information

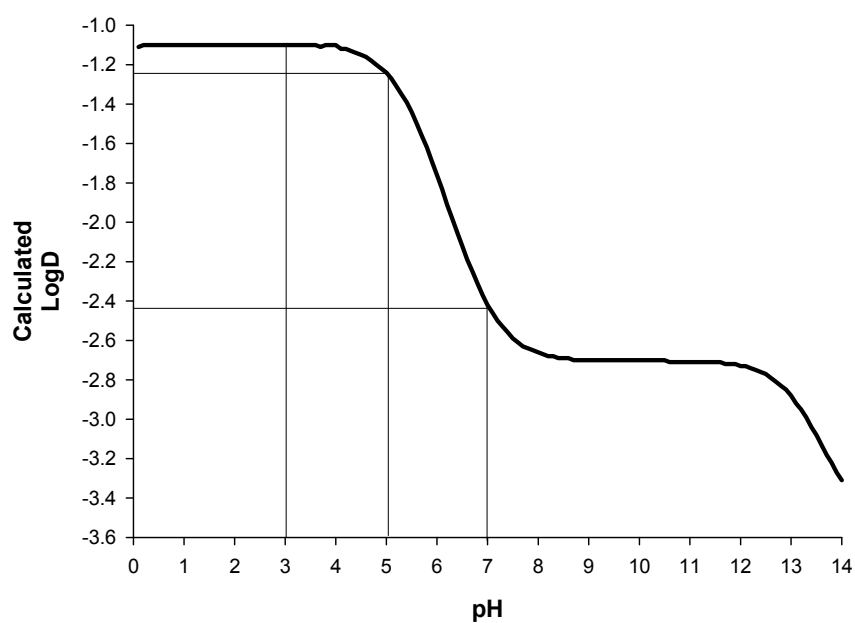


Figure S1: Variation of the value of the calculated log D in dependence of pH for SO1 of SP1.

TableS1: Characteristics of the SPs adopted in this study

In-house developed columns (Codes)	Type	%C	%H	%N	%S	%P	Surface A [m ² /g]	Sel. amt. [mmol/g]	Sel. amt. [μmol/m ²]	Particle Size [μm]
P1	MM	9.08	1.92	0.78	1.74	0.79	300	0.25	0.83	5
SP2	MM	6.25	1.45	0.32	1.98	0.41	300	0.13	0.43	5
SP3	MM	8.21	1.78	0.68	1.80	0.54	300	0.18	0.58	5
SP4	MM	6.53	1.50	0.55	1.97	0.37	300	0.12	0.39	5
SP5	MM	11.14	2.24	0.83	1.91	0.86	300	0.28	0.92	5
SP6	MM	8.93	1.86	0.57	2.21	0.56	300	0.18	0.60	5
C-Chocolate [17]	HILIC	5.10		1.70			300		2.09	3
SH modified	MM	4.96	1.20	-	2.11	-	300	0.65	2.17	5
WU070507_1 TV-AQ/RPWAX	MM	17.12	2.83	1.00	5.28	-	300	0.36	1.19	5
RN030504 RPWAX DMAE Amid C11	MM	12.62	2.21	1.27	1.86	-	300	0.42	1.40	5
RN080904 RPWAX	MM	13.99	2.35	1.20	3.11	-	300	0.36	1.21	5
Commercial columns										
Dionex Acclaim Mixed Mode WAX-1	MM	12.70	2.50	1.46	-		300	0.52 (2N) ^{a)}	1.74	5
Interchim Uptisphere 5 MM3	MM	8.14	1.79	0.19	-		320	0.14 (1N) ^{a)}	0.43	5
Sielc Primesep B2	MM	8.38	1.83	0.65	-		n/a	0.46 (1N) ^{a)}	n/a	5
Sielc Obelisc R	MM	8.93	1.92	0.66	0.222		n/a	0.47 (1N) ^{a)}	n/a	5
Sielc Obelisc N	MM	4.59	1.21	0.30	-		n/a	0.21 (1N) ^{a)}	n/a	5
Chiralpak QN-AX (Chiral Technologies)	Chiral WAX	15.14	2.38	1.59	1.84		300	0.38	1.3	5
Phenomenex Luna 5 μ NH ₂ 100 A	Amino	10.09	2.31	2.84	-		400	2.32	5.8	5
BioBasic AX	Amino	3.7	0.77	0.58	-		100	0.22	2.2	5
3-(<i>N,N</i> -Dimethylamino)propyl-silica	WAX	4.59	1.11	0.75	-		300	0.40	1.33	5
Phenomenex Synergi 4 μ Fusion-RP 80	RP-PEC	12.00	n/a	-	-		475	n/a	n/a	4
TSKGel Amide-80	HILIC	11.06	1.99	2.46	-		n/a	1.76 (1N) ^{a)}	n/a	5
Polysulfoethyl A (PolyLC)	HILIC/SCX	9.95	1.74	3.47	1.76		100	0.55 (1S) ^{a)}	5.50	5
SeQuant ZIC-HILIC	HILIC	8.74	1.77	1.02	1.90		140	0.59 (1S) ^{a)}	4.24	5
M&N	HILIC	-	-	-	-		n/a	n/a	n/a	5
Merck Chromolith Performance Si	Silica	-	-	-	-		300*	-	-	-
Shiseido PC-HILIC	HILIC	-	-	-	-		n/a	n/a	n/a	5

^{a)} Exact surface chemistry undisclosed. Element used for calculations and its assumed number in the ligand in parenthesis

Table S2. Chromatographic results for the HILIC test for test set 1

	$k_{\text{thymidine}}$	$k_{\text{adenosine}}$	k_{uridine}	k_{cytidine}	$k_{\text{guanosine}}$
In-house developed Hilic/Mix mode columns					
SP1	0.38	0.88	0.63	1.87	2.44
SP2	0.14	0.40	0.14	0.64	0.64
SP3	0.36	0.66	0.62	1.15	1.96
SP4	0.24	0.56	0.49	1.11	1.79
SP5	0.36	0.66	0.66	1.15	1.97
SP6	0.33	0.67	0.60	1.26	2.01
GSCH- c-choc	1.11	3.19	2.04	6.49	11.06
SH mod	with t_0	0.11	with t_0	0.15	0.15
RP/WAX-AQ360	0.79	1.59	1.89	4.12	7.52
RP/WAX-DMAE	0.66	1.13	3.82	9.18	17.62
RP/WAX-BAMQO	0.13	1.31	1.09	2.33	4.59
Commercial/comparison columns					
Acclaim Mixed Mode WAX-1 (Dionex)	0.88	1.67	1.90	4.18	7.15
Uptisphere 5 MM3 (Interchim)	with t_0	0.15	0.15	0.81	1.05
Primesep B2 (Sielc)	with t_0	0.10	with t_0	0.22	0.22
Obelisc R (Sielc)	0.09	0.48	0.48	2.15	2.69
Obelisc N (Sielc)	0.23	0.59	0.48	2.75	1.61
Chiralpak QN-AX (Chiral Technologies)	0.15	0.15	0.15	0.29	0.29
Luna NH ₂ (Phenomenex)	1.21	3.80	3.80	11.99	19.18
BioBasic AX (Thermo Scientific)	0.35	0.84	0.75	2.18	3.42
Synergi Fusion-RP (Phenomenex)	with t_0	0.04	with t_0	0.16	0.04
TSKGel Amide-80 (Tosoh)	1.27	3.12	3.45	10.20	12.80
PolysulfoethylA (PolyLC)	0.77	2.08	3.14	15.02	16.69
ZIC-HILIC (SeQuant)	0.89	2.09	3.24	9.54	12.63
Nucleodur HILIC	0.91	1.64	2.08	5.05	6.53
Chromolith Performance Si (Merck)	0.29	0.76	0.61	2.26	2.04
PC-HILIC (Shiseido)	1.00	2.29	1.66	4.70	5.21

Table S3. Chromatographic results for the HILIC test for test set 3

	k_{caffeine}	$k_{\text{theobromine}}$	$k_{\text{theophylline}}$
In-house developed HILIC/Mix mode columns			
SP1	0.19	0.38	0.55
SP2	0.21	0.33	0.48
SP3	0.06	0.21	0.37
SP4	0.06	0.18	0.35
SP5	0.00	0.17	0.44
SP6	0.01	0.30	0.56
GSCH- c-choc	0.23	0.73	0.98
SH mod	with t_0	with t_0	with t_0
Synergi Fusion-RP (Phenomenex)	with t_0	with t_0	with t_0
RP/WAX-AQ360	0.17	0.35	1.11
RP/WAX-DMAE	0.10	0.28	0.76
RP/WAX-BAMQO (Fig. 1d)	0.03	0.18	0.80
Commercial/comparison columns			
Acclaim Mixed Mode WAX-1 (Dionex)	0.10	0.26	0.84
Uptisphere 5 MM3 (Interchim)	with t_0	with t_0	with t_0
Primesep B2 (Sielc)	0.02	0.02	0.11
Obelisc R (Sielc)	0.06	0.14	0.26
Obelisc N (Sielc)	0.15	0.22	0.22
Chiralpak QN-AX (Chiral Technologies)	0.10	0.24	0.44
Luna NH ₂ (Phenomenex)	0.31	0.67	3.19
BioBasic AX (Thermo Scientific)	0.08	0.18	0.18
Synergi Fusion-RP (Phenomenex)	with t_0	with t_0	with t_0
TSKGel Amide-80 (Tosoh)	0.40	0.76	1.16
PolysulfoethylA (PolyLC)	0.20	0.45	0.51
ZIC-HILIC (SeQuant)	0.28	0.63	0.63
Nucleodur HILIC	0.36	0.67	0.67
Chromolith Performance Si (Merck)	0.19	0.19	0.19
PC-HILIC (Shiseido)	0.60	1.03	1.03

a) Conditions see Experimental

Table 6. Chromatographic results for the HILIC test for test set 2.

	k_{thiamine}	$k_{\text{pyridoxine}}$	$k_{\text{riboflavine}}$	$k_{\text{ascorbic acid}}$	$k_{\text{nicotinic acid}}$
In-house developed HILIC/Mix mode columns					
SP1	58.44	0.83	1.24	-0.10	0.00
SP2	78.24	0.42	0.42	-0.13	-0.13
SP3	7.89	0.49	0.98	0.19	0.52
SP4	9.86	0.69	1.27	0.06	0.40
SP5	30.31	0.52	1.5	0.16	0.00
SP6	43.51	0.58	1.58	0.15	-0.11
SH mod	0.3	0.21	0.099	-0.18	with t_0
Synergi Fusion-RP (Phenomenex)	14.94	0.11	with t_0	with t_0	0.44
GSCH- c-choc	30.23	1.80	5.42	14.82	12.33
RP/WAX-AQ360	0.09	1.17	2.17	n/d	34.37
RP/WAX-DMAE	0.17	0.88	1.03	15.03	16.32
RP/WAX-BAMQO	0.73	0.57	0.40	7.46	15.04
Commercial/comparison columns					
Acclaim Mixed Mode WAX-1 (Dionex)	0.17	1.11	1.66	n/d	31.14
Uptisphere 5 MM3 (Interchim)	0.60	0.13	0.13	5.27	3.03
Primesep B2 (Sielc)	3.92	0.36	0.04	0.04	0.73
Obelisc R (Sielc)	10.11	0.78	0.78	2.73	10.11
Obelisc N (Sielc)	n/d	6.65	1.15	1.15	0.66
Chiralpak QN-AX (Chiral Technologies)	1.17	0.41	0.32	n/d	3.52
Luna NH ₂ (Phenomenex)	0.95	2.64	3.10	28.74	24.90
BioBasic AX (Thermo Scientific)	0.43	0.43	0.89	n/d	10.88
Synergi Fusion-RP (Phenomenex)	14.94	0.11	with t_0	with t_0	0.44
TSKGel Amide-80 (Tosoh)	43.54	1.49	4.77	20.70	5.49
PolysulfoethylA (PolyLC)	26.81	2.73	3.10	n/d	2.73
ZIC-HILIC (SeQuant)	29.30	1.20	2.20	35.13	4.89
Nucleodur HILIC	99.31	1.73	1.78	6.26	1.78
Chromolith Performance Si (Merck)	28.20	0.65	0.65	1.41	1.85
PC-HILIC (Shiseido)	95.49	1.91	2.66	6.65	2.05

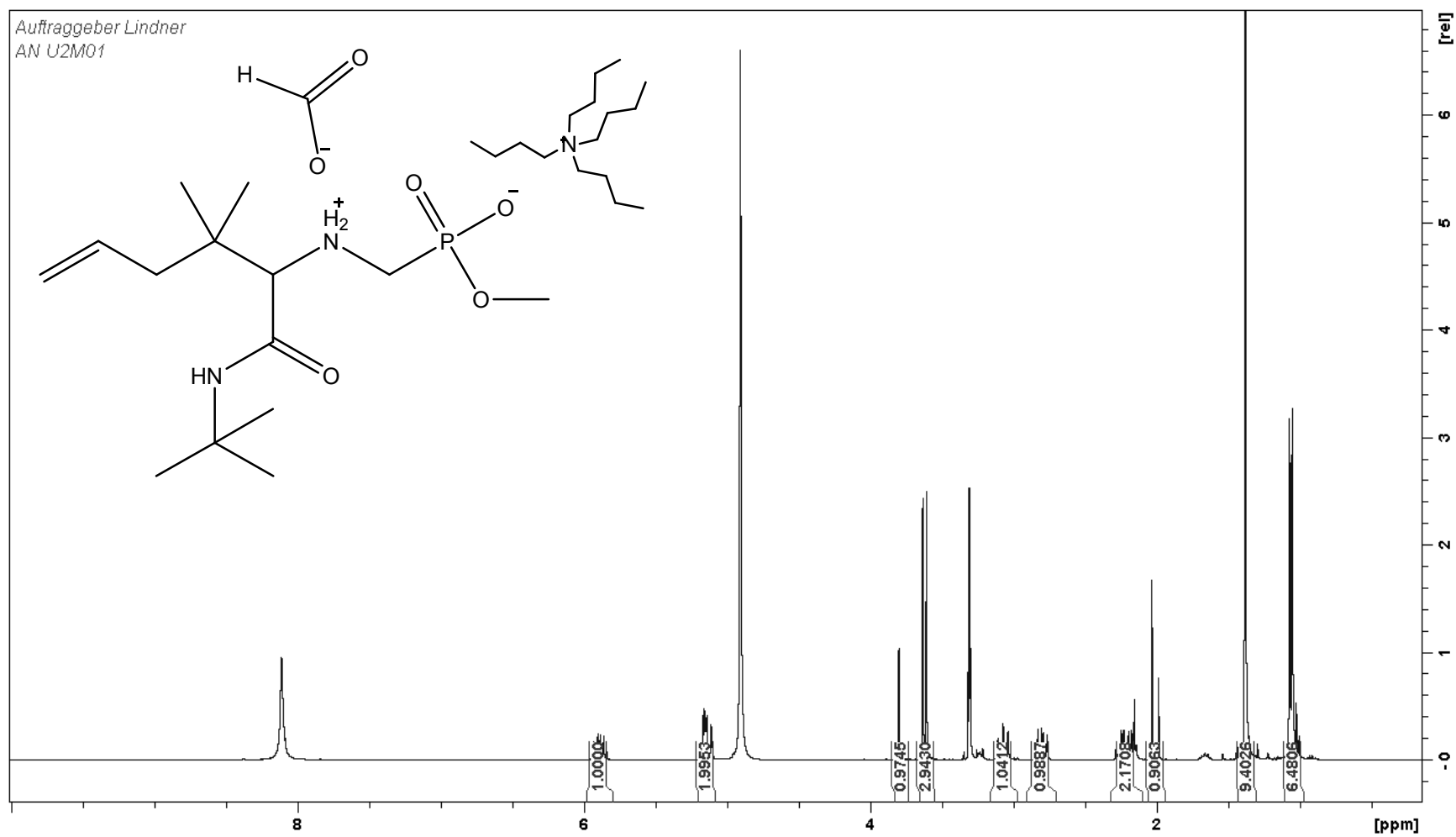
^{a)} Conditions see Experimental. n/d, not detected

Table S4. Chromatographic results for the RP test set 4

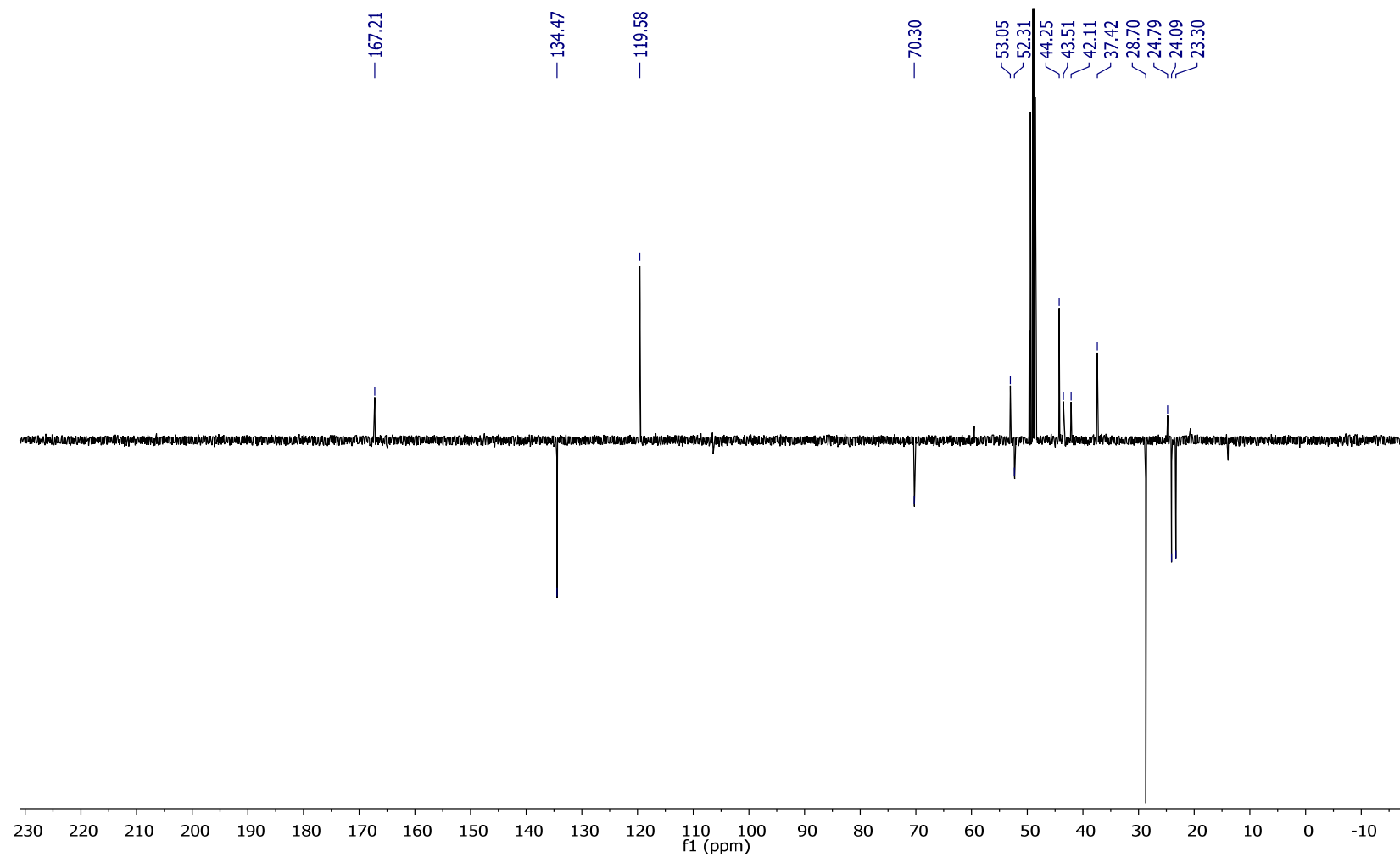
	k_{BuB}	k_{PeB}	k_{DETP}	$k_{\text{BocProPhe}}$	α_{CH2}
In-house developed HILIC/Mix mode columns					
SP1	2.04	2.69	-0.20	-0.13	1.32
SP2	3.79	5.17	-0.20	0.00	1.36
SP3	4.56	6.30	0.17	0.60	1.38
SP4	4.79	6.63	0.03	0.46	1.38
SP5	9.96	15.12	-0.23	0.01	1.52
SP6	16.56	24.84	-0.20	0.12	1.50
SH mod	5.02	6.33	with t_0	with t_0	1.26
Synergi Fusion-RP (Phenomenex)	24.17	43.28	with t_0	0.06	1.79
GSCH- c-choc	with t_0	with t_0	0.33	0.33	-
RP/WAX-AQ360	11.80	18.36	25.71	45.91	1.56
RP/WAX-DMAE	4.43	6.35	14.35	30.57	1.43
RP/WAX-BAMQO	10.36	15.99	26.68	30.27	1.54
Commercial/comparison columns					
Acclaim Mixed Mode WAX-1 (Dionex)	5.52	8.47	14.45	34.75	1.53
Uptisphere 5 MM3 (Interchim)	27.73	48.89	0.19	0.28	1.76
Primesep B2 (Sielc)	9.97	15.59	1.97	5.36	1.56
Obelisc R (Sielc)	6.22	9.47	3.59	10.97	1.52
Obelisc N (Sielc) ^{b)}	1.00	1.35	4.00	3.64	1.35
Chiralpak QN-AX (Chiral Technologies)	4.11	5.76	5.76	7.69	1.40
Luna NH ₂ (Phenomenex)	with t_0	with t_0	4.39	1.76	-
BioBasic AX (Thermo Scientific)	with t_0	with t_0	1.05	0.53	-
WAX (in-house)	with t_0	with t_0	0.12	0.22	-
Synergi Fusion-RP (Phenomenex)	24.17	43.28	with t_0	0.06	1.79
TSKGel Amide-80 (Tosoh)	with t_0	with t_0	with t_0	with t_0	-
PolysulfoethylA (PolyLC)	with t_0	with t_0	with t_0	with t_0	-
ZIC-HILIC (SeQuant)	with t_0	with t_0	0.14	with t_0	-
Nucleodur HILIC	with t_0	with t_0	with t_0	with t_0	-
Chromolith Performance Si (Merck)	with t_0	with t_0	with t_0	with t_0	-
PC-HILIC (Shiseido)	with t_0	with t_0	with t_0	with t_0	-

^{a)} Conditions see Experimental, all measurements at pH 6.0

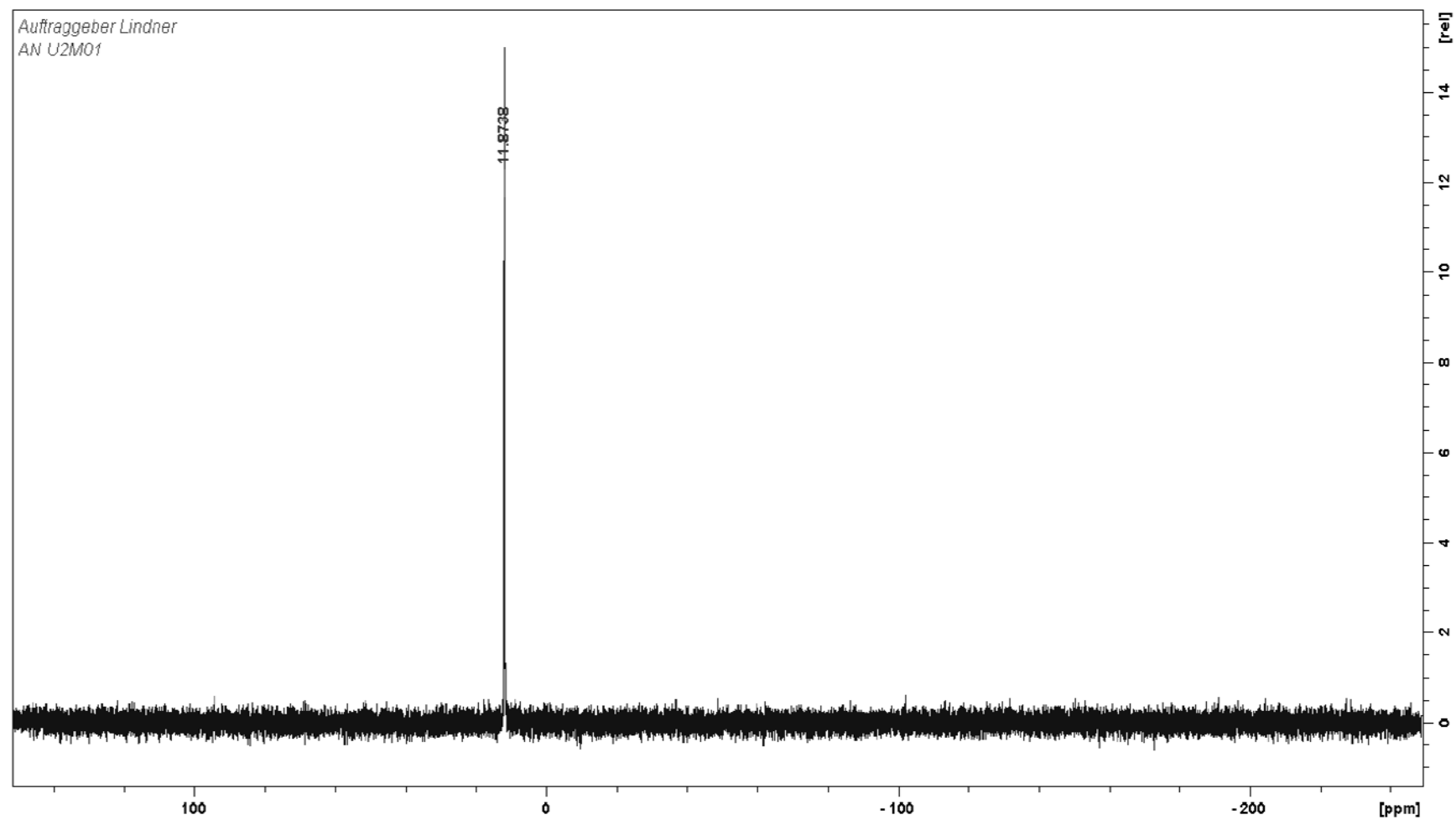
^{b)} Same conditions but pH 4.5

**Figure S2 (a)**

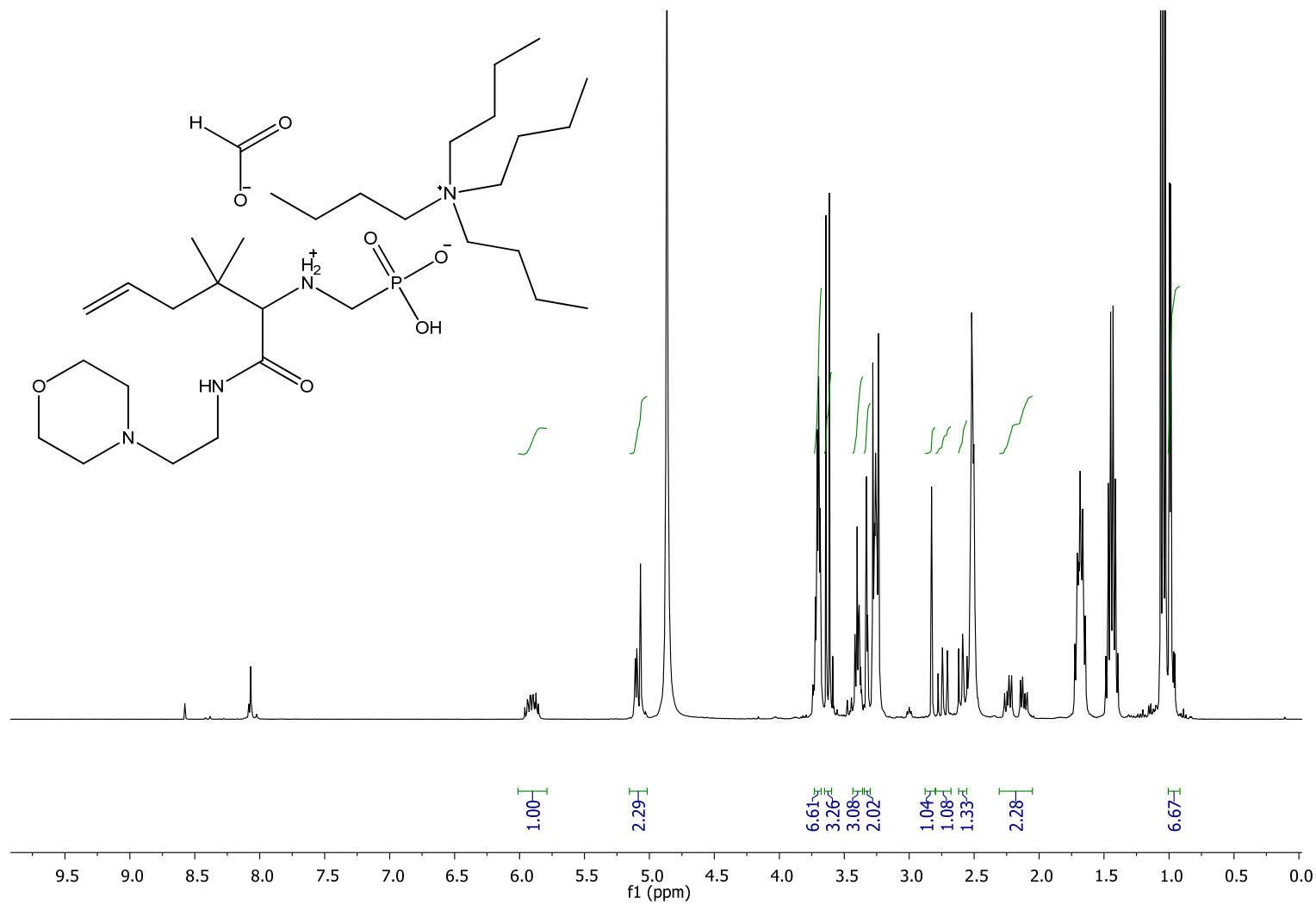
¹H-NMR spectrum in CD₃OD of SO₁ (SP1)

**Figure S2 (b)**

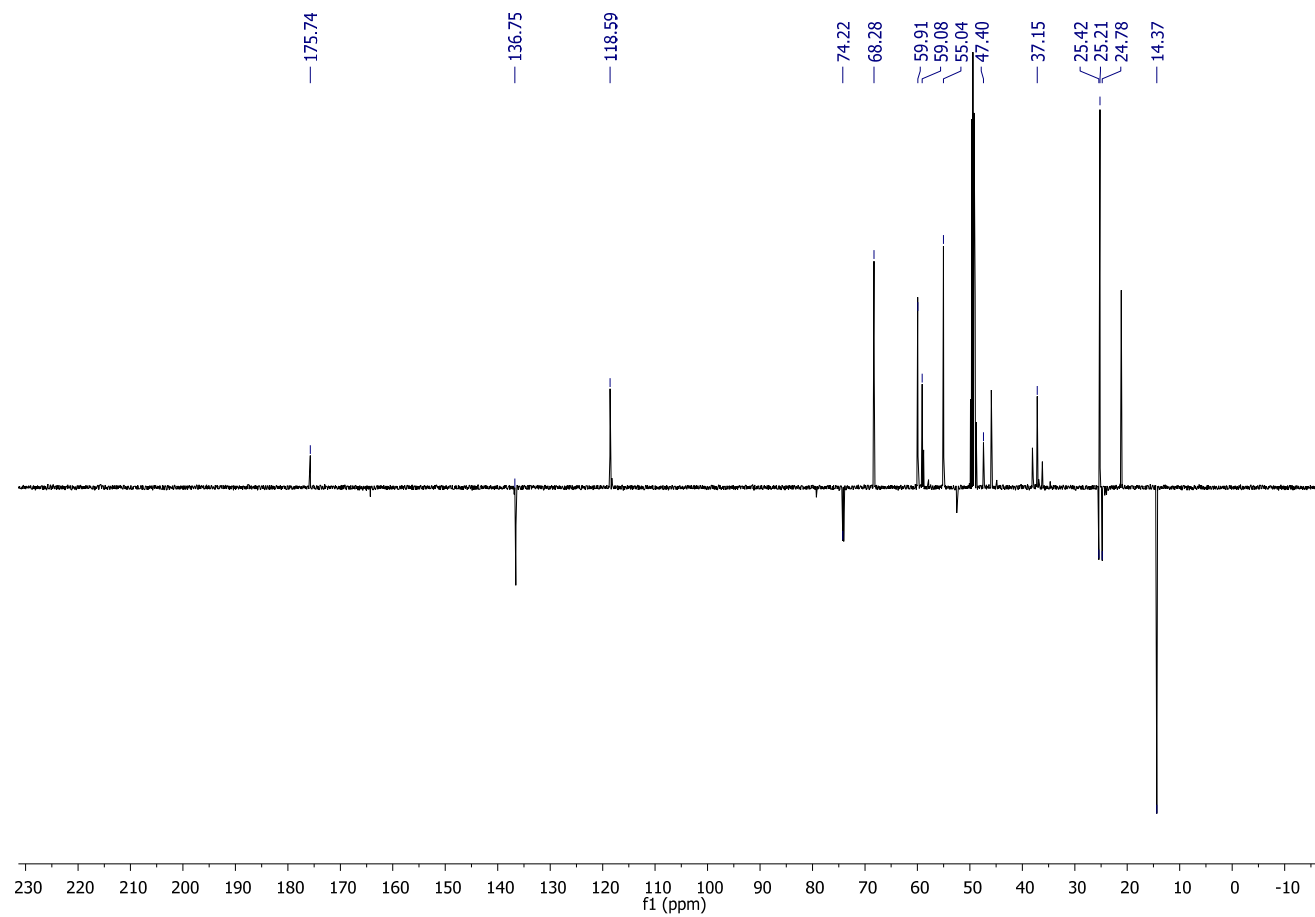
¹³C-NMR spectrum in CD₃OD of SO₁ (SP1)

**Figure S2 (c)**

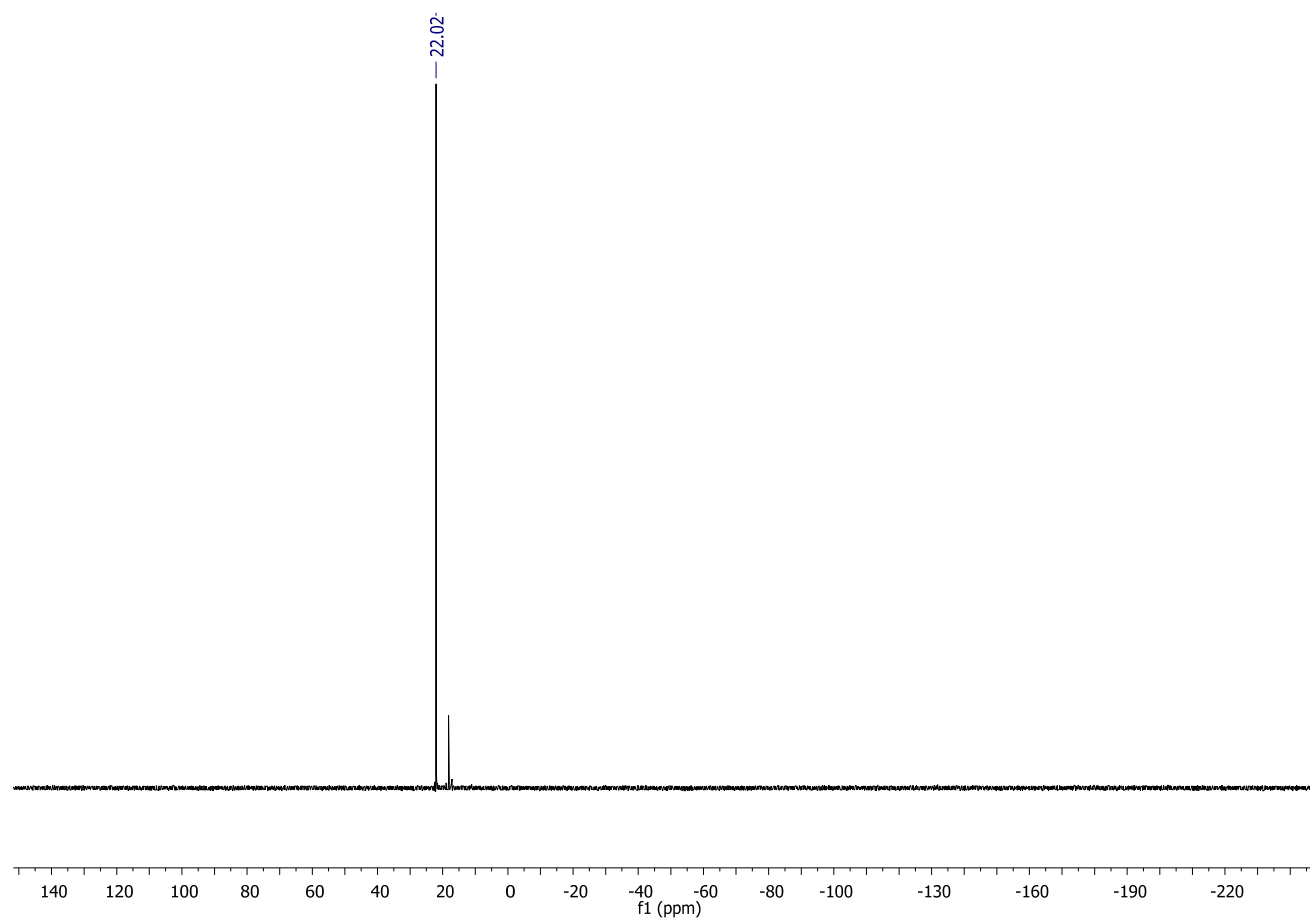
^{31}P -NMR spectrum in CD_3OD of SO_1 (SP1)

**Figure S3 (a)**

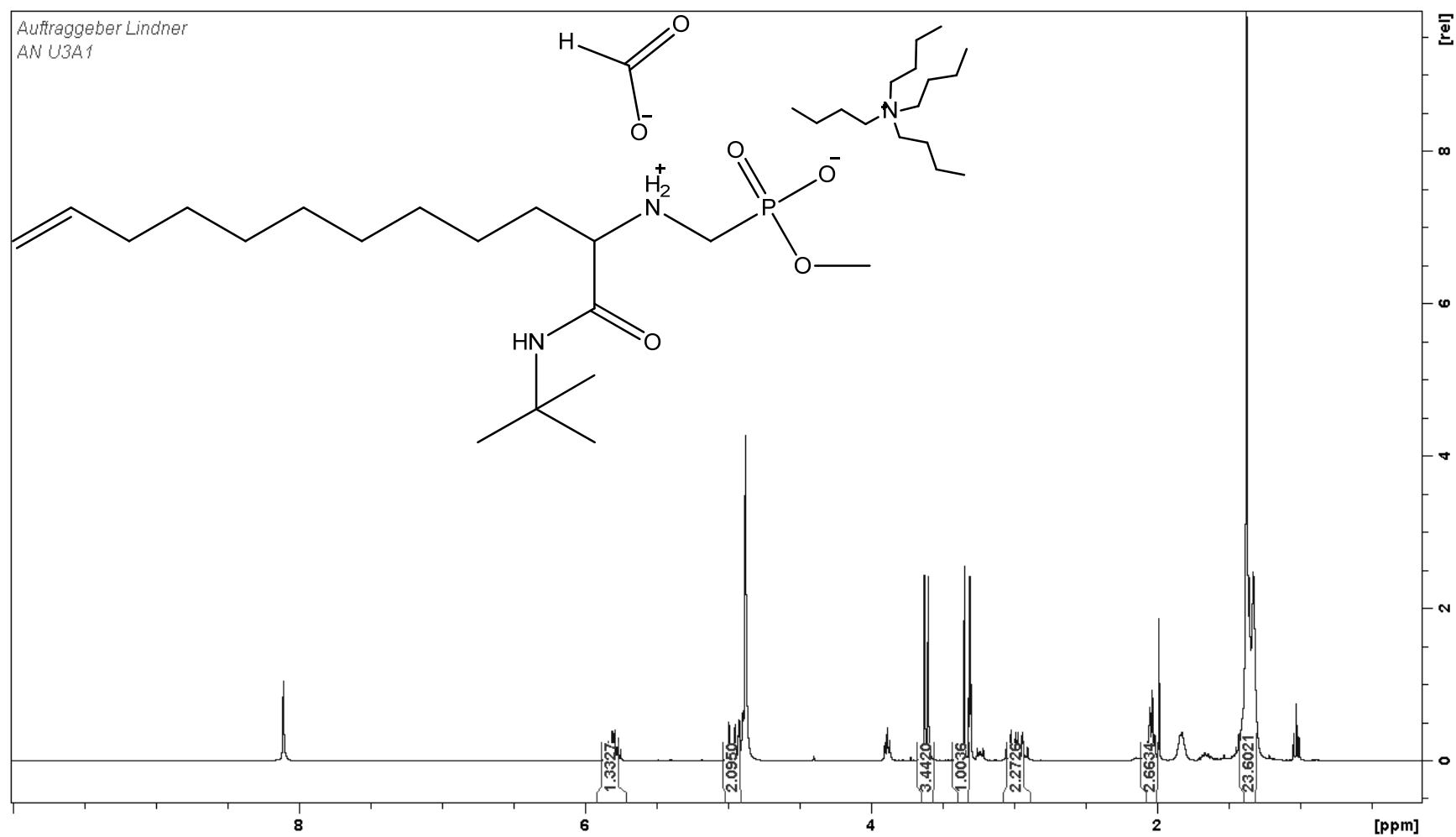
¹H-NMR spectrum in CD₃OD of SO₃ (SP3)

**Figure S3 (b)**

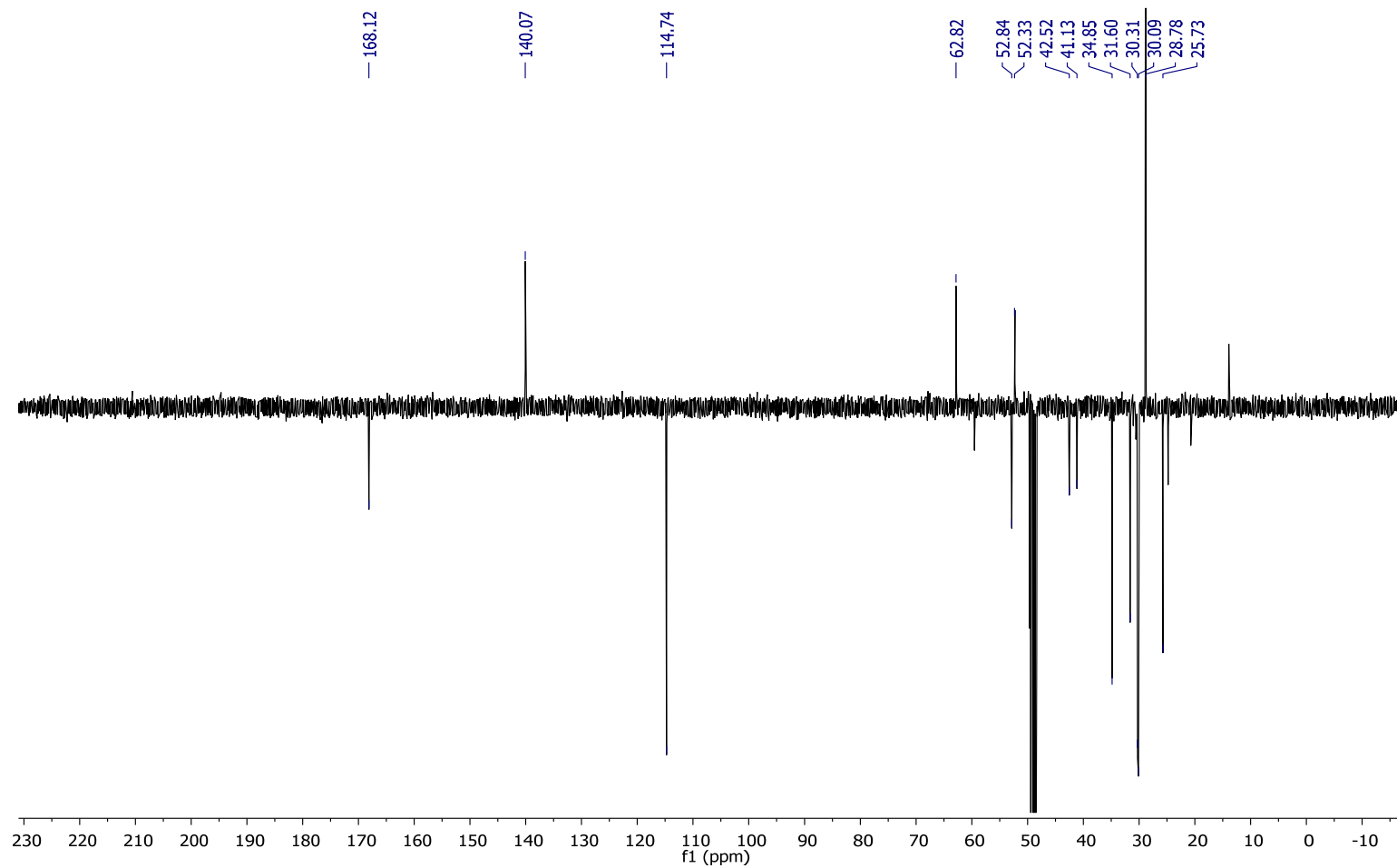
¹³C-NMR spectrum in CD₃OD of SO₃ (SP3)

**Figure S3 (c)**

^{31}P -NMR spectrum in CD_3OD of SO_3 (SP3)

**Figure S4 (a)**

¹H-NMR spectrum in CD₃OD of entry SO₅ (SP5)

**Figure S4 (b)**¹³C-NMR

spectrum

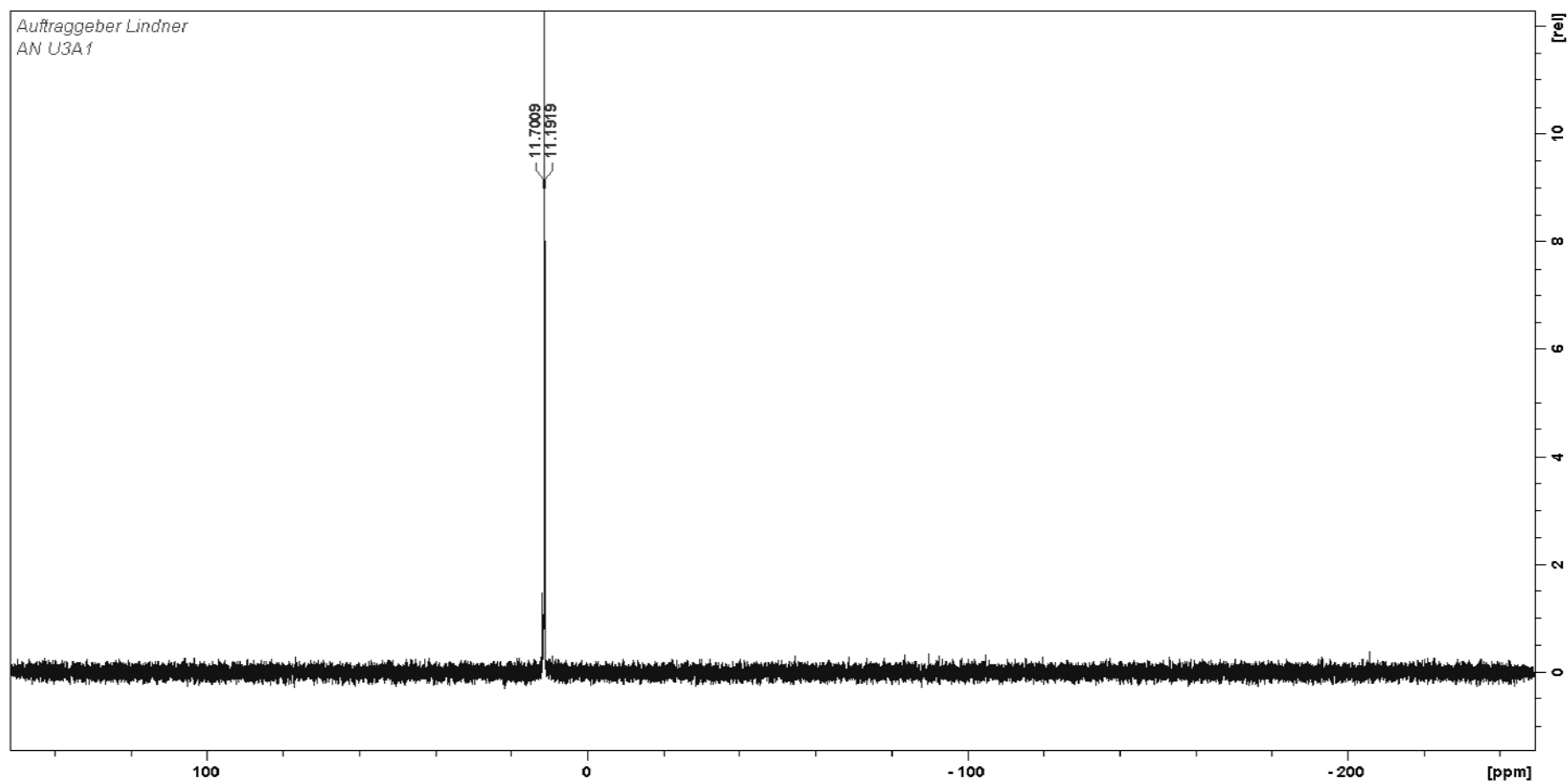
in

CD₃OD

of

SO₅

(SP5)

**Figure S4 (c)**

^{31}P -NMR spectrum in CD_3OD of SO_5 (SP5)

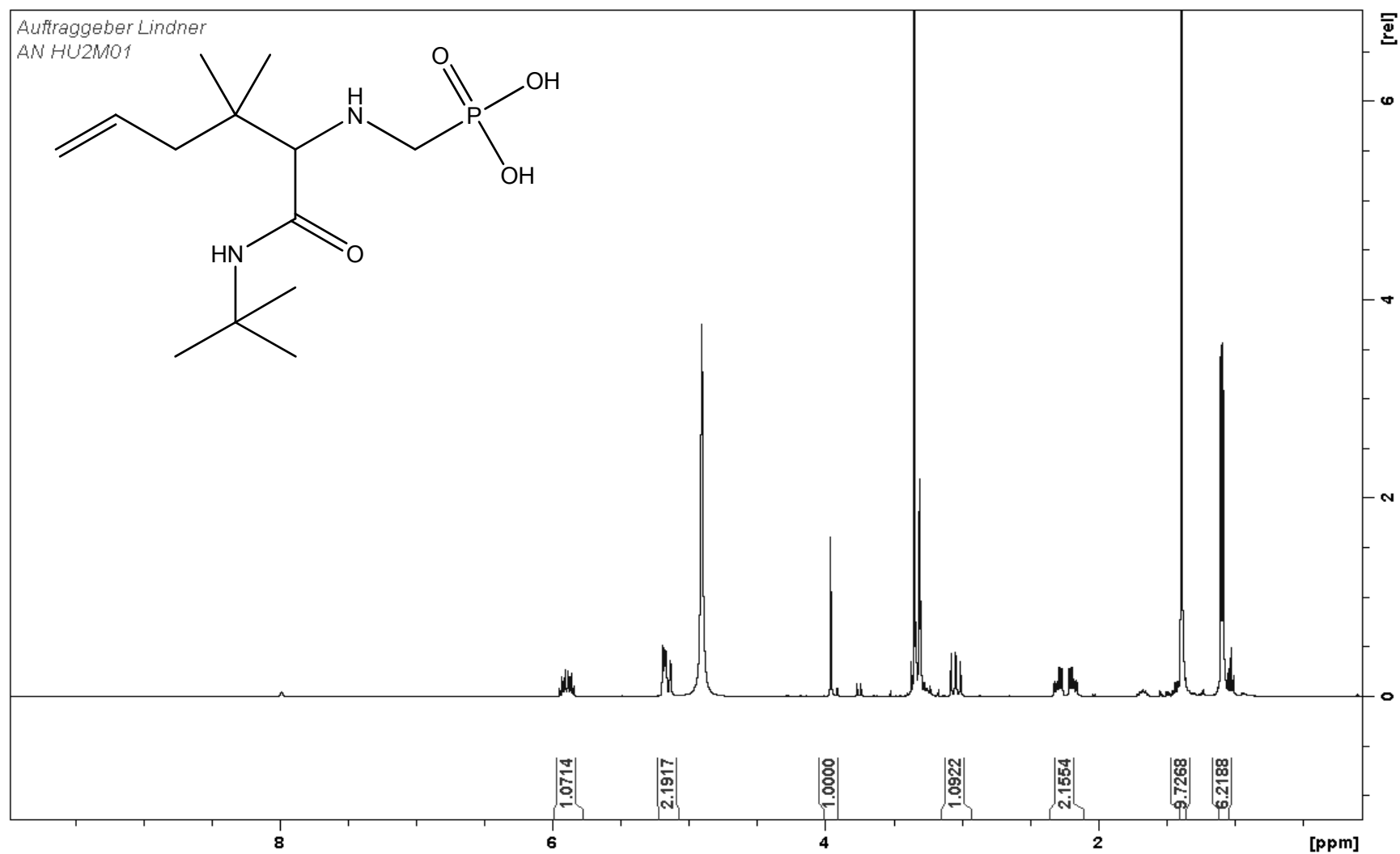
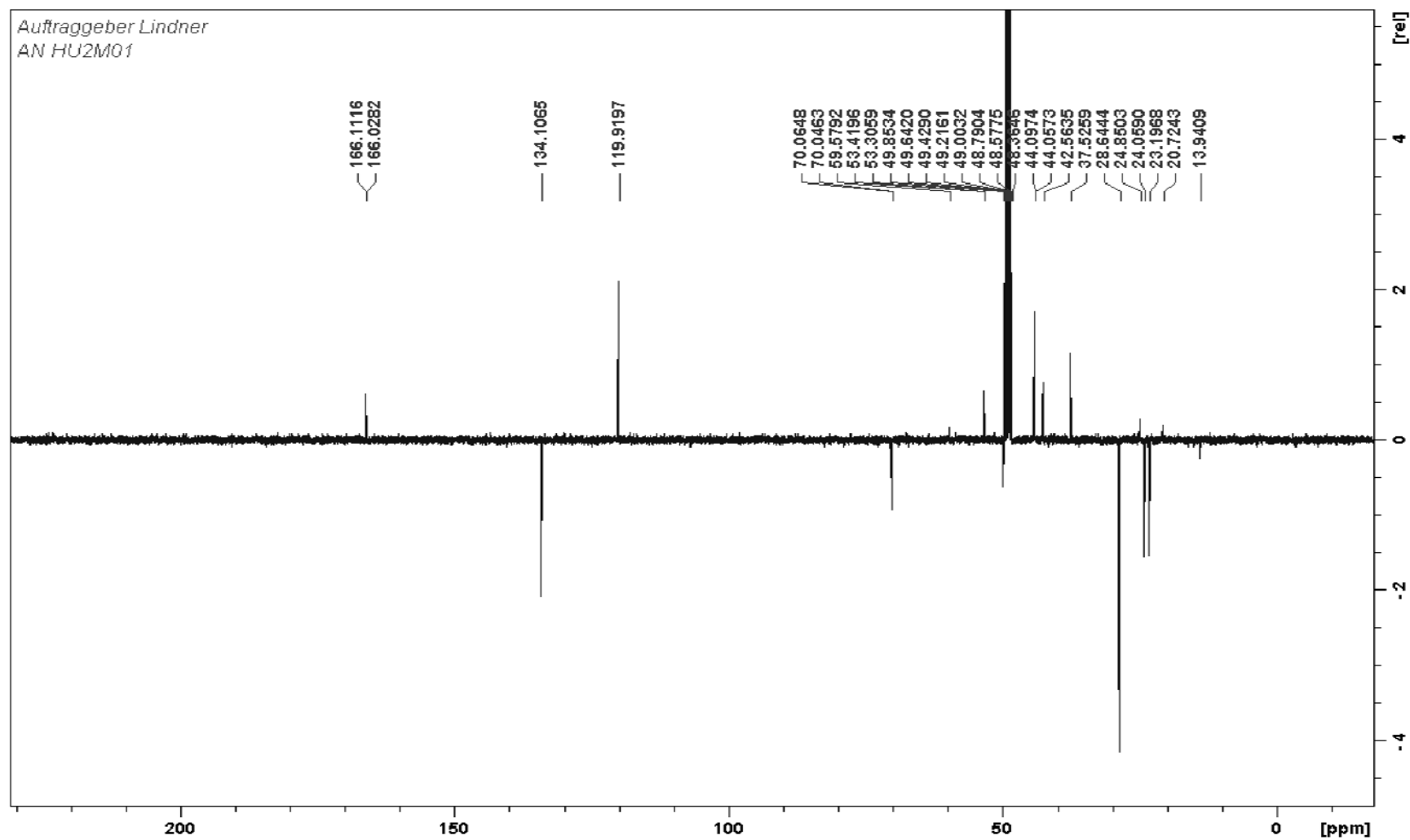
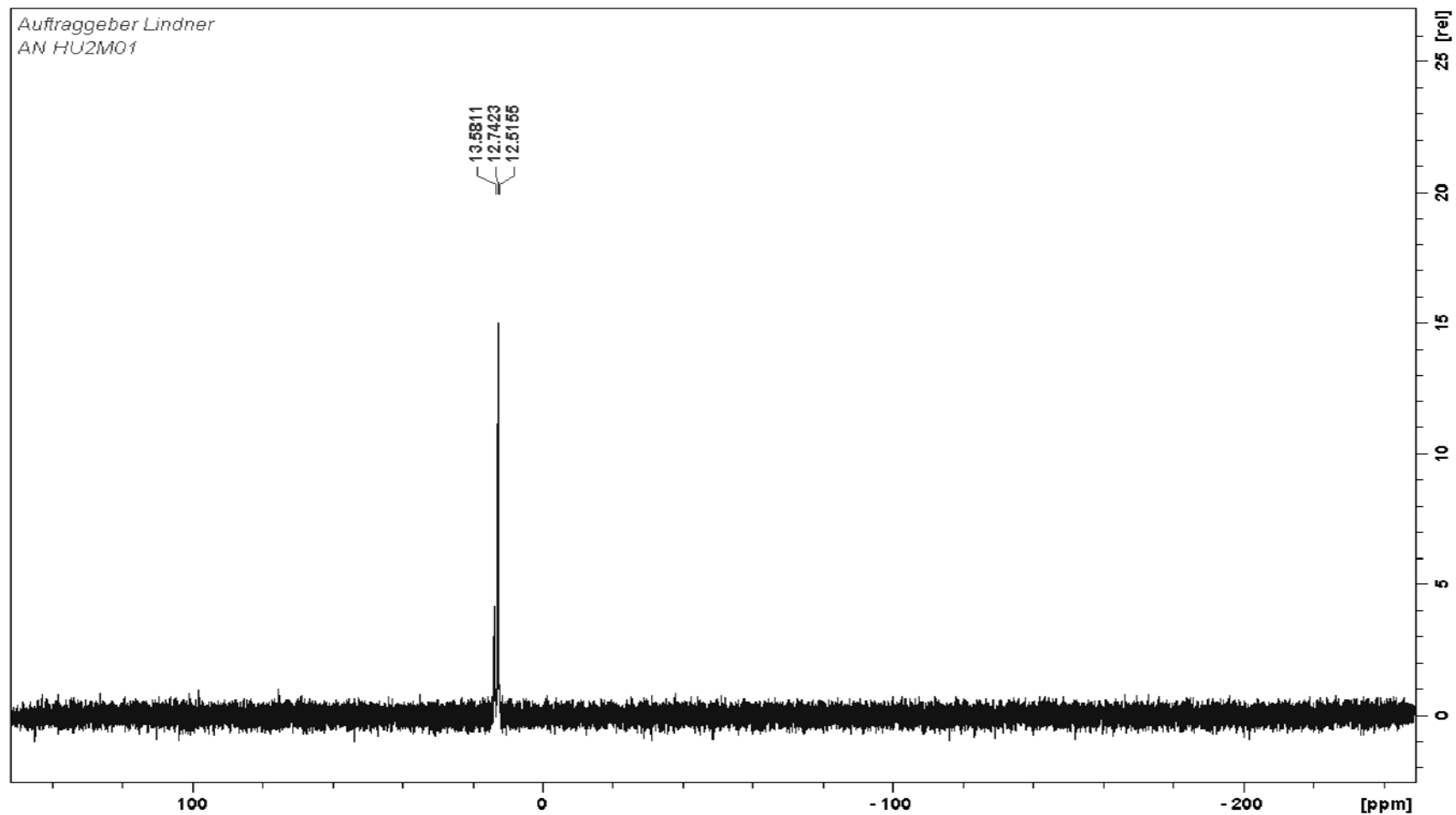


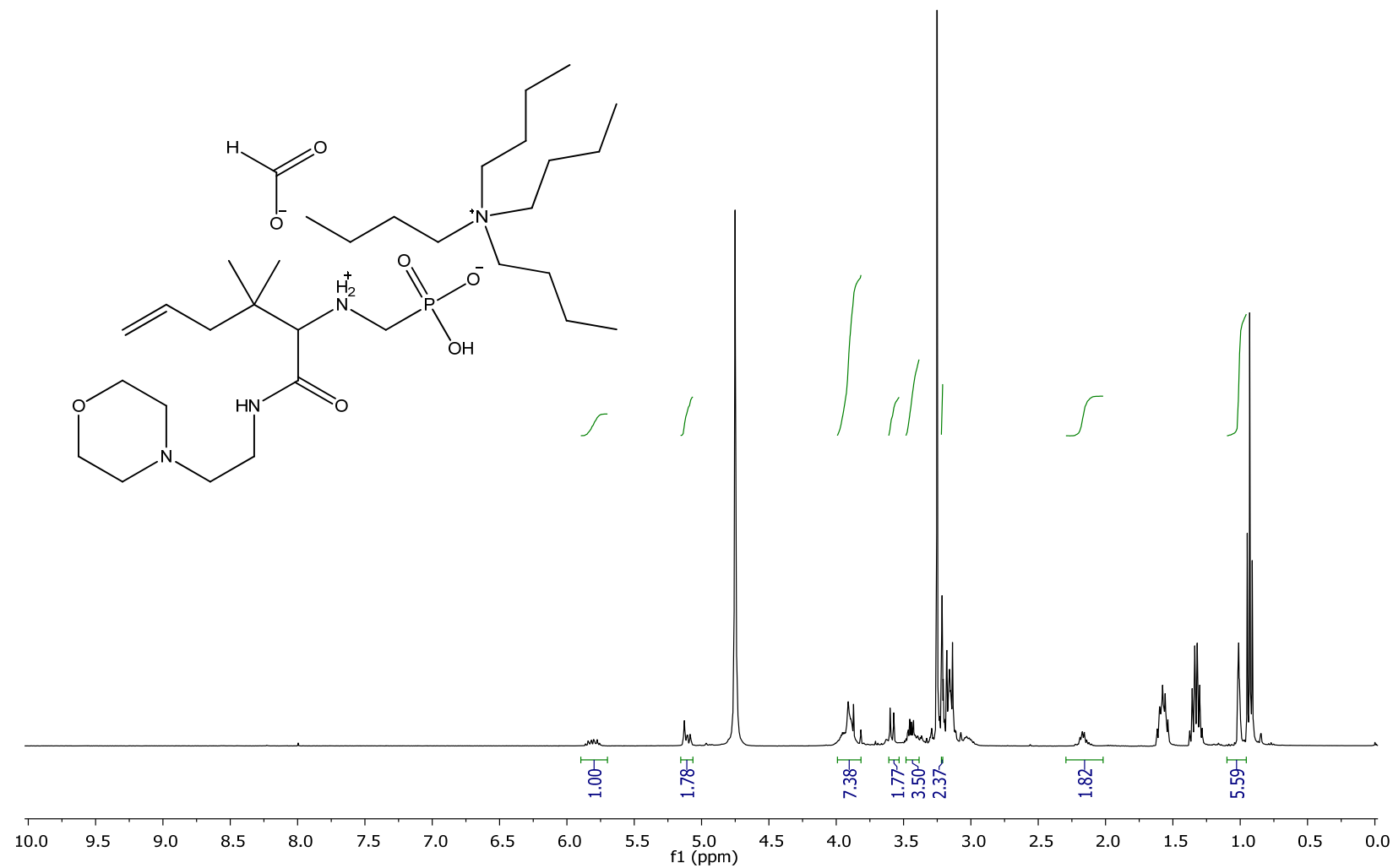
Figure S5 (c)
¹H-NMR spectrum (CD₃OD) of SO₂ (SP2)

**Figure S5 (b)**

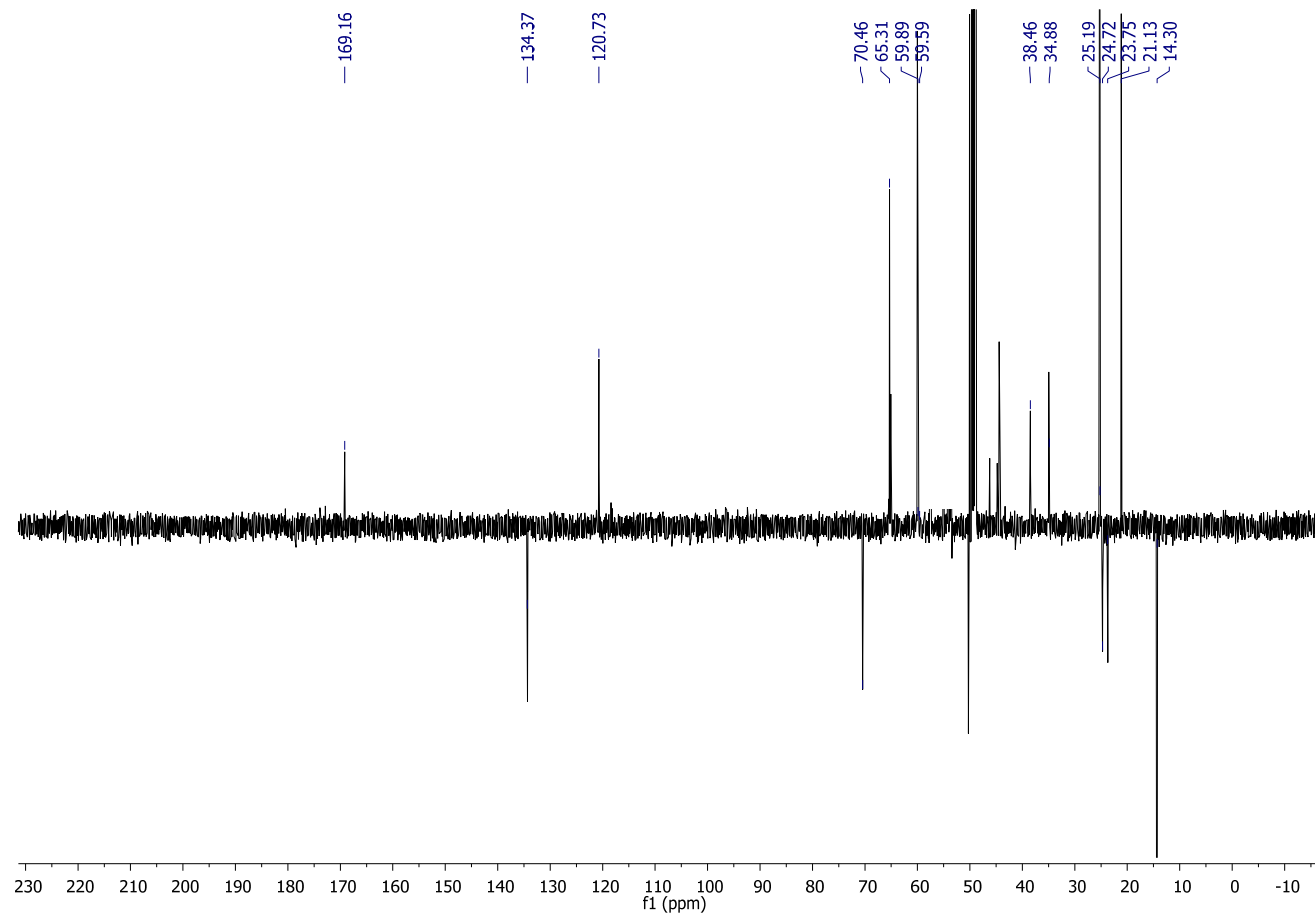
^{13}C -NMR spectrum (CD_3OD) of SO_2 (SP2)

**Figure S5 (c)**

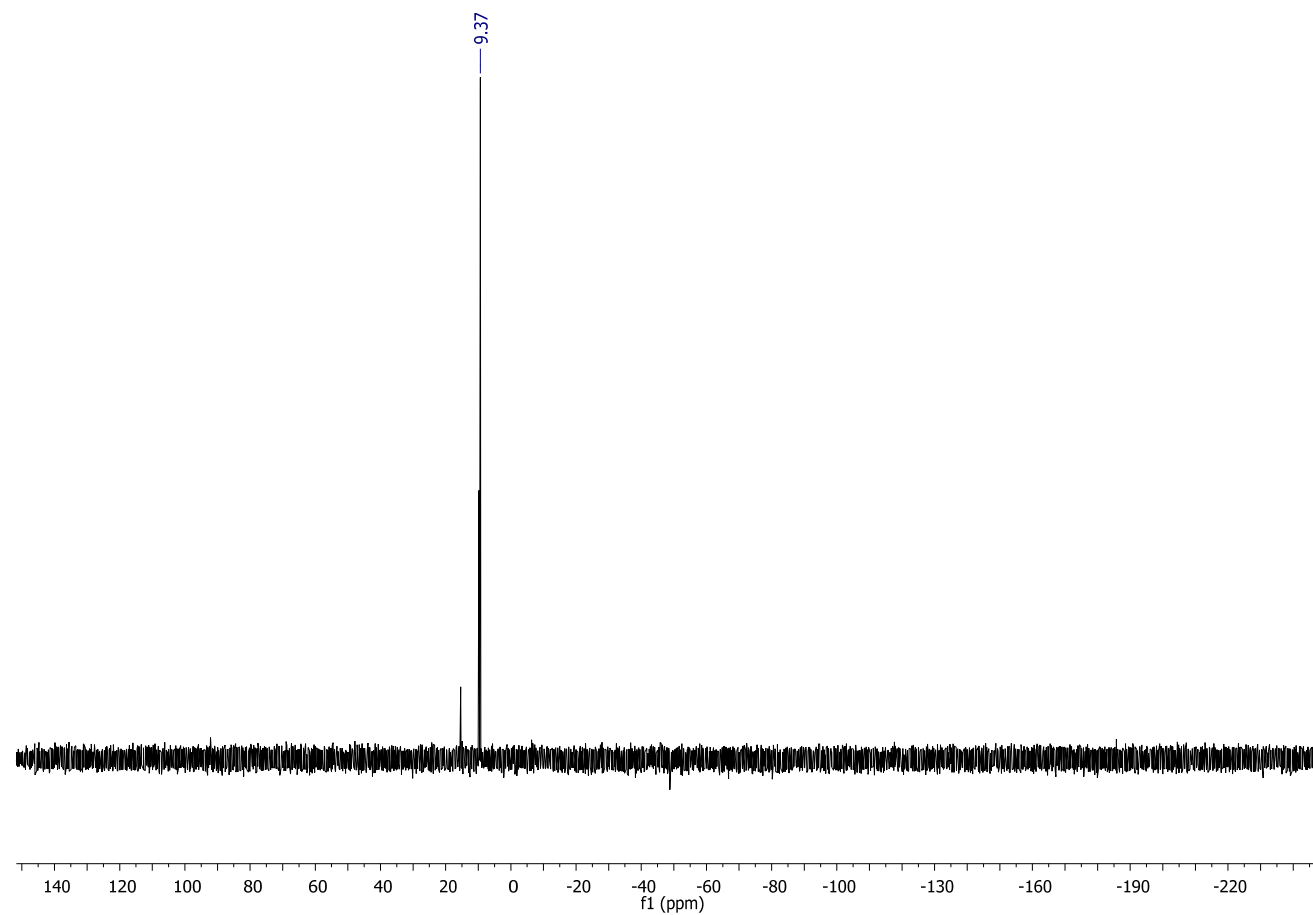
^{31}P -NMR spectrum (CD_3OD) of SO_2 (SP2)

**Figure S5 (a)**

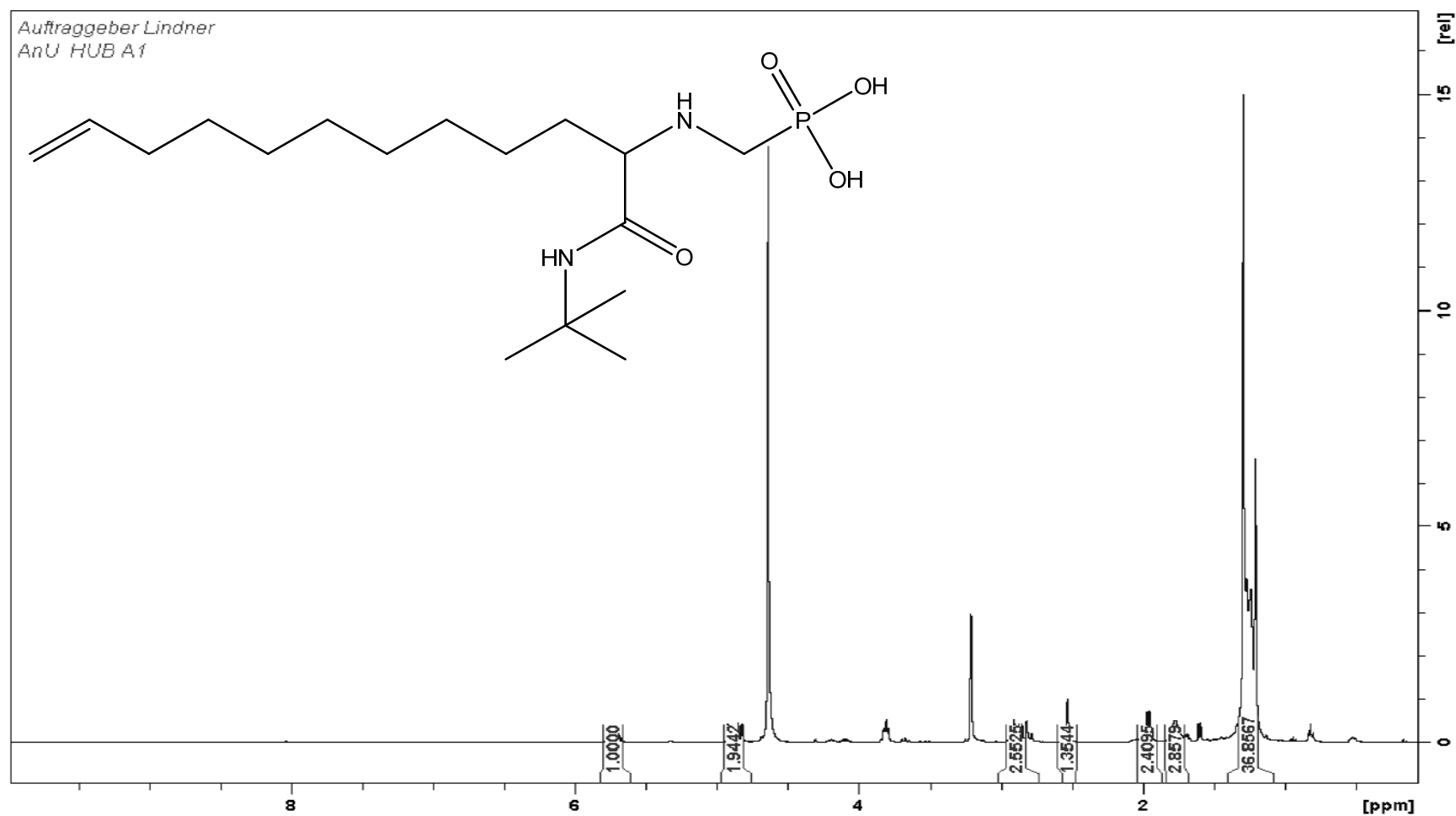
¹H-NMR spectrum (CD₃OD) of SO₄ (SP4)

**Figure S5 (b)**

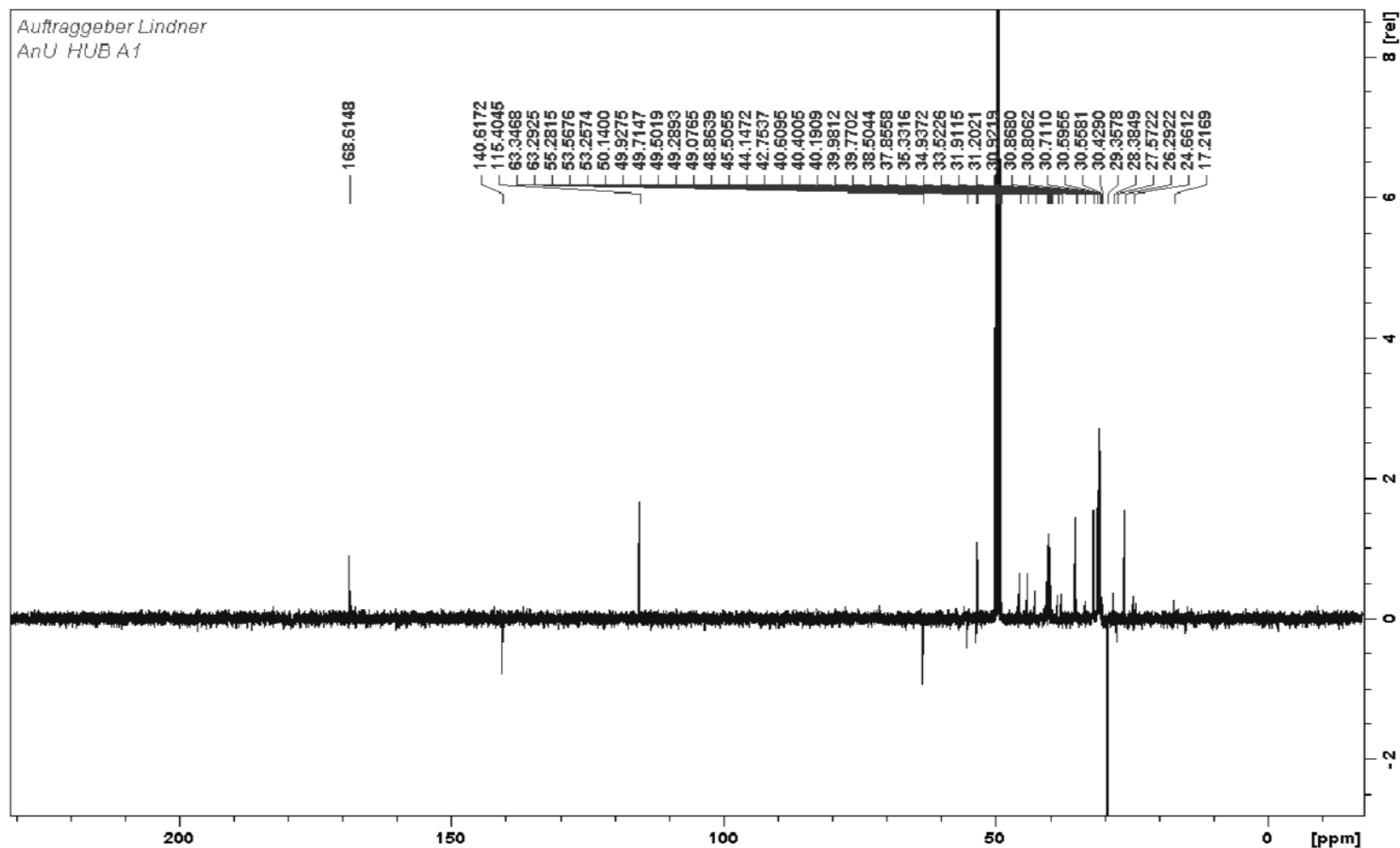
¹³C –NMR spectrum (CD₃OD) of SO₄ (SP4)

**Figure S5 (c)**

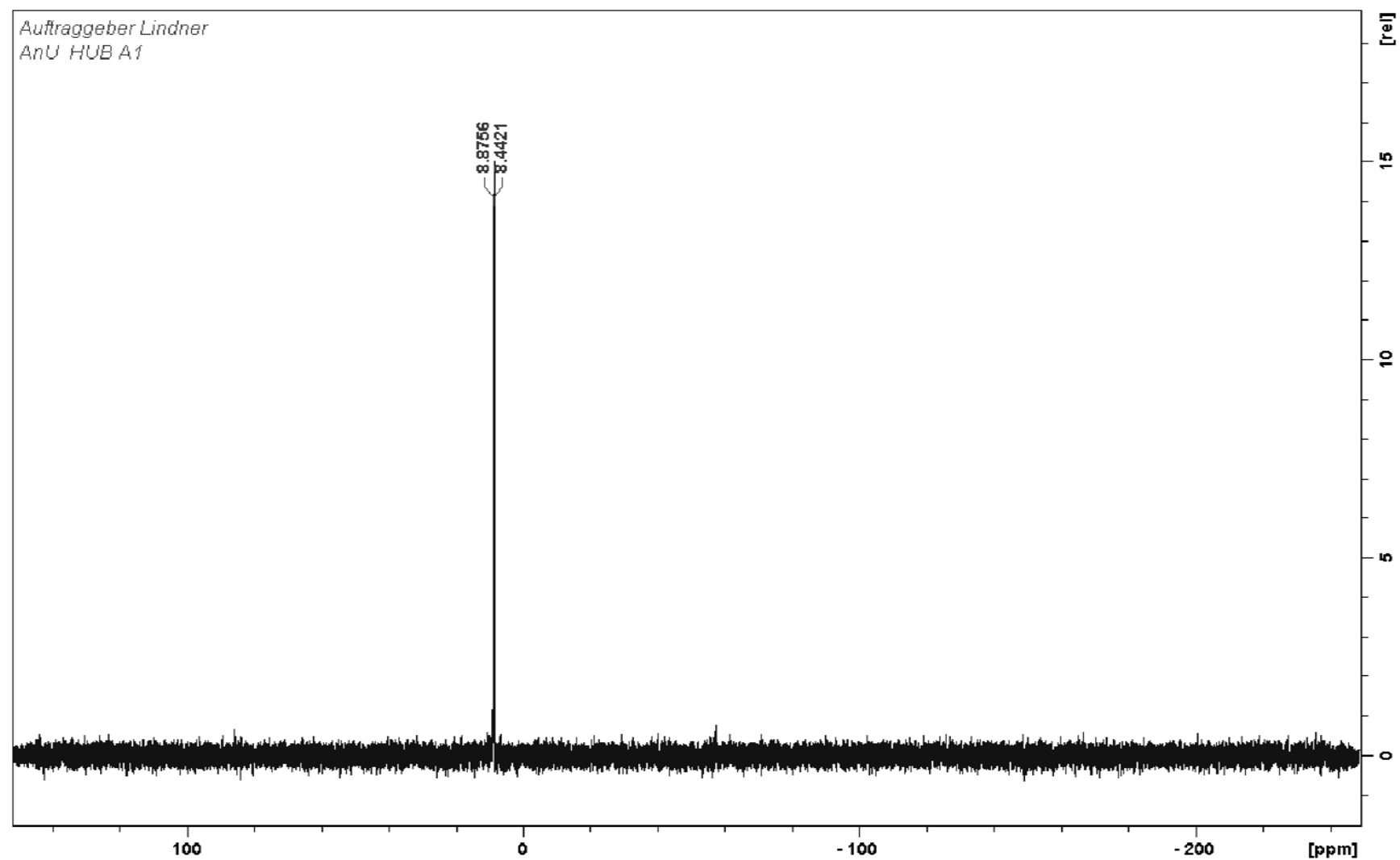
^{31}P –NMR spectrum (CD_3OD) of SO_4 (SP4)

**Figure S8 (a)**

¹H-NMR spectrum (CD₃OD) of SO₆ (SP6)

**Figure S8 (b)**

^{13}C -NMR spectrum (CD_3OD) of SO_6 (SP6)

**Figure S8 (c)**

^{31}P -NMR spectrum (CD_3OD) of SO_6 (SP6)

E. Thesis statistics:

Thesis word count: 40703

N°	Word	1 every .. word
1845	the	22.1 (4%)
189	phase	215.4
186	chromatography	218.8
162	chiral	251.3
158	reaction	257.6
128	retention	318.0
119	stationary	342.0
119	phases	342.0
114	separation	357.0
109	mobile	373.4
105	phosphonate	387.6
102	aminophosphonic	399.0
79	Ugi	515.2
60	novel	678.4

Table-: Repetition of single word in the whole text

F. Acknowledgements³

L'ordine del sorvegliante,

11/03/2013, Vienna (Au)

This thesis with its abstract vectorial sketches, peaks (the more the better), tables, graph and words (a lot) summarize 3 years of me, tens of thousands of hours of work and of my life. It's hard to keep my heart beat low and avoid shivering while I'm writing this couple of words that precede the word end in this story (as consequence what follows might be cheese, a Bit).

I would like to express my gratitude to my super-visor professor Lämmerhofer, your support and spur made this thesis. In these years I enjoyed challenging you, learning to lose (or at least how to lose better; learning) has not been easy but taught me something more than just chemistry.

Many thanks go to professor Lindner and to the separation science working group of the University of Vienna. I haven't been just working at the second floor of the department of chemistry; I've been part of a stimulating group in which we supported ourselves in the difficult quest of demonstrating our capability (or better proving ourselves) through our results (*Figure A1-*). Among the people I've been working a special thanks goes to Georgie, Rock and Roly, Stef(ph)anie, Sissy, Heli, Reini and Marek.

I acknowledge also the people that I've been working with at the R&D center of Astra Zeneca for the good and interesting time I had in Sweden and in particular Dr. Leek and Dr. Pavonine for their support and suggestions.

A special thanks goes to who educated me scientifically (Dr. Jana Krenkova, Dr. Caterina Temporini, Professor František Švec and Professoressa Gabriella Massolini). It's also their fault if now I'm here.

Ending this thesis to me mean also to virtually close an experience of three years not only form a scientific prospective. I there-fore like to use this chance to thanks the people that made this time my time (and not just a serious time). My acknowledgments go to Professor Binder (Mr. B, a guide in the world of life and rock music), Andrea Mastro Pasozzi (my fuzzy brother), Erfris Ciribilli (pag 43), Jacopo Padano Lucchesi, Joshua Circuitore Beretta, Irene Beltram Lavini, Lyla, Macho, Iniesta and Steph Pretzle, Ernesto, Marius, Dosi, Sophie, Muraccher, Gg, Cla, Camy, Chiara, Sara, Silvia, Oyster Mellon, Ulf Hamburger, Dr. Yushi, Heidi, Ingo, Shain and SS Ms E. Your names may contains misspell, it was about time to give some less formal style to this contribution.

Last but not least I thank my family for the choices they took for me in the past and for offering me life examples to get inspired by.

THE END.A

³ Epic word consisting a complicated combination of letters that I can hardly spell correctly.



FigureA1: Apple in Agarose

Andrea F.G. Gargano

G. Curriculum Vitae

PERSONAL DETAILS

Full Name

Andrea Francesco Giuseppe Gargano

Address

Stammgasse 9/6 1030A Wien, Austria;
Via Sabbionina n°3 25075 Nave (Brescia), Italy



Telephone

+43 1 4277 52 323

e-mail

andrea.gargano@univie.ac.at;
garganandrea@gmail.com

Date of
birth

05/09/1985

Nationality

Italian

Gender

Male

Current Position: PhD Student, Department of Analytical Chemistry, University of Vienna

Mother Tongue: Italian

Other Languages: English, Deutsch

European level*		Understanding		Speaking		Writing
		Listening	Reading	Spoken interaction	Spoken production	
	English	C1	C1	C1	C1	B2
	Deutsch	A1	A1	A1	A1	-

(*) [Common European Framework of Reference for Languages](#)

EDUCATIONAL BACKGROUND

Dates	Course, University	Qualification	Subjects
11/2012 01/2013	ASTRAZENECA R&D, Mölndal (Gö) Sweden	Internship in the AZ R&D, Structural Analysis Mölndal	-Characterization of novel developed aminophosphonate stationary phases Development of novel protein based affinity chromatography materials
02/ 2012	University of Vienna: Mass Spectrometry Fundamentals and Applications course		MS-based approaches in the analysis of small and large molecules, including peptides and proteins
09/ 2010	ASAC* NMR Summerschool		1D- and 2D-NMR Spectroscopy in Liquids
01/ 2010- on-going?	Institute of Analytical Chemistry, Faculty of Chemistry, University of Vienna, Austria	PhD.Study in Pharmaceutical and Bioanalytical chemistry	Chromatography Bioanalytical Chemistry Synthesis of novel chromatographic selectors for HILIC, Mixed Mode, Ion exchange and Chiral Chromatography and evaluation of chromatographic properties
01/ 2009- 06/ 2009	Lawrence Berkeley National Laboratory, California, USA	Master thesis	Development of novel monolithic stationary phases for ion exchange chromatography
09/ 2004- 07/ 2009	Institute of Analytical Chemistry, Faculty of Pharmacy , University of Pavia, Italy	Master of Science degree 110/110	Pharmaceutical analysis Medicinal chemistry Pharmaceutical technology
09/ 1999- 06/ 2004	High-school, Liceo Scientifico “Leonardo”, Brescia, Italy	High school leaving qualification 90/100	

* Austrian Society of Analytical Chemistry,

CONFERENCE CONTRIBUTIONS

Dates	Type of Contribution	Conference	Title
06/ 2012	Talk	38 th HPLC conference ¹ Anaheim, CA	"Novel aminophosphonate multimodal selectors for liquid chromatography based on UGI-multicomponent reaction"
06/ 2012	Poster	38 th HPLC conference ¹ Anaheim, CA	"Pore-size influence on the separation efficiency of silica based quinine stationary phases for plasmid DNA isoform separation"
06/ 2012	Talk	8 th ASAC JunganalytikerInnen meeting Salzburg, AU	"Novel aminophosphonate multimodal selectors for liquid chromatography based on UGI-multicomponent reaction"
09/ 2011	Poster	14 th RDPA meeting Pavia, IT	"Stereoselective determination of D- and L-lactic acid by the use of HPLC on quinine based chiral stationary phases"
06/ 2011	Poster*	37 th HPLC conference ¹ Budapest, HU	"Selectivity of mixed-mode chromatography for structural isomers of phosphorylated carbohydrate metabolites "*"
06/ 2011	Poster	37 th HPLC conference ¹ Budapest, HU	"Amino acid grafted poly(glycidyl methacrylate-co-ethylene glycol dimethacrylate) capillary monoliths for plasmid DNA isoform separation"

¹ International symposium on high performance liquid phase separations and related techniques

² Austrian Society of Analytical Chemistry, young analytical forum

³Recent developments in pharmaceutical analysis conference

* **Poster Award:Third place**

TEACHING ACTIVITY

WS ¹ SS ² 2011, 2012	Faculty of Chemistry, University of Vienna	Practical Course: HPLC analysis of bioactive compounds
SS ² 2011	Faculty of Chemistry, University of Vienna	Practical Course: Capillary Electrophoresis
WS ¹ 2008	Faculty of Pharmacy, University of Pavia	Practical Course: Instrumental Methods for Analytical Chemistry

¹ Winter Semester

² Summer Semester

PUBLICATIONS

A. F.G. Gargano, W.Lindner, M. Lämmerhofer	Enantioseparation of chiral amido-aminophosphonate scaffolds from a novel Ugi multi-component Reaction by liquid chromatography on quinidine-based chiral anion exchangers (manuscript, to be published)
A. Gargano, S. Buchinger, M. Kohout, W. Lindner, M. Lämmerhofer	Facile route to phosphopeptidomimetics by single step Ugi Multicomponent Reaction (manuscript, to be published)
A.F.G Gargano , T.Leek W. Lindner, M.I Lämmerhofer	Novel amido-aminophosphonate mixed mode chromatographic selectors form UGI multicomponent reaction (manuscript,to be published)
A.F.G. Gargano, P. Macíková , M. Kohout , M. Lämmerhofer, W. Lindner	Direct liquid chromatographic enantioseparation of free α , β and γ -aminophosphonic acids employing cinchona-based chiral zwitterionic exchangers (manuscript accepted, An.Bioan.Chem. 2013)
P. Franco, T. Zhang, A. Gargano, M. Mahut, M. Lämmerhofer, W. Lindner	Enantiomer and Topoisomer Separation of Acidic Compounds on Anion-Exchanger Chiral Stationary Phases by HPLC and SFC LC GC Europe 2012;
M. Mahut, A. Gargano, W. Lindner, M. Lämmerhofer	Chemoaffinity material with condition-dependent switchable selectivity between separation of plasmid DNA isoforms and circular topoisomers An. Chem. 2013
H. Hinterwirth M. Lämmerhofer B. Preinerstorfer A. Gargano R.Reischl W. Bicker O. Trapp W. Lindner	Selectivity issues in targeted metabolomics: Separation of phosphorylated carbohydrate isomers by mixed-mode hydrophilic interaction/weak anion exchange chromatography J. Sep. Sci 2010
M. Lämmerhofer A. Gargano	Monoliths with chiral surface functionalization for enantioselective capillary electrochromatography. J. Pharm. Biomed. Anal 2010
J Krenkova, A. Gargano, N. A. Lacher J. M. Schneiderheinze F. Svec,	High binding capacity surface grafted monolithic columns for cation exchange chromatography of proteins and peptides J.Chrom. A 2009
